Magnetic Nanostructures Investigated by Small Angle Neutron Scattering

Albrecht Wiedenmann

VIII School of Neutron Scattering
„Francesco Paolo Ricci“
Structure and Dynamics of magnetic systems

http://www.hmi.de/bereiche/SF/SF3/methods/sans/index_en.html

Acknowledgements

SANS-Crew at hmi

Elvira Garcia-Matres André Heinemann Armin Höll
Martin Kammel Uwe Keiderling Olivier Perroud

SANSPOL

Thomas Keller (TU München), Thomas Krist (hmi), Ferenc Mezei (hmi)

POLARIS

Axel Rupp (hmi) Werner Heil (Univ. Mainz)

Ferrofluids

Martin Buske (Berlin heart), Helmut Bönnemann (MPI Mühlheim/Ruhr)
Roland P. May (ILL Grenoble), Charles Dewhurst (ILL Grenoble)

Magnetic alloys

Joachim Kohlbrecher (PSI Switzerland), Jürgen Eckert (TU-Darmstadt)
Helmut Herrmann (IFW Dresden)

Time-resolved techniques

Roland Gähler (ILL), Klaus Habicht (hmi), Margareta Russina (hmi)

Funding

German Research Society (DFG) Projects Wi-1151/2, Wi 1151/3

Berlin Neutron Scattering Center (BENSC)

Access to spectrometers

2/3 of beam-time for external users

Application : 15 February
15 September

Scientific committee decides

http://www.hmi.de/bensc/

HEAVY OVERLOAD

Content

I. Basics of SANS technique

Scattering law

Nuclear and magnetic scattering

Scattering of polarised neutrons (SANSPOL, POLARIS)

II. Applications to Materials Science

Magnetic colloids

Soft and hard magnetic materials

III. Practice of SANS

SANSPOL instrument V4

Data aquisition, data reduction and analysis techniques

IV. Tutorial - Problem Class

V. New developments-Dynamical studies

I. Basics of SANS technique - outline

1.1 Introduction

1.2 Conventional Small Angle Scattering (SANS)
Scattering cross section, scattering length, Scattering law, pair correlation function ,General results,Particle scattering, Polydisperse systems,Structure factors

1.3 Magnetic scattering

1.4 Polarised neutrons: POLARIS, SANSPOL,SANS

1.5 Instrument

Small Angle Neutron Scattering

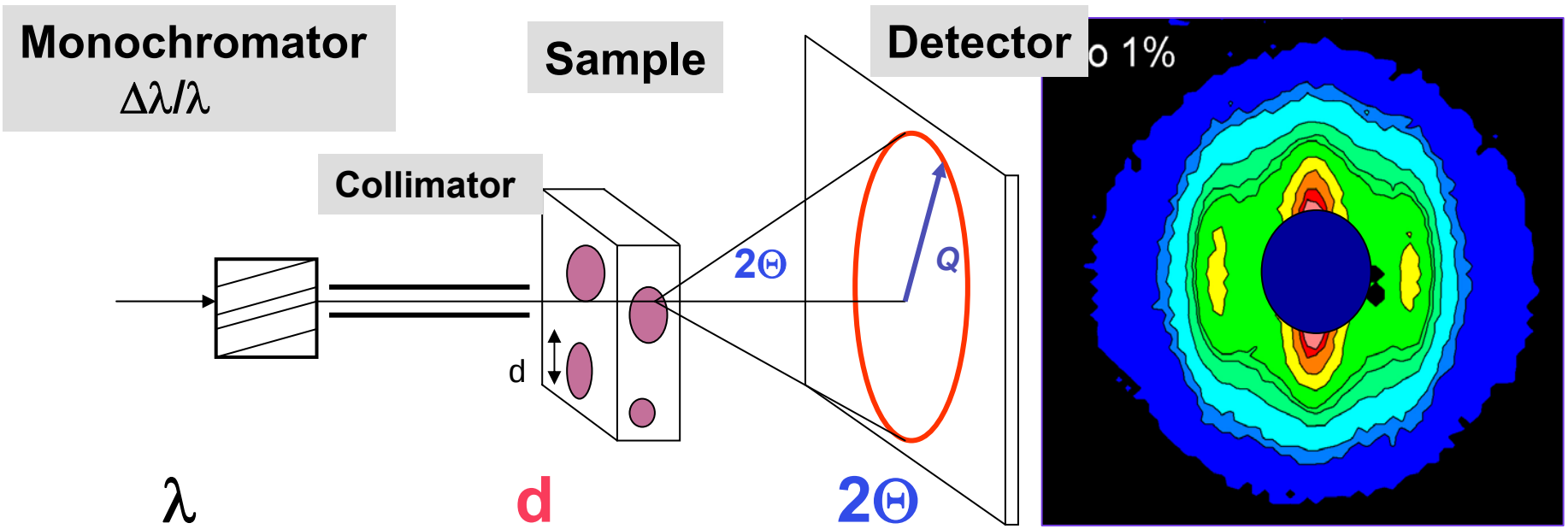

λ	d	2Θ
0.5-2 nm	0.5-300nm	0.1-20°

fluctuations of density, composition, magnetization

Nano-analytics on length scale 0.5 nm-500 nm

TEM (Transmission electron microscopy)

FIM (Field ion microscopy)

Local

SAXS (X-rays): Interaction with electrons:

Scattering length: $b_x = Z*0.282\ 10^{-12}$ cm

SANS (neutrons): Interaction with nucleous

Integral

Scattering length: b_n (^{1}H: -0.2, ^{2}D: +0.5)

Between neutron spin and magnetic moment μ

Scattering length: $b_{mag} = 0.27 * 10^{-12} * \mu$

Scattering cross-section

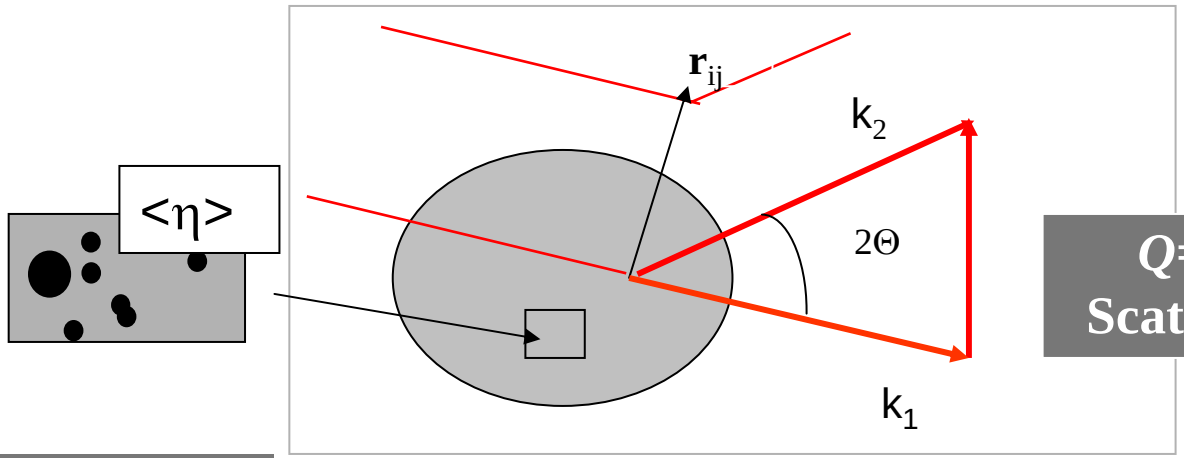

$Q = 4\pi \sin\Theta/\lambda$
Scattering vector

General $I(Q) = \sum\sum b_i b_j \exp[iQr_{ij}]$

For SANS Scattering length density: nuclear $\eta(r) = \sum c_i b_i \rho_i$

magnetic $\eta(r) \propto \sum c_i M_i^{\perp} \rho_i$

Correlation function $\gamma(r) = \eta_0 \eta(r) / \langle\eta^2\rangle$

$$I(Q) = \langle\eta^2\rangle \int \gamma(r)\, d^3r \exp[i\, Q\, r]$$

Fourier transform of c.f.

The prefactor $<\eta^2>$ in a two-phase system

phase 1 $\eta_1 = \sum c_i b_i / \Omega_i$ volume fraction f

phase 2 $\eta_2 = \sum c_i b_i / \Omega_i$ volume fraction (1-f)

average scattering length density

$$<\eta> = f\,\eta_1 + (1-f)\,\eta_2$$

Deviation from $<\eta>$:

$$\delta_1 = \eta_1 - <\eta> = (1-f)(\eta_2 - \eta_1)$$

$$\delta_2 = \eta_2 - <\eta> = f\,(\eta_2 - \eta_1)$$

Mean square fluctuation of scattering length densities

$$<\eta^2> = f\,\delta_1^2 + (1-f)\,\delta_2^2 = f(1-f)\,(\eta_1 - \eta_2)^2$$

Nuclear contrast-matching

Scattering from different parts of particle (Micelles in solvents)

a) Isotope mixtures of solvents

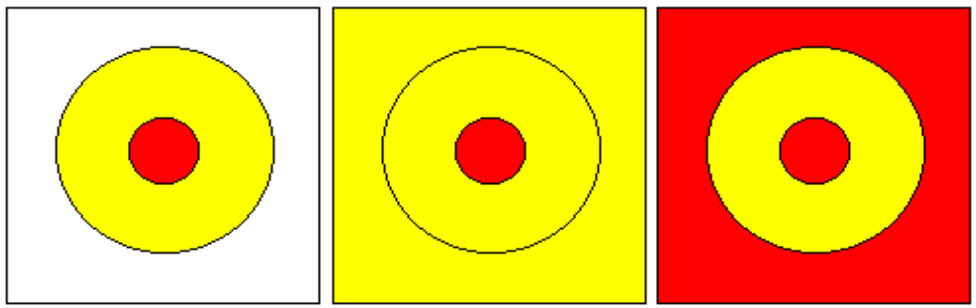

b) Isotope substitution (H by D) in molecules

Scattering law

$$I(Q) = \langle\eta^2\rangle \int\gamma(r)d^3r \exp[i\,Qr]$$

For isotropic, centro-symmetric scatterers

$$\langle\exp[i\,Qr]\rangle = \sin(Qr)/Qr$$

$$I(Q) = \langle\eta^2\rangle \int\gamma(r)\, 4\pi\, r^2 dr \sin(Qr)/Qr$$

Fourier transform

$$\gamma(r) = (2\pi^2\langle\eta^2\rangle)^{-1} \int I(Q)\, Q^2\, dQ \sin(Qr)/Qr$$

Limits

$r = \infty$: $\gamma(\infty) = 0$

$r = 0$: $\gamma(0) = 1$

Pair distance distribution function p (r)

$$p(r) = 4\pi r^2 \gamma(r)$$

e.g: spheres of Radius R

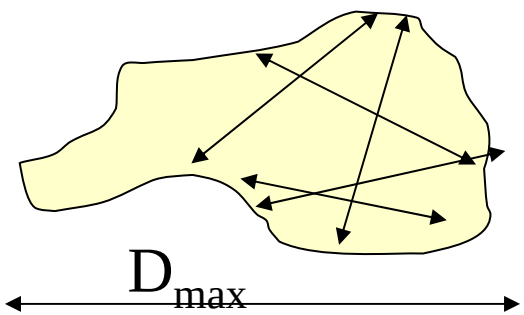

$r = 0$

$p(r)=0$

$r > D_{max}$

$p(r)=0$

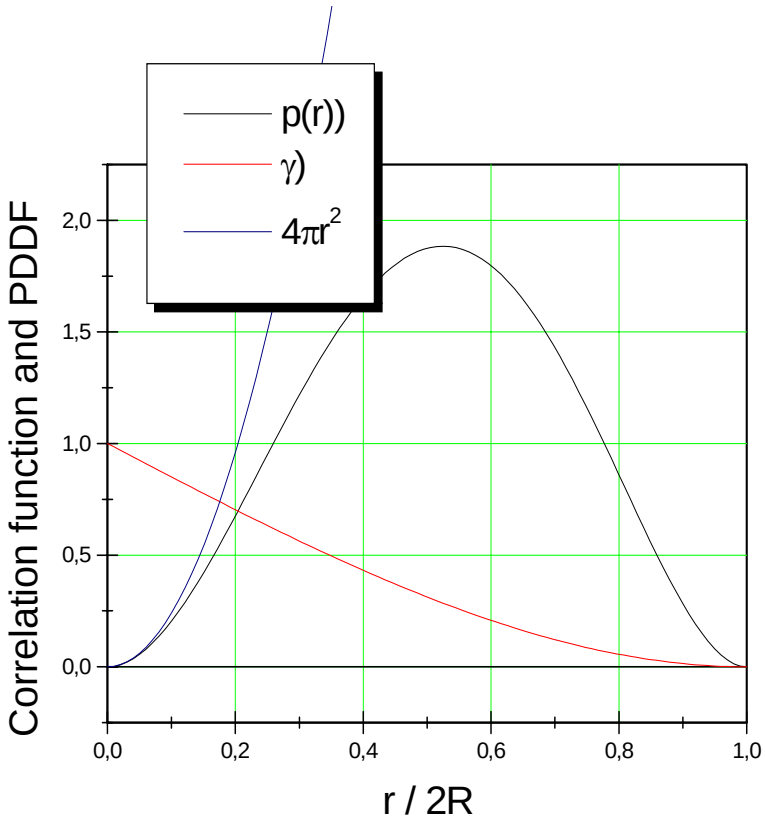

General results from SANS

"Invariant", independent of shape:

$$\int I(Q)\, Q^2\, dQ = 2\pi^2 \langle\eta^2\rangle$$

Extrapolation to Q = 0:

$$I(0) = \langle\eta^2\rangle \int \gamma(r)\, 4\pi\, r^2\, dr = \langle\eta^2\rangle\, V_p$$

Combination $\Rightarrow$ **Volume :**

$$I(0) / \int I(Q)\, Q^2\, dQ = V_p / 2\pi^2$$

Guinier-approximation (small Q) $\Rightarrow$ **Radius of gyration**

$$I(Q) = \langle\eta^2\rangle \int \gamma(r)\, 4\pi\, r^2\, [1 - Q^2 r^2 / 3! + ..]\, dr$$

$$= I(0) \exp(-R_g^2\, Q^2 / 3)$$

$$R_g = \int \gamma(r)\, r^4\, dr / \int \gamma(r)\, r^2\, dr$$

Porod-approximation (large Q) $\Rightarrow$ **Surface S:**

$$\gamma(r) \propto 1 - Sr/4\,V + .. \Rightarrow I(Q) \propto S / Q^4$$

Real space *versus* reciprocal space

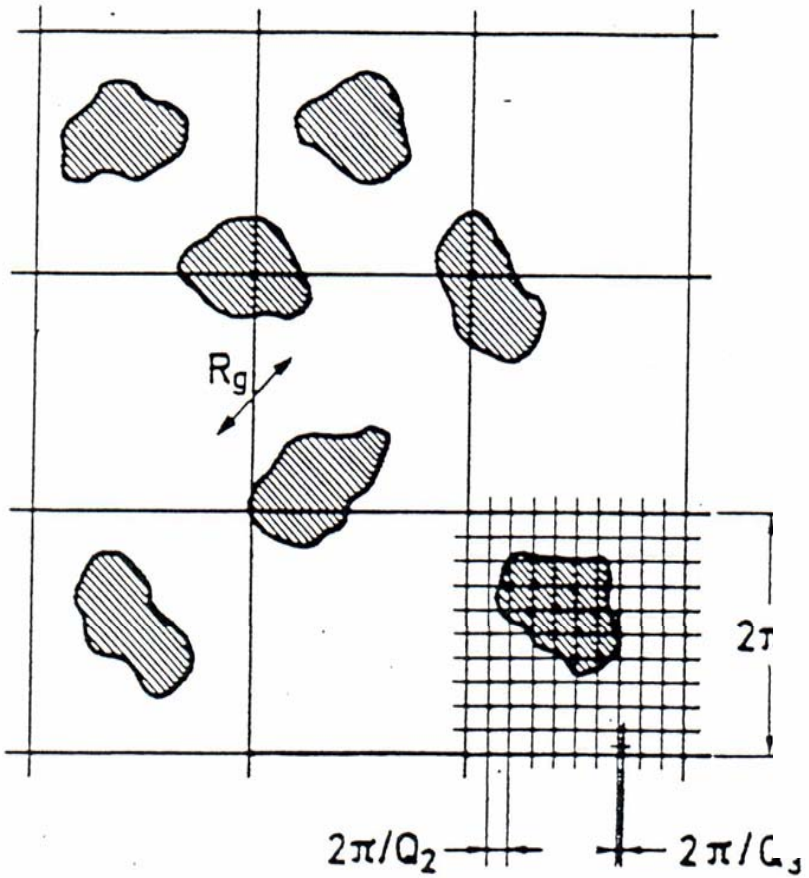

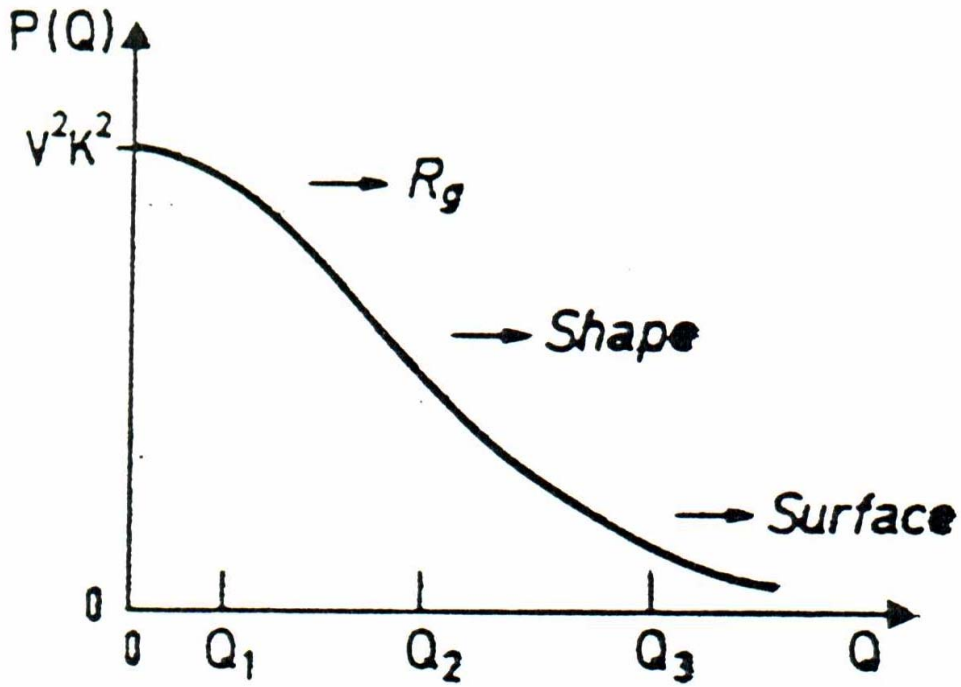

Particles Scattering : Spheres

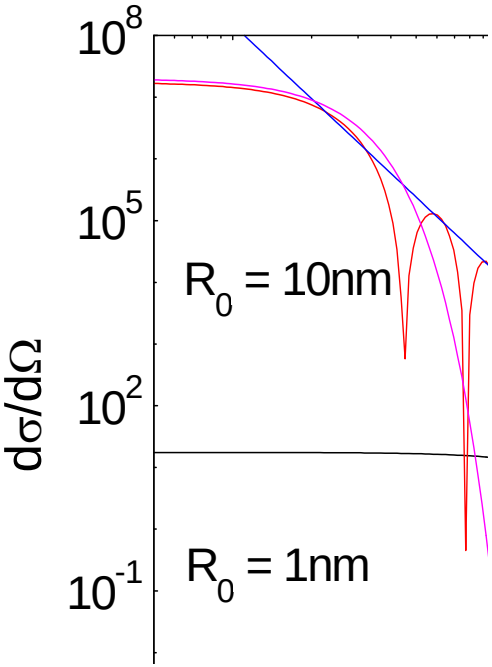

Guinier-approximation:
(for $QR_g < 1.5$)

$$I(Q) = \Delta\eta^2 V_p^2 \exp-(R_g^2 Q^2/3)$$

$$I_0 = \Delta\eta^2 V_p^2$$

$$R_g = (3/5)^{1/2} R_0$$

Porod approximation:
(for $QR_g > 2.5$)

$$I(Q) = 2\pi\Delta\eta^2 S^* Q^{-4} = P\, Q^{-4}$$

$$S = 4\pi R_0^2 \quad , V_p = 4\pi/3 R_0^3$$

Combination

$$R_0^4 = 9\, I_0 / 2\, P$$

$$I(Q) = \Delta\eta^2 V_p^2 [3(\sin(QR)-(QR)\cos(QR))/(QR)^3]^2$$

Form-factors for special shapes

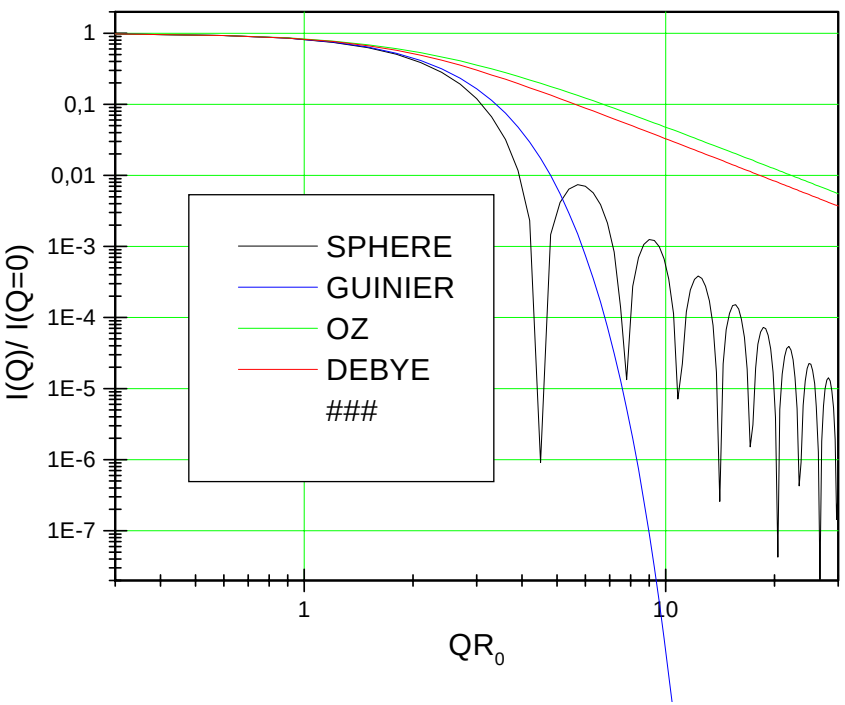

Cylinders of length L and radius Rc

$$F^2(Q) = V^2 \Delta\eta^2 \exp(-Q^2 R_c^2/2) / (QL)$$

Flat particles with area A and thickness T

$$F^2(Q) = AT^4 \Delta\eta^2 \, [\sin(-QT/2) / (-QT/2)]^2 / (QT)^2$$

Random coil (Debye)

$$F^2(Q) = 2 / (QR_g)^4 \, [(QR_g)^2 - 1 + \exp(-Q^2 R_g^2)]$$

Critical fluctuations (Ornstein-Zernicke)

$$F^2(Q) = 1/ [1 + (Q^2 \zeta^2)] \quad \text{with} \quad \zeta^2 = R_g^2 / 3$$

Poly-disperse multi-phase systems

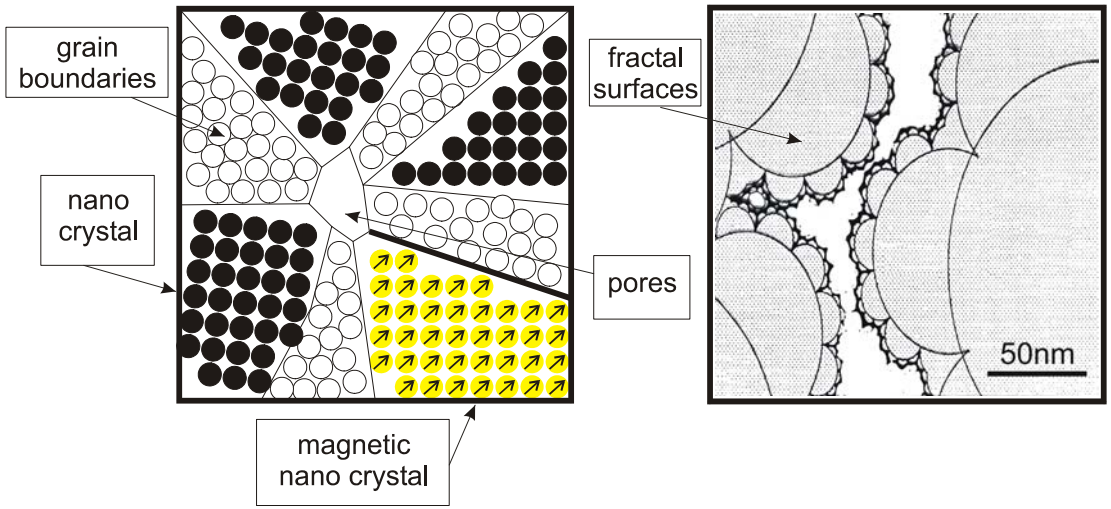

$$I(Q) = \int\int F_i^{\,2}(QR)\; N_i(R)\; S_i(QR)\; dR \otimes Res(Q)$$

Form-factor: $F(QR) = \Delta\eta\; V(R)\; f(QR)$

contrast

volume

shape-factor

size-distribution

structure factor

instrument resolution

Inter-particle correlations

$$I(Q)= \langle |F(Q)|^2 \rangle \{1+ |\langle F(Q)\rangle|^2/\langle |F(Q)|^2\rangle (S(Q)-1)\}$$

monodisperse hard-spheres

$$I(Q)=N V^2 \Delta\rho^2 |F_s(QR)|^2 S(Q)$$

$$S(Q)=1-8\phi F_s(Qd)$$

Volume fraction

$$\phi = 4 / 3 \pi R^3 / d^3$$

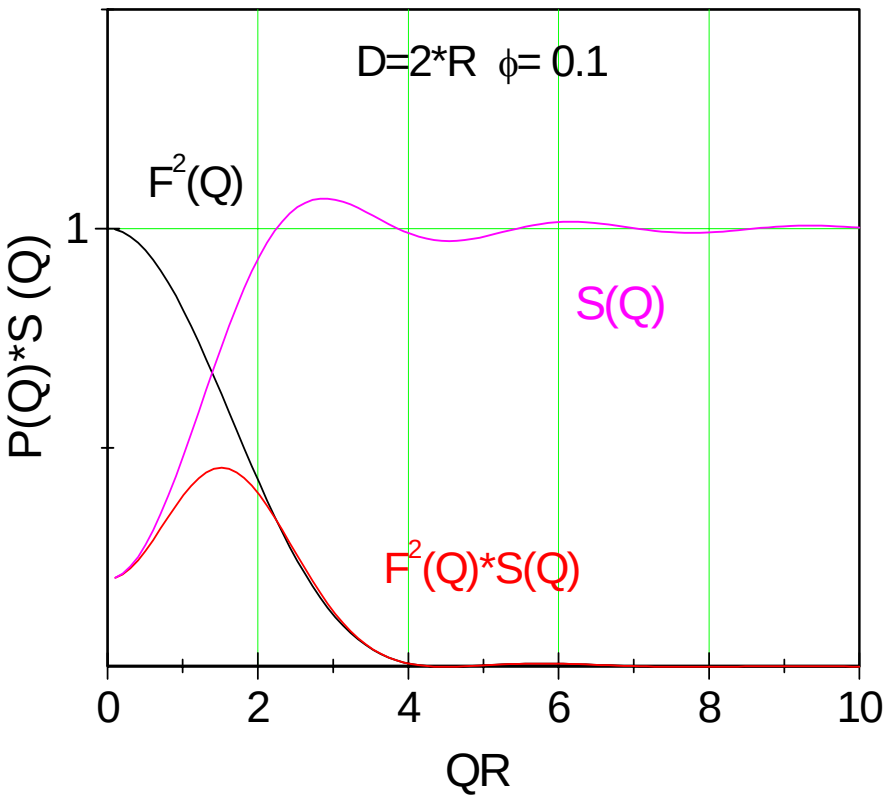

Structure factor S(Q)

$$S(Q) = 1 + N_p \int [g(r) - 1] \exp(iQr)\, dr$$

Pair correlation function g(r) :

$$g(r) = 1 + (1/2\pi^2 N_p) \int [S(Q)-1] \sin(QR)/QR\, Q^2 dQ$$

S(Q) = 1	**ideal gas**
S(Q) < 1	**repulsive potential:**
	Excluded volume, electrostatic repulsion
S(Q) > 1	**attractive interaction**

In practice

$$\boxed{S(Q, \alpha) = I(Q,\alpha)_{\text{measured}} / I(Q,\alpha)_{\text{non-interacting}}}$$

for diluted samples

Magnetic scattering

Magnetic amplitude

$$p=(\gamma e^2/2mc^2)\ g\ S\ f_m(Q)=0.27\ 10^{-12}\ cm/\mu_B\ |M|\ f_m(Q)$$

Magnetic scattering lengh density

$$\eta_{mag} = 0.27\ 10^{-12}\ cm/\mu_B \sum M^{\perp}_i\, c_i / \Omega_i$$

Magnetic contrast

$$\Delta\eta_{mag} = \eta_{mag}(particle) - \eta_{mag}(matrix)$$

Magnetic contrast variation

Magnetic Scattering from different parts

a) Change of magnitude and /or direction of applied magnetic field

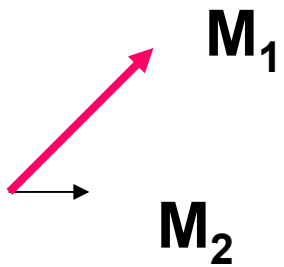

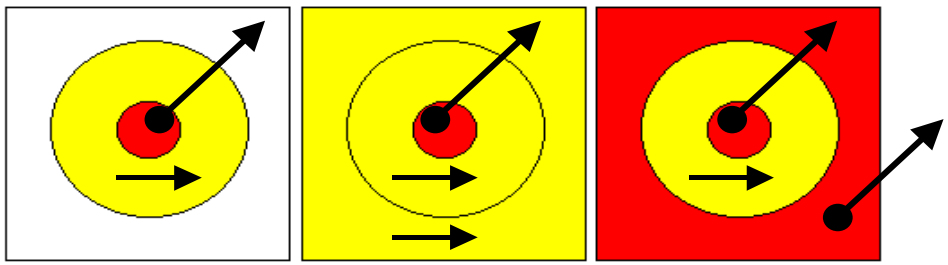

Magnetic contrasts

$\Delta\eta_{core} \propto M_1 - M_{matrix}$	$M_1^{\perp}$	$M_1^{\perp} - M_2^{\perp}$	0
$\Delta\eta_{shell} \propto M_2 - M_{matrix}$	$M_2^{\perp}$	0	$M_1^{\perp} - M_2^{\perp}$
$\Delta\eta_{c\text{-}sh} \propto M_1 - M_2$	$M_1^{\perp} - M_2^{\perp}$	$M_1^{\perp} - M_2^{\perp}$	$M_1^{\perp} - M_2^{\perp}$

Magnetic particle scattering: $M^{\perp}$

$M^{\perp}$: Projection of magnetization onto a plane perpendicular to the scattering vector Q

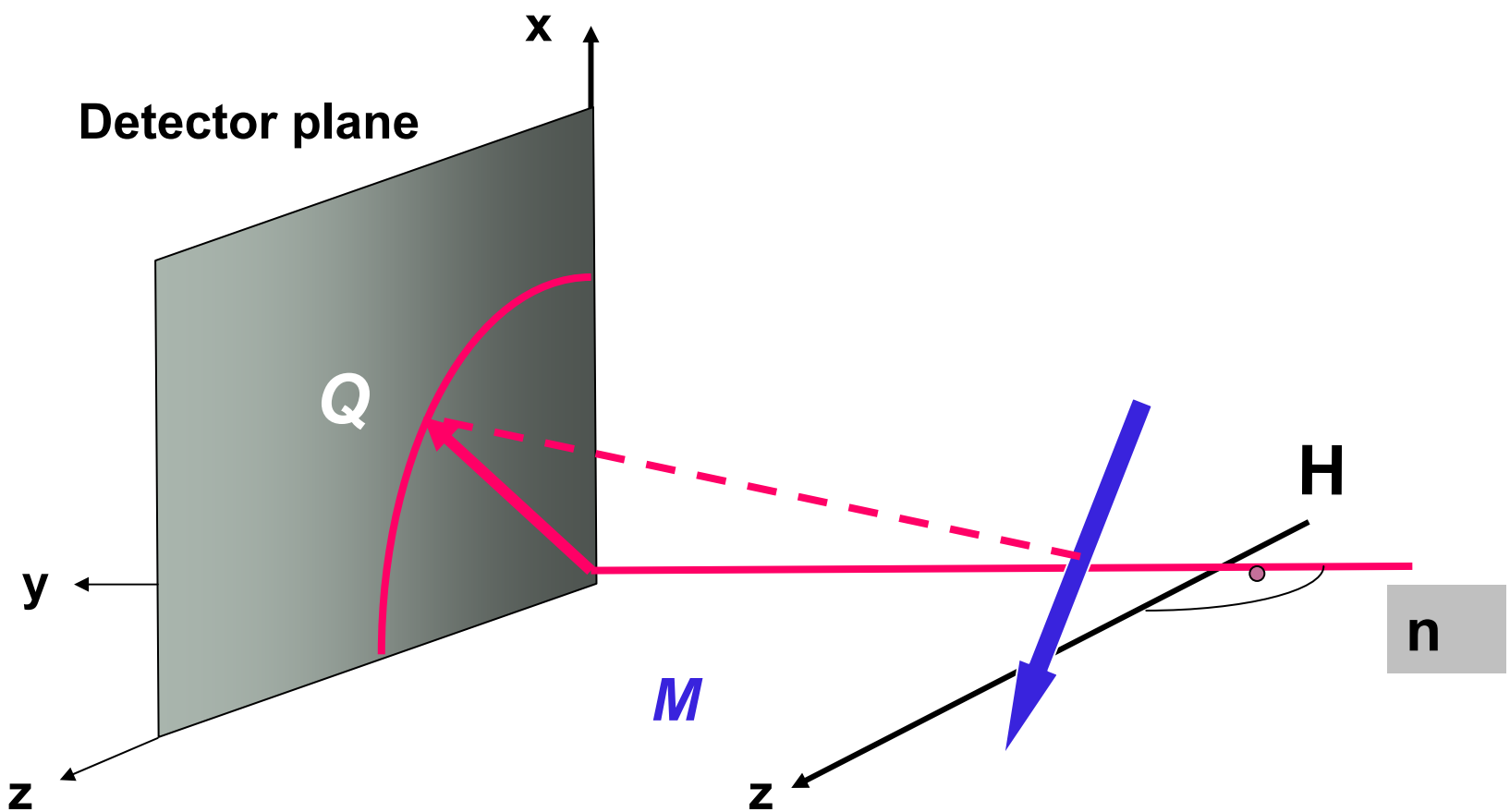

Magnetic particle scattering : $M^{\perp}$

$M^{\perp}$: Projection of magnetization onto a plane perpendicular to the scattering vector Q

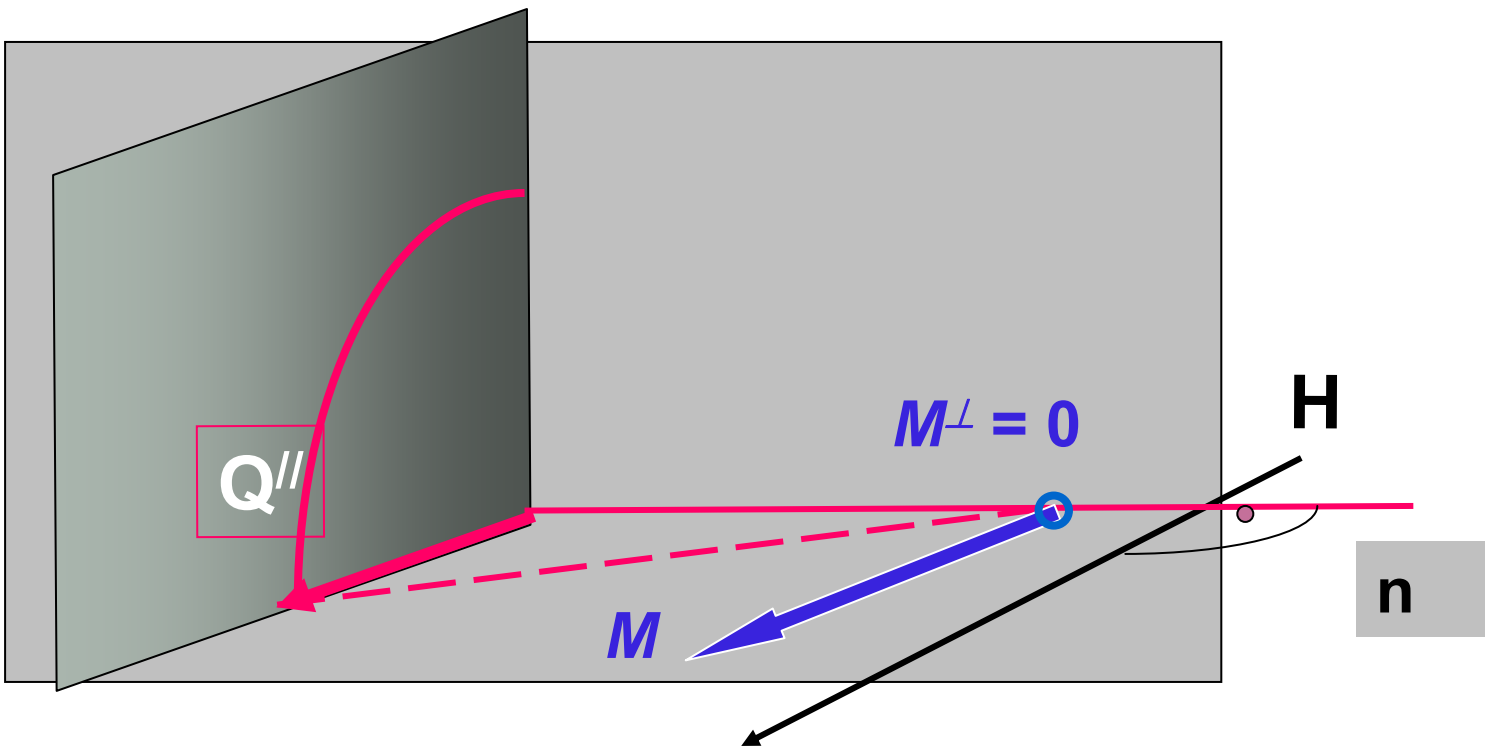

Magnetic particle scattering : $M^{\perp}$

$M^{\perp}$: Projection of magnetization onto a plane perpendicular to the scattering vector Q

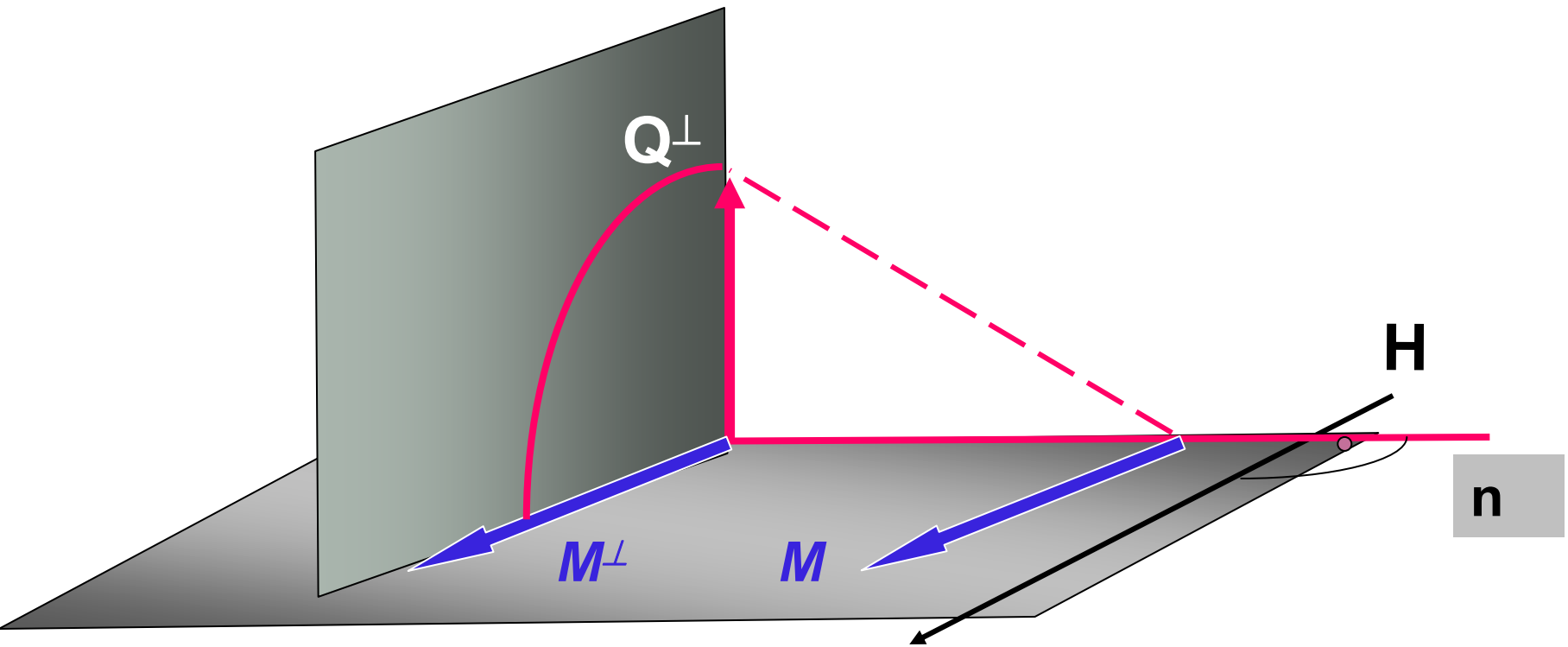

Non polarised neutrons (SANS)

$$I(Q) = A(Q) + B(Q)\sin^2\alpha$$

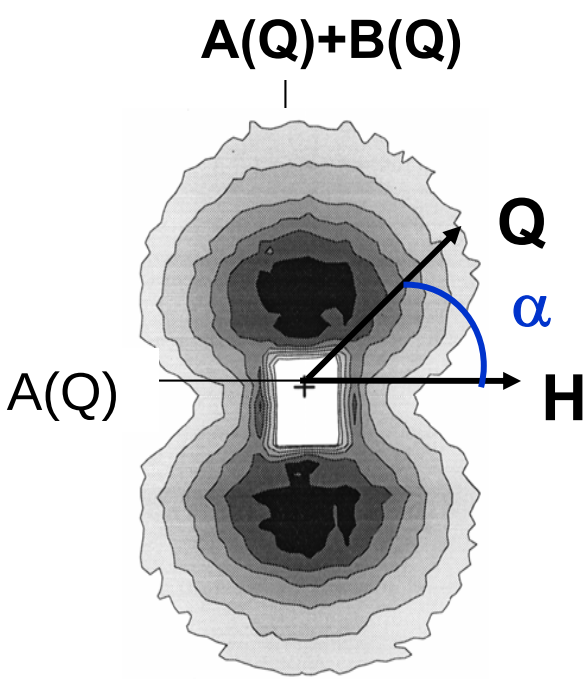

Nuclear scattering

$$A(Q) \propto F^2_N \propto \Delta\eta_{nuc}^2$$

Magnetic scattering

$$B(Q) \propto F^2_M \propto \Delta\eta_{mag}^2$$

$$I(Q) \propto \Delta\eta_{nuc}^2 + \Delta\eta_{mag}^2 \sin^2\alpha$$

Polarised neutrons: Production

Transmission-Polariser

$P = (n^+ - n^-) / (n^+ + n^-)$

Critical angle for total reflection:

$\Theta_{c\,(-)}$ [mrad]= m * 1.73 λ

$\Theta_{c\,(+)}$ [mrad]= 0.7* λ

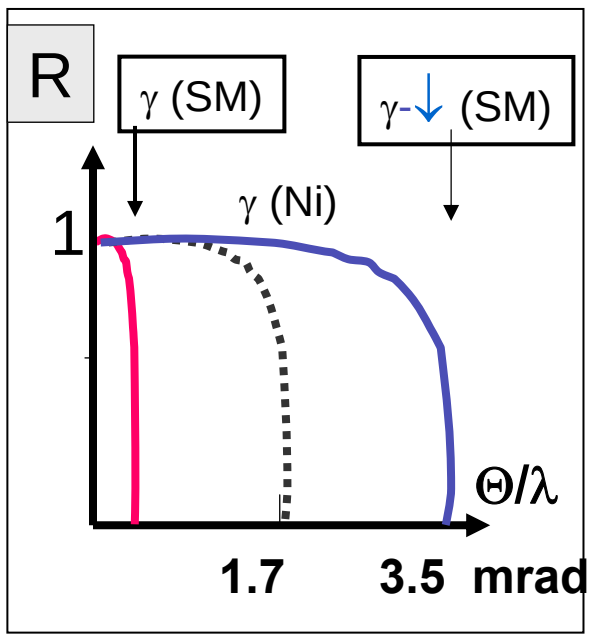

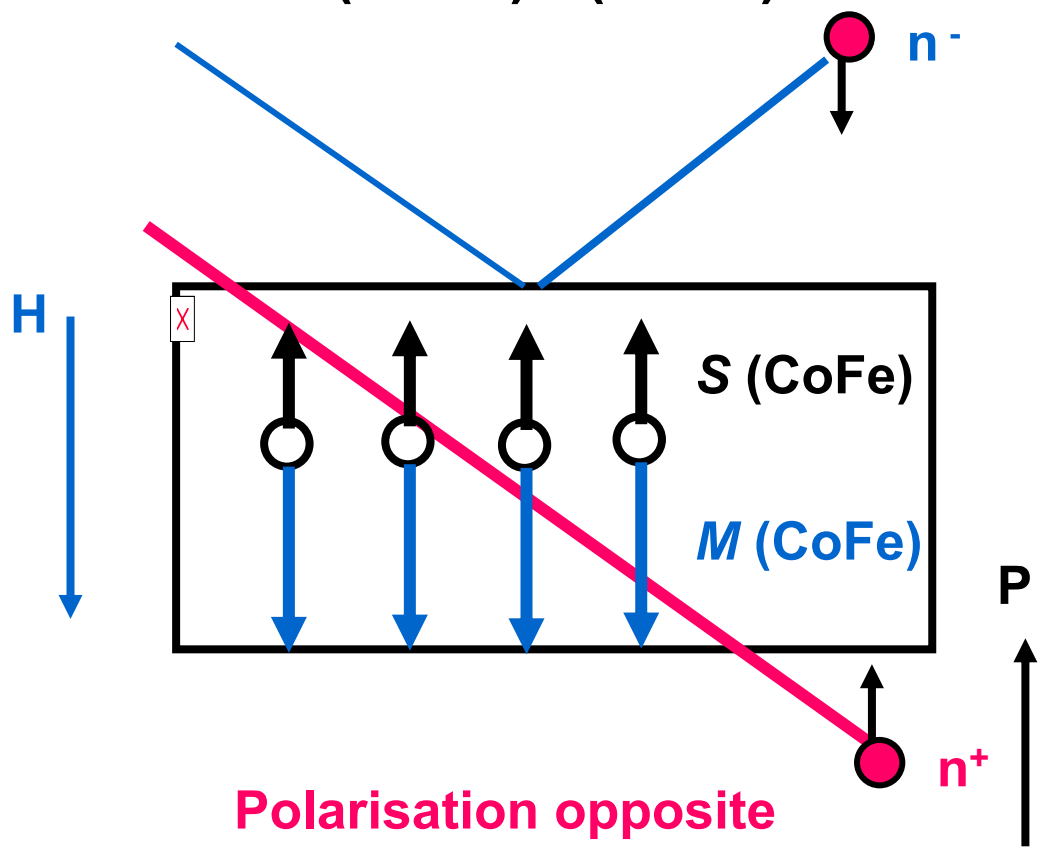

Polarisation opposite to magnetic field

Polarised neutrons

Polarisation

$P = (n^+ - n^-) / (n^+ + n^-)$ $n^{+:}$ Neutron spin opposite to $H//z$

Magnetic amplitude

$$p = (\gamma e^2/2mc^2)\ g\ S\ f_m(Q) = 0.27\ 10^{-12}\ cm/\mu_B\ |M|\ f_m(Q)$$

Atomic scattering amplitudes

$$a^{s,s'} = \langle s' | b_i - p_i\ M_i\perp\ \sigma | s \rangle$$

$M_i\perp$: Component of the magnetic moment perpendicular to Q

σ : neutron-spin operator

Spin-non flip	$a(++) = b - p\ M\perp^z$	$a(--) = b + p\ M\perp^z$
Spin-flip	$a(+-) = -p(M\perp^x + i\ M\perp^y)$	$a(-+) = -p(M\perp^x - i\ M\perp^y)$

SANS with polarised neutrons

Amplitudes

Spin-non flip $a(++) = \Delta\eta_N - p\Delta M\perp^z$ $\quad a(--) = \Delta\eta_N + p\Delta M\perp^z$

Spin-flip $a(+-) = -p(\Delta M\perp^x + i\,\Delta M\perp^y)$ $\quad a(-+) = -p(\Delta M\perp^x - i\,\Delta M\perp^y)$

Form-factors

$p = 0.27\ 10^{-12}\ \mathrm{cm}/\mu_B\,|\,\Delta M\,|\,f_m(Q)$, $F_N = \Delta\eta_N V_p f(Q)$, $F_M = p\,V_p f(Q)$

$F(++) = F_N - F_M\,\Delta M\perp^z$ $\quad F(--) = F_N + F_M\,\Delta M\perp^z$

$F(+-) = -F_M\,(\Delta M\perp^x + i\,\Delta M\perp^y)$ $\quad F(-+) = -F_M\,(\Delta M\perp^x - i\,\Delta M\perp^y)$

SANS with polarised neutrons

Amplitudes

Spin-non flip $a(++) = \Delta\eta_N - p\Delta M\perp^z$ $\quad a(--) = \Delta\eta_N + p\Delta M\perp^z$

Spin-flip $a(+-) = -p(\Delta M\perp^x + i\,\Delta M\perp^y)$ $\quad a(-+) = -p(\Delta M\perp^x - i\,\Delta M\perp^y)$

Form-factors

$p = 0.27\ 10^{-12}\ cm/\mu_B\,|\,\Delta M\,|\,f_m(Q)$, $F_N = \Delta\eta_N V_p f(Q)$, $F_M = p\,V_p f(Q)$

$F(++) = F_N - F_M\,\Delta M\perp^z$ $\quad F(--) = F_N + F_M\,\Delta M\perp^z$

$F(+-) = -F_M\,(\Delta M\perp^x + i\,\Delta M\perp^y)$ $\quad F(-+) = -F_M\,(\Delta M\perp^x - i\,\Delta M\perp^y)$

Intensities (for $M\perp^y=0$)

$I{++}(Q) = \langle |F{++}|^2 \rangle$ $\quad I{--}(Q) = \langle |F{--}|^2 \rangle$

$I{+-}(Q) = \langle |F{+-}|^2 \rangle$ $\quad I{-+}(Q) = \langle |F{-+}|^2 \rangle$

SANS with polarised neutrons

$M^{\perp}$: Projection of magnetization onto a plane perpendicular to the scattering vector Q

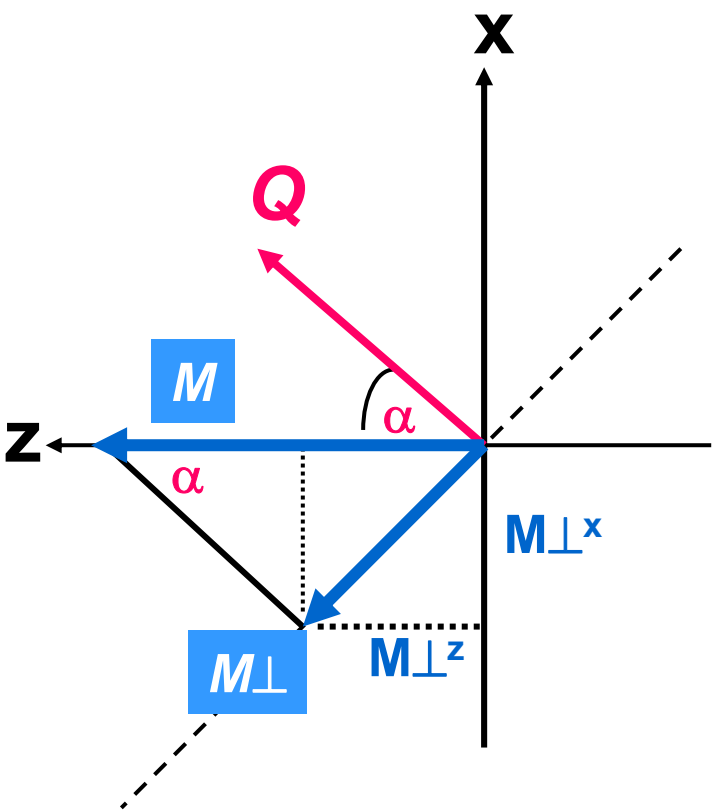

$$P \,//\, M \,//\, H \,//\, z$$

$$|M\perp| = |M| \sin\alpha$$

$$M\perp^{z} = |M\perp| \cos(90°-\alpha) = |M\perp| \sin(\alpha) = |M| \sin^2\alpha$$

$$M\perp^{x} = |M\perp| \sin(90°-\alpha) \quad |M| \sin\alpha \cos\alpha$$

$$M\perp^{y} = 0$$

POLARIS: SANS with analysis of polarisation

Spin non-flip scattering (for $M_{\perp}^{y}=0$)

$$I^{++}(Q) = (F_N - F_M \sin^2\alpha)^2$$

$$I^{--}(Q) = (F_N + F_M \sin^2\alpha)^2$$

Spin -flip scattering (for $M_{\perp}^{y}=0$)

$$I^{+-}(Q) = (F_M \sin\alpha \cos\alpha)^2$$

$$I^{-+}(Q) = (F_M \sin\alpha \cos\alpha)^2$$

SANSPOL and SANS

Without polarisation analysis of scattered neutrons

$$I^{+}(Q) = \langle |F^{++}|^2 \rangle + \langle |F^{+-}|^2 \rangle = F_N^2 + \{F_M^2 - 2F_N F_M\} \sin^2\alpha$$

$$I^{-}(Q) = \langle |F^{--}|^2 \rangle + \langle |F^{-+}|^2 \rangle = F_N^2 + \{F_M^2 + 2F_N F_M\} \sin^2\alpha$$

Anisotropic scattering profile

$$I^{\pm}(Q) = A(Q) + B^{\pm}(Q) \sin^2\alpha$$

Magnetic-nuclear cross term

$$I^{-}(Q) - I^{+}(Q) = 4 F_N F_M \sin^2\alpha$$

Sum signal ≡ I (non-polarised SANS)

$$(I^{+} + I^{-}) / 2 = F_N^2 + F_M^2 \sin^2\alpha$$

Nuclear scattering contrast

Scattering length density η

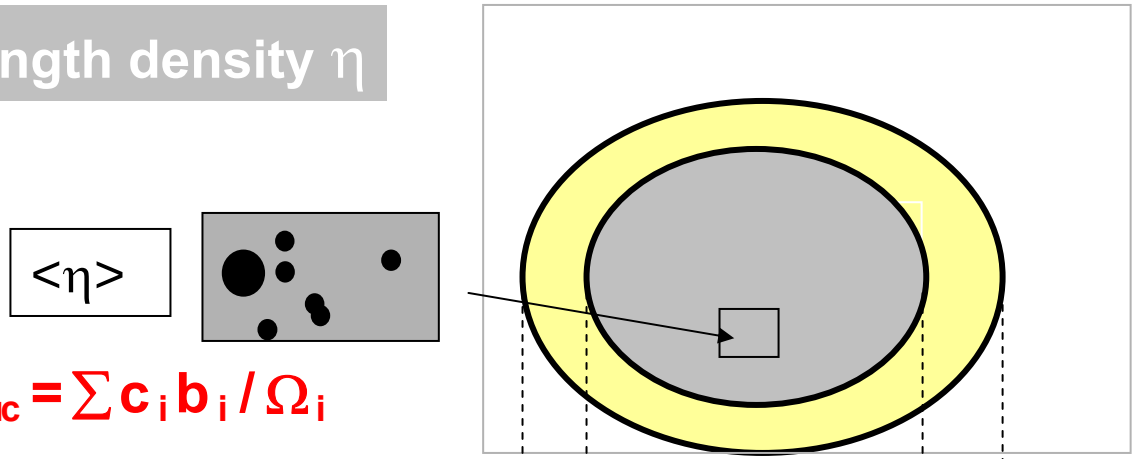

Nuclear $\eta(r)_{nuc} = \sum c_i b_i / \Omega_i$

contrast $\Delta\eta$

$\Delta\eta(r)_{nuc} = \eta_{nuc\,(particle)} - \eta_{nuc\,(matrix)}$

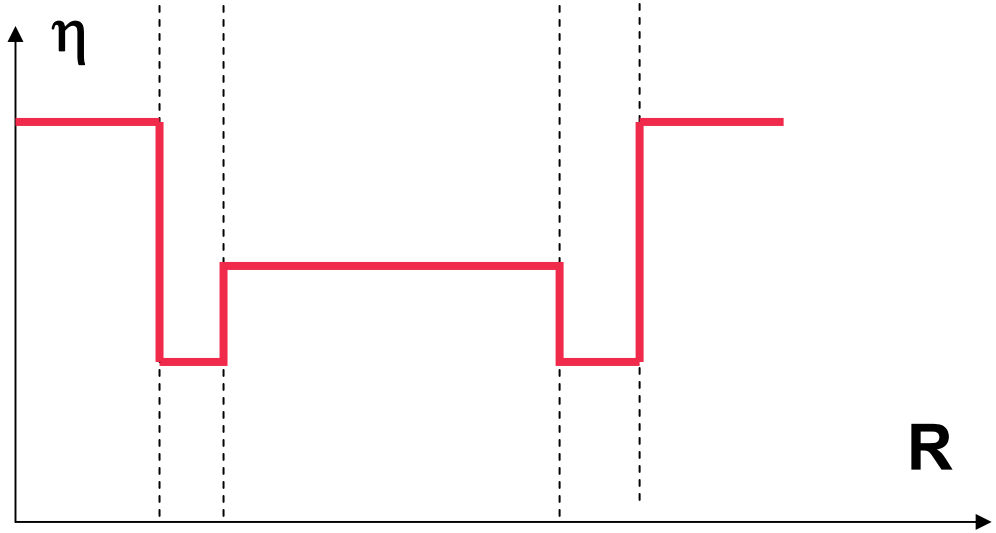

Nuclear and magnetic scattering contrast

Scattering length density η

$\langle\eta\rangle$

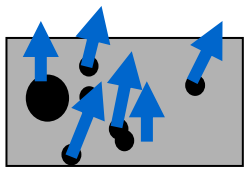

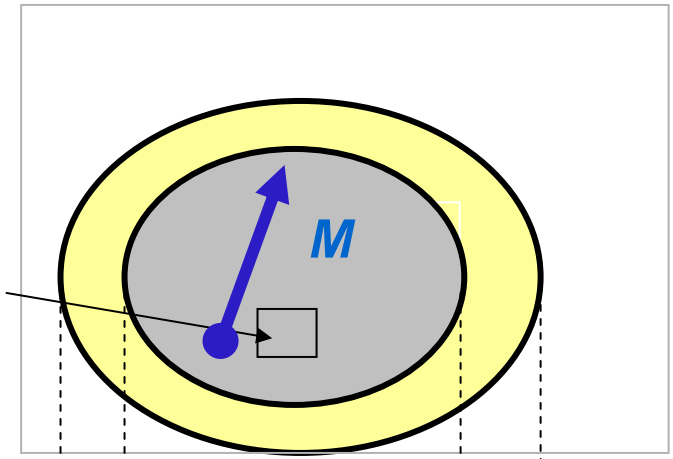

Nuclear

$$\eta(r)_{nuc} = \sum c_i b_i / \Omega_i$$

Magnetic

$$\eta(r)_{mag} = 0.27\ 10^{12} \sum c_i M^{\perp}_i / \Omega_i$$

contrast $\Delta\eta$

$$\Delta\eta(r)_{nuc} = \eta_{nuc\,(particle)} - \eta_{nuc\,(matrix)}$$

$$\Delta\eta(r)_{mag} = \eta_{mag\,(particle)} - \eta_{mag\,(matrix)}$$

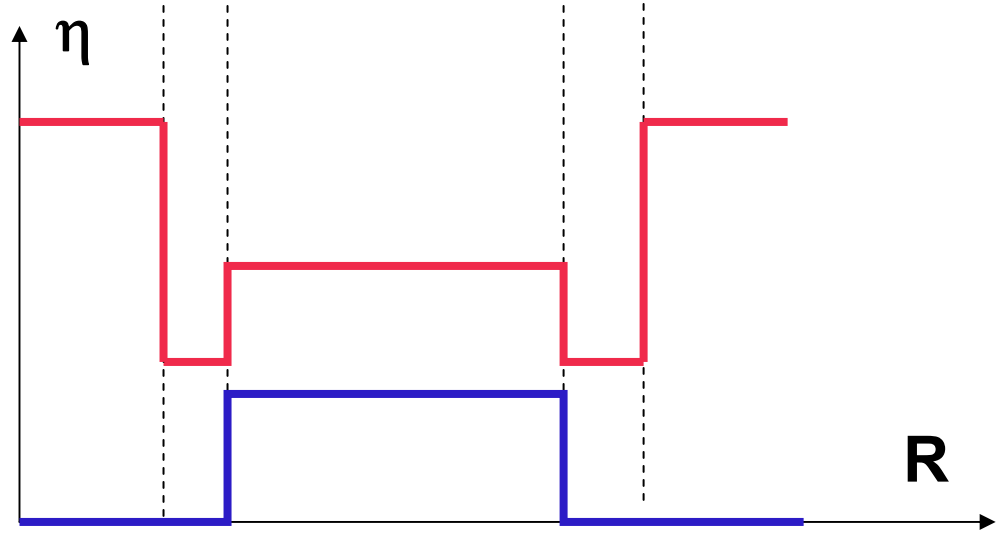

Polarised neutrons: SANSPOL

Scattering length density η

<η>

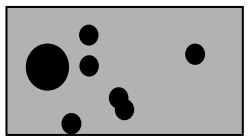

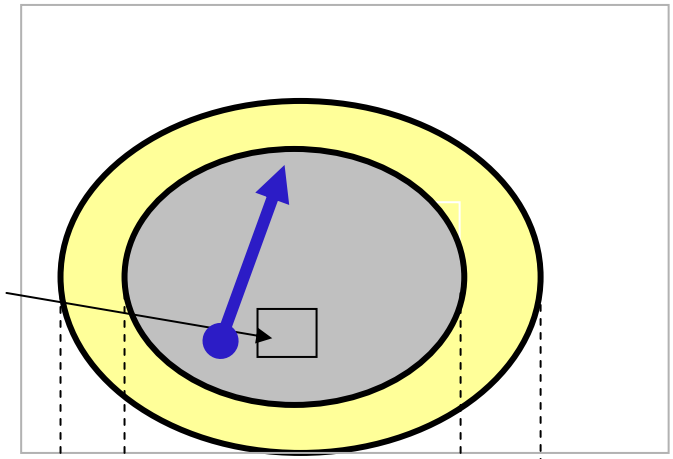

Nuclear $\eta(r)_{nuc} = \sum c_i b_i / \Omega_i$

Magnetic $\eta(r)_{mag} = \sum c_i M^{\perp}_i / \Omega_i$

contrast Δ η

$\Delta\eta(r) = \eta_{(particle)} - \eta_{(matrix)}$

$\eta_{(particle)}(-) = \eta_{nuc} + \eta_{mag}$

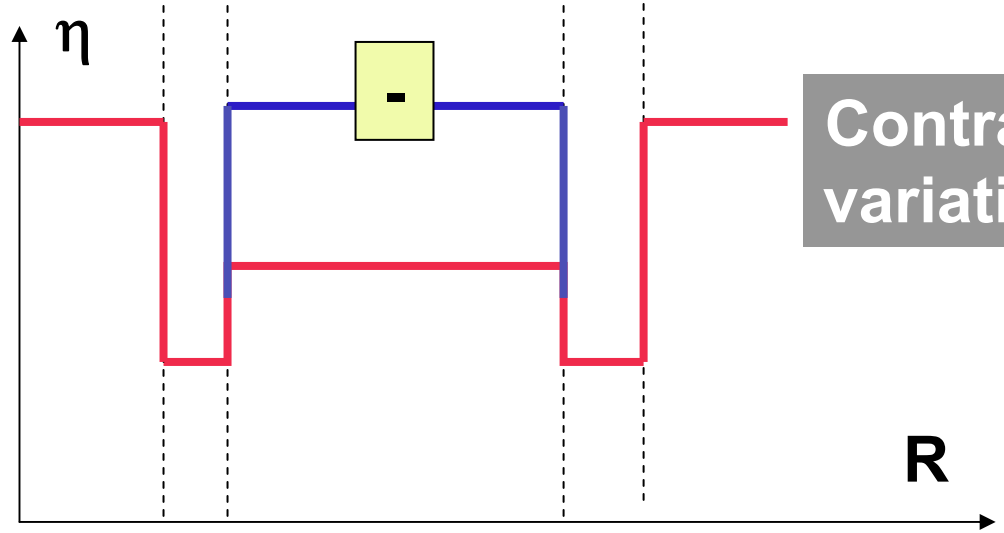

Contrast variation

Polarised neutrons: SANSPOL

Scattering length density η

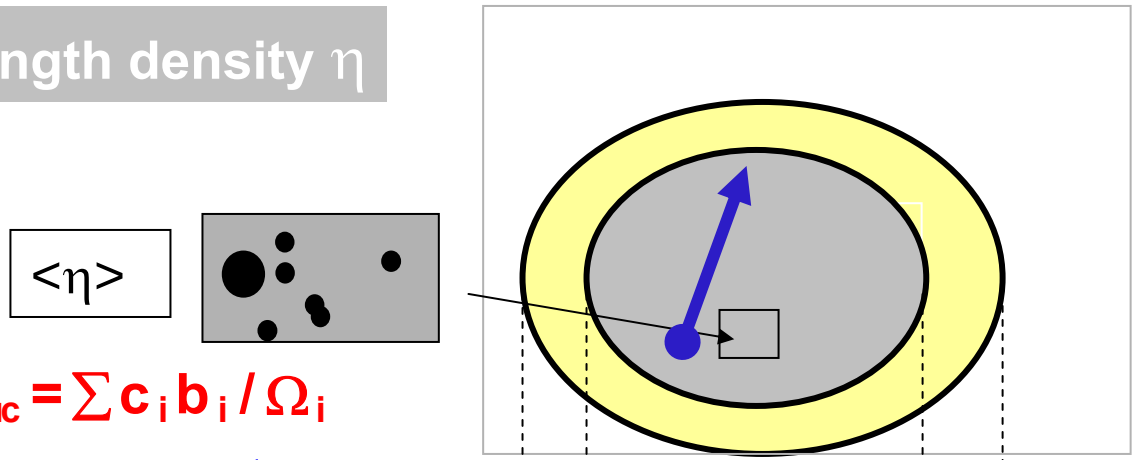

Nuclear $\eta(r)_{nuc} = \sum c_i b_i / \Omega_i$

Magnetic $\eta(r)_{mag} = \sum c_i M^{\perp}_i / \Omega_i$

contrast $\Delta\eta$

$\Delta\eta(r) = \eta_{(particle)} - \eta_{(matrix)}$

$\eta_{(particle)}(+) = \eta_{nuc} - \eta_{mag}$

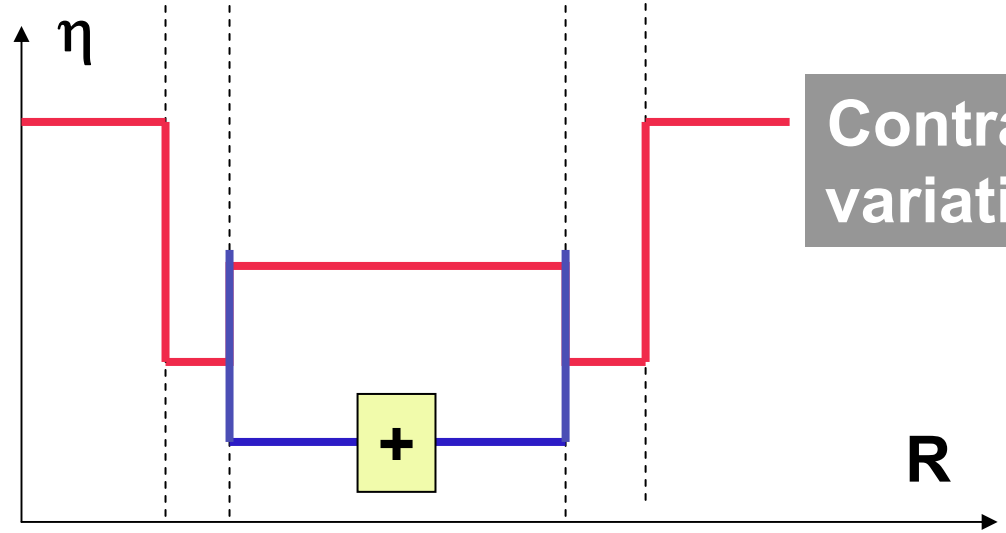

Contrast variation

Polarised neutrons (SANSPOL)

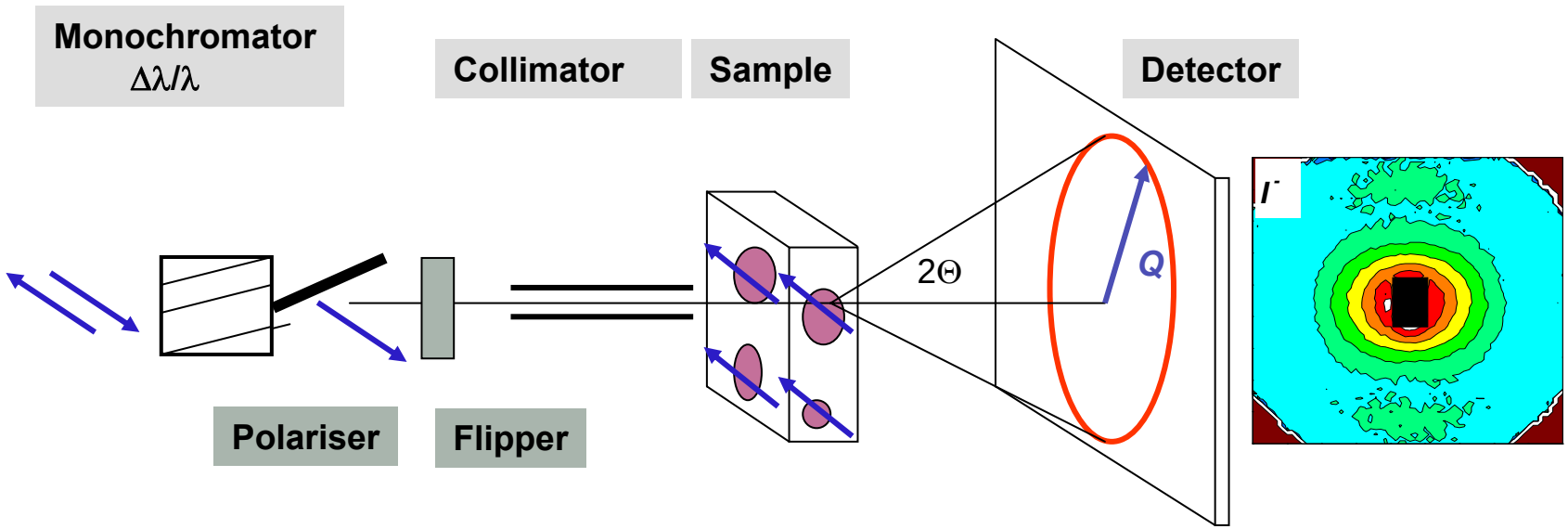

$$I(Q)\ (-) \propto \Delta\eta_N^2 + \{\Delta\eta_M^2 + 2\Delta\eta_M\Delta\eta_N\}\sin^2\alpha$$

Polarised neutrons (SANSPOL)

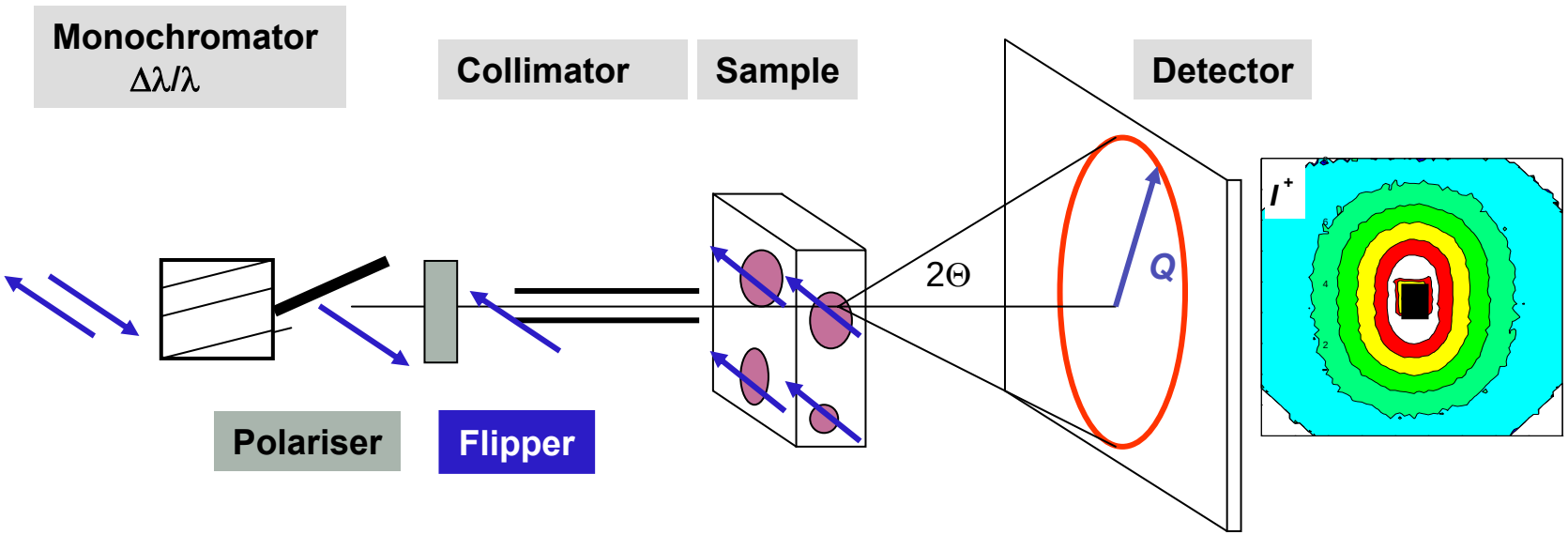

$$I(Q)\ (+) \propto \Delta\eta_N^2 + \{\Delta\eta_M^2 \ - \ 2\Delta\eta_M\Delta\eta_N\}\ \sin^2\alpha$$

SANSPOL Instrument V4

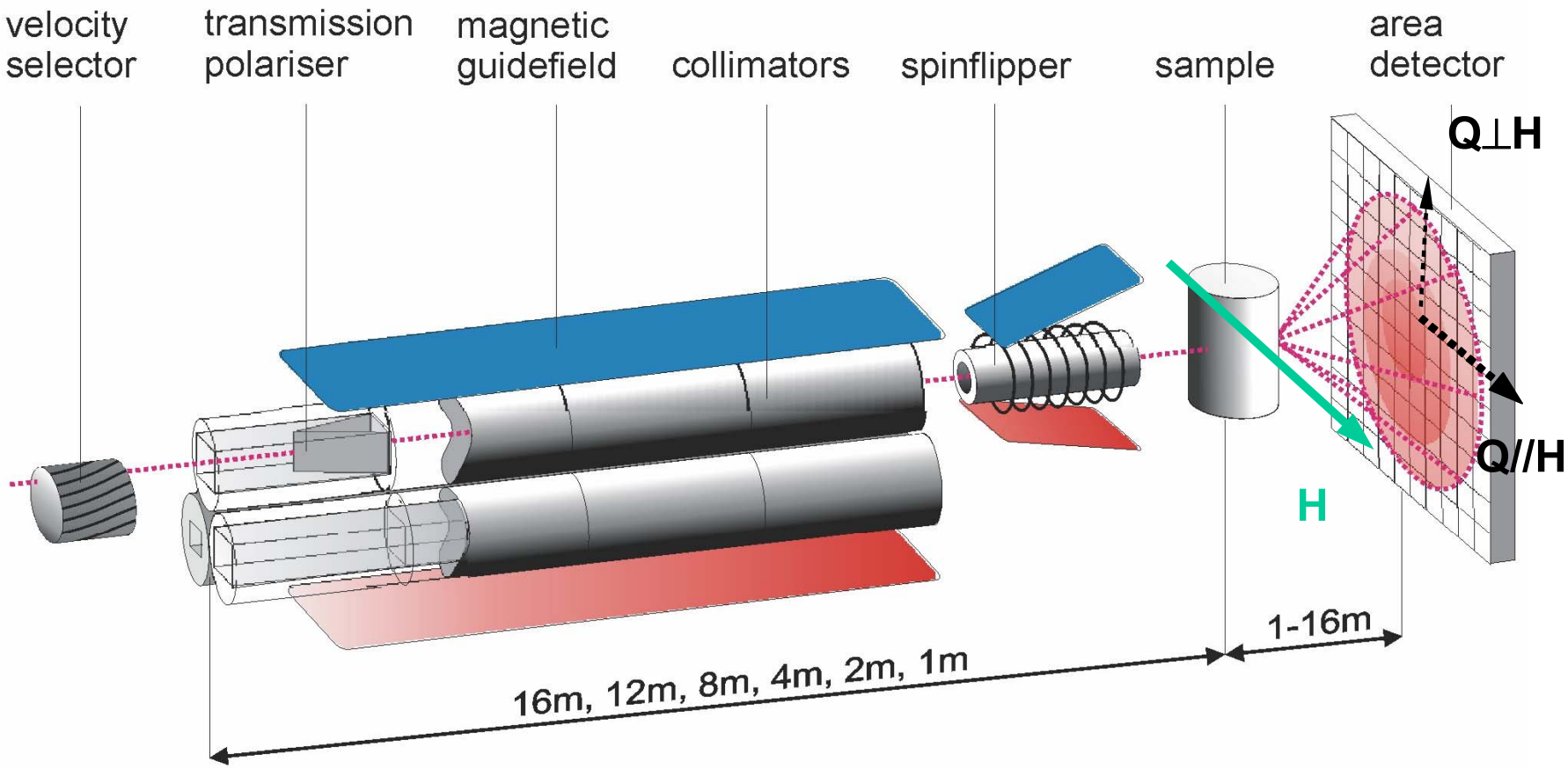

Th. Keller et al (2000) Nucl. Instr.

II. Applications

1. **Magnetic colloids: "Ferrofluids"**

2. **Amorphous magnetic alloys: Soft magnetic materials Bulk Amorphous Hardmagnets**

Magnetic Liquids

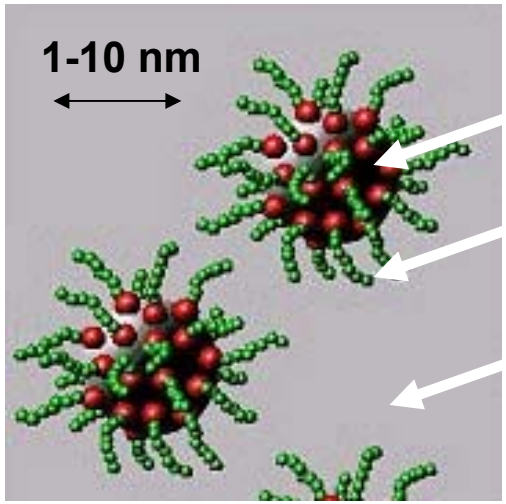

Magnetic core

Nonmagnetic shell of surfactant

Carrier liquid

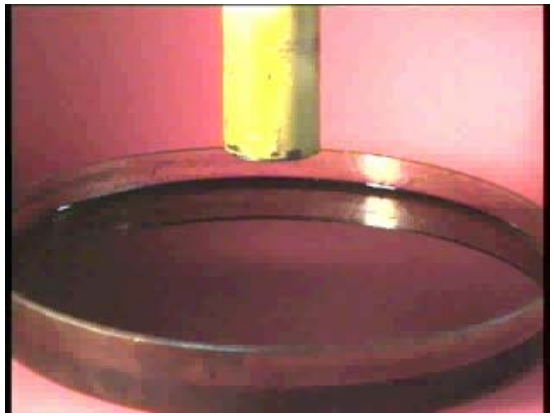

Applications

Magnetic „drug-targeting“

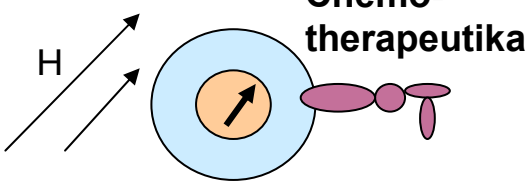

Transport in strong H- field-gradient

Diagnostic

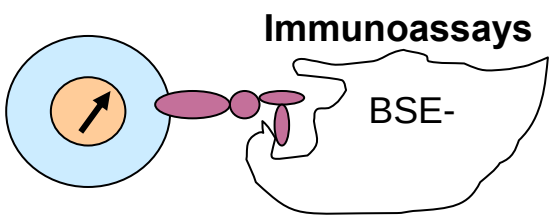

Change of relaxation time (SQUID)

Therapy: Hyperthermie

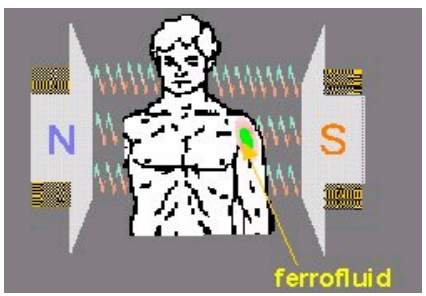

Reverse of magnetisation in ac field:(400kHz):local increase of temperature to 50-55°C

Questions

Core:
Size, Density,
Shape, Distribution?

Shell:
Composition,
Density, Thickness,
Shielding,?

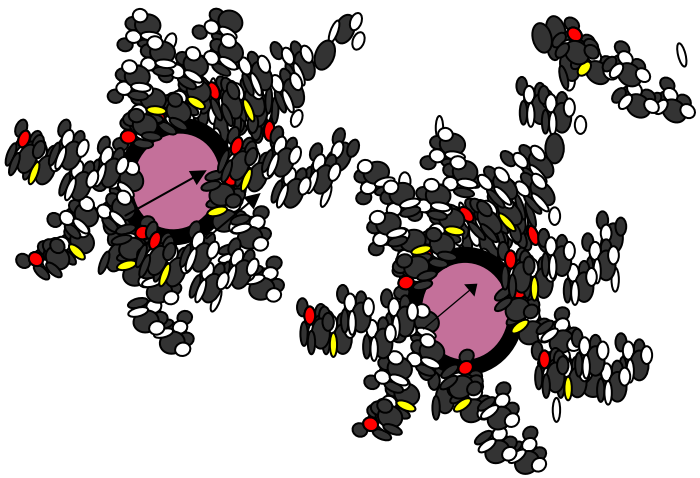

Magnetic Nanostructure:
Moment-value , orientation,
single-domain, interfaces?

Solvent
Penetration?

Aggregation:
formation of chains,
influence of magnetic field?

Materials

Core	Co	Fe_3C	Fe_3O_4	Ba-Ferrite
Shell	$C_{21}H_{39}NO_3$ +surfact.	$C_{21}H_{39}NO_3$ +surfact.	Charge Dextrane L-M	$C_{21}H_{39}NO_3$
Magnet. Moment	1.7 μ_B / at	1.6 μ_B / at	1.24 μ_B / at	0.9 μ_B / at
Carrier liquid	C_7H_8	$C_{10}H_{22}$	H_2O	$C_{12}H_{26}$
Concentration	0.5- 5 vol.%	0.5- 5 vol.%	1- 6 vol. %	2.5 -4 vol.%

2D-SANSPOL scattering patterns

e.g. Co-Ferrofluid

$I(Q) = A(Q)+B^{\pm}(Q)\sin^2\alpha$

$A(Q) = F_N^2$

$B^+(Q) = F_M^2 - F_N F_M$

$B^-(Q) = F_M^2 + F_N F_M$

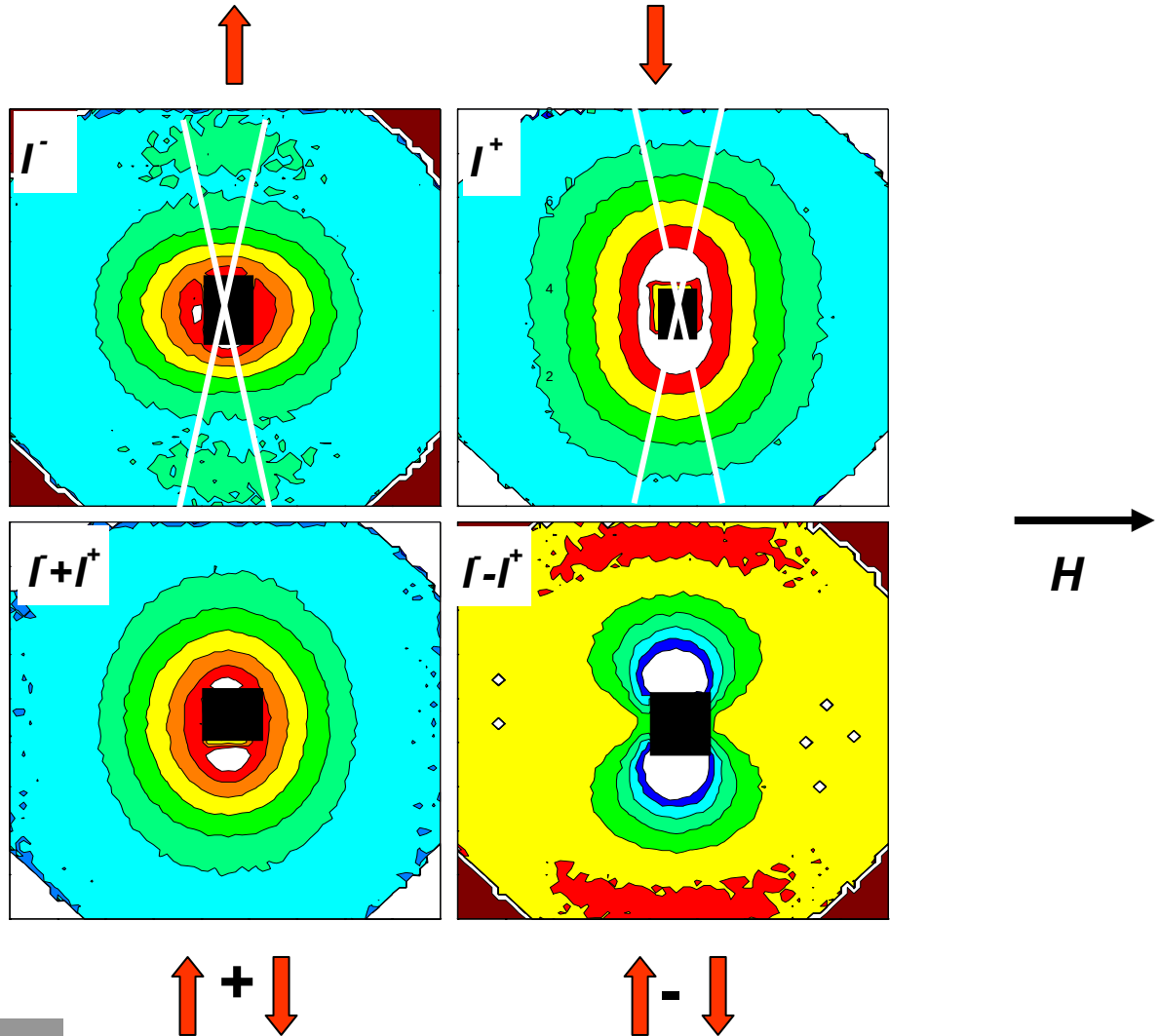

A.W. Physica B 297 (2001) 226 - 233

SANSPOL sector perpendicular to H

Co-FF in C_7D_8

$I(\perp)=A(Q)+B^{\pm}(Q)$

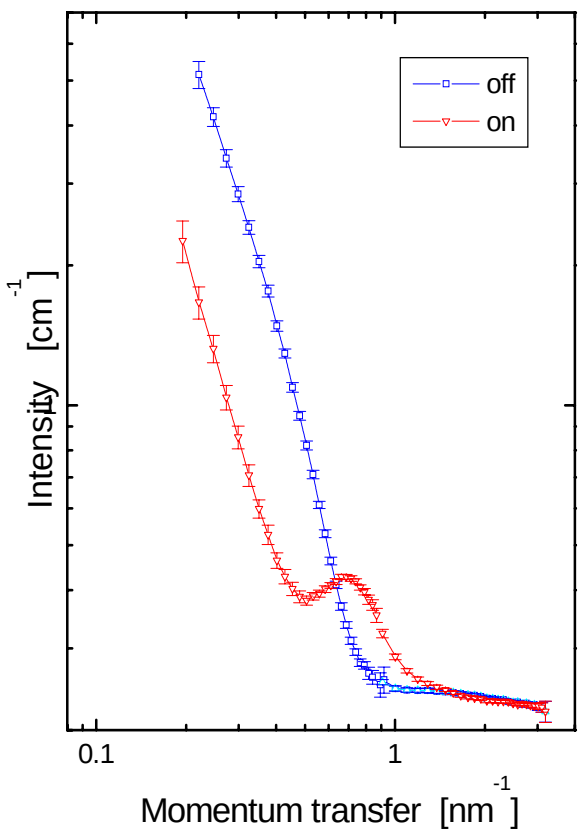

Flipping ratio I(-) / I(+)

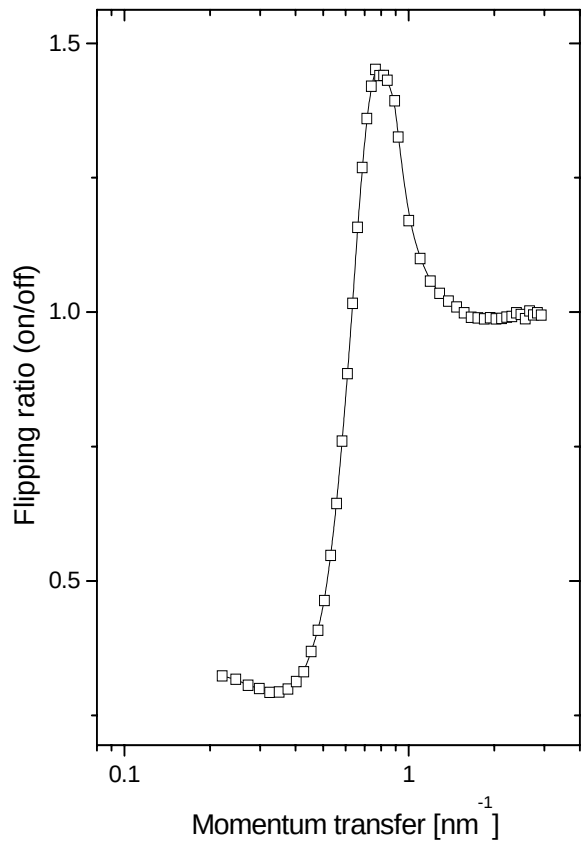

Combined contrast variation

H/D mixtures and SANSPOL

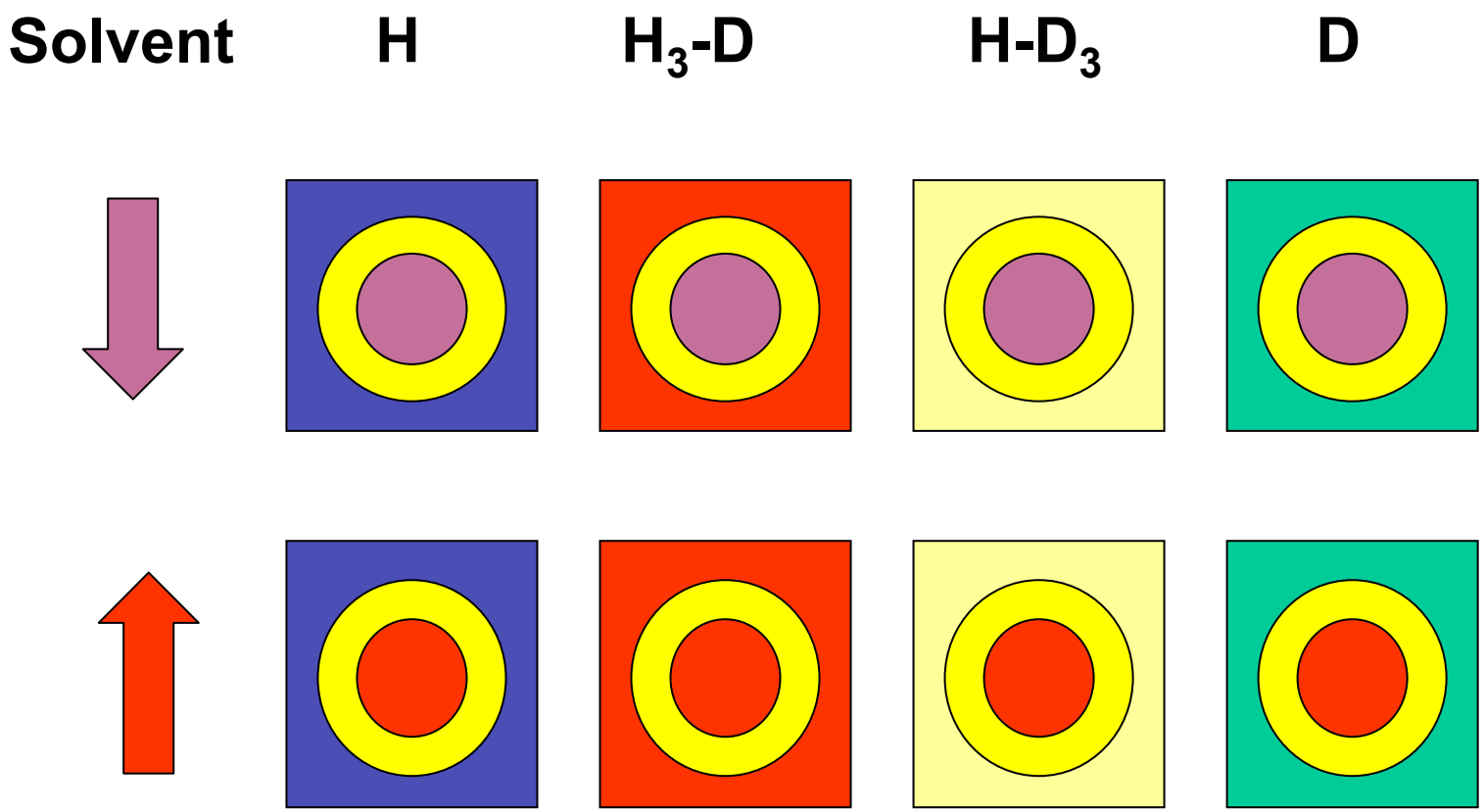

AW,1999,00,01

$$\Delta\eta^{(\pm)} = \eta^{nuc} \pm \eta^{mag} - \eta_{solvent}$$

Contrast variation in Co-Ferrofluids

$C_{21}H_{39}NO_3$
surfactant

Solvent
C_7H_8- C_7D_8

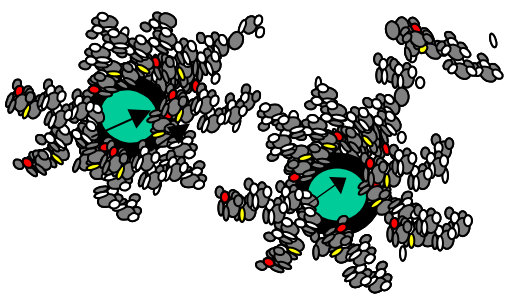

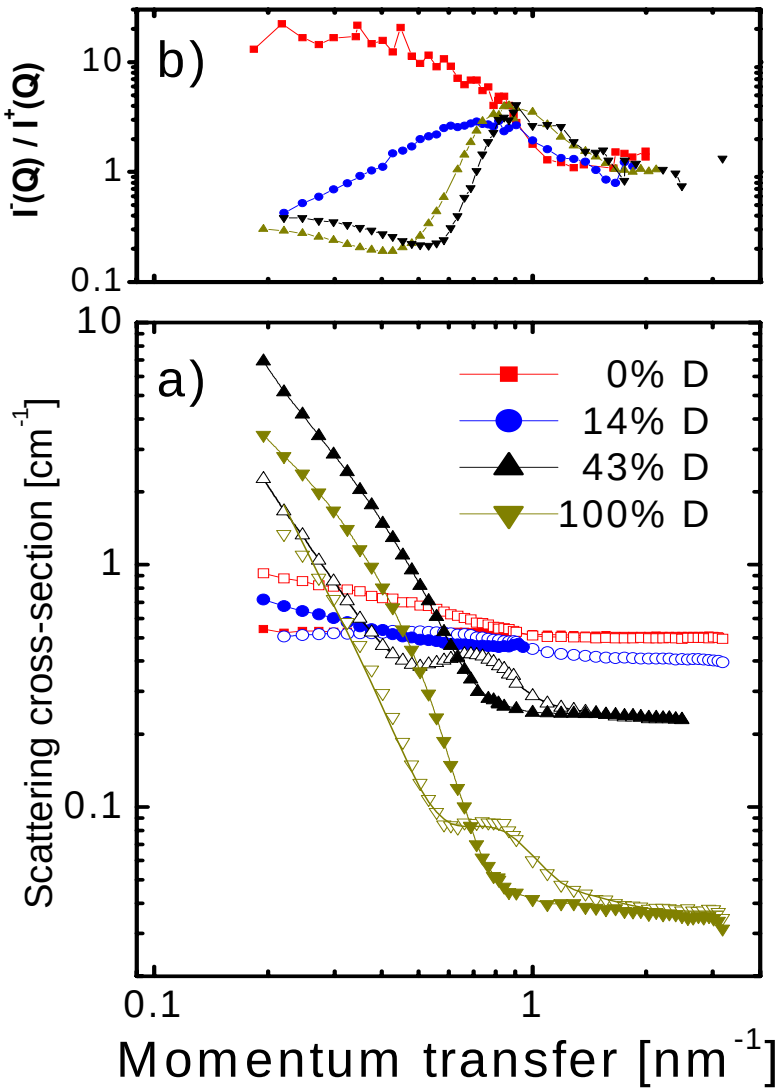

AW, Physica B(2001)226-233

Density profile in Co-Ferrofluid

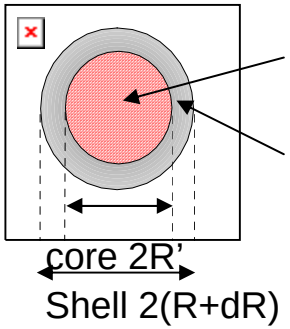

$$\Delta\eta_1^{(\pm)} = \eta_1^{nuc} \pm \eta_1^{mag} - \eta_{matrix}$$

$$\Delta\eta_2 = \eta_2^{nuc} - \eta_{matrix}$$

Volume distribution

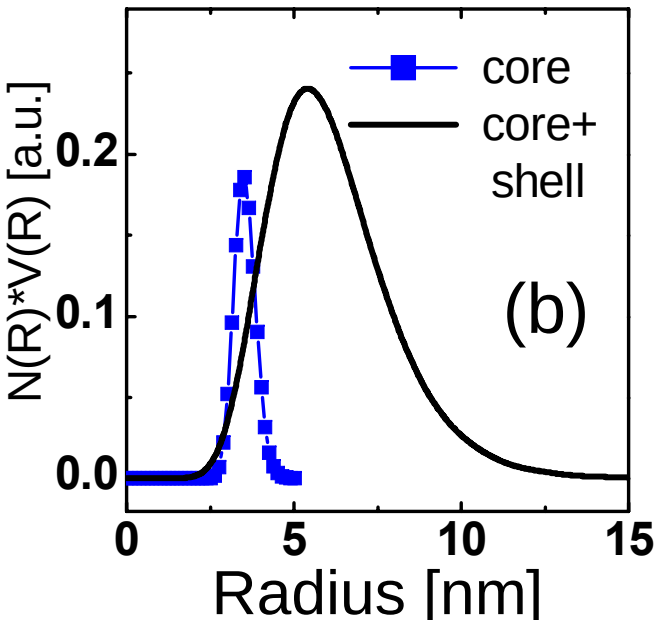

Density profile

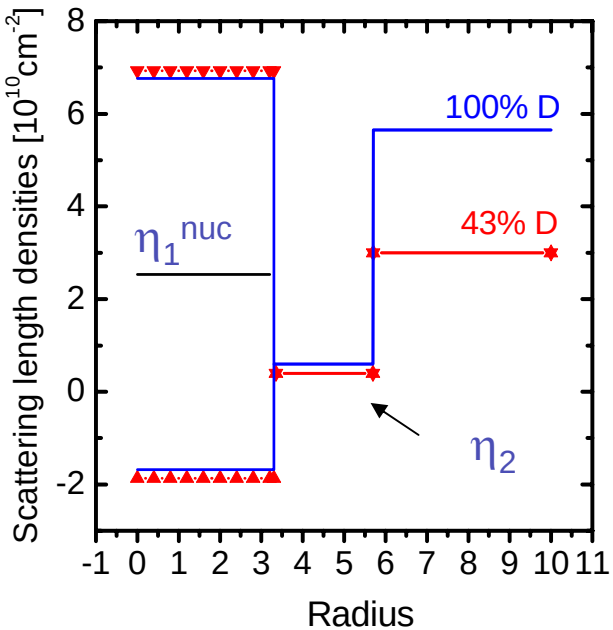

η_2^{nuc} **independent of solvent:**

⇩

Shell is impenetrable for solvent

AW, J. Appl.Cryst. 33 (2000) 428-435

Optimization by simultaneous fits

SANSPOL intensities

$I(on) = F_N^2 + \{F_M^2 + 2F_N F_M\}$

$I(off) = F_N^2 + \{F_M^2 - 2F_N F_M\}$

$I(on)-I(off) = 4F_N F_M$

SANS intensities

$I(nuc) = F_N^2$

$I(mag) = F_M^2$

using contraints on parameters e.g.:

$\Delta\eta_1 (on) = \Delta\eta_1 (nuc) + \eta_1(mag)$

$\Delta\eta_1 (off) = \Delta\eta_1 (nuc) - \eta_1(mag)$

Software

SASFIT	(J. Kohlbrecher)
MATHEmatica	(A. Heinemann)
FISH	(R. Heenan)

Field variation of magnetization in superparamagnetic particles

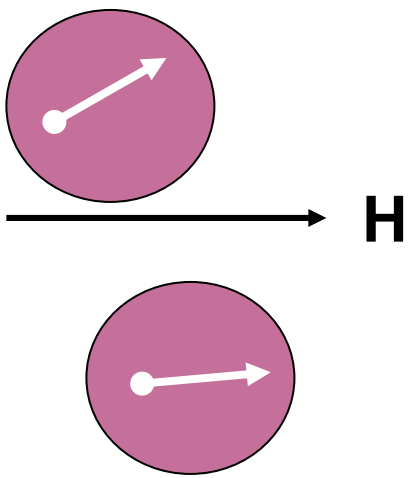

$$\sigma/\sigma_\infty = L(M_{cr}V_p\mu_0H_{eff} / kT)$$

Langevin function:

$$L(x)=\coth(x)-1/x$$

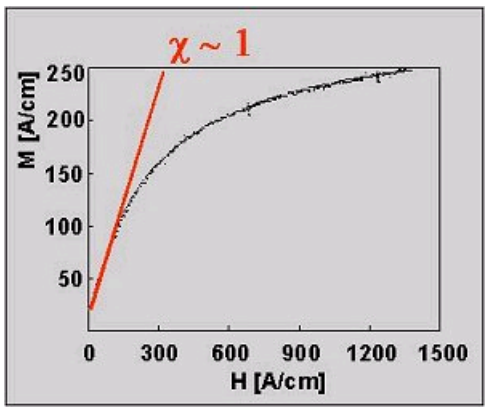

Field variation of SANSPOL cross-term

$$I^-(Q,\alpha) - I^+(Q,\alpha) = 4\, F(Q)_{nuc}\, F(Q)_{mag}\, L(x) \sin^2\alpha$$

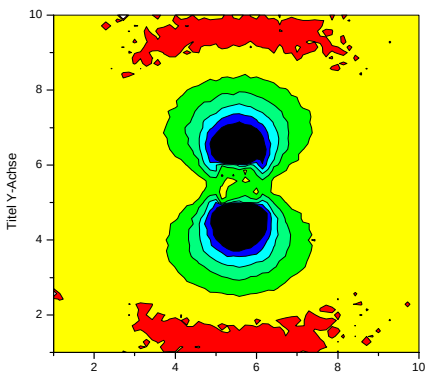

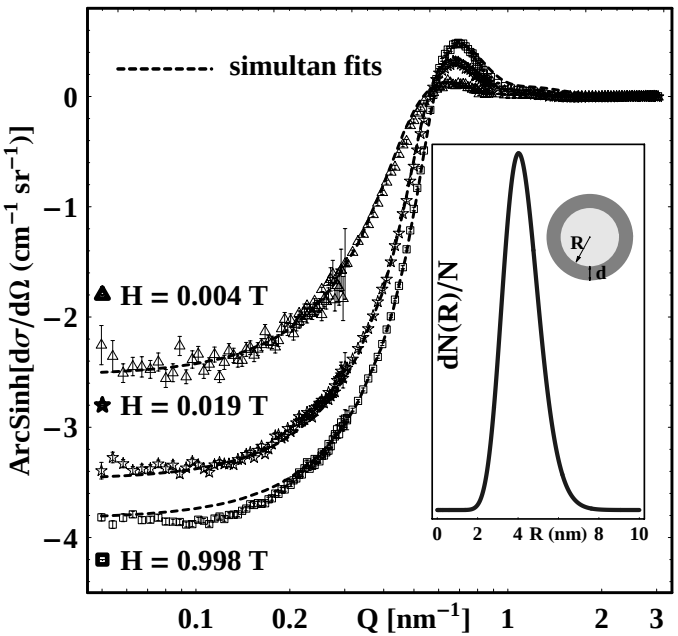

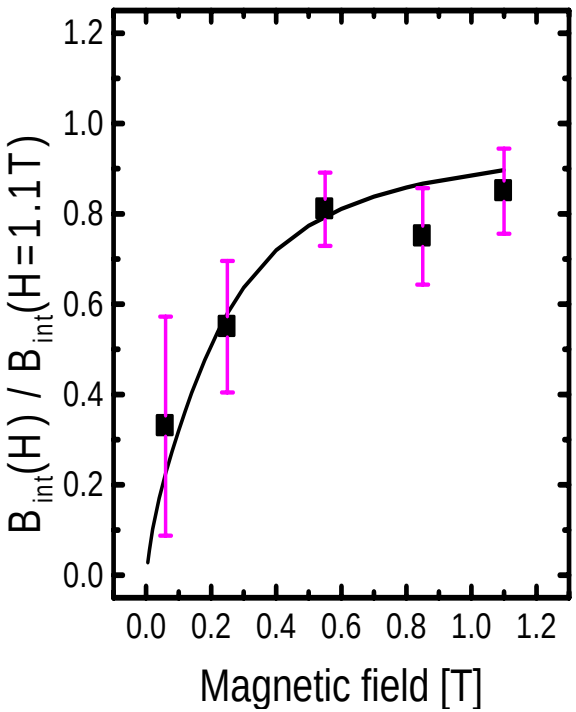

AW, Physica B (2001) 226-233
A. Heinemann et al AOC(2004)

Superparamagnetic behaviour of non-interacting single domains

Diluted poly-disperse systems

I^- (on) - I^+ (off)

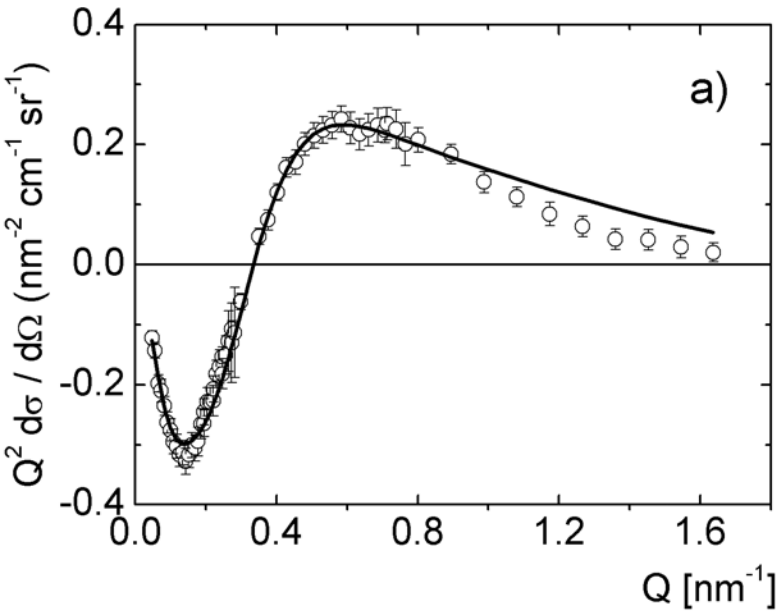

I^- (on) , I^+ (off)

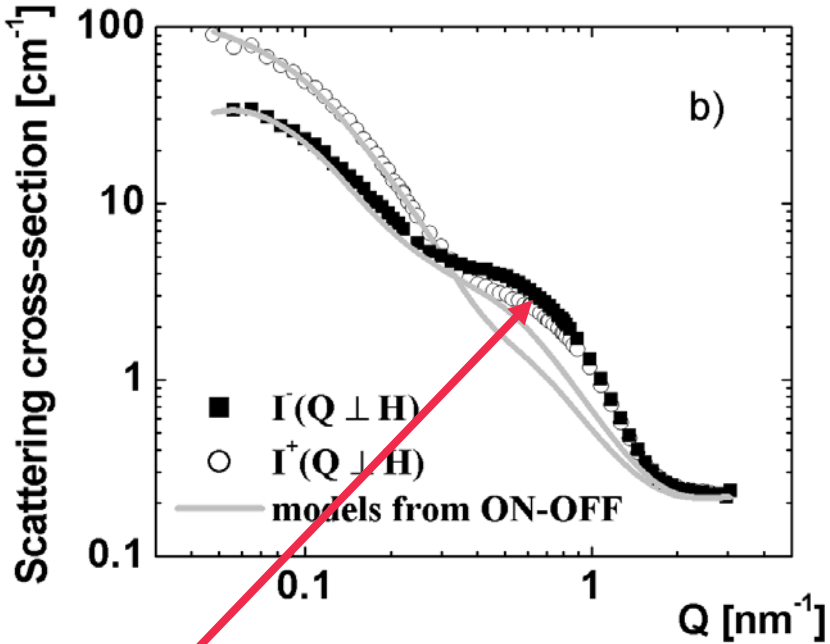

Probes only magnetic particles

Additional non-magnetic contributions: micelles

Heinemann et al JAC 2002

Magnetite-FF: Contrast Variation

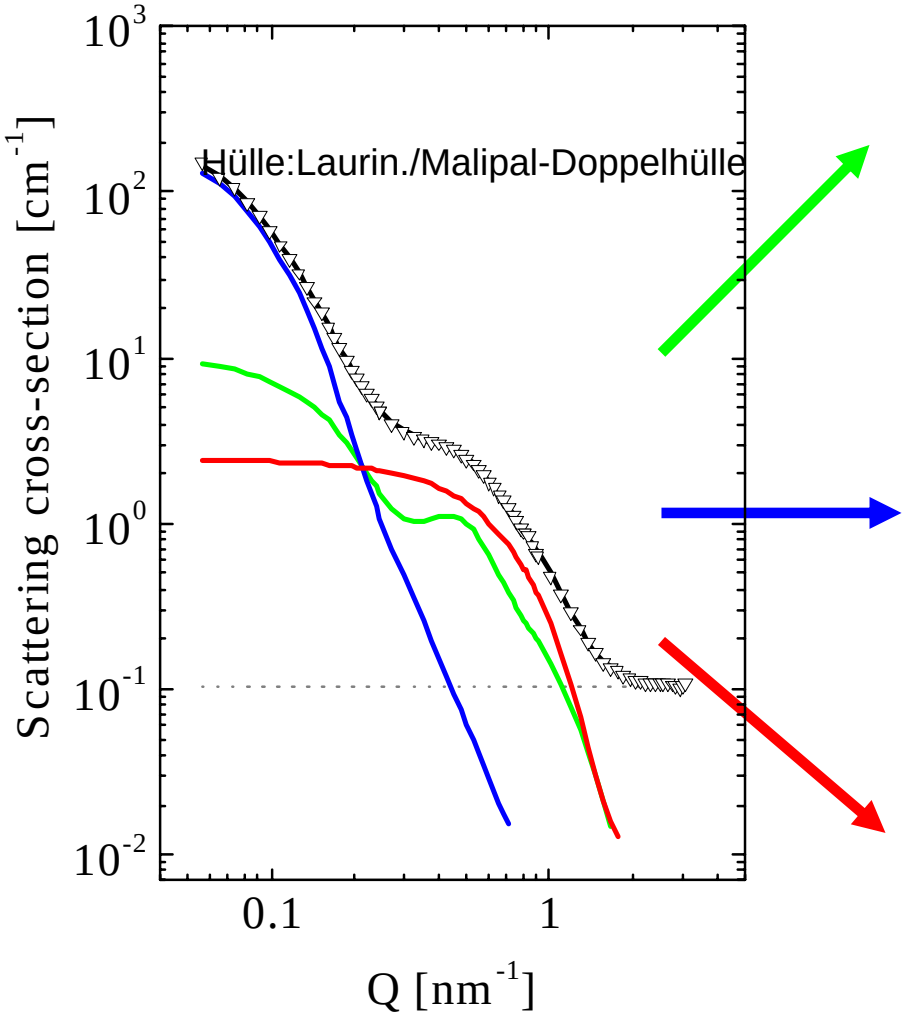

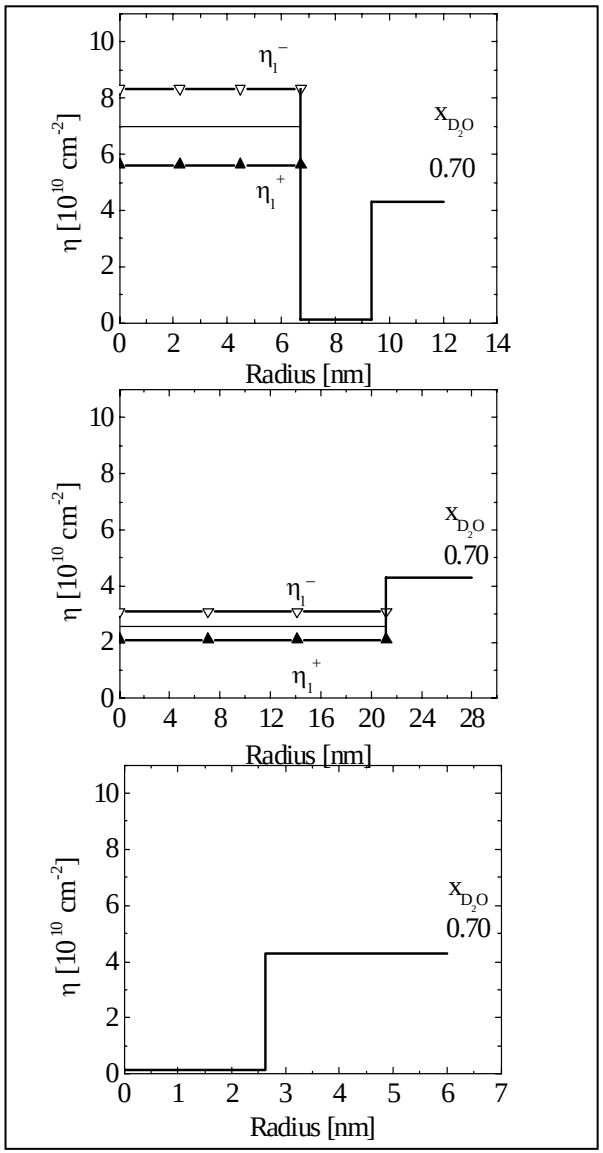

Magnetic core-shell particles

Magnetic aggregate

Non-magnetic micelles

M. Kammel , A. Hoell, A.W., JMMM 2002

Interparticle correlations: Structure factor S(Q)

$$S(Q) = 1 + N_p \int [g(r) - 1] \exp(iQr)\, dr$$

g(r) : Pair correlation function

S(Q) = 1	ideal gas
S(Q) < 1	repulsive potential:
	Excluded volume, electrostatic repulsion
S(Q) > 1	attractive interaction

In practice

$$S(Q, \alpha) = I(Q,\alpha)_{\text{measured}} / I(Q,\alpha)_{\text{non-interacting}}$$

for diluted samples

Field induced ordering

Non-polarised neutrons, H=1 T

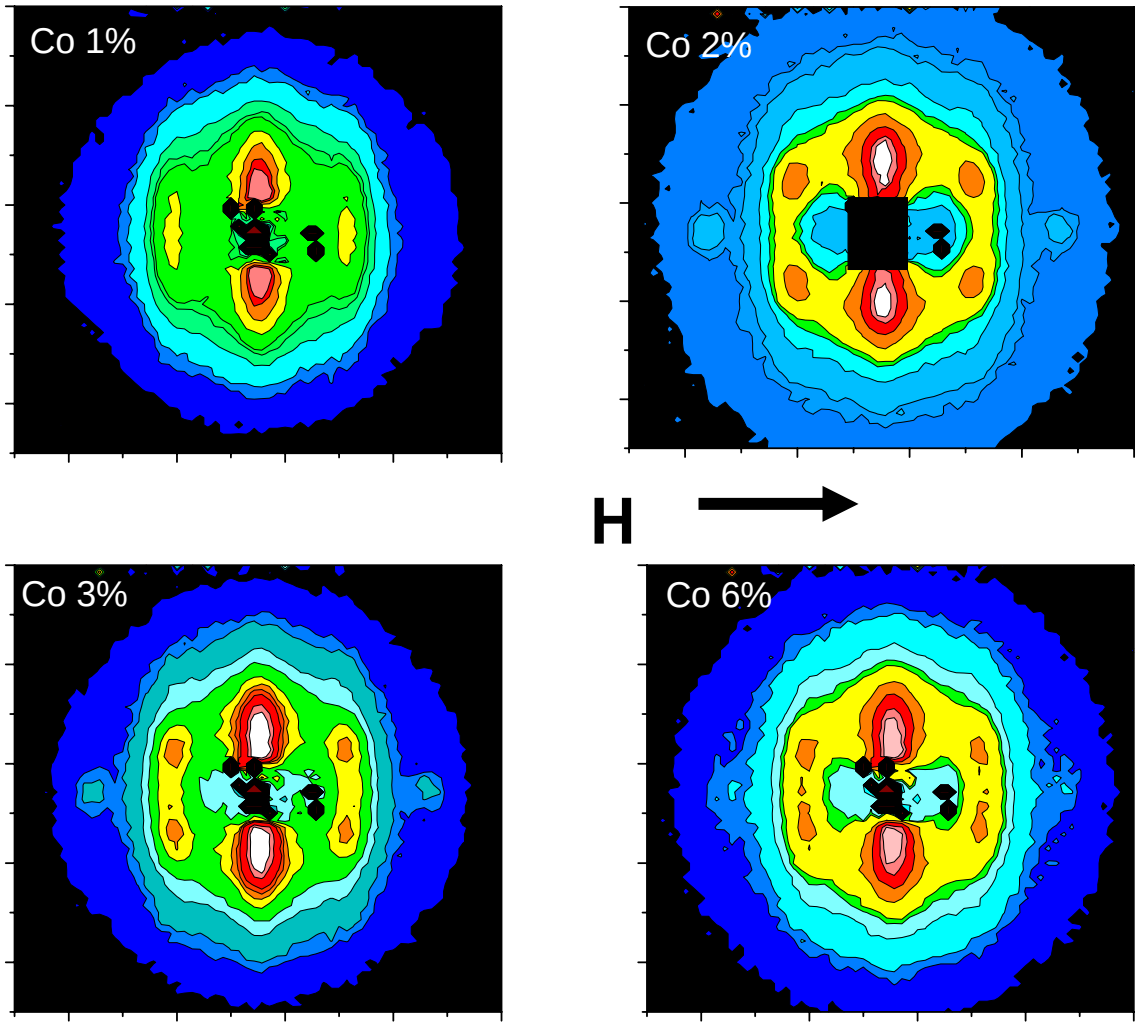

For Co-concentrations above 1 vol. % :

Peaks ! disappear at H=0

A.Wiedenmann et. al. Phys Rev E 2003

3 vol.% Co-FF:SANSPOL

Polarised neutrons

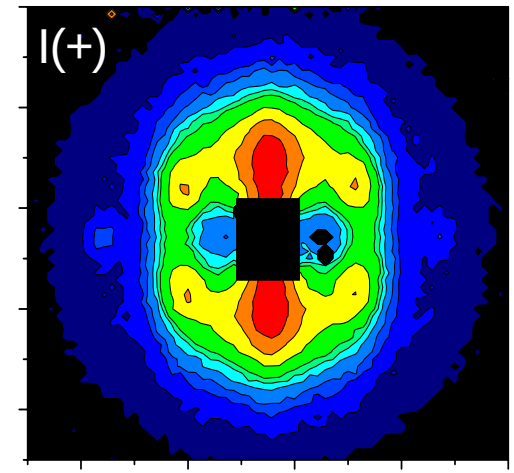

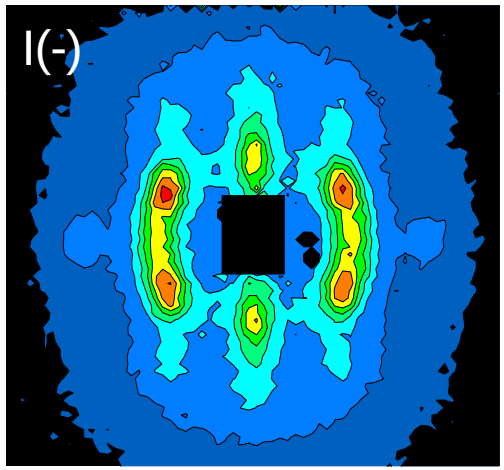

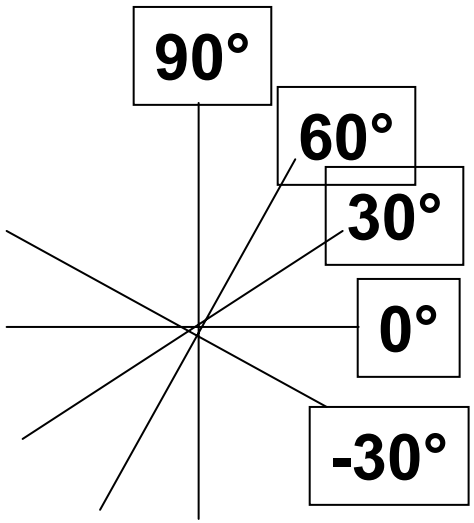

H →

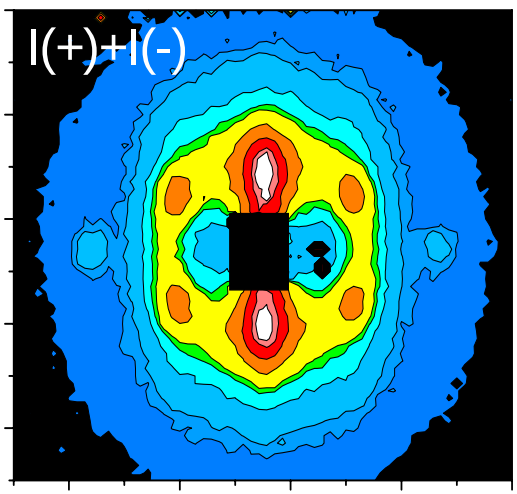

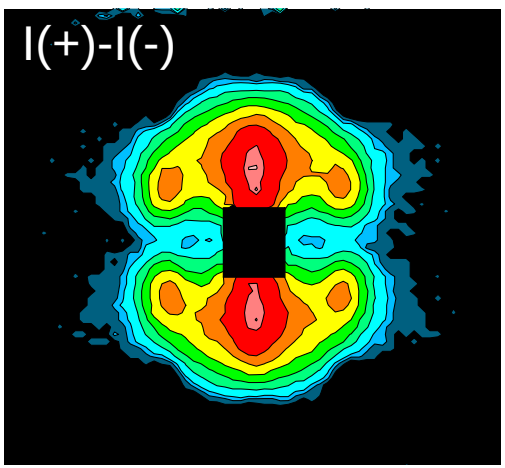

Sectors of 2D-SANSPOL

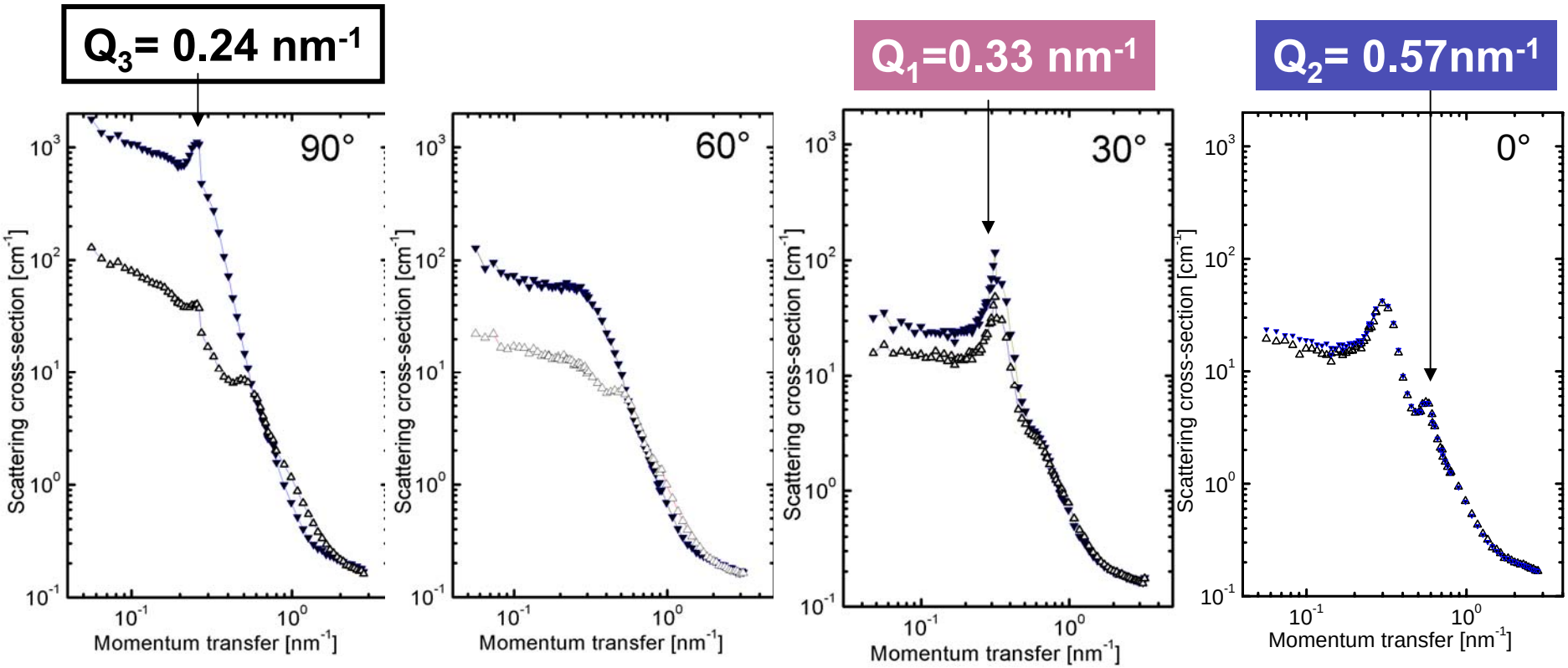

Anisotropic in-plane structure factors

$$\frac{I(Q,\alpha)}{I\ (model)}$$

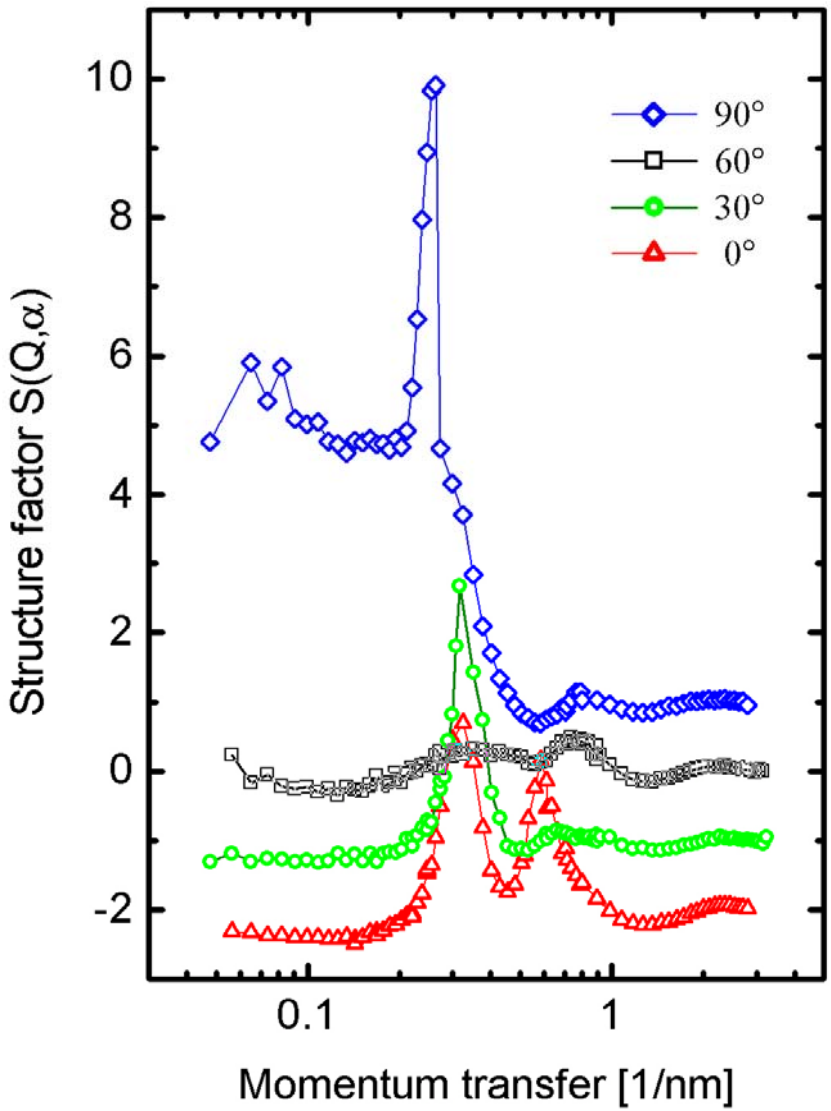

Peaks at

Q_1= 0.33 nm^{-1}
Q_2= 0.57 nm^{-1}
Q_3= 0.24 nm^{-1}

Streaks at

Q_x= 0.0 nm^{-1}
Q_x= 0.29 nm^{-1}

Neutrons parallel to H

Radial averaged SANSPOL

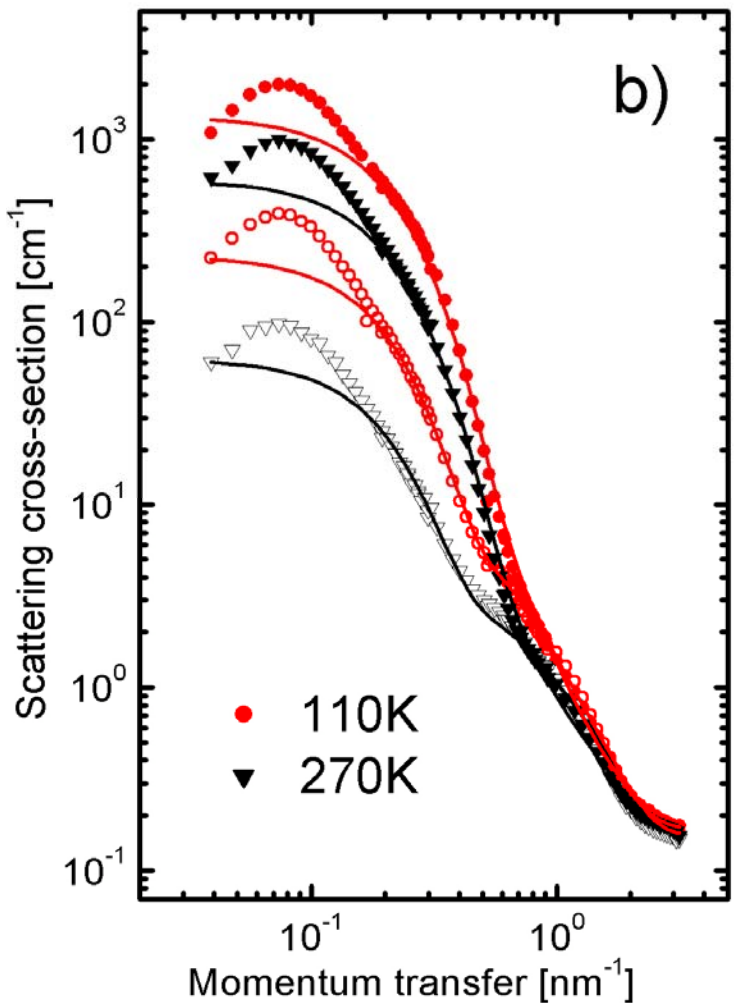

Model fits at high Q from diluted samples using form-factors alone

Neutrons parallel to H

Radial averaged SANSPOL „Debye-Scherrer ring“

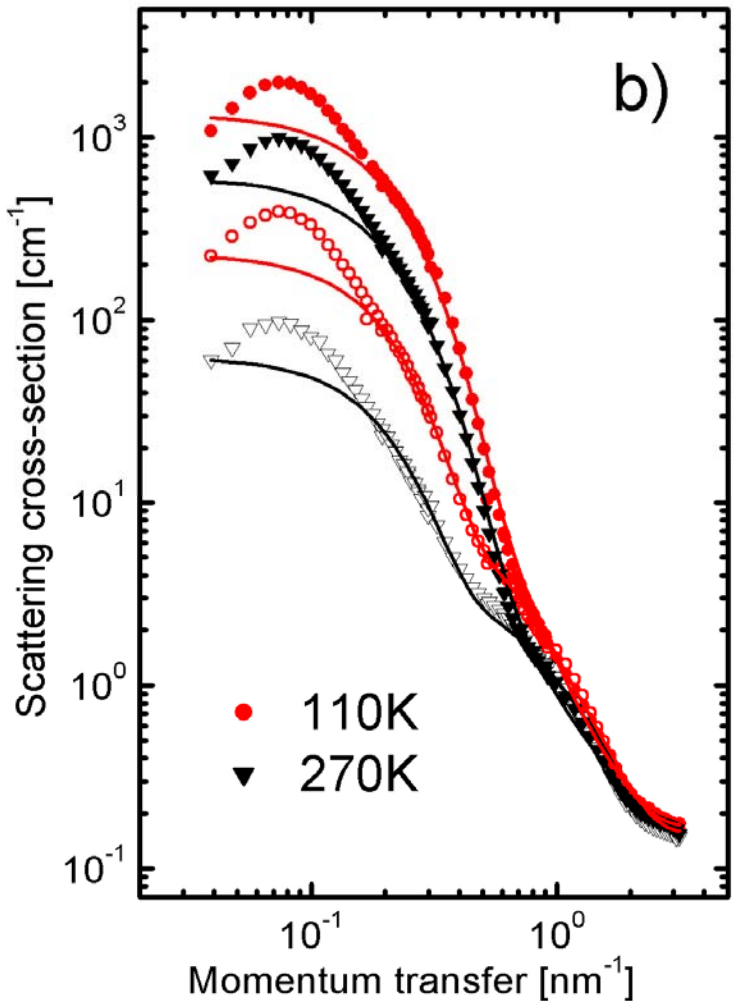

Stucture factor (n // H)

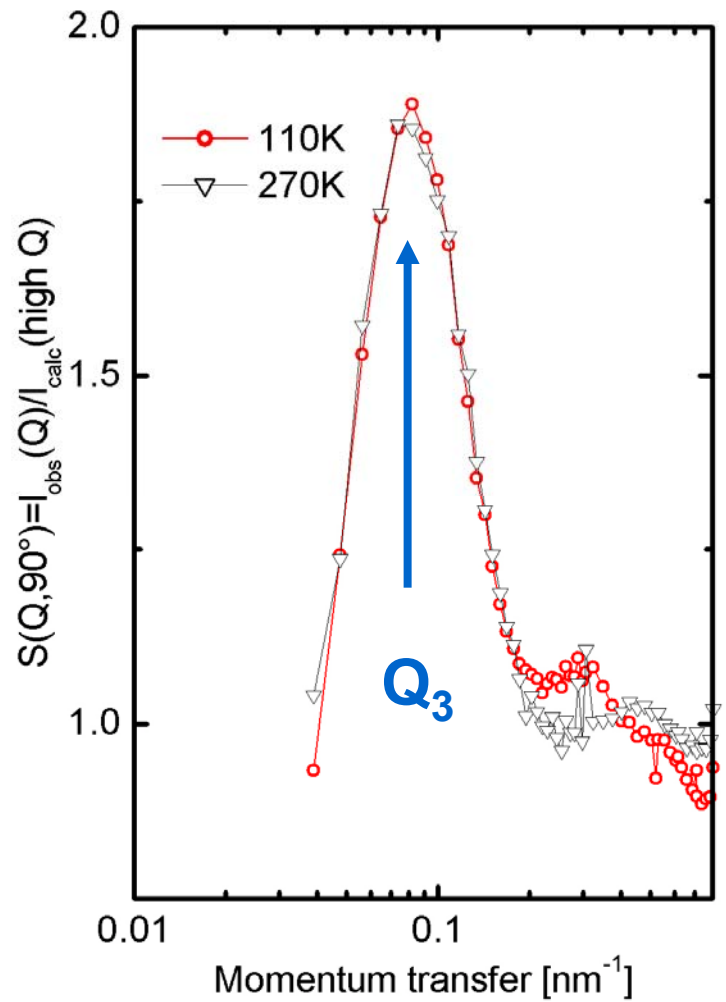

Nature of field induced ordering

Hexagonal symmetry

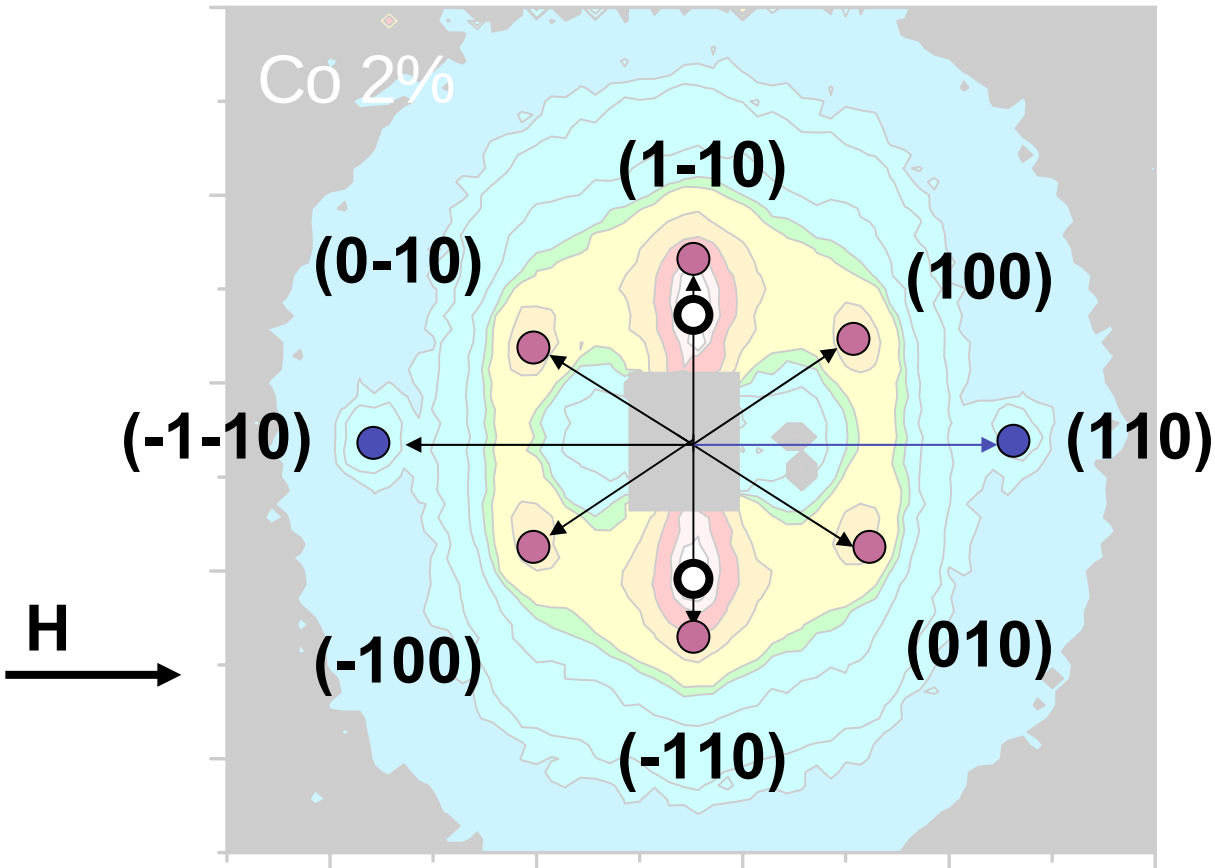

Q_1=0.33 nm^{-1}

Q_2= 0.57nm^{-1}

$Q_2 / Q_1 = \sqrt{3}$

Q_3= 0.24 nm^{-1}

(0 0 1), (0 0-1)

a_{hex} = 21.3 nm

c_{hex}= 26.1 nm

$$Q\,(hkl) = 2\pi / \{4(h^2+k^2+hk)/3a^2 + l^2/c^2\}^{1/2}$$

Pseudo-crystalline hexagonal ordering

Texture type I

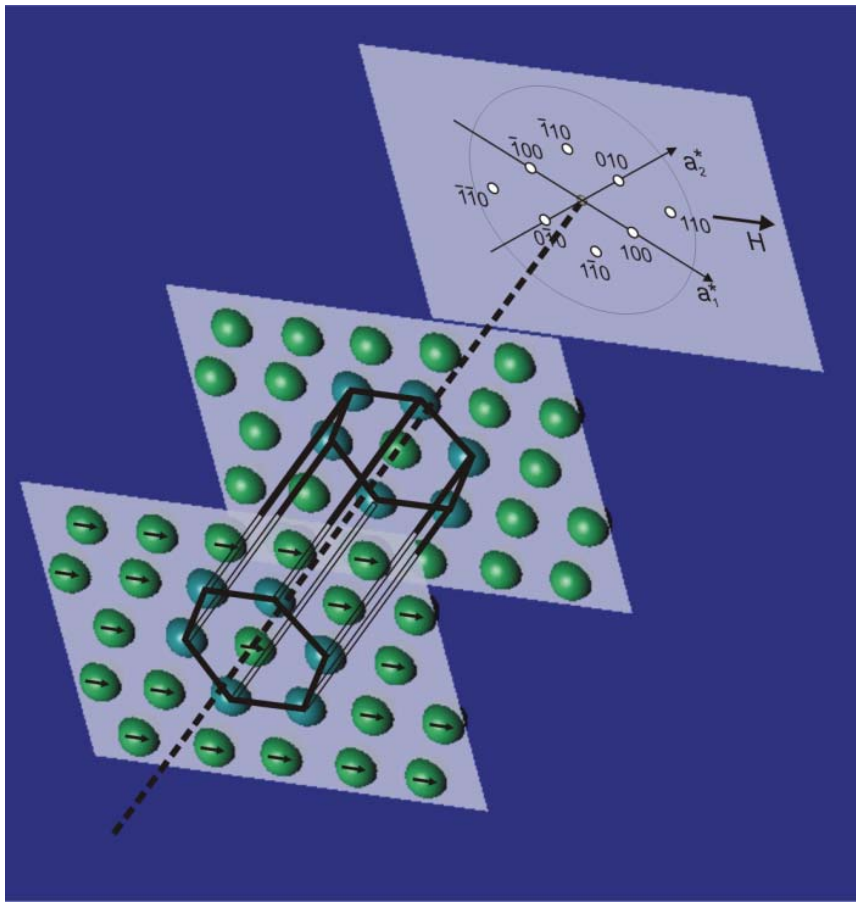

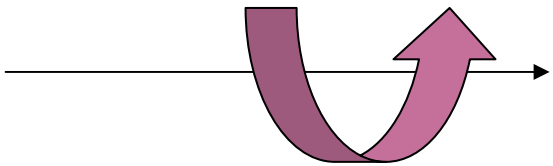

Turn around [110] direction of magnetic field by 90°

Particle moments *M* // [110] along H

Field induced ordering

Pseudo-crystalline hexagonal particle alignment

Texture type I

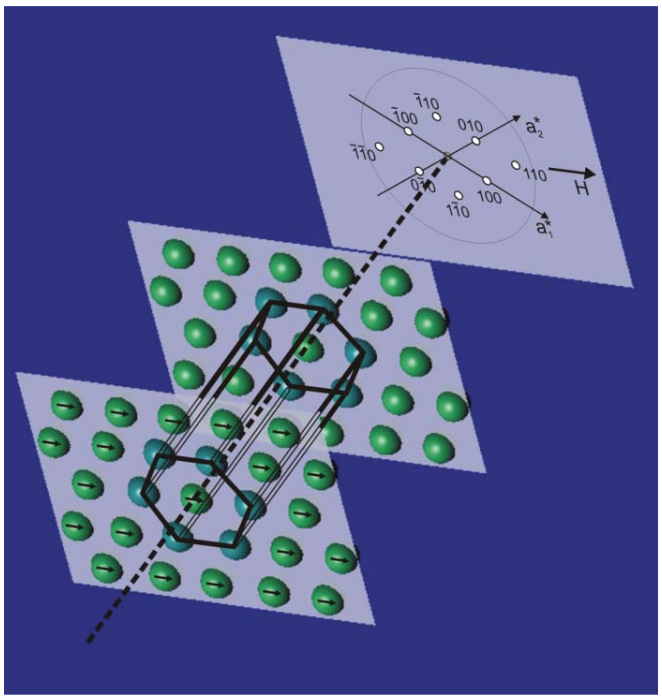

Texture type II

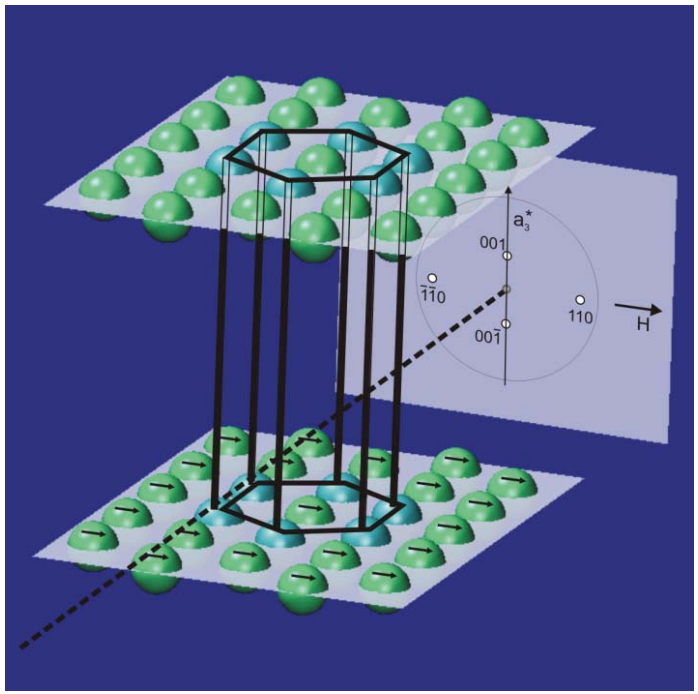

R_c = 3.8 nm, d=1.9 nm
a_{hex}= 21 nm
c_{hex}= 25…70 nm

A.Wiedenmann, A. Hoell, M. Kammel, Phys Rev E 2003

Field induced ordering: 1 vol.% Co-FF

Diffraction planes perpendicular to H

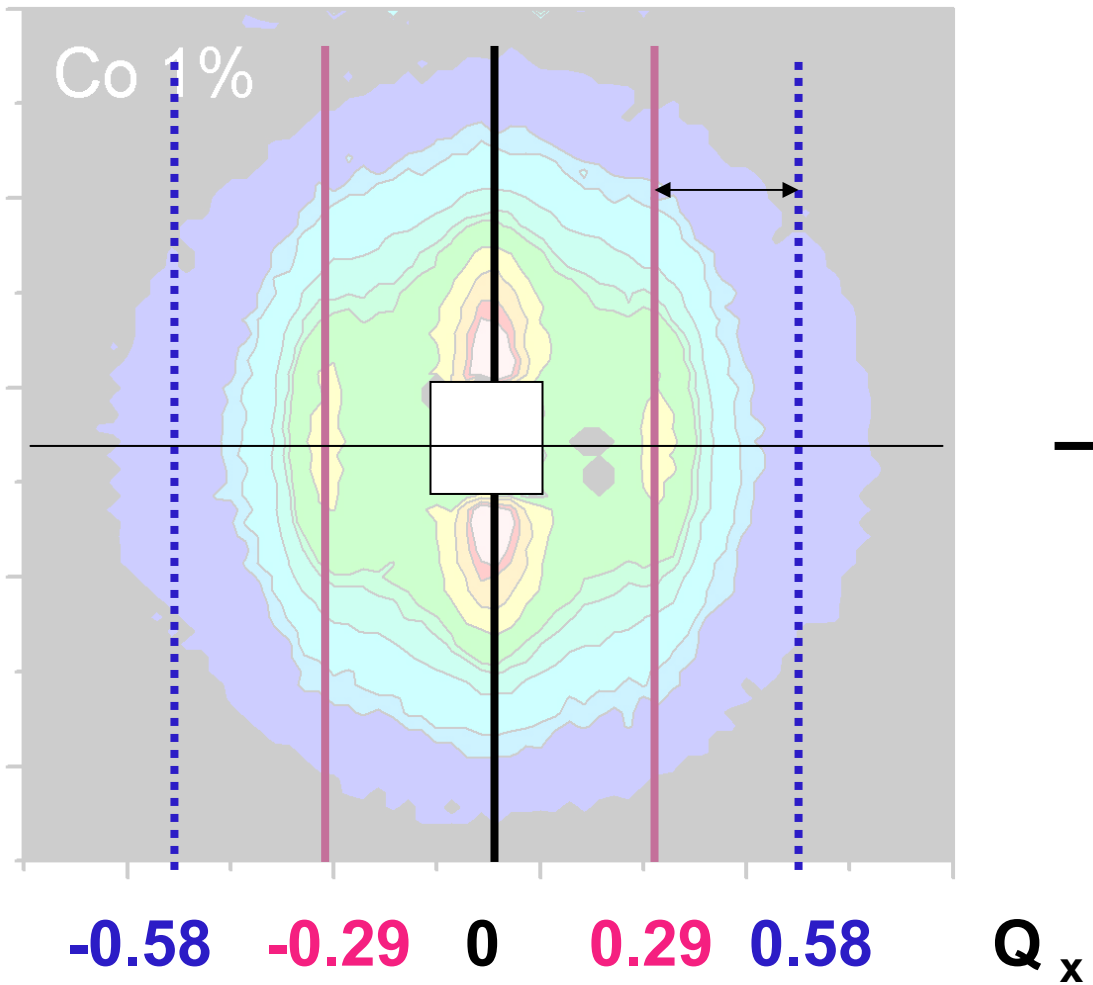

Δ Q= 0.29 nm^{-1}

H

1 vol.% Co-FF: Field induced ordering

Diffraction planes perpendicular to H

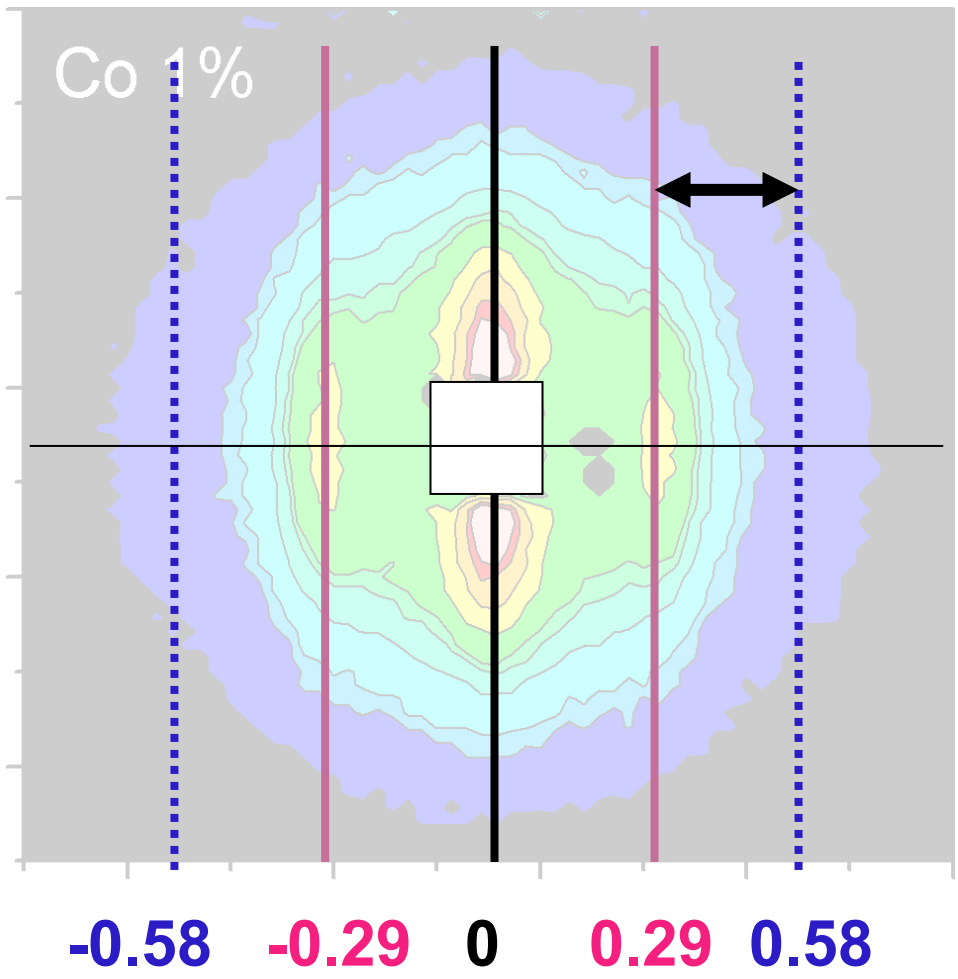

Δ Q= 0.29 nm^{-1}

Chain-like structures

Nearest neighbour distances

σ (1D) = $2\pi / \Delta Q$
= 21 nm
= a_{hex}

Ordering- 1st step:chaining

SANSPOL Co-3 vol.%

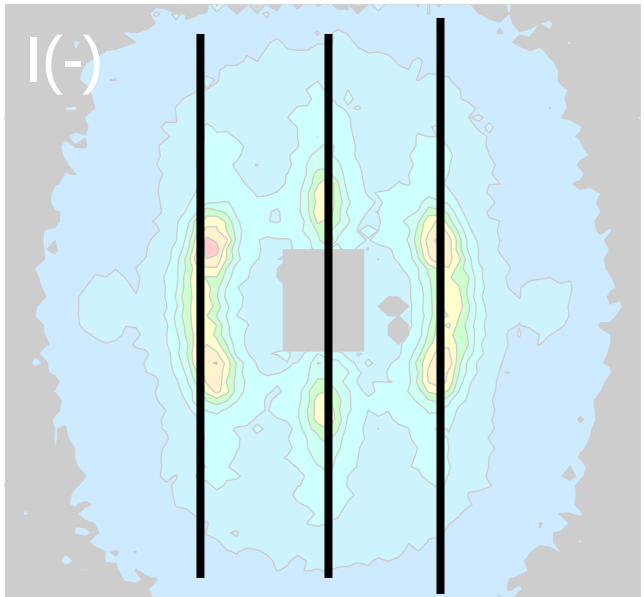

Intensity I(Q⊥H) at low Q:

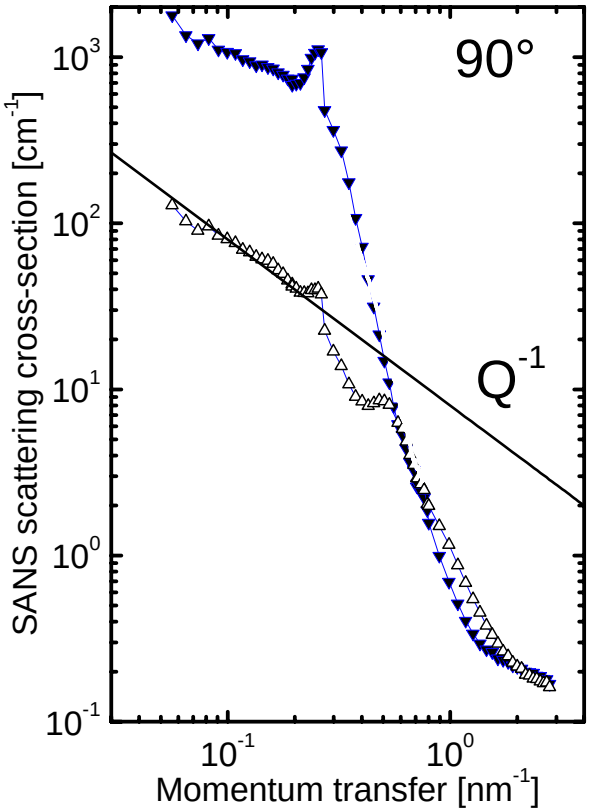

Co-existence of uncorrelated chains with hexagonal ordered domains

$$I(Q) \propto Q^{-1}$$

$$S(Q,90°) > 1$$

Ordering - 1st step:chaining

Particle size
$\langle R_c \rangle$ = 3.8 nm, d=1.9 nm

Shortest possible distance
11.4 nm

OBSERVED :

Diffraction planes from quasi-1D chains

σ (1D) =2π /ΔQ= 21 nm

σ (1D) = a $_{hex}$

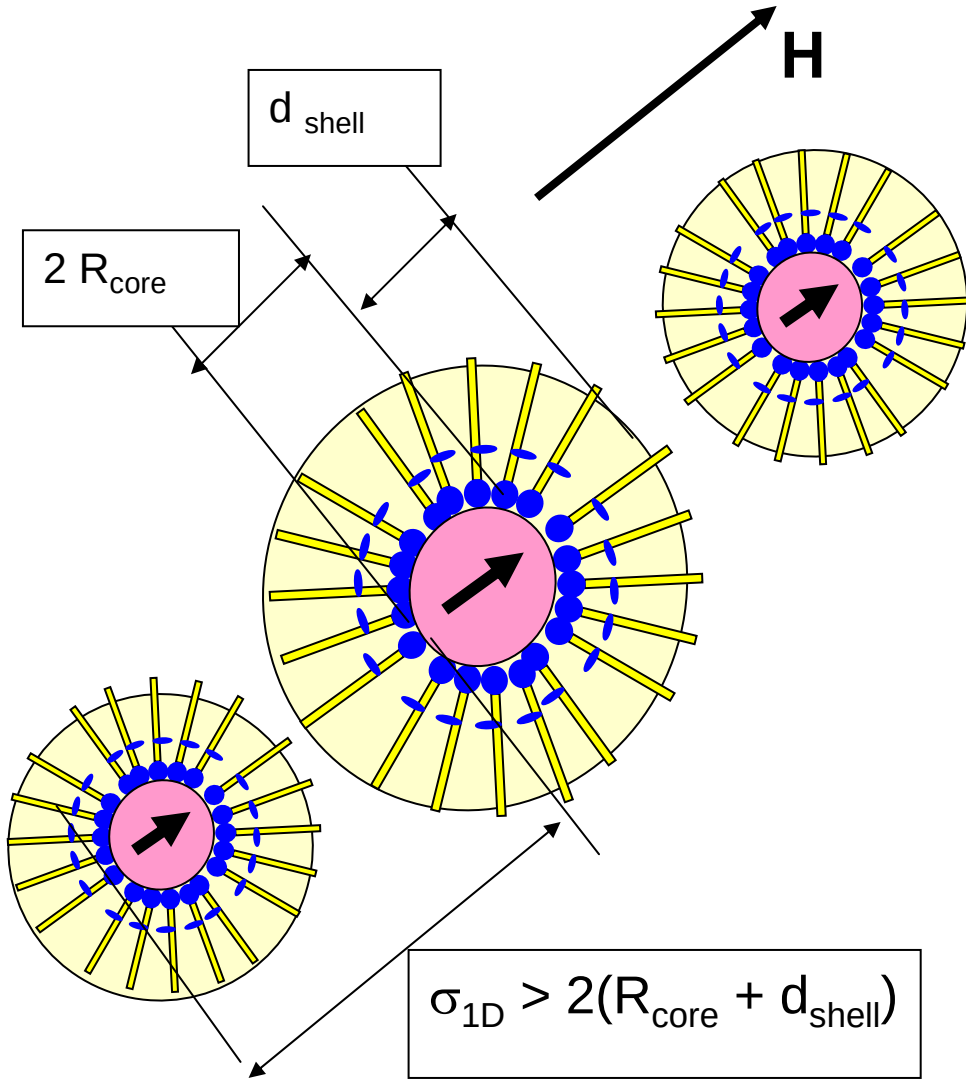

Second example: Co-L9

SANS H=1 T

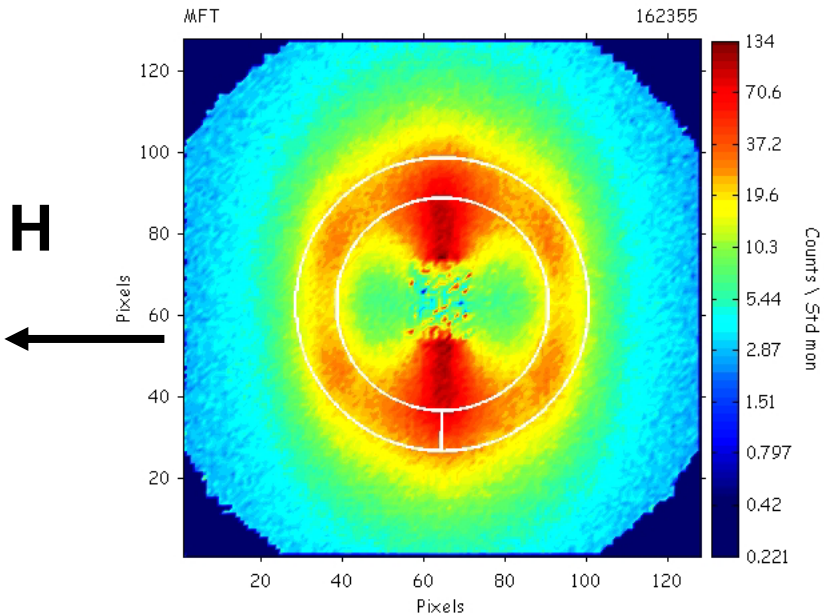

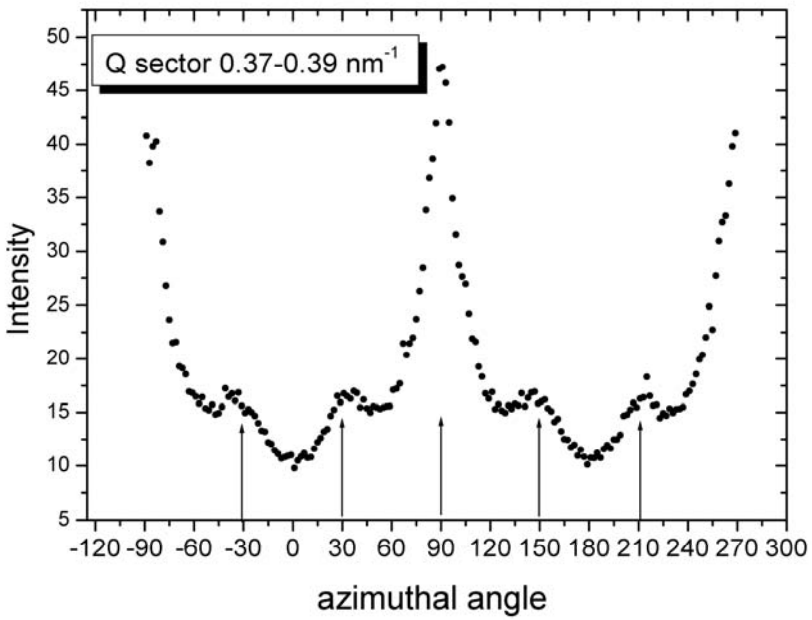

Confirmation of hexagonal symmetry

Field dependence of ordering

6 vol.% Co in Oil L9 **SANS H=1 T Saturation**

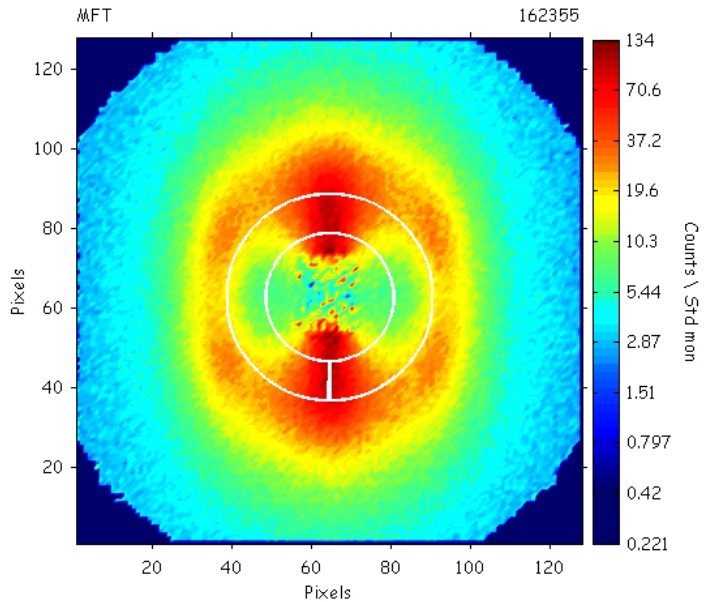

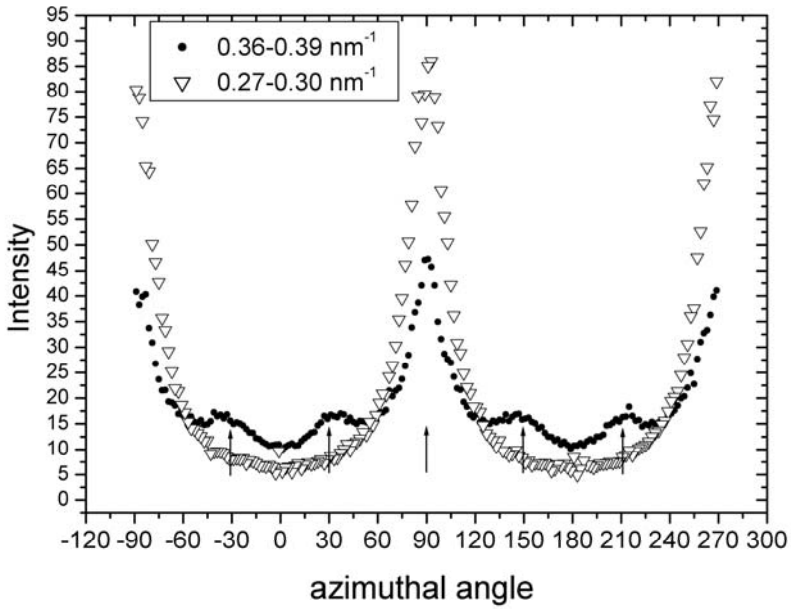

$$I(Q,\alpha) = [F_M^2 L^2(x)\sin^2\alpha + F_N^2]\ S(Q,\alpha)$$

$$+\ [2L(x)/x - \sin^2\alpha(L^2(x) - 1 + 3L(x)/x)]\ F_M^2$$

SANSPOL : Co-L9

$I(+) - I(-) / \sin^2\alpha$

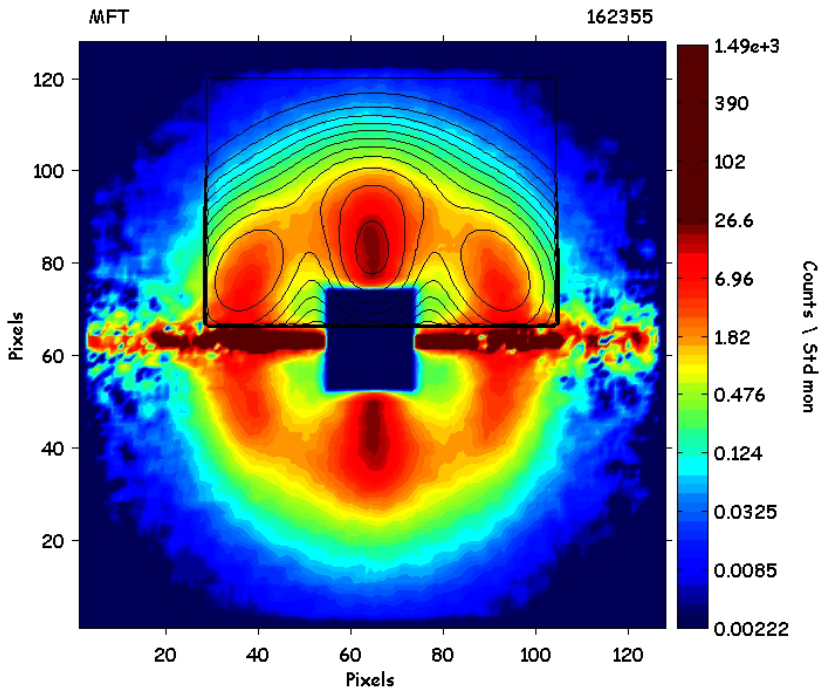

$= 4\, F_N F_M\, L(x)\, S(Q,\alpha)$

2D Gaussian fits

At H=1 T:

Hexagonal ordering

$a_{hex} = 18.9$ nm

$c_{hex} = 21.9$ nm

Co-L9

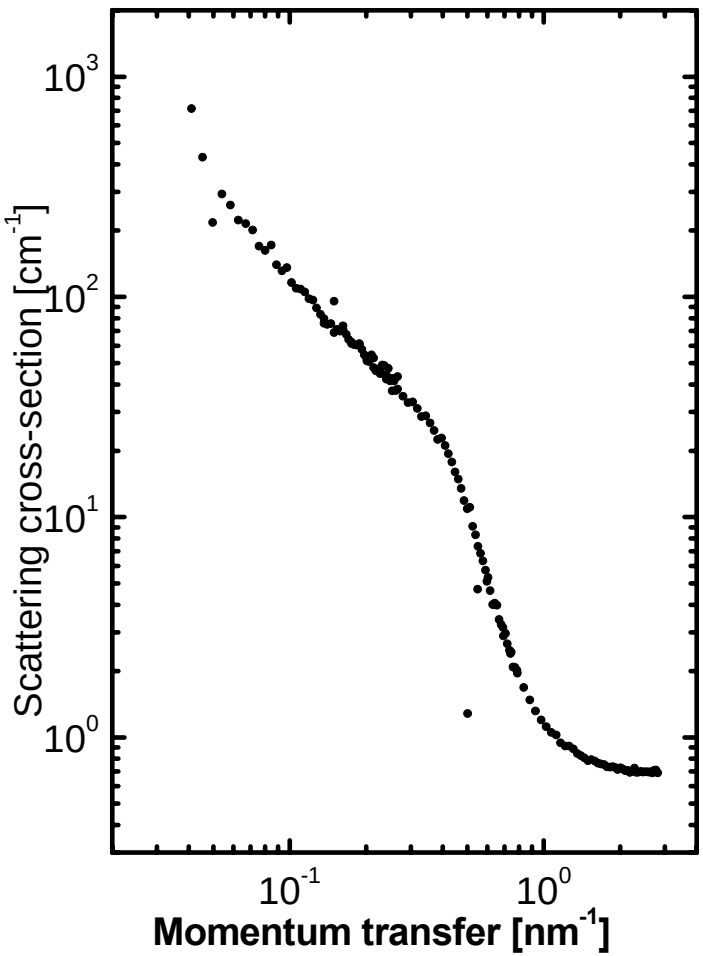

At H=0

Isotropic scattering:
no peaks

Cylinders
L= 80 nm R=4.3 nm
(5-6 core-shell particles)

Spontaneous formation of chains
$I(Q) \sim Q^{-1}$

Co-L9

At H=1 T

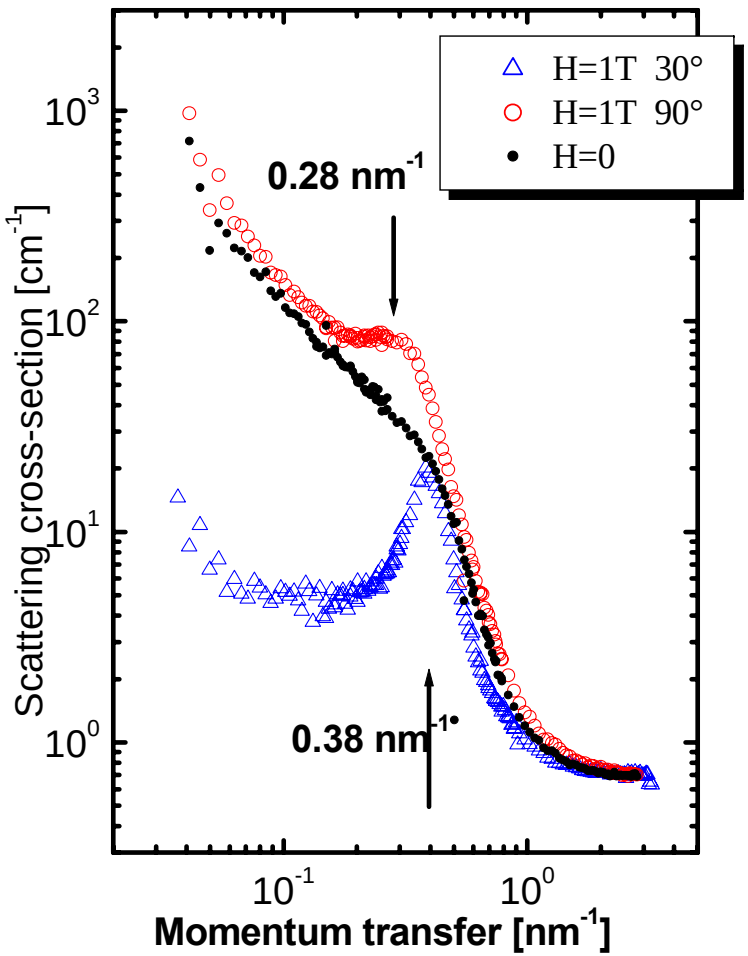

Anisotropic scattering peaks

Perpendicular to H
Q_3= 0.28 nm^{-1}

Sectors ± 30°
Q_1= 0.38 nm^{-1}

Co-existence with chain segments

$I(Q) \sim Q^{-1}$

Co-L9

SANS sector 90°: Difference I_H- $I_{H=0}$

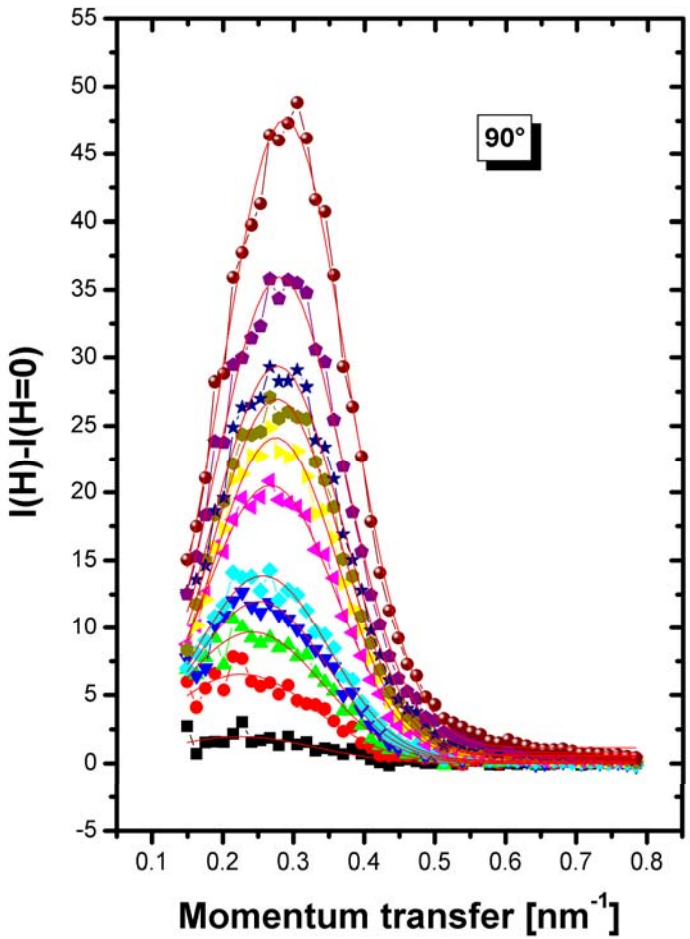

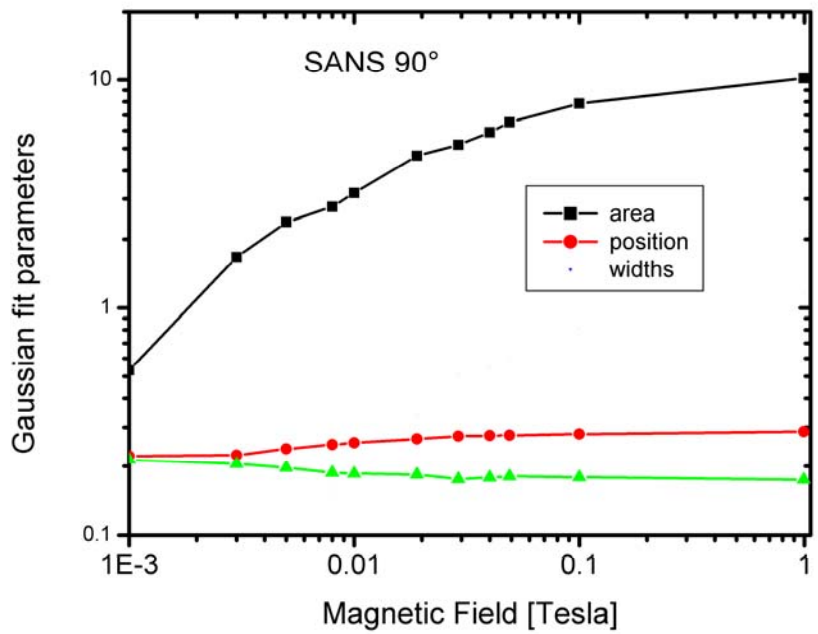

Shift of peak

c(0.005T) = 25.5 nm

c(1T) = 21.9 nm

Area: ~ $L^2(x)$ Langevin

Structure evolution in magnetic field

SANSPOL sector 30° I(on)-I(off)

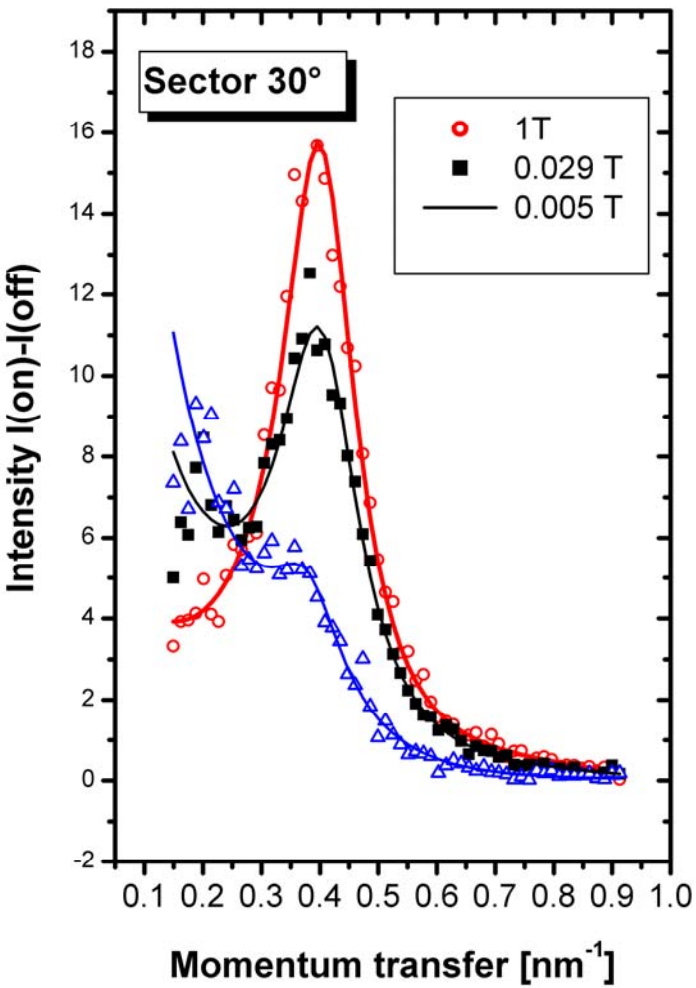

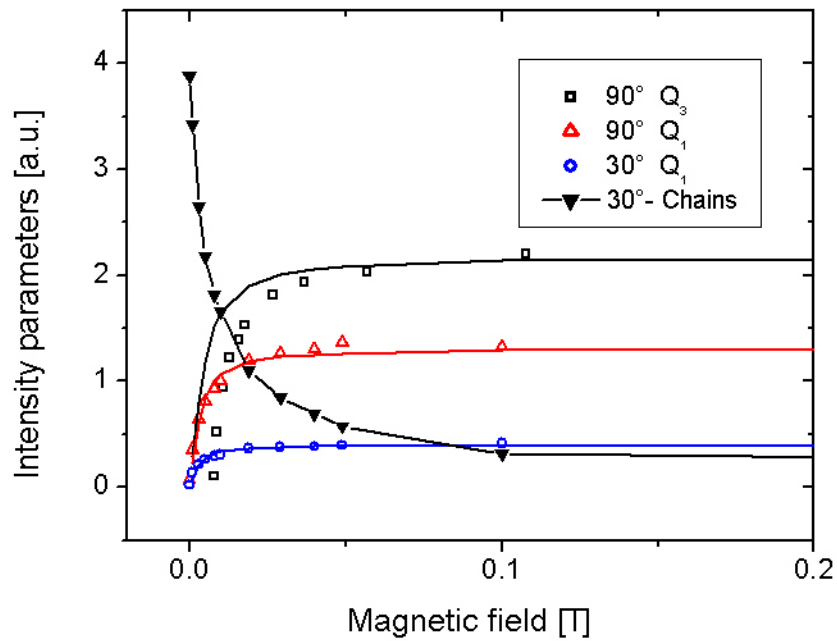

Hexagons:

Contrast ~L(x)

Cylinders:

get aligned along H

A. Wiedenmann. A. Heinemann JMMM(2005)

Transition from chain-like to lamellar ordering

Competition between magnetic dipol-interaction and thermal energy

$$\gamma = M^2_{sat} V^2_c \mu_o / 4\pi k_B T \sigma^3.$$

Present range $1.4 < \gamma < 8$

Computer simulations (MSA):
Chaining in head-to tail conformation (de Gennes)

Lateral attractions
Molecular dynamics predicts close-packed structures (Hess)

SANSPOL with Polarisation Analysis

A. Wiedenmann Physica B 2005

^{3}He filter

Spin selective neutron absorption:
(Passell, Schermer; 1966)

$$^3He\uparrow + n\downarrow \rightarrow [^4He^*] \rightarrow t + p + 0.76\ MeV$$

$$\sigma\uparrow\downarrow \approx 3000\ barn \cdot \lambda[Å]$$

$$^3He\uparrow + n\uparrow \rightarrow {}^3He\uparrow + n\uparrow \qquad \sigma\uparrow\uparrow \approx 5\ barn$$

<u>Advantages:</u>

- **Unlimited angular acceptance**
- **Broad range of usable wavelength**
- **No deflection of neutrons**
- **Polarisation of white beams**

Compression of polarised ^{3}He

Piston compressor at University of Mainz

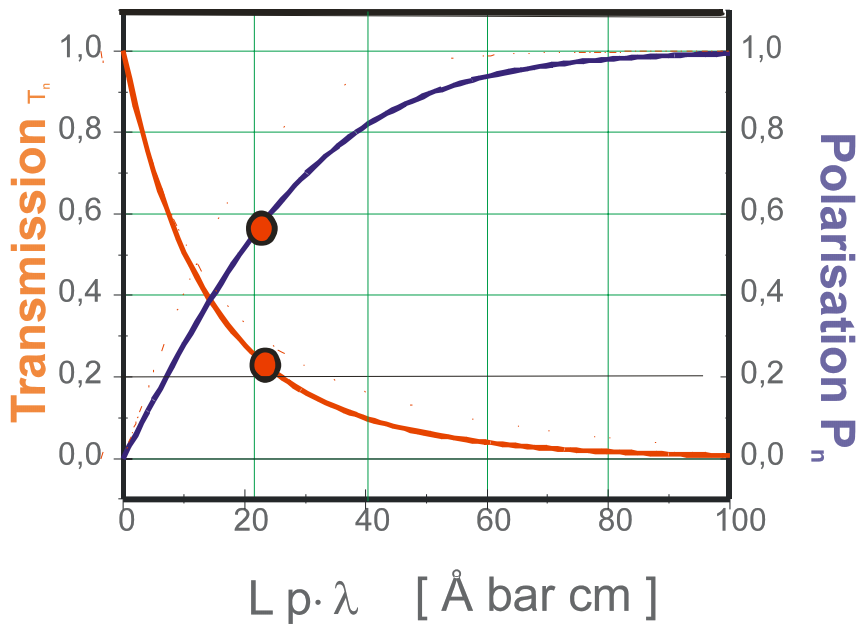

Neutron polarisation P_n

$P_n = \tanh(x P_{He})$

Transmission

$T(+) = \exp[-x (1 - P_{He})]$

$T(-) = \exp[-x (1+ P_{He})]$

$T_0 = \exp[-x]$

Neutron optique filter thickness : $x = N_{He} \sigma L = 0.0733 \, p \, \lambda \, L$

Performance of ^{3}He filter

^{3}He polarisation from flipping-ratio n^-/n^+:

$P_{He} = 1/2x \ln (n^- / n^+)$

Decay with time:

$P_{He}(t) = P_0 \exp[-t/\tau]$

$P_{He}(0) = 41\ \%$

$\tau = 40$ h

Transmissions

T (on) = 6-8%

T(off) = 25-18%

T_0 = 14%

Neutron polarisation

60% - 38%

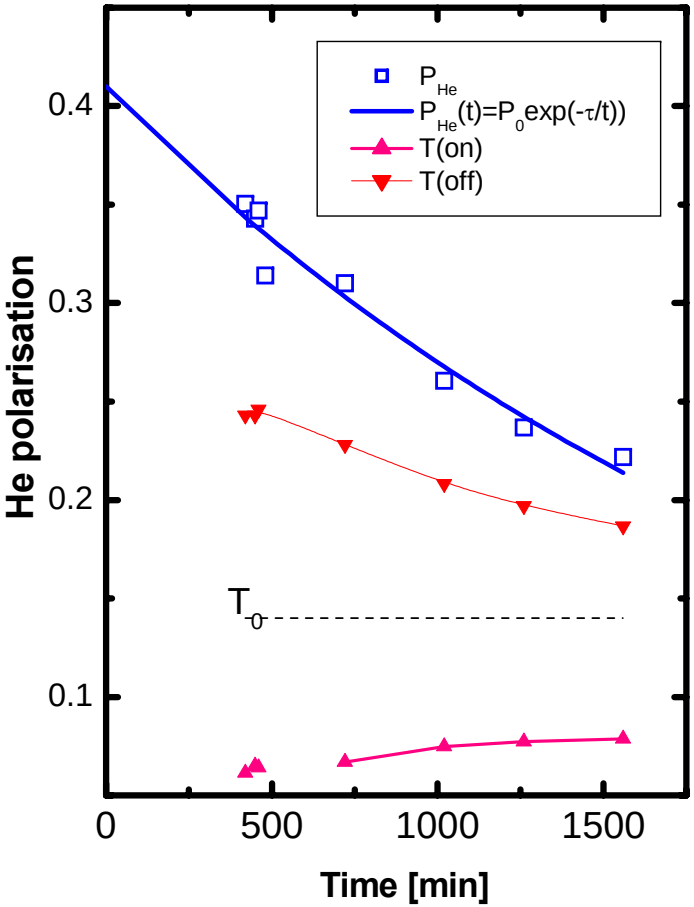

p(^{3}He) =0.5 bar, λ=0.6nm, L=9cm

$\Rightarrow$ x=1.905

Outlook:Polarisation analysis at V4

2d-Detector ^{3}He filter coil sample flipper polarizer

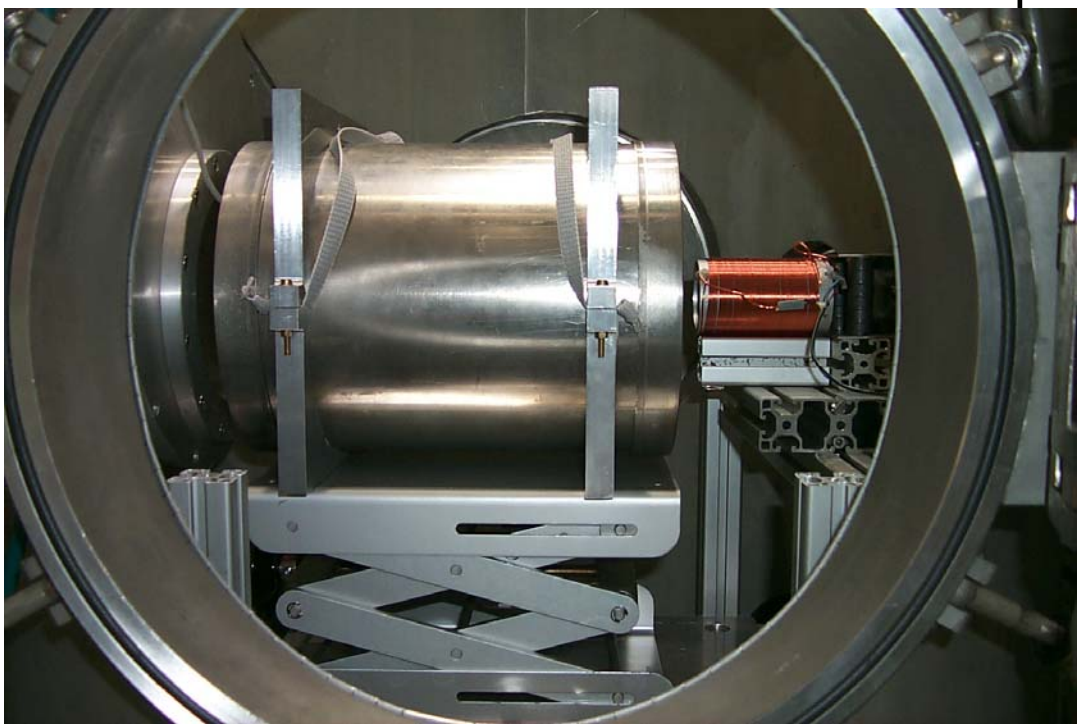

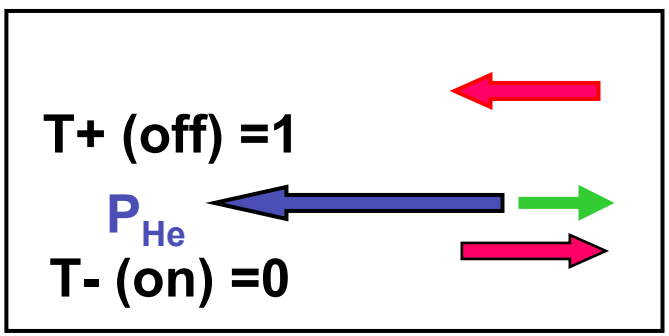

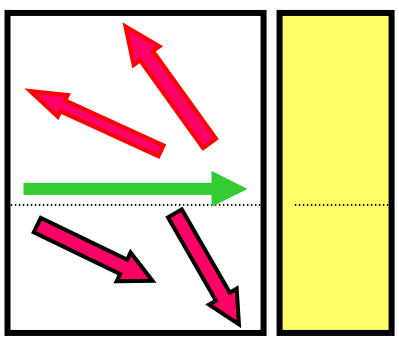

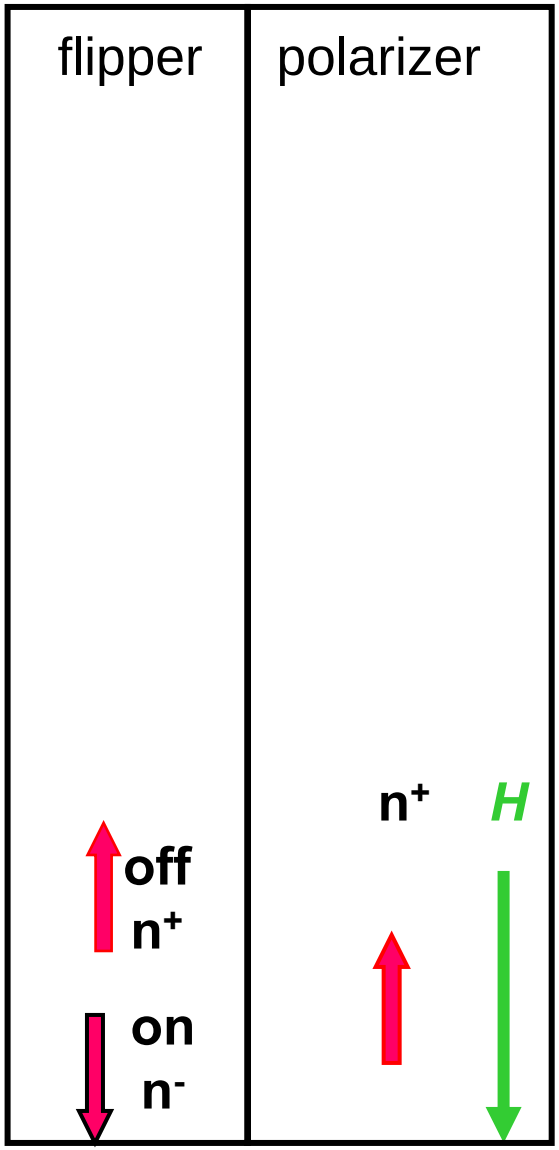

Outlook:Polarisation analysis at V4

2d-Detector ^{3}He filter coil sample flipper polarizer

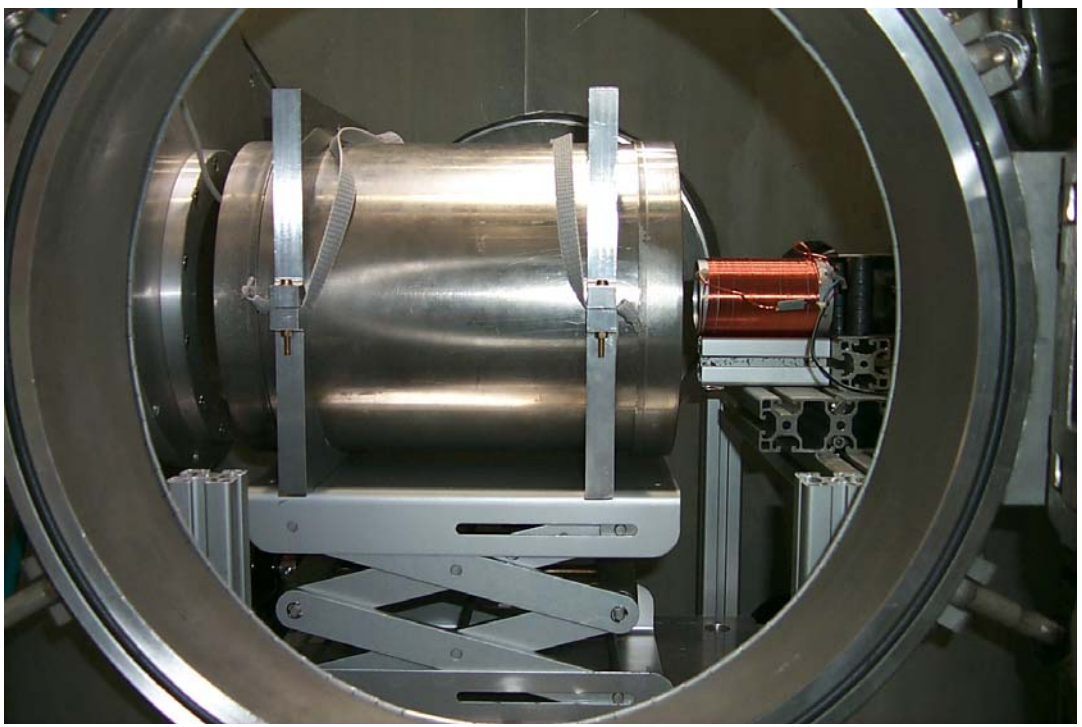

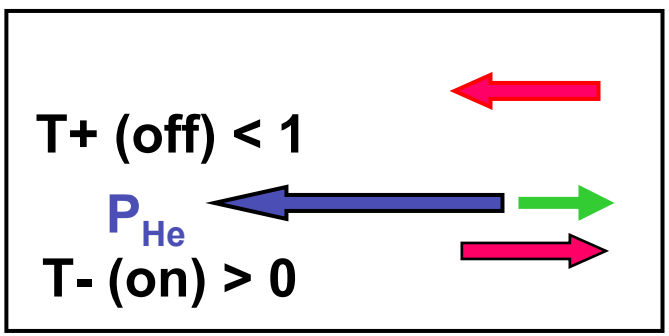

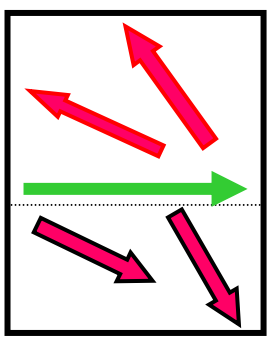

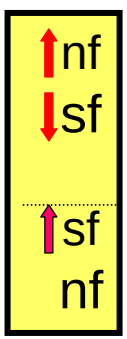

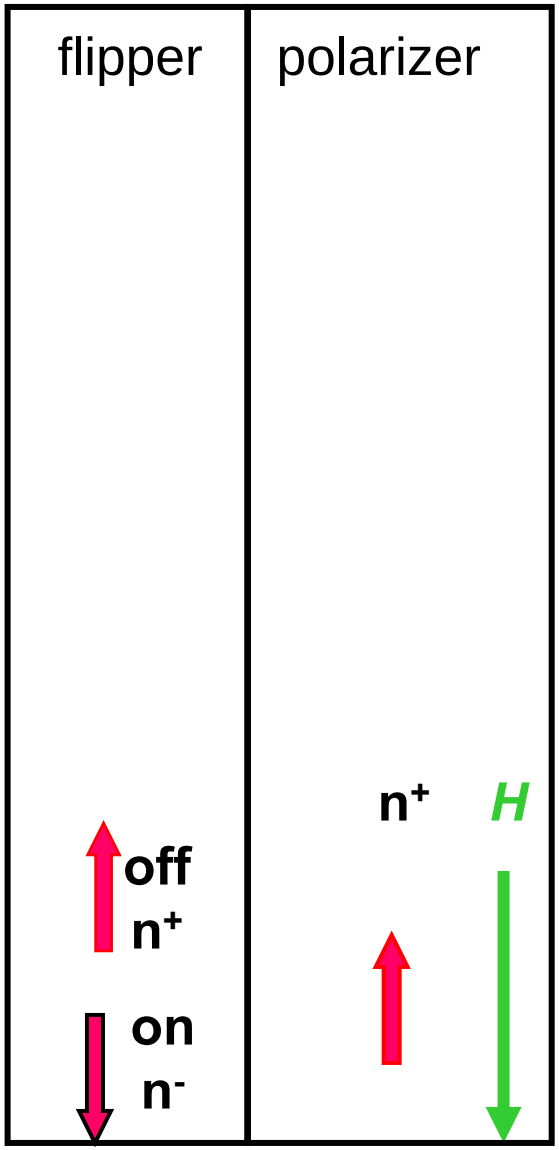

Outlook: *POLARIS*ation analysis at V4

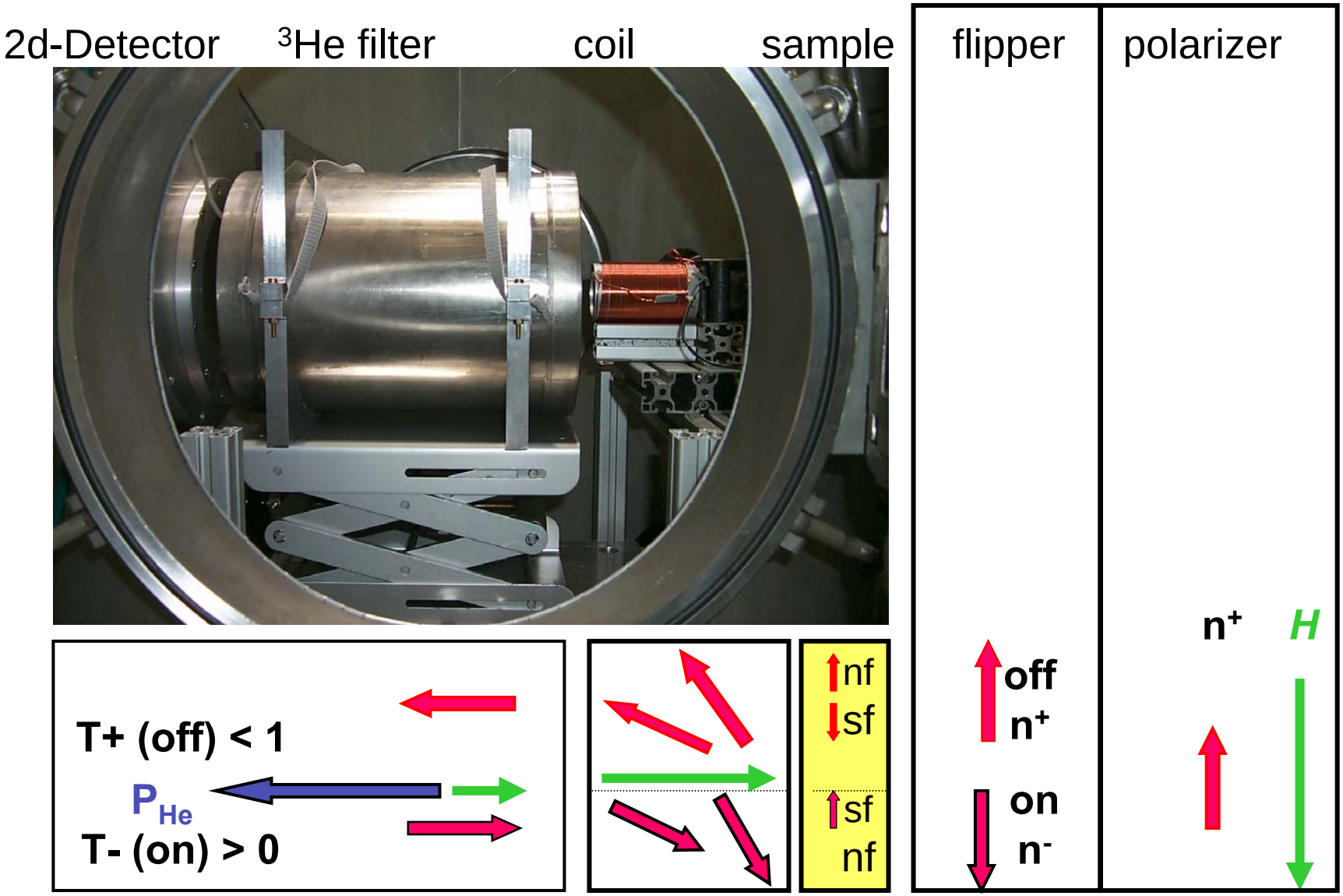

Magnetic single-domain particles

Neutron Scattering cross-sections *

spin-non-flip ++, --
spin flip + -, -+

$$d\sigma/d\Omega(ij)(Q,\alpha,x) = C_{ij}\, S(Q,\alpha) + D_{ij} F_M^2(Q)$$

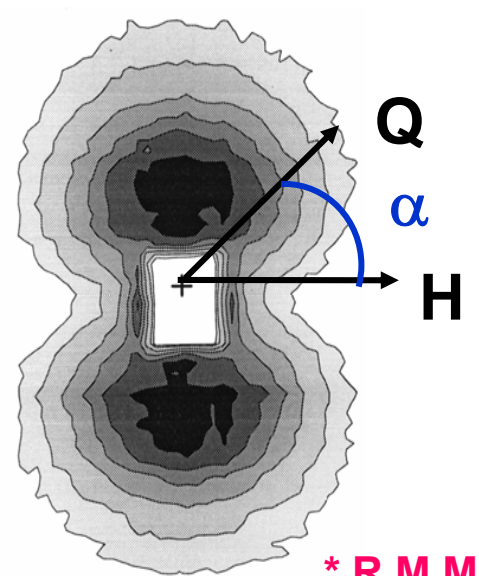

Nuclear Magnetic contributions

Misalignment of magnetic moment

* R.M.Moon,T.Riste, W.C. Koehler(1969) and R.Pynn, J.Hayter (1983)

$d\sigma/d\Omega\ (ij)(Q,\alpha) = C_{ij}\ S(Q,\alpha) + D_{ij}\ F_M^2(Q)$

$a(x)= L(x) / x$, $b(x)= L^2(x)-1+3\ a(x)$ $x=M_{cr}V_p\mu_0H_{eff} / kT$

ij	C_{ij}	D_{ij}
POLARIS		
I(++)	$[F_M\ L(x)\ \sin^2\alpha\ -\ F_N]^2$	$a\ \sin^2\alpha - b\ \sin^4\alpha$
I(- -)	$[F_M\ L(x)\ \sin^2\alpha\ +\ F_N]^2$	$a\ \sin^2\alpha - b\ \sin^4\alpha$
I(+ -),I(-+)	$[F_M\ L(x)\ \sin\alpha * \cos\alpha]^2$	$a(2-\sin^2\alpha) - b\ [\sin\alpha * \cos\alpha]^2$
SANSPOL		
I(+)	$[F_M^2L^2(x) - 2F_MF_NL(x)]\sin^2\alpha + F_N^2$	$a - b\ \sin^2\alpha$
I(-)	$[F_M^2L^2(x) + 2F_MF_NL(x)]\ \sin^2\alpha + F_N^2$	$a - b\ \sin^2\alpha$
I(-) - I(+)	$4\ F_MF_N\ L(x)\ \sin^2\alpha$	0
SANS		
I(Q)	$F_M^2\ L^2(x)\ \sin^2\alpha + F_N^2$	$2a - b\ \sin^2\alpha$

$d\sigma/d\Omega\ (ij)(Q,\alpha) = C_{ij}\ S(Q,\alpha) + D_{ij}\ F_M^2(Q)$

$a(x)= L(x) / x$, $b(x)= L^2(x)-1+3\ a(x)$ $x=M_{cr}V_p\mu_0H_{eff} / kT$

ij	C_{ij}	D_{ij}
	POLARIS	
I(++)	$[F_M\ L(x)\ \sin^2\alpha\ -\ F_N]^2$	$a\ \sin^2\alpha - b\ \sin^4\alpha$
I(- -)	$[F_M\ L(x)\ \sin^2\alpha\ +\ F_N]^2$	$a\ \sin^2\alpha - b\ \sin^4\alpha$
I(+ -),I(-+)	Purely magnetic	Purely magnetic
	SANSPOL	
I(+)	$[F_M^2L^2(x) - 2F_MF_NL(x)]\sin^2\alpha + F_N^2$	$a - b\ \sin^2\alpha$
I(-)	$[F_M^2L^2(x) + 2F_MF_NL(x)]\ \sin^2\alpha + F_N^2$	$a - b\ \sin^2\alpha$
I(-) - I(+)	$4\ F_MF_N\ L(x)\ \sin^2\alpha$	0
	SANS	
I(Q)	$F_M^2\ L^2(x)\ \sin^2\alpha + F_N^2$	$2a - b\ \sin^2\alpha$

Concentrated sample: SANSPOL

Field induced ordering?- Non-perfect alignment of M?

5 vol % Co-FF in C_6D_8 H=0.05 T

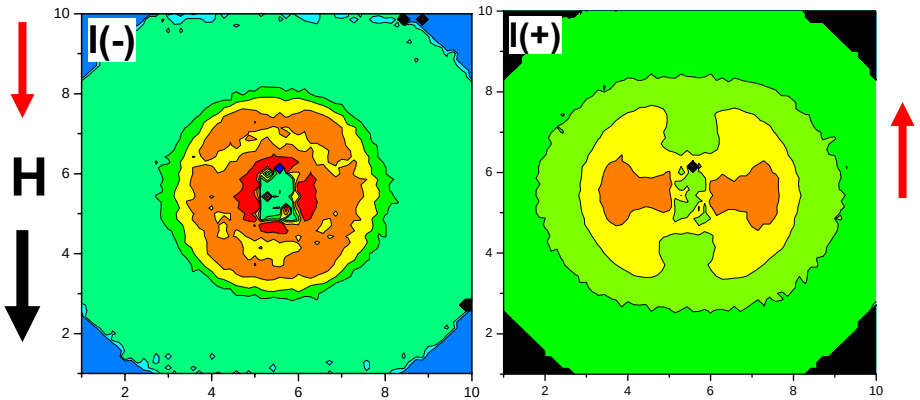

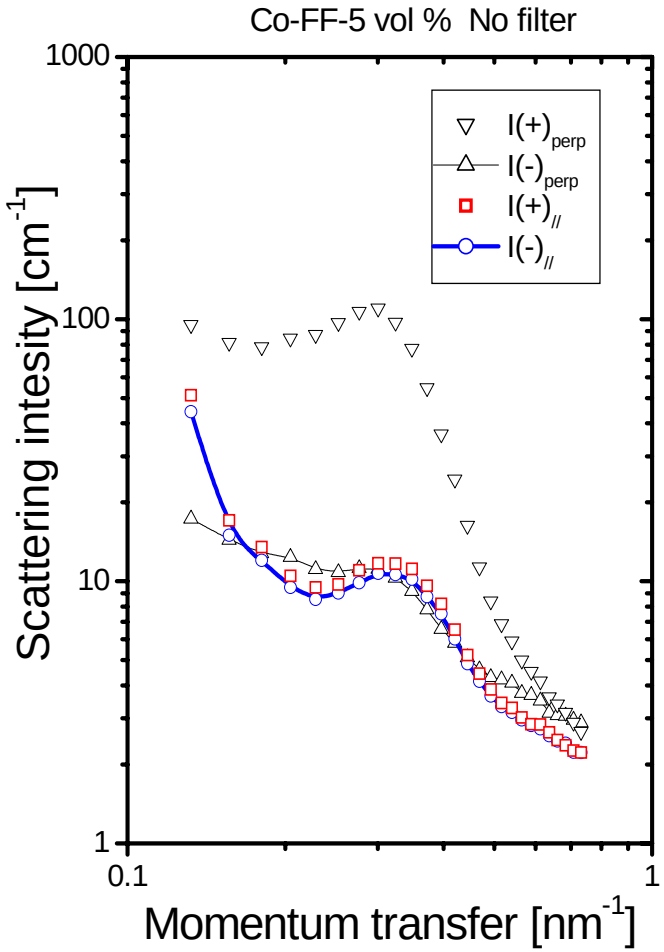

Q⊥H: $I_{\perp}(-) < I_{\perp}(+)$

$S(Q, \perp)$

$Q_{max} = 0.28\ nm^{-1}$

Q//H: $I_{//}(-) = I_{//}(+)$

$S(Q, //)$

$Q_{max} = 0.32\ nm^{-1}$

Concentrated sample:POLARIS

Field induced ordering?- Non-perfect alignment of M?

5 vol % Co-FF in C_6D_8 H=0.05 T

Spin-flip **spin non-flip**

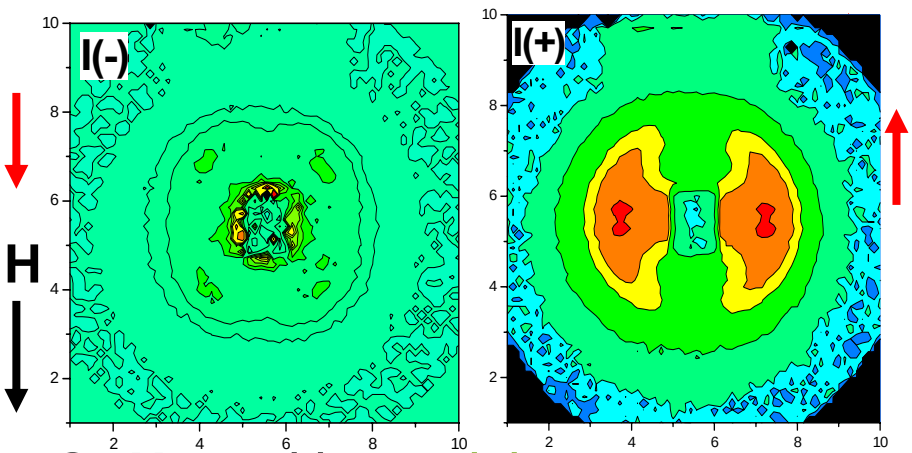

Q⊥H: $I_{\perp}(-)$ < $I_{\perp}(+)$

Q//H: $I_{//}(-)$ < $I_{//}(+)$

S(Q, ⊥) Q_{max} = 0.28 nm^{-1} only in I(+)

S(Q, //) Q_{max} = 0.32 nm^{-1} only in I(+)

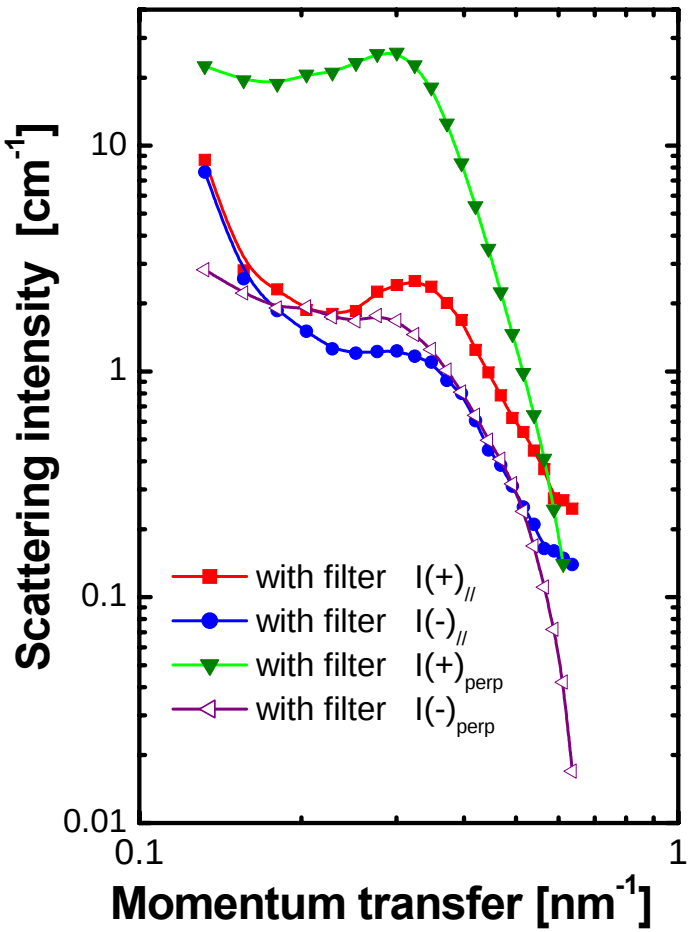

POLARIS I(-): spin-flip

$$I_{sf}(Q) = F_M^2 \{[L^2(x)\, S(Q) - L^2(x) + 1 - 3L(x)/x]\, [\sin^2\alpha * \cos^2\alpha] + (2 - \sin^2\alpha) L(x)/x\}$$

H

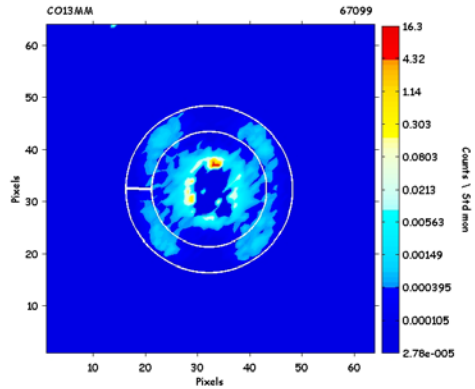

$$I_{sf}(Q)_{x\to\infty} = F_M^2 S(Q,\alpha)\, (\sin\alpha * \cos\alpha)^2$$

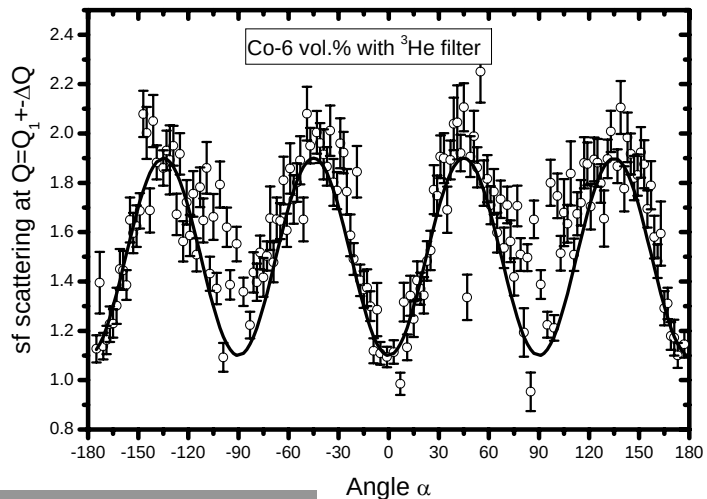

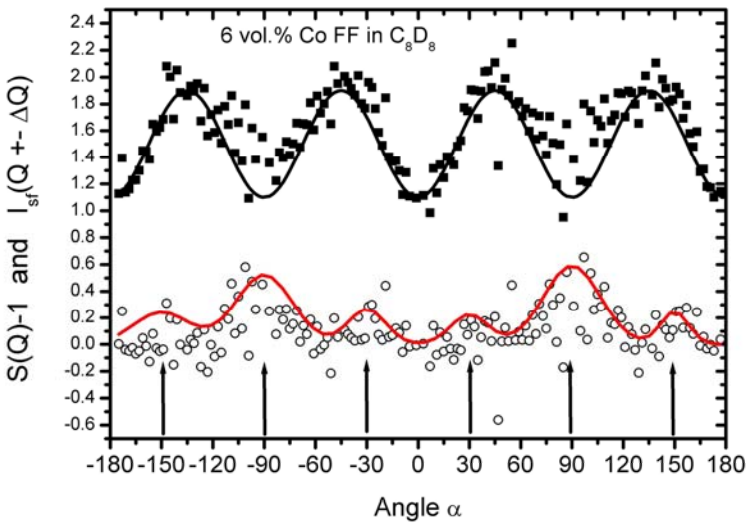

AW Physica B 2005

Polarisation analysis using ^{3}He filters

Uniaxial polarisation analysis in SANS: Additional contrast variation technique

Imperfect alignment of magnetic particle moments

Field induced correlations S(Q,α):
Separation of purely magnetic contribution and purely nuclear contributions

Summary: Nanostructures in Ferrofluids

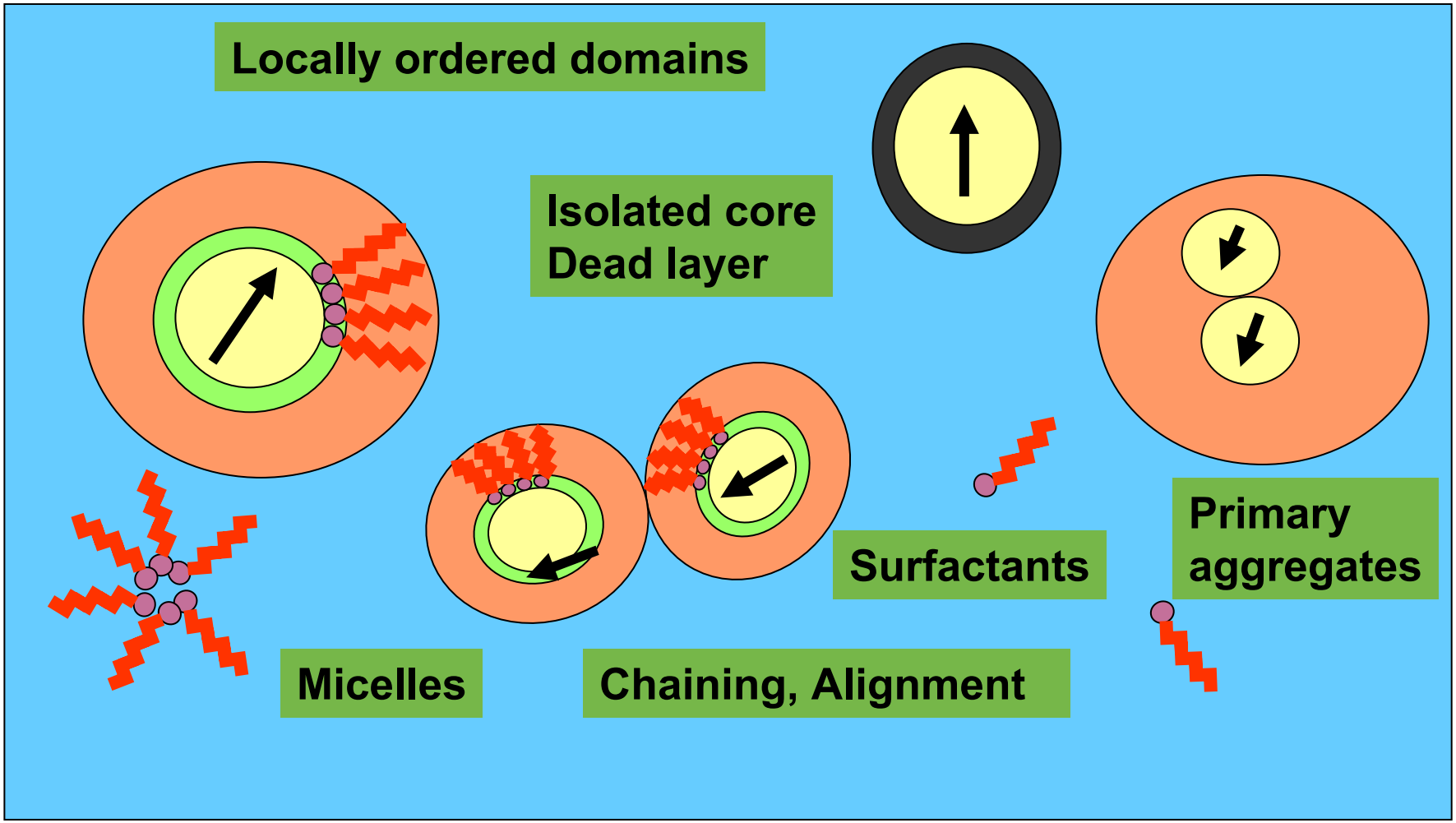

Competing interactions

Magnetic dipol-interaction versus thermal energy

$$\gamma = M^2_{sat}\, V^2_c\, \mu_o / 4\pi\, k_B T$$

Actual ran

Chaining in head-to

Lateral at

DYNAMICAL STUDIES ?

See 3. Oct. 2006

?

ucts:

from uni-axial to lamellar close-packed

uctures (Hess)

II. Applications

1. Magnetic colloids:
   "Ferrofluids"

2. Amorphous magnetic alloys:

   Soft magnetic materials
   Bulk amorphous hardmagnets

Soft magnetic alloys

$Fe_{73.5}$ Si $_{15.5}B_7Nb_3$ Cu_1 : Amorphous ferromagnetic alloy

Improvement of soft magnetic properties by heat treatment

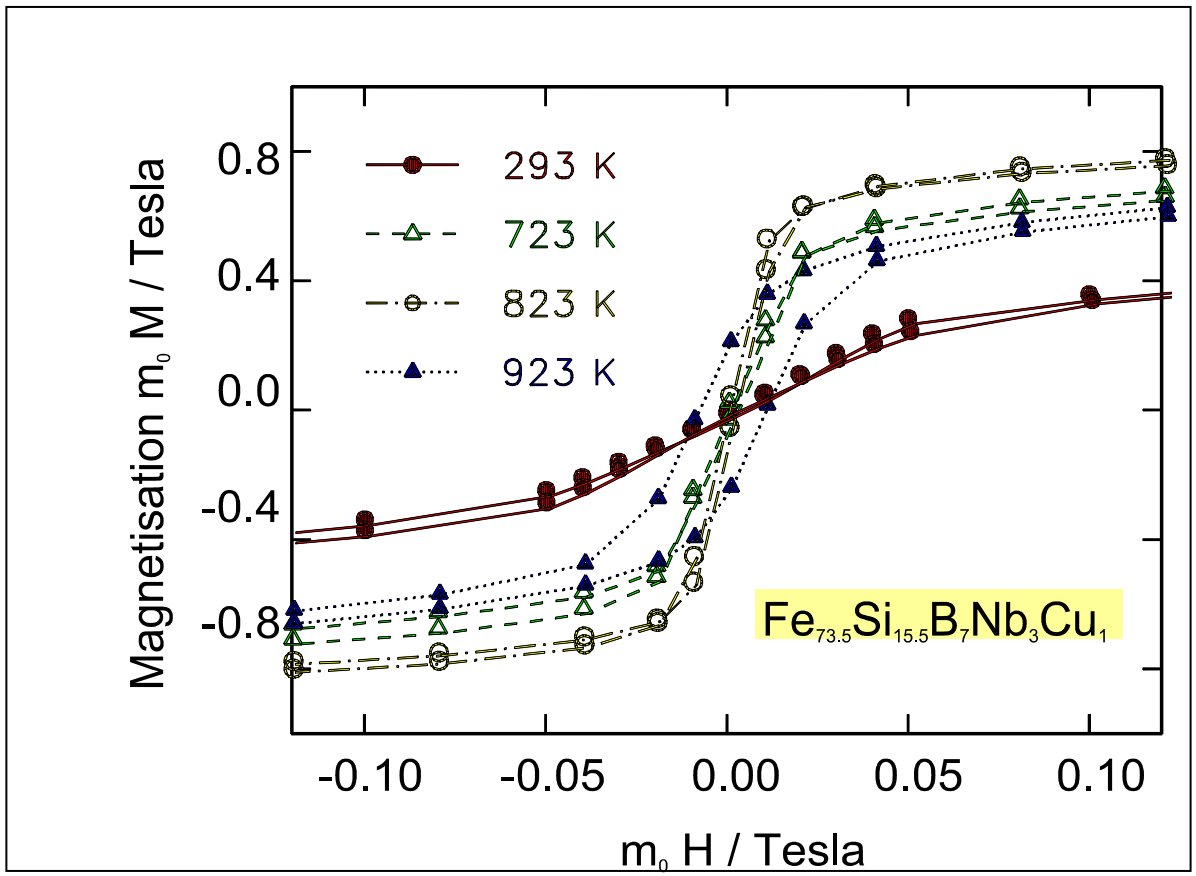

Soft magnetic properties Tc, Hc, Ms

⇕

Magnetic microstructure M(R)

⇕

Crystalline Nanostructure <R> , N(R)

Magnetic contrast variation

Kohlbrecher et al 1997

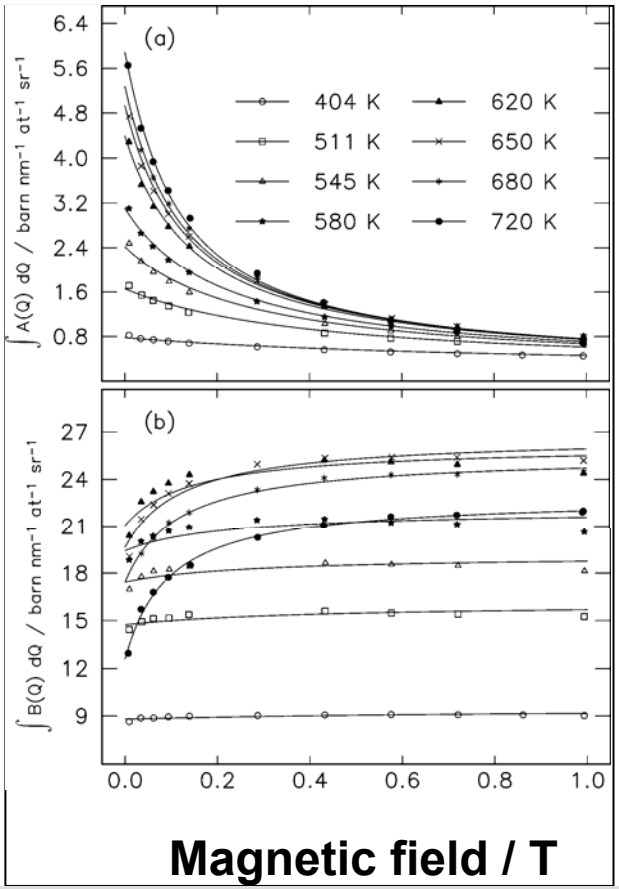

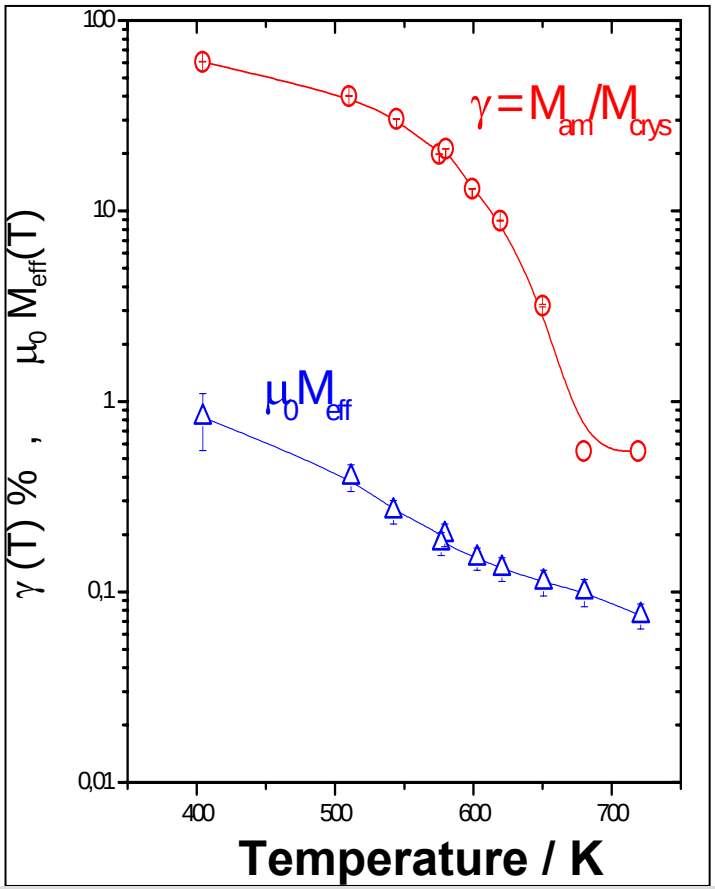

Ferromagnetic single domain in ferromagnetic matrix
Magnetisation ratio $\gamma(T) = M^{am} / M^{cr}$
Effective magnetic field $M_{eff}(T)$

SANSPOL in $Fe_{0.8}\,Nb_{0.07}\,B_{0.125}$: n-Fe (bcc)

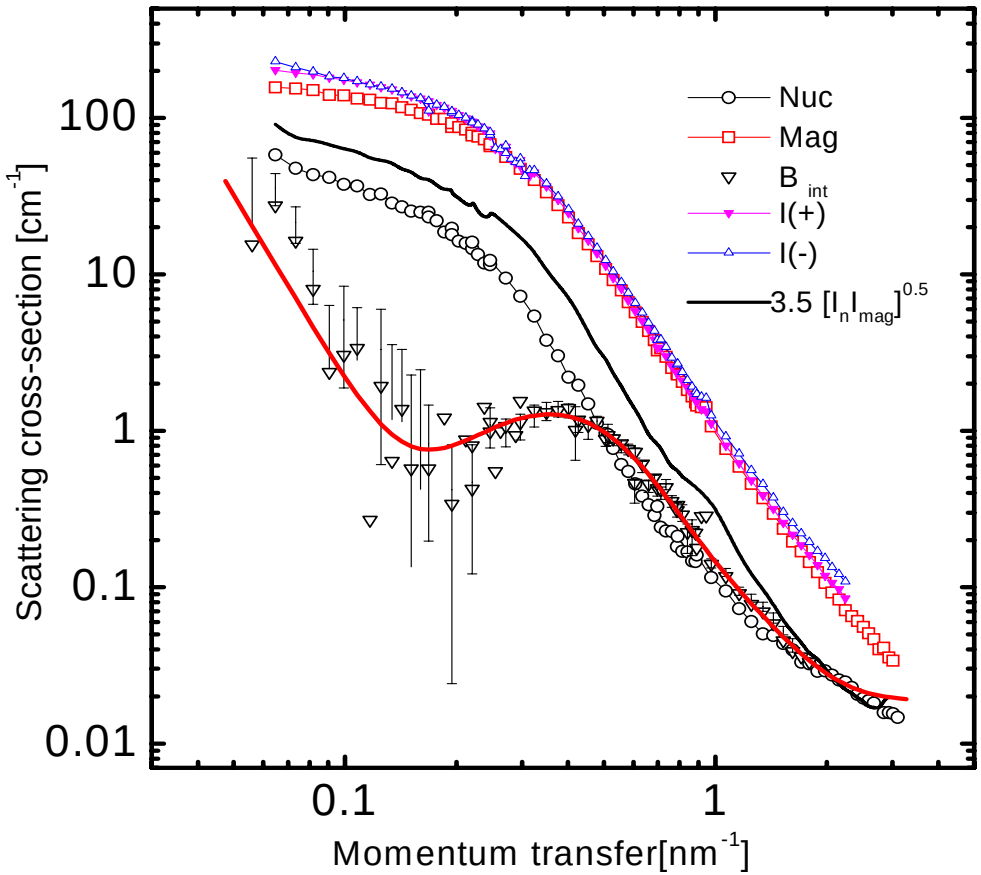

$\Delta\eta^{mag}$ (core) / $\Delta\eta^{mag}$(shell) = 3:
Reduced magnetisation inside the shell

$B_{int}(Q) < 4\,[A(Q)*B(Q)]^{0.5}$
Additional non-magnetic phase

SANSPOL :Fe-Si-B-Nb-Cu 2 % n-Fe_3Si

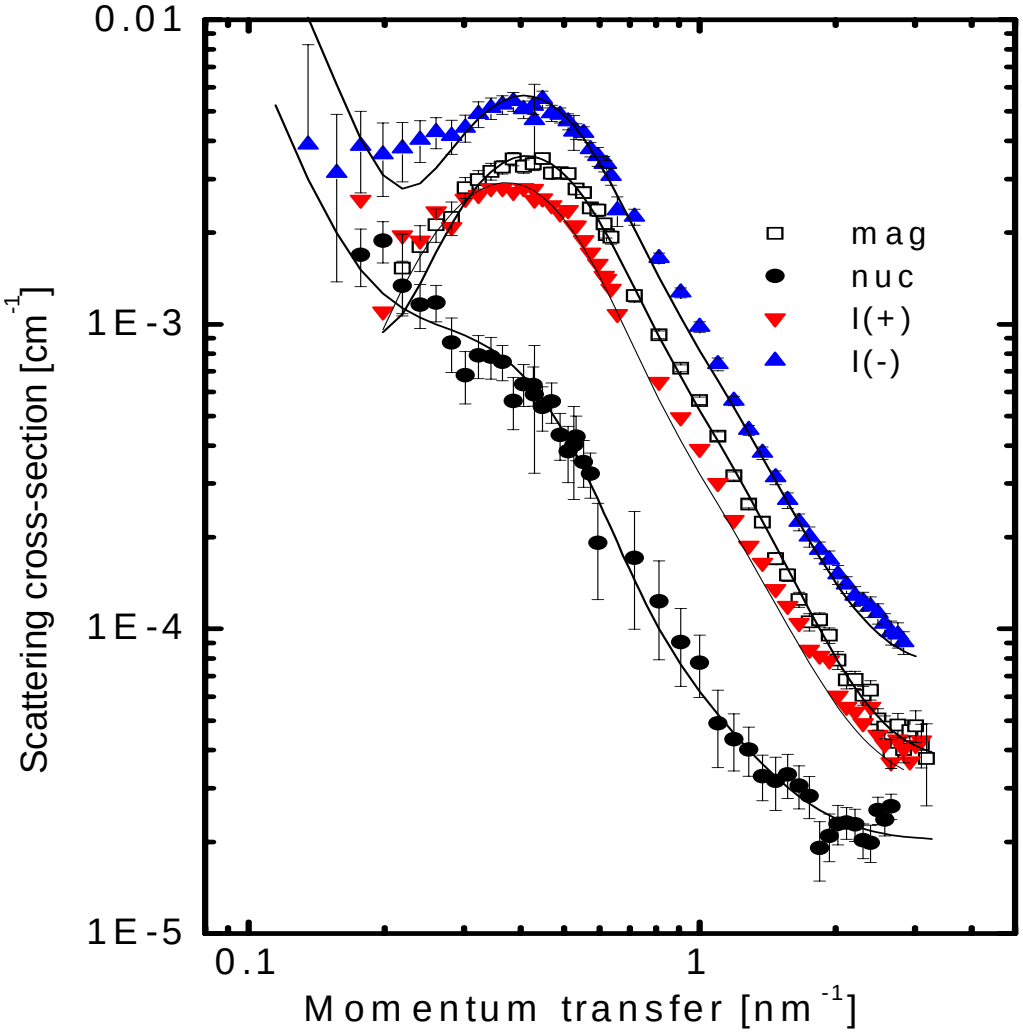

A.W. Physica B (2001) 226-233, Heinemann et al 1999

Diffusion zone: Enrichment of Nb

Contrasts for magnetic core, shell and matrix

$$\Delta\eta_1^{(\pm)} = \eta_1^{nuc} \pm \eta_1^{mag} - \eta_m^{(\pm)}$$
$$\Delta\eta_2^{(\pm)} = \eta_2^{nuc} \pm \eta_2^{mag} - \eta_m^{(\pm)}$$
$$\eta_m^{(\pm)} = \eta_m^{nuc} \pm \eta_m^{mag}$$

$\eta_2^{mag} / \eta_1^{mag} = 0.3$

$\eta_m^{mag} / \eta_1^{mag} = 0.7$

Density profile

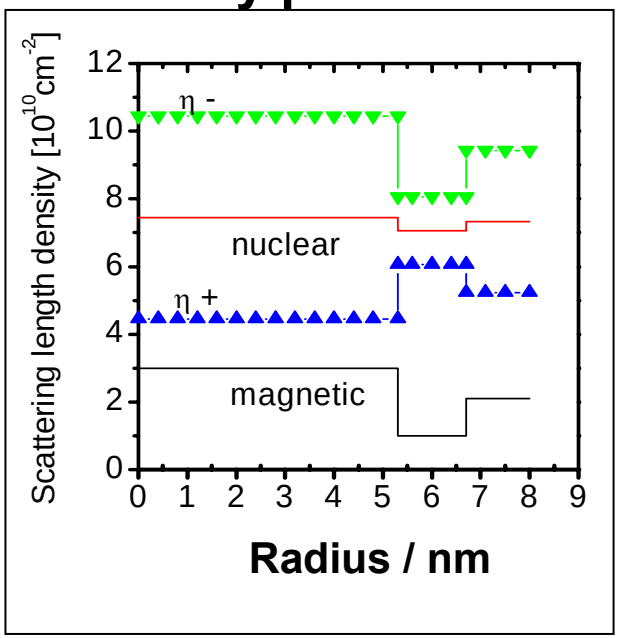

Size distribution

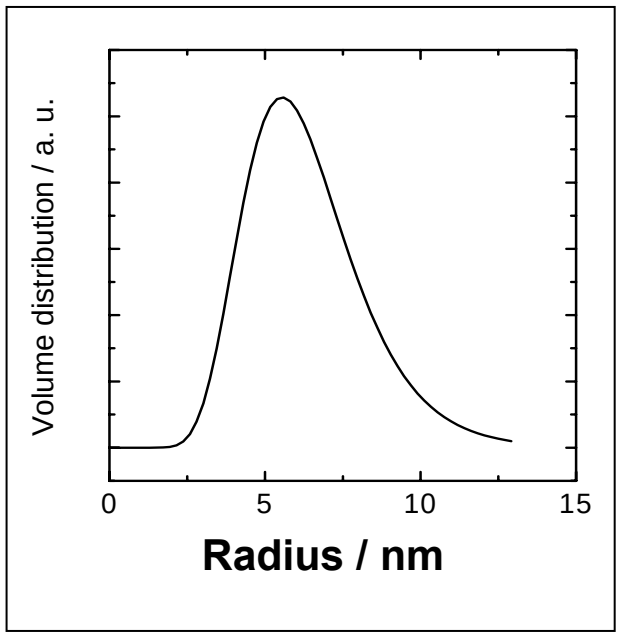

Weak magnetization in the interface between n- Fe_3Si matrix

Magnetic particle scattering

$M^{\perp}$: Projection of magnetization onto a plane perpendicular to the scattering vector Q

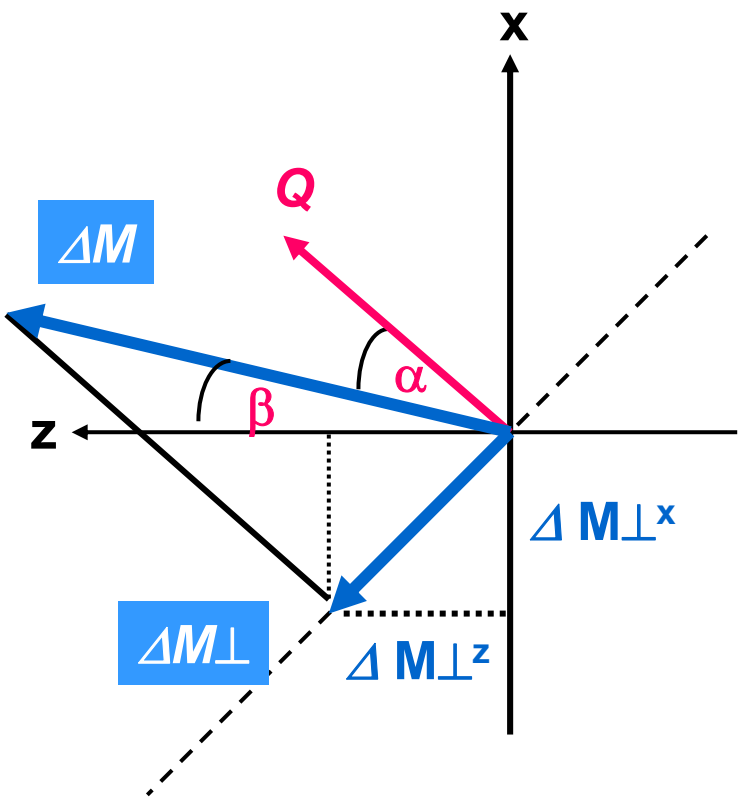

$\angle\beta\,(\Delta M\,,\,z)$

$|M\perp| = |M|\sin\alpha$

$$M\perp^{z} = |M\perp|\cos(90° - (\alpha+\beta)) = |M\perp|\sin(\alpha+\beta) = |M|\sin\alpha\,\sin(\alpha+\beta)$$

$$M\perp^{x} = |M\perp|\sin(90° - (\alpha+\beta)) \quad |M|\sin\alpha\,\cos(\alpha+\beta)$$

$$M\perp^{y} = 0$$

Results: Soft magnetic metallic glasses

Diffusion controlled enrichment of Nb around nanocrystals: magnetic dilution:

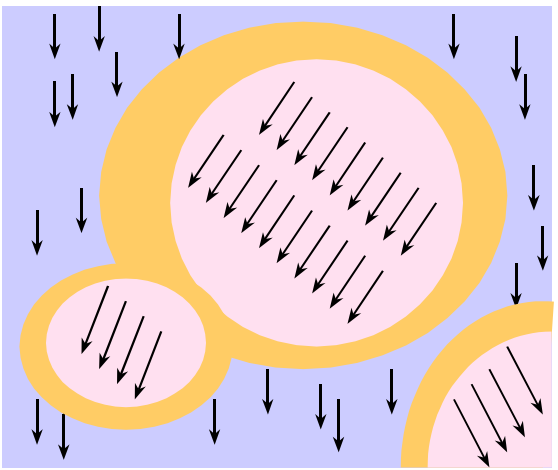

$$\eta_1^{(\pm)} = \eta_1^{nuc} \pm \eta_1^{mag}$$

$$\eta_2^{(\pm)} = \eta_2^{nuc} \pm \eta_2^{mag}$$

$$\eta_m^{(\pm)} = \eta_m^{nuc} \pm \eta_m^{mag}$$

Weak magnetic interlayer reduces ferromagnetic coupling between matrix and nanocrystals

$Nd_{60}Fe_xCo_{30-x}Al_{10}$ alloys

Magnetic Properties

Non-magnetic

Soft-magnetic

hard-magnetic

versus

compositions and cooling conditions

Mold-casting

Melt-spinning

Magnetic and crystalline microstructure

Present example : $Nd_{60}Fe_{20}Co_{10}Al_{10}$

Magnetization at H=1T

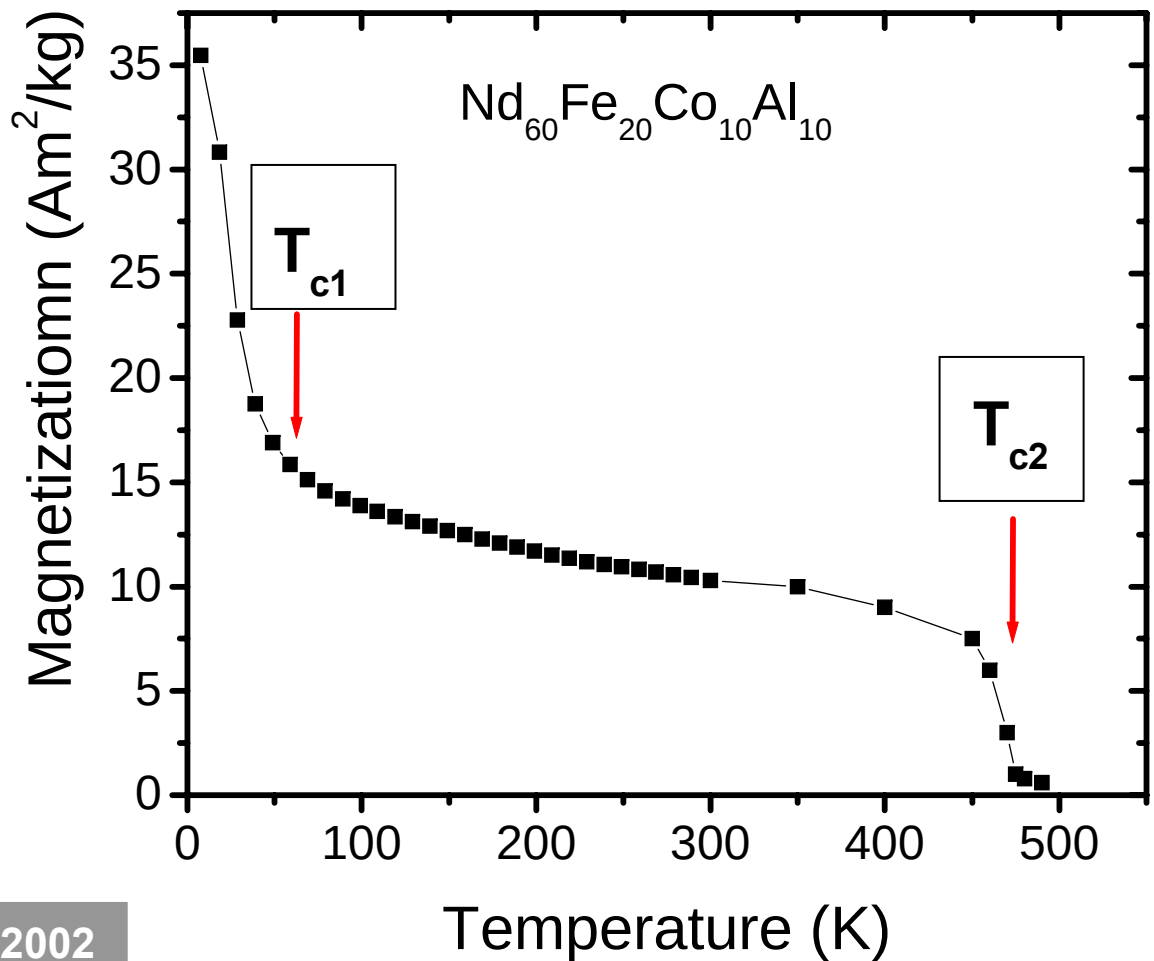

Kumar et al. 2002

Non-polarised SANS in $Nd_{60}Fe_{20}Co_{10}Al_{10}$

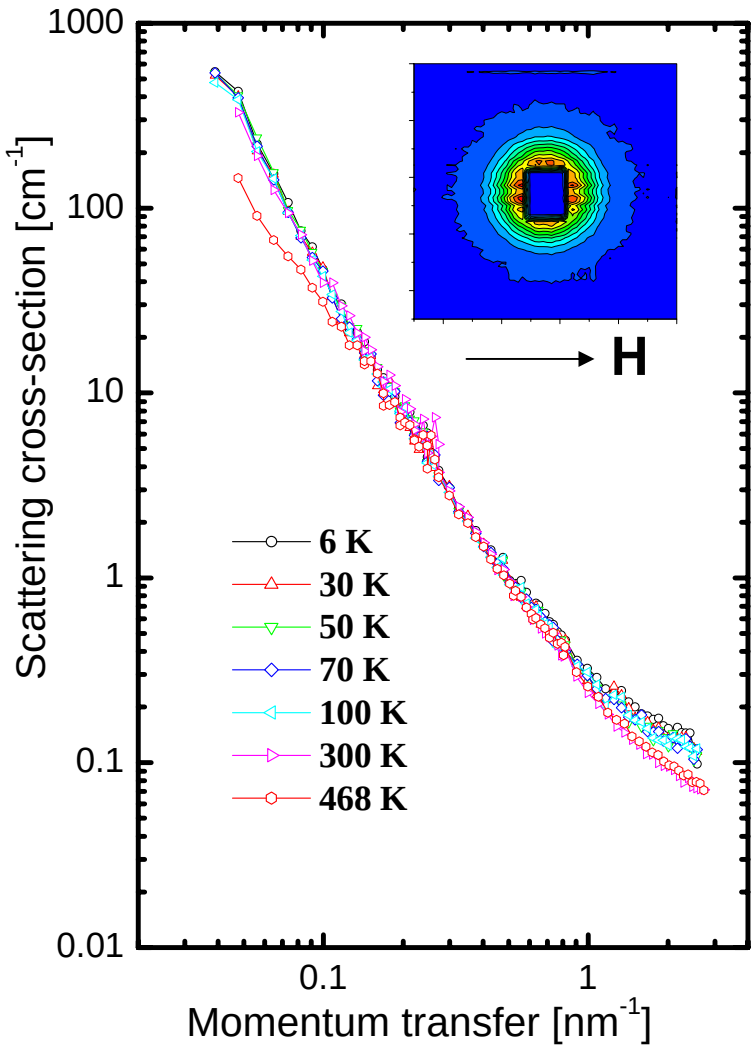

H= 1T

Almost isotropic patterns

Near Tc_2: Decrease of I(Q) at low Q

Weak magnetic contribution

SANSPOL in $Nd_{60}Fe_{20}Co_{10}Al_{10}$

I(on) and I(off)

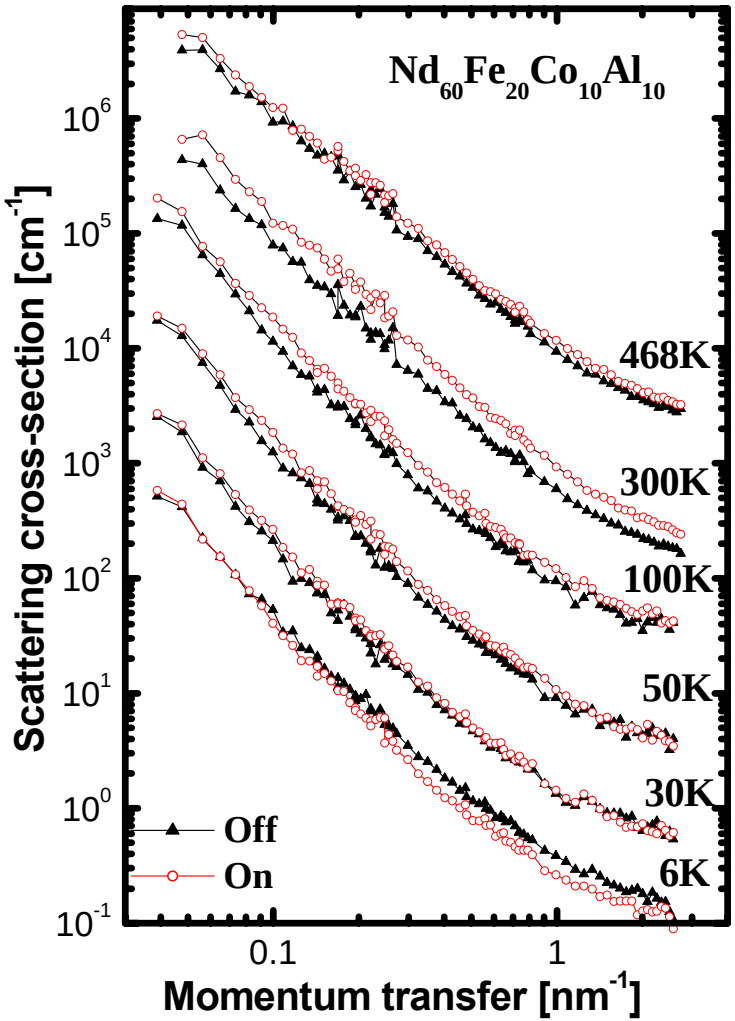

I(on)-I(off)

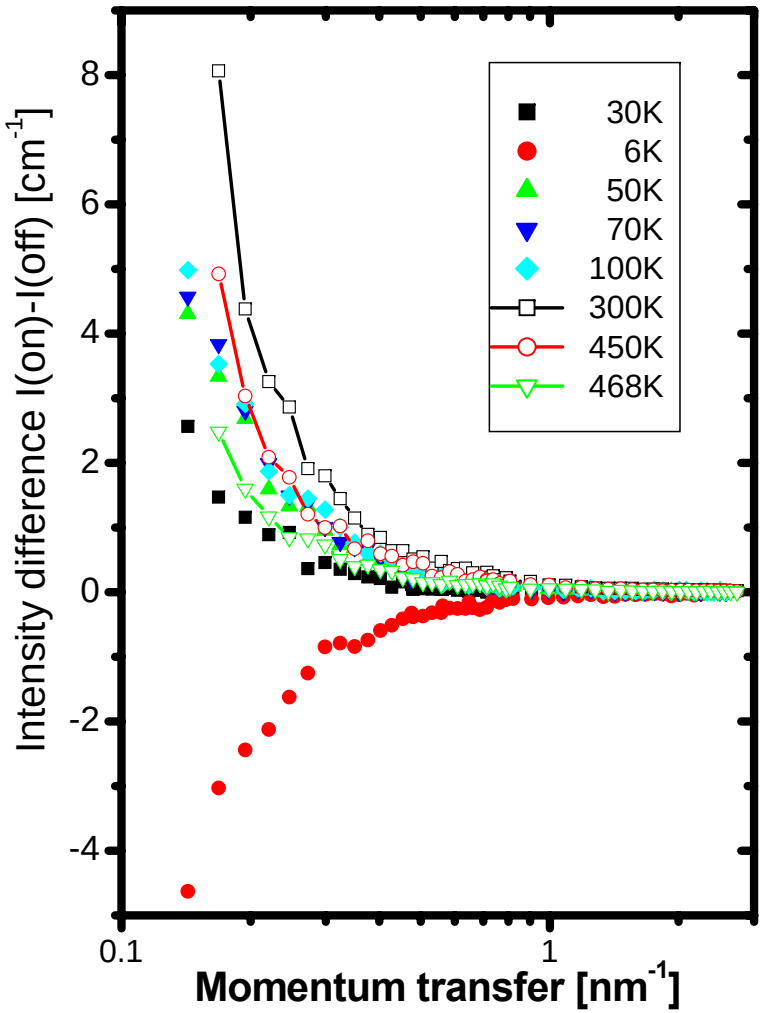

$Nd_{60}Fe_{20}Co_{10}Al_{10}$

Volume distributions

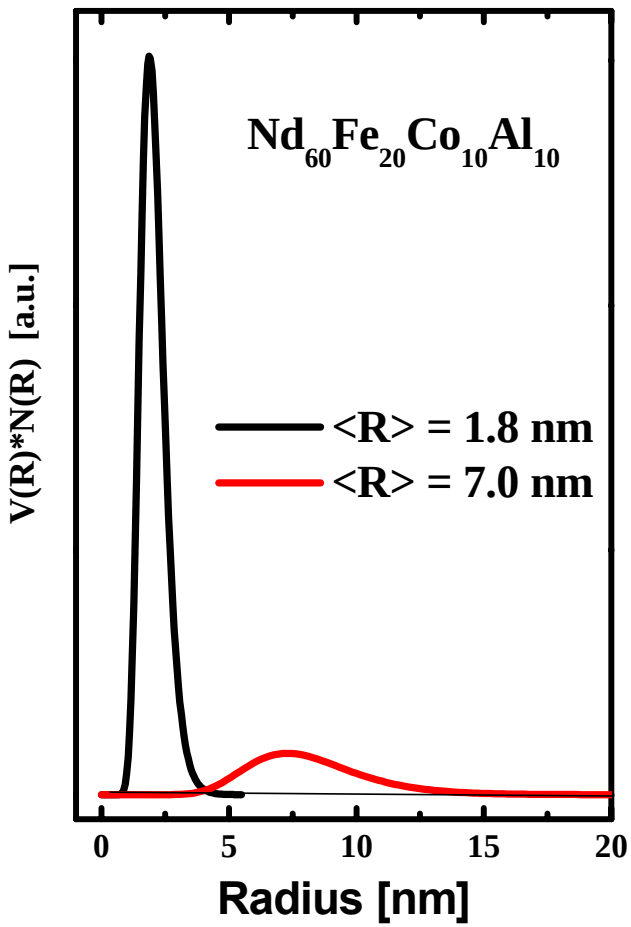

Scattering contrasts

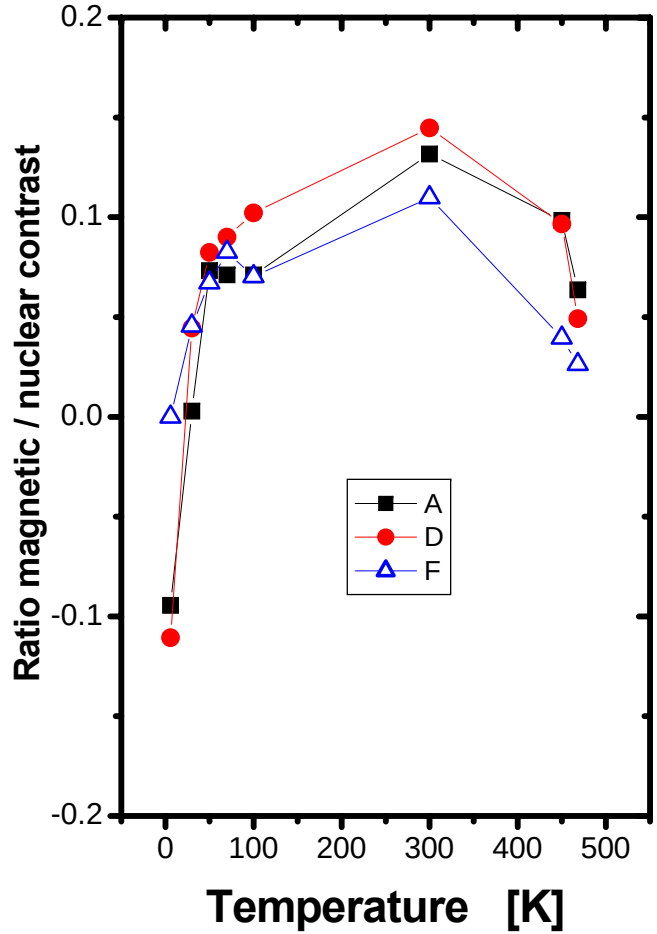

Scattering length densities in $Nd_{60}Fe_{20}Co_{10}Al_{10}$

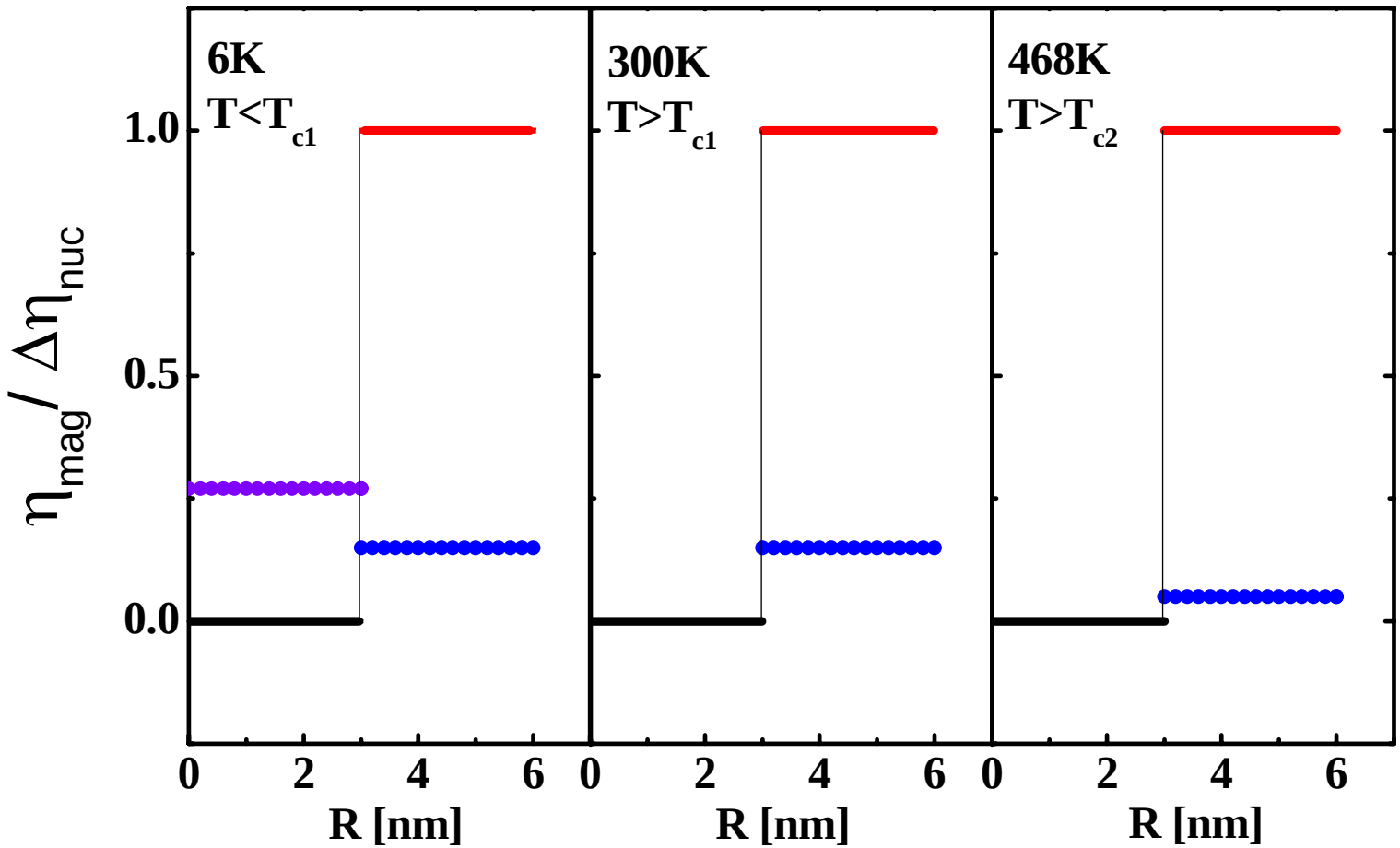

Microstructure model $Nd_{60}Fe_{20}Co_{10}Al_{10}$

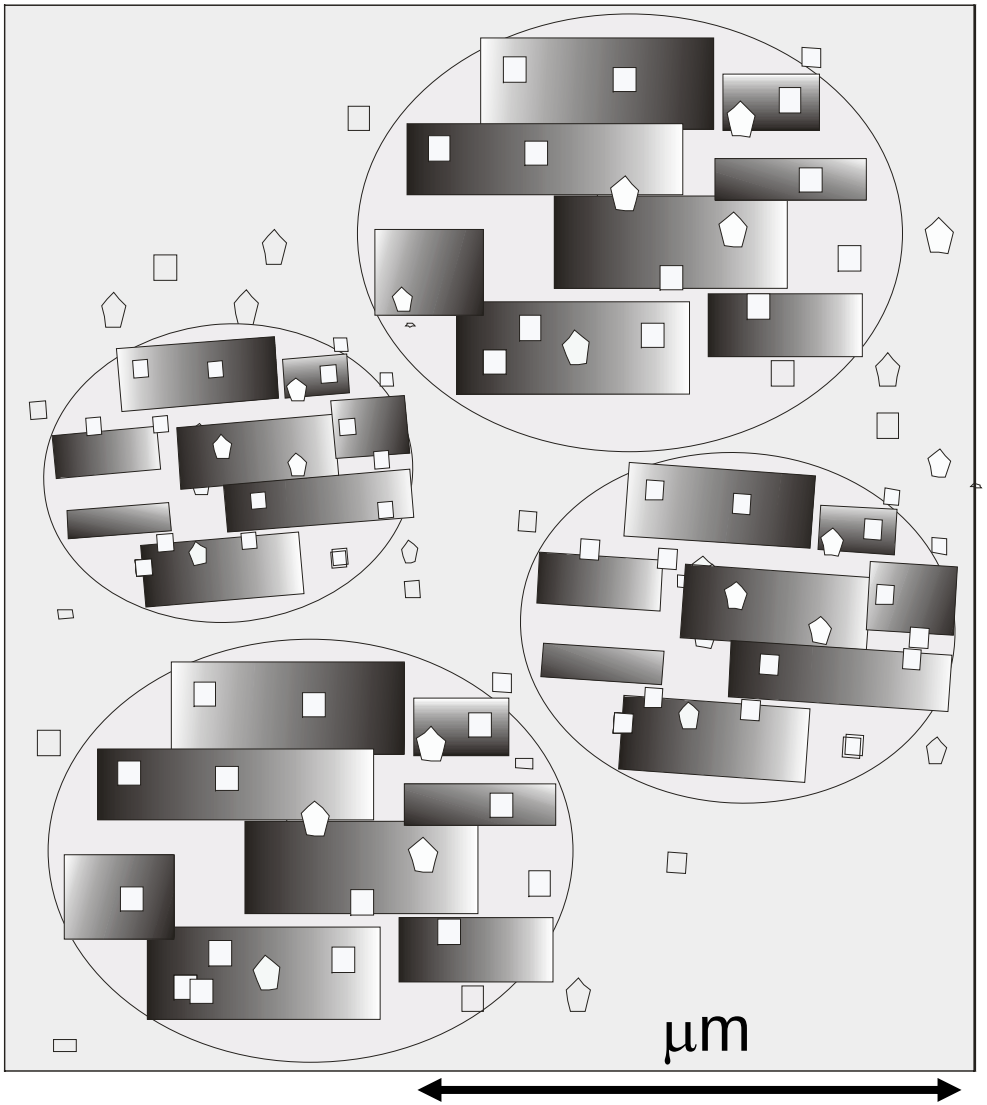

Fe-rich crystalline phase

Nd-rich crystalline phases f_1 and f_2

Nd-rich amorphous phase f_3

Nanostructure $Nd_{60}Fe_{20}Co_{10}Al_{10}$ $T > T_{c2}$

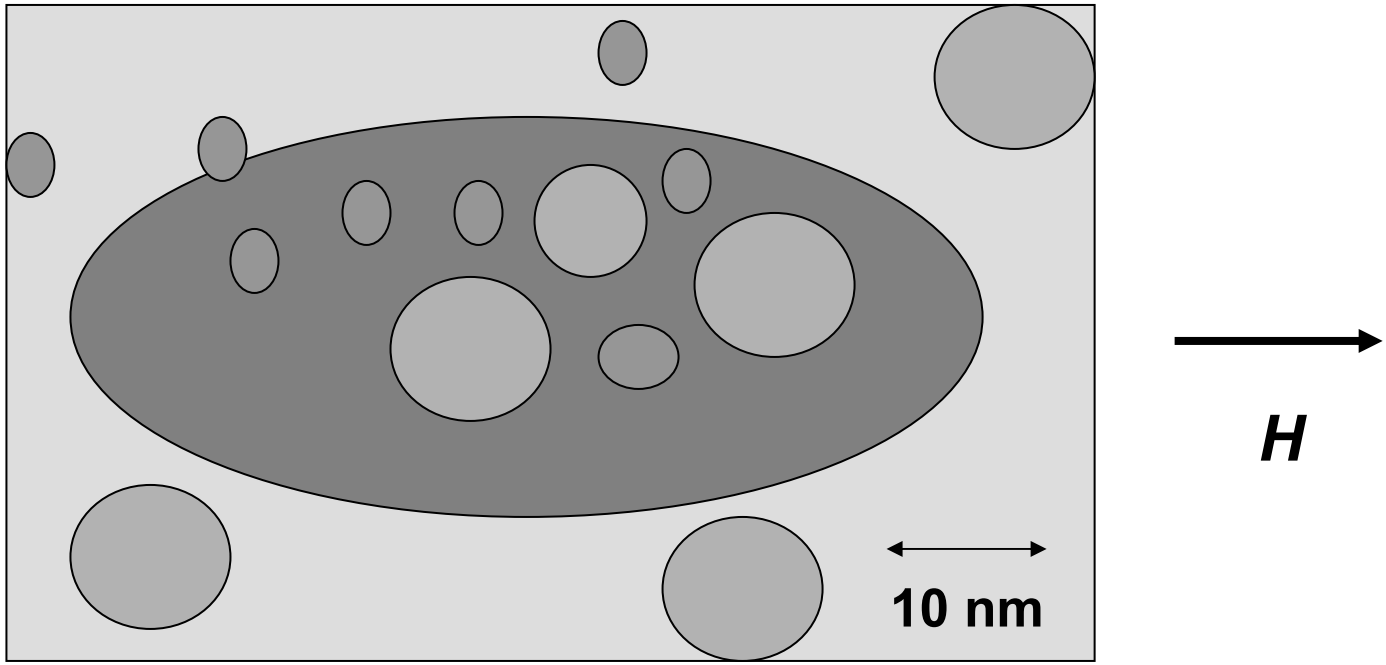

Nd-rich Amorphous f_3	Nd-rich crystalline f_1 and f_2	Fe-rich crystalline

$Nd_{60}Fe_{20}Co_{10}Al_{10}$ $Tc_1 < T < Tc_2$

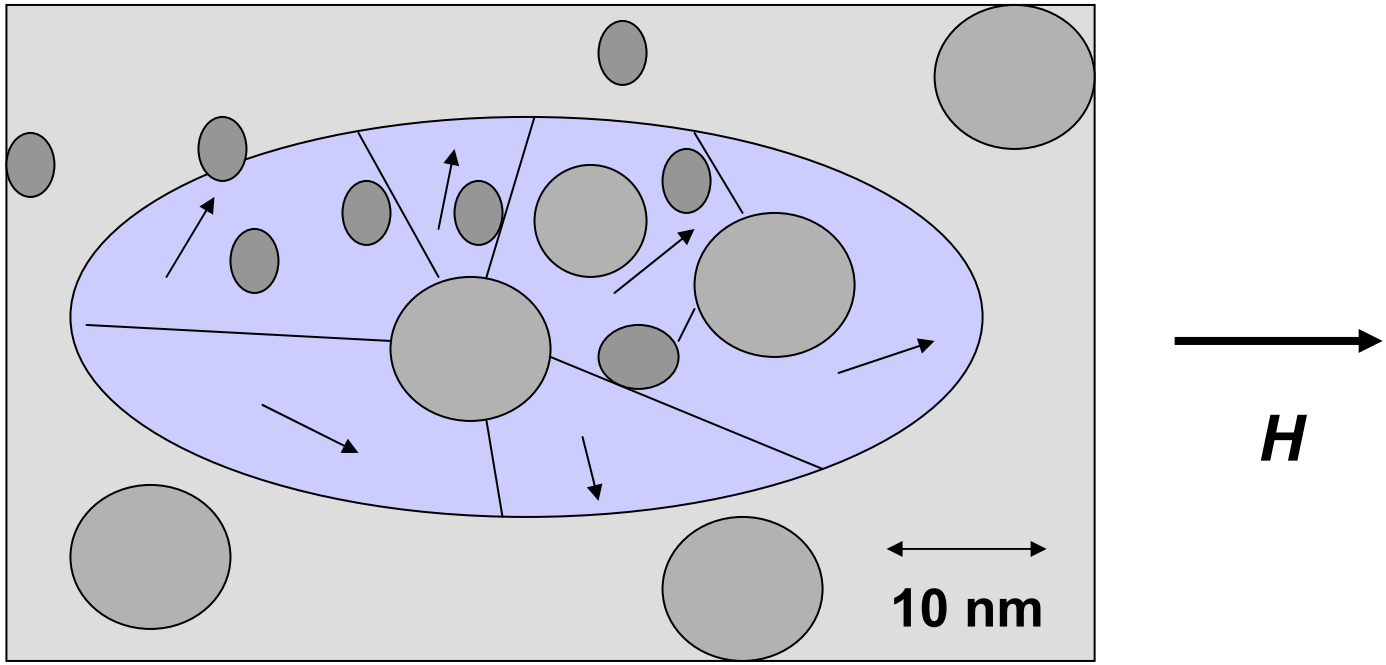

Nd-rich amorphous paramagnetic	Nd-rich crystalline paramagnetic	Fe-rich crystalline Magnetic domains
Pinning centers		Hard magnetic

$Nd_{60}Fe_{20}Co_{10}Al_{10}$ $T < Tc_1$

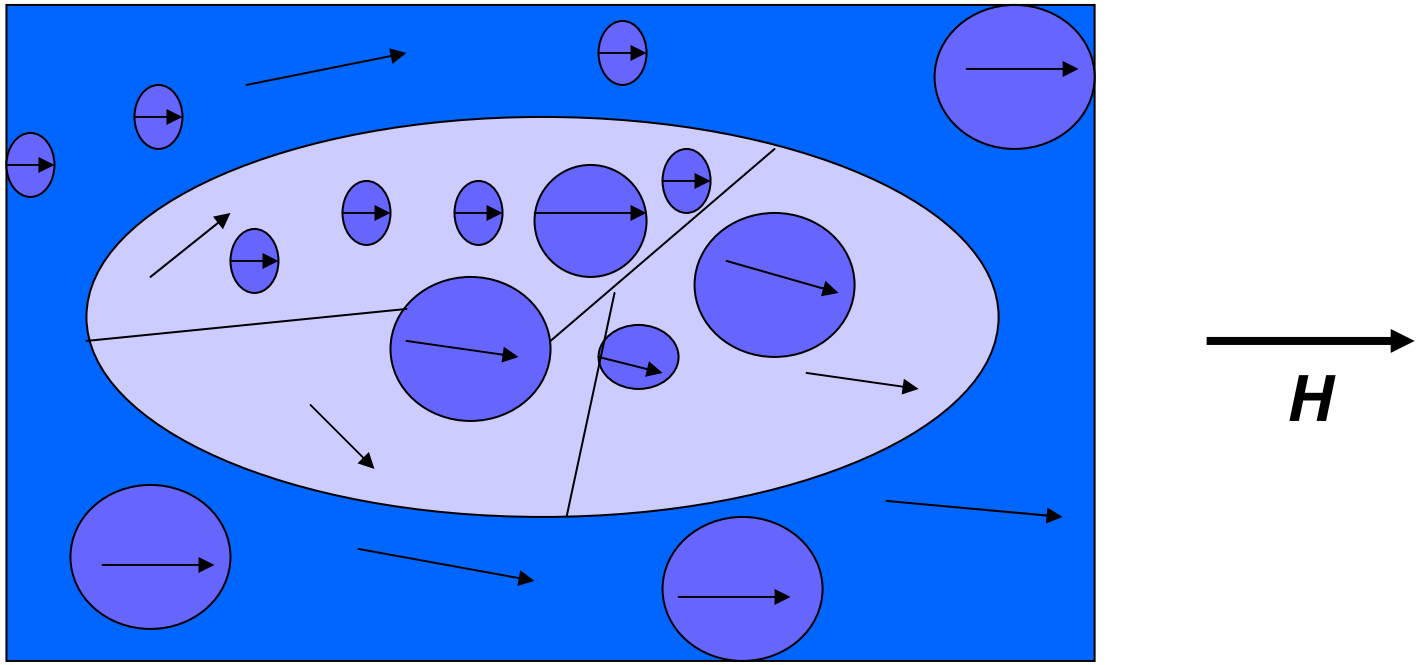

Nd-rich amorphous ferromagnetic

Nd-rich crystalline ferromagnetic

Fe-rich crystalline ferromagnetic

Soft-magnetic

Results Nd-Fe-Al-Co alloys

- Nanosized Nd-rich crystalline and amorphous particles embedded in Fe-rich ferromagnetic crystals.
- They are paramagnetic between T_{c1} and T_{c2}.
- They act as pinning center for magnetic domains (hard-magnetic behaviour).
- Below T_{c1} they are ferromagnetic with higher magnetization than Fe-rich crystals.

Magnetic Nanostructures Investigated by Small Angle Neutron Scattering

Albrecht Wiedenmann

VIII School of Neutron Scattering
„Francesco Paolo Ricci“
Structure and Dynamics of magnetic systems

http://www.hmi.de/bereiche/SF/SF3/methods/sans/index_en.html

III. Practice of SANS

1. Instrument V4

2. SANS-Experiment,
Data Reduction and analysis

3. Tutorial and problem class

SANSPOL Instrument (V4 at hmi)

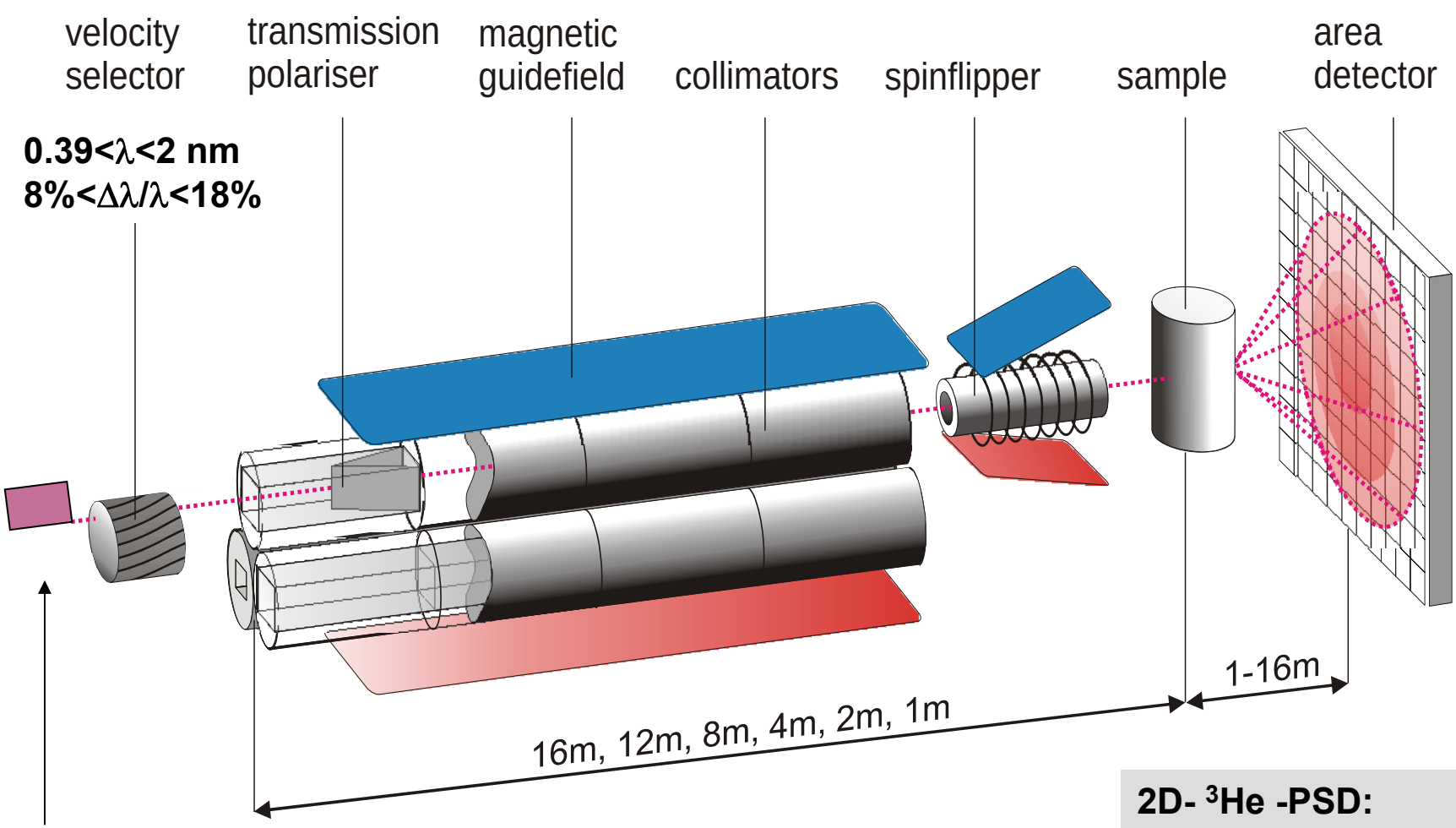

Curved neutron guide:
λ_{cutoff}= 0.39 nm

2D- ^{3}He -PSD:
64 cm*64 cm
1cm^2/pixel

SANSPOL Instrument V4

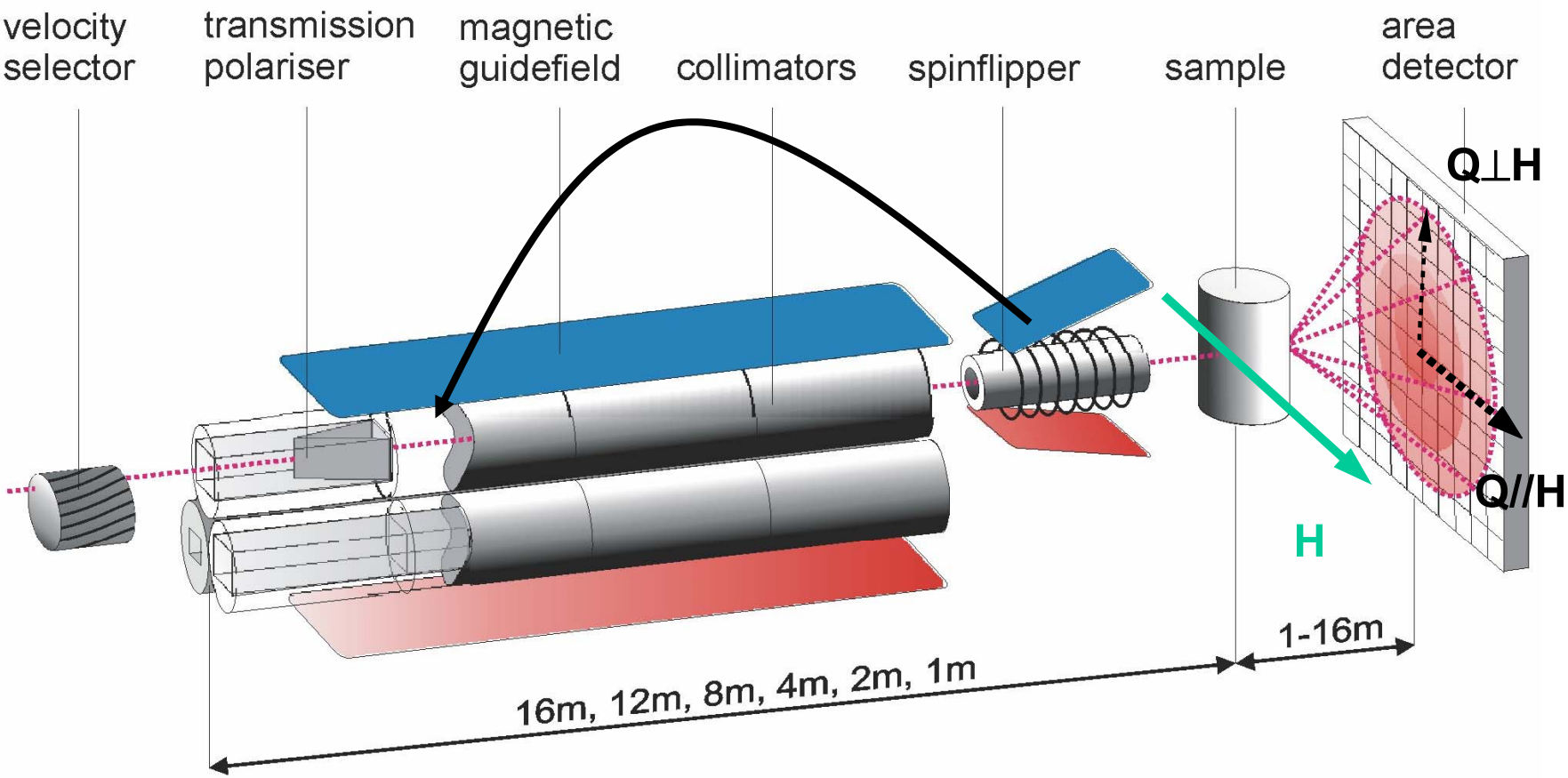

Th. Keller et al (2000) Nucl. Instr.

SANSPOL components

Transmission-Polariser $\lambda > 0.48$ nm

V-shaped l = 1.8m, α = 8.33 mrad

CoFe/Si Supermirror m = 2

FeNdB magnets: 7*100mm H=1kGs

Magnetic guide field

Permanent magnets NdFeB on steel rods

Steel plates ST37, H= 10 Gs in centre

Spin-flipper

B_0=100Gs , dB/dl=3Gs/cm

RF-coil l=5cm, 3 w/cm:

$\omega_0 = \gamma B_0$= 300kHz =Larmor frequency

B_1= 20 Gs

Collimator

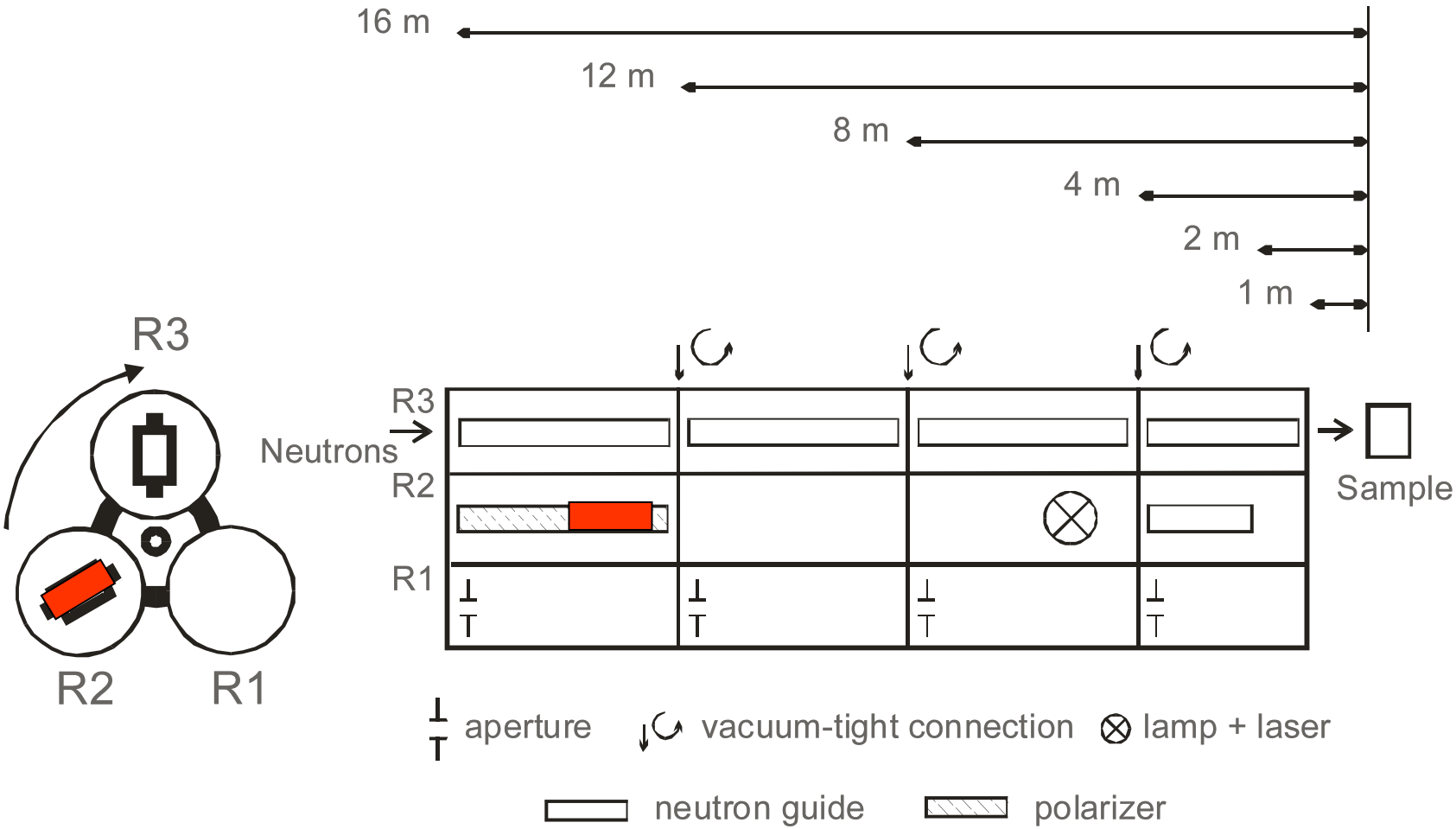

Transmission -Polariser

Transmission-Polariser

Critical angle for total reflection:

$\Theta_{c\,(up)}$ **[mrad]= m * 1.73 λ**

$\Theta_{c\,(dn)}$ **[mrad]= 0.7* λ**

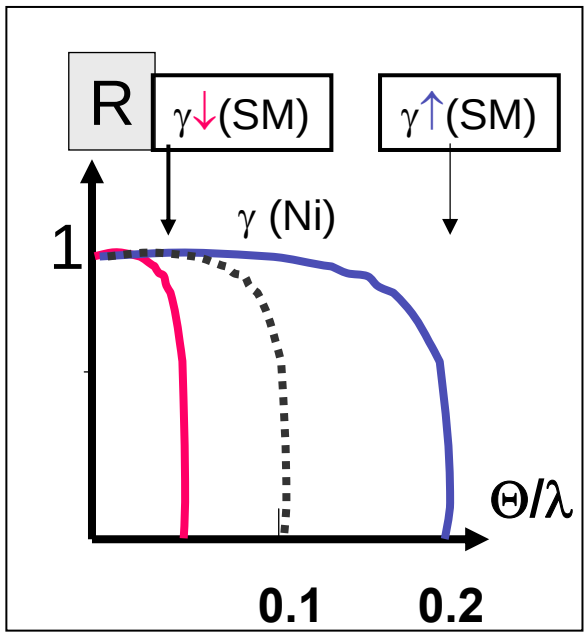

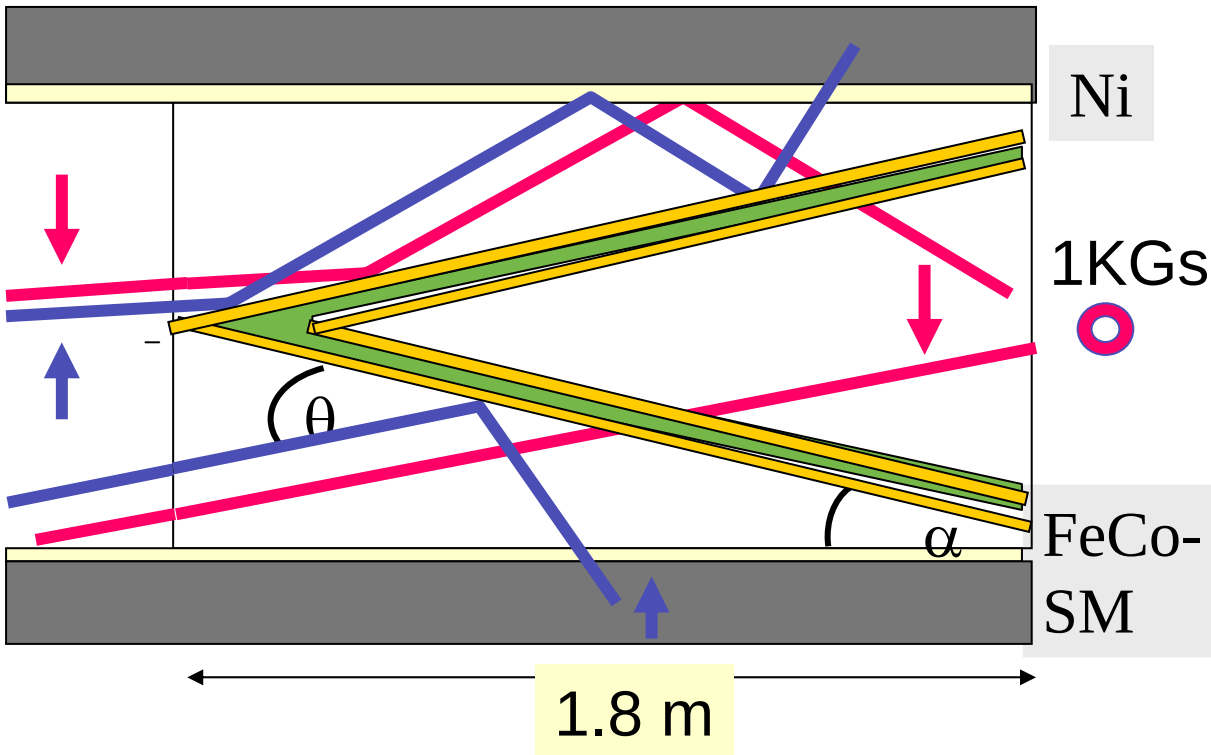

α = 8.33 mrad

m = 2

No divergence of incident neutrons

$$\Theta_{eff} = \alpha$$

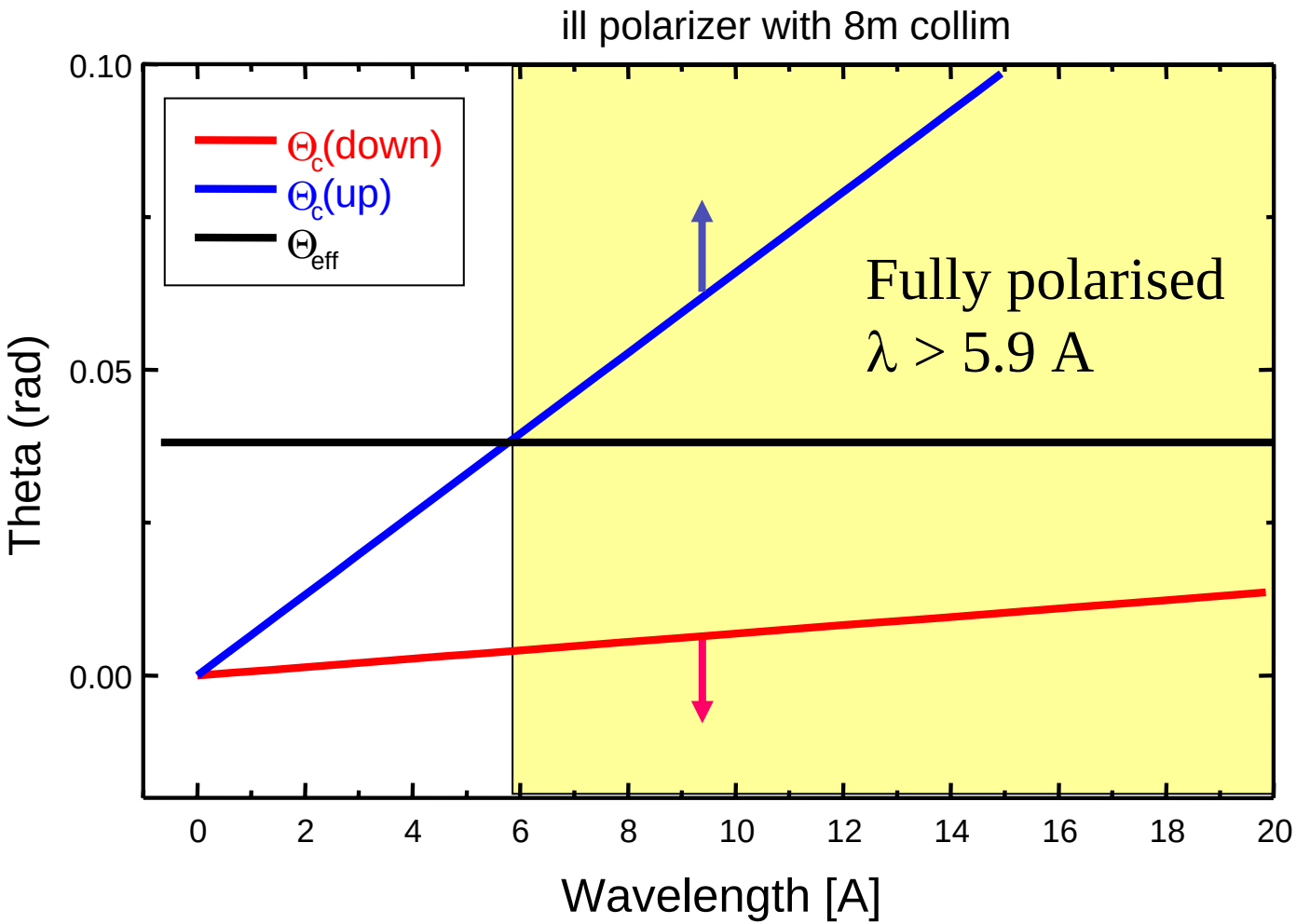

Divergence of incident neutrons

Critical angle for total reflection:

$\Theta_{c\ (up)}$ [mrad]= m * 1.73 λ

$\Theta_{c\ (dn)}$ [mrad]= 0.7* λ

Prototype Fe-Si SM m=3.8

$$\Theta_{eff} = \alpha \pm \delta iv$$

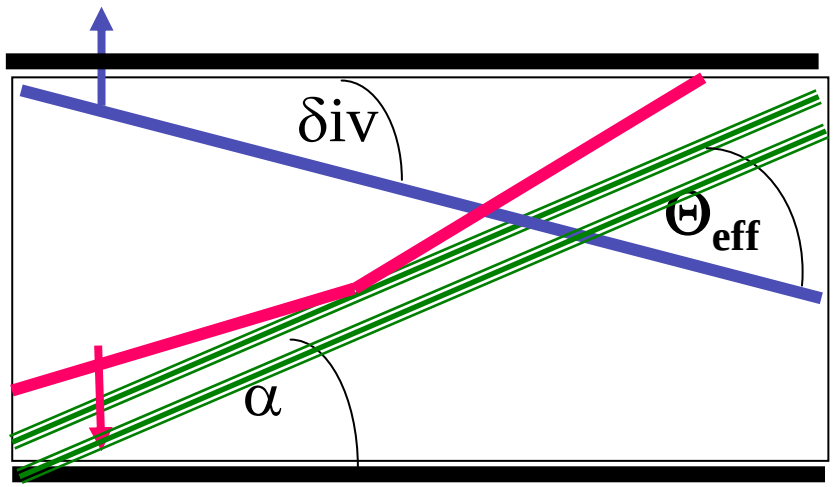

For collimators:

$$\delta iv = \phi / L$$

For neutron guides m=1

$$\delta iv = 1.73\ \lambda$$

Decrease of Polarisation

Divergence from collimators

$$\Theta_{eff} = \alpha \pm \phi / L$$

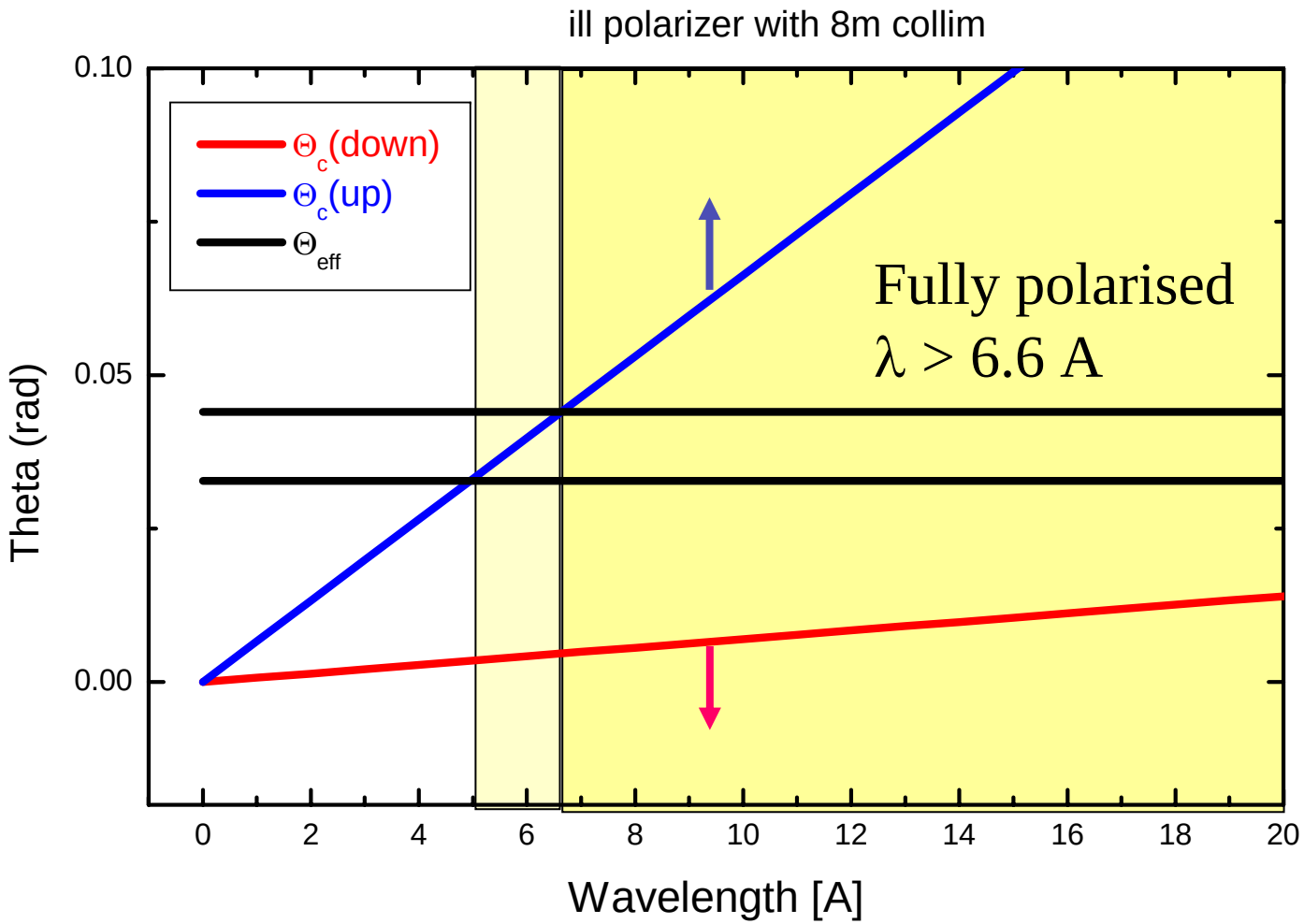

Divergence from a neutron guide

Ni-guide: m=1 $\Theta_{eff} = \alpha \pm 1.73 * \lambda$

ILL prototype polariser behind a Ni-guide

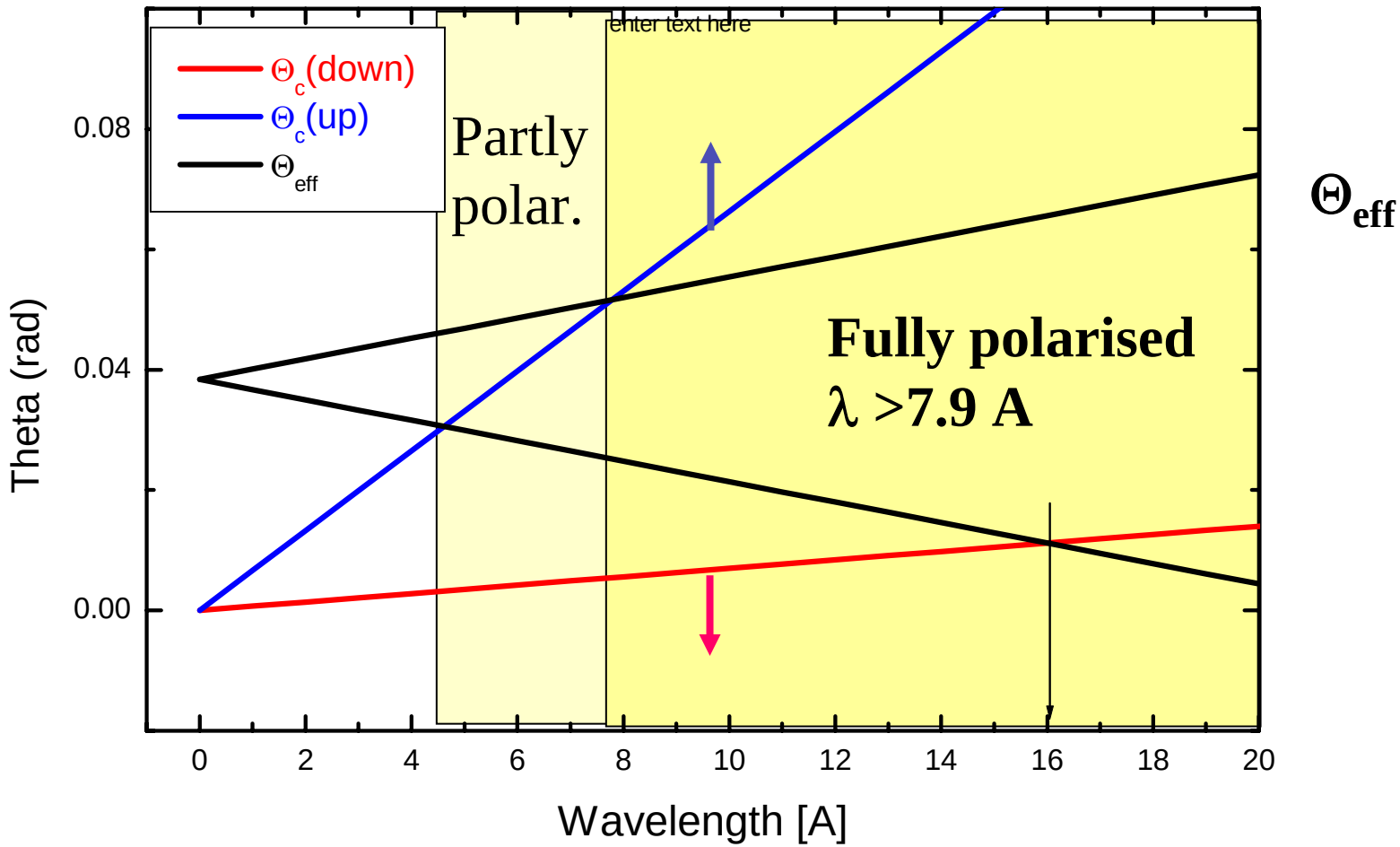

V4 polariser behind a neutron guide

Ni-guide: m=1 $\Theta_{eff} = \alpha \pm 1.73 * \lambda$

V4-m=2 polariser behind a Ni-guide

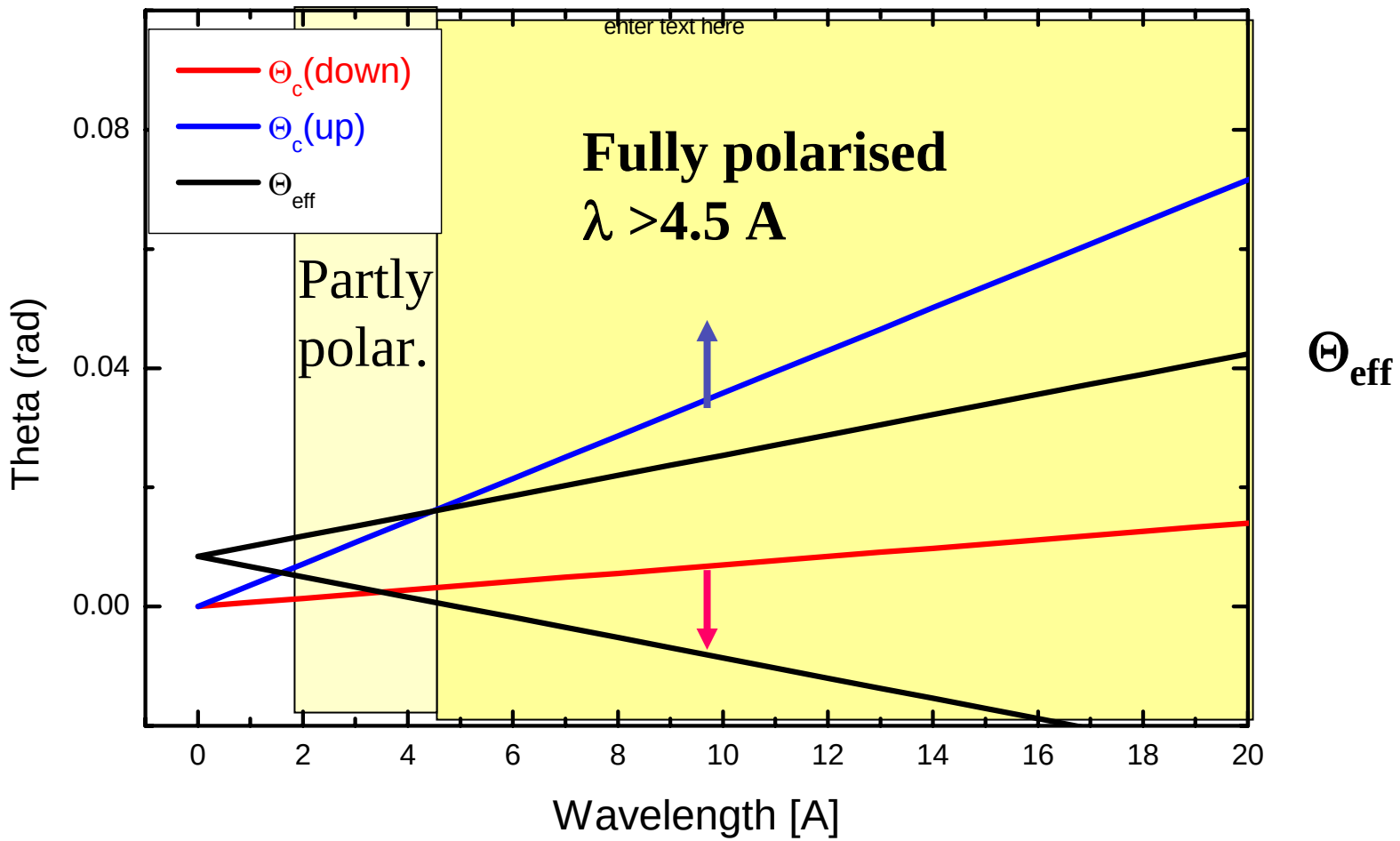

Magnetic guide-field

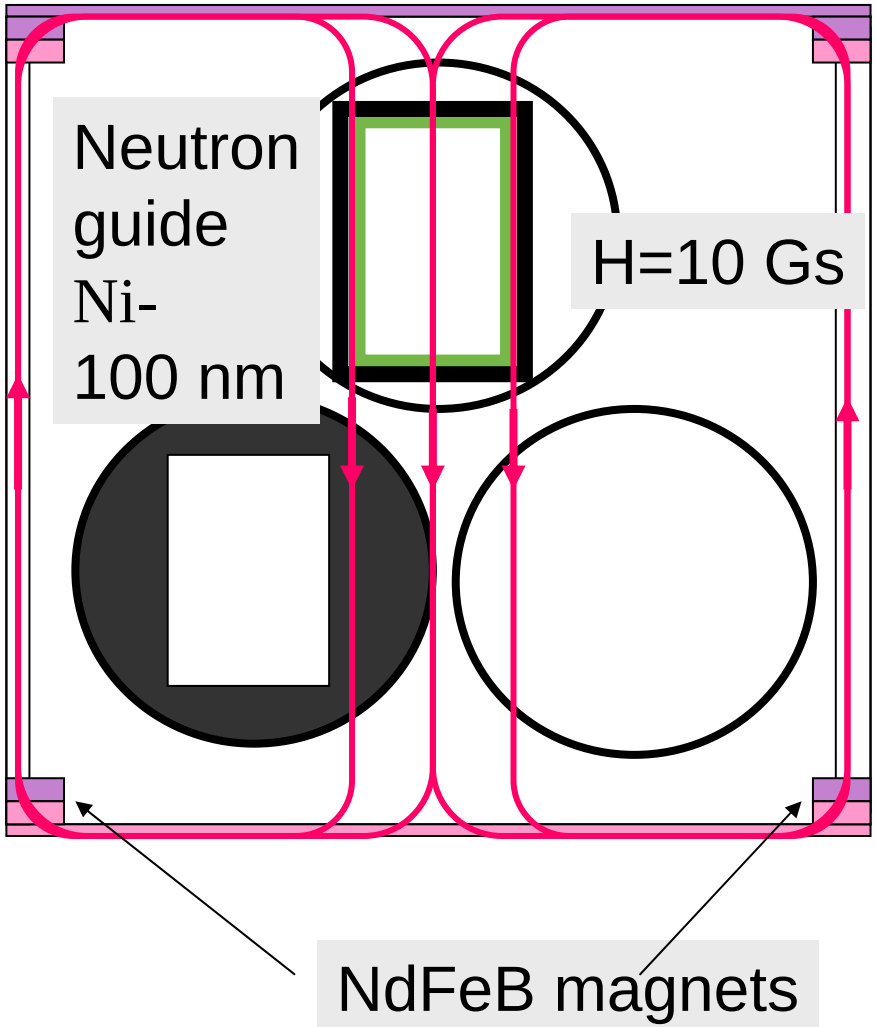

Spin-flipper

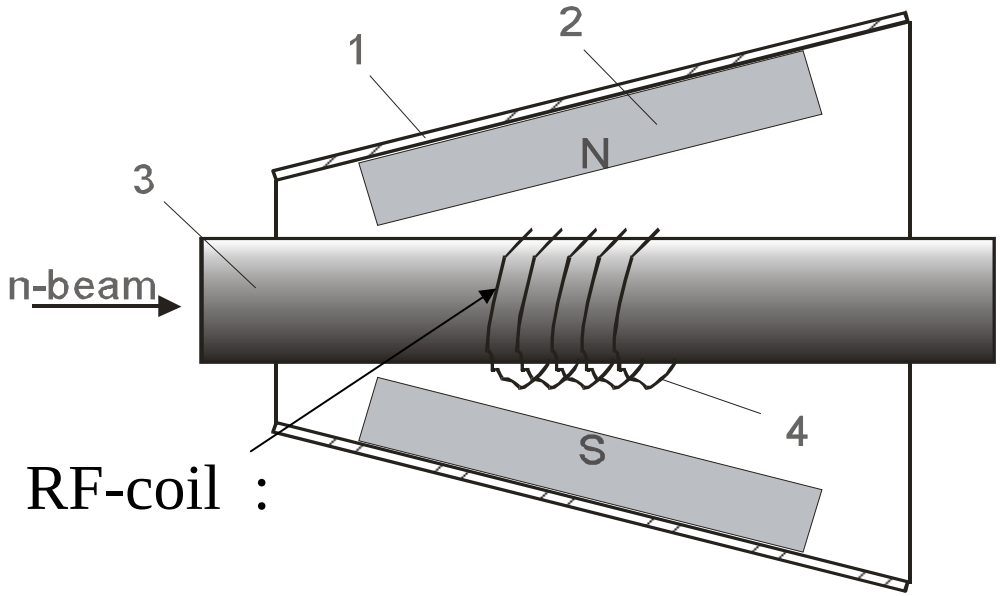

RF-coil :

$B_{eff} = B - \omega_0/\gamma + B_1$

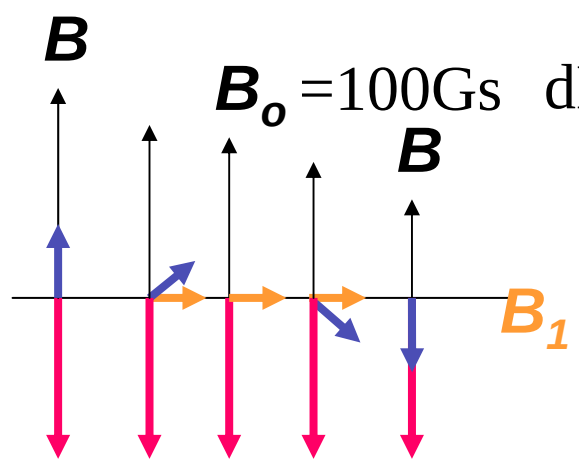

B_o =100Gs dB/dl=3Gs/cm

$\omega_0 = \gamma B_0 = 300$kHz

$-\omega_0/\gamma$ B_1= 20 Gs

Performance of SANSPOL

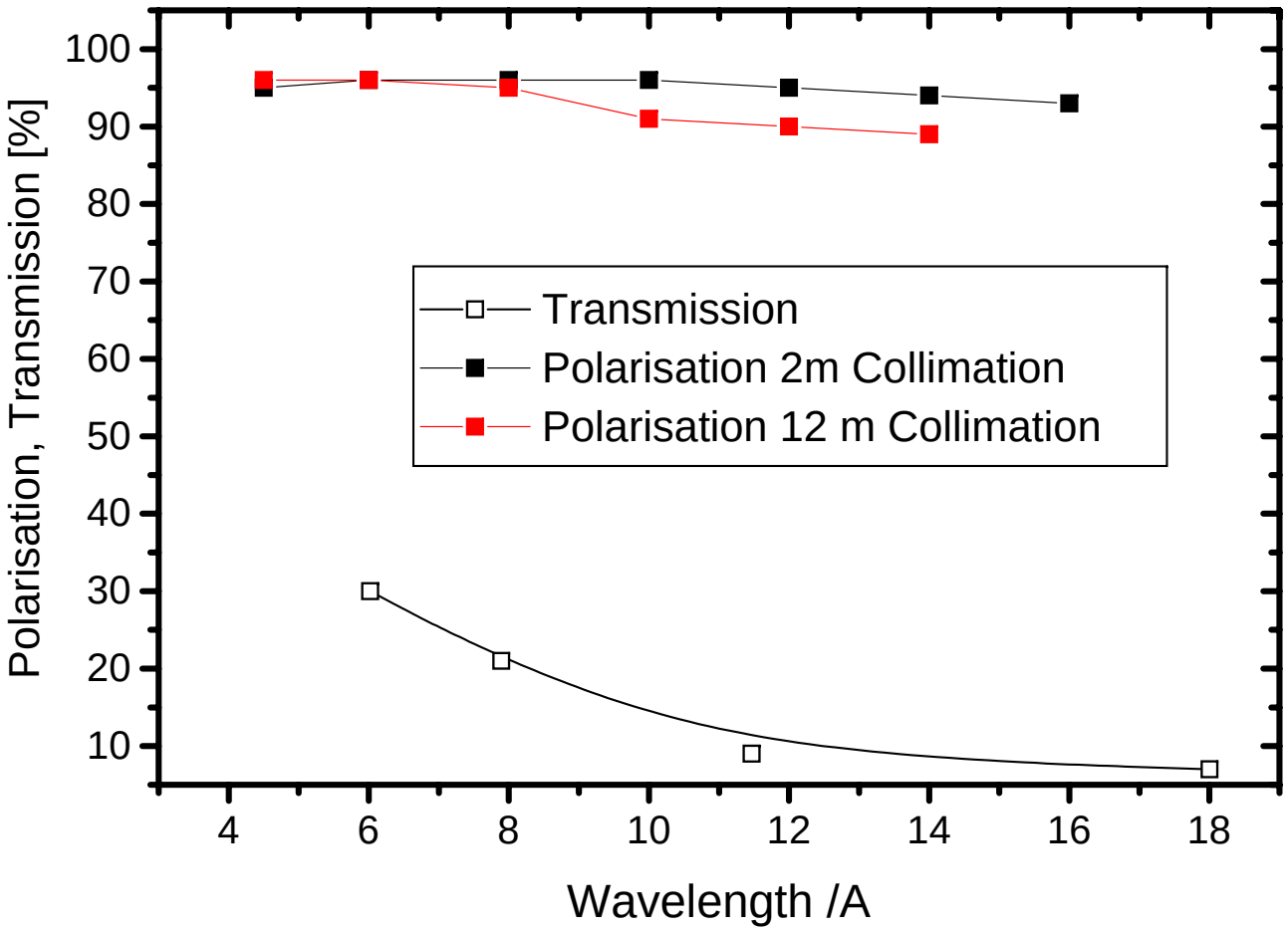

T. Keller, T. Krist, A. Danzig, U. Keiderling, F. Mezei, A. Wiedenmann

J. Nuclear Instruments A451(2000), 474-479

III. Practice of SANS

1. Instrument V4

2. SANS-Experiment,
Data Reduction and analysis

3. Practice and sensitivity of SANSPOL

Choice of Q-range

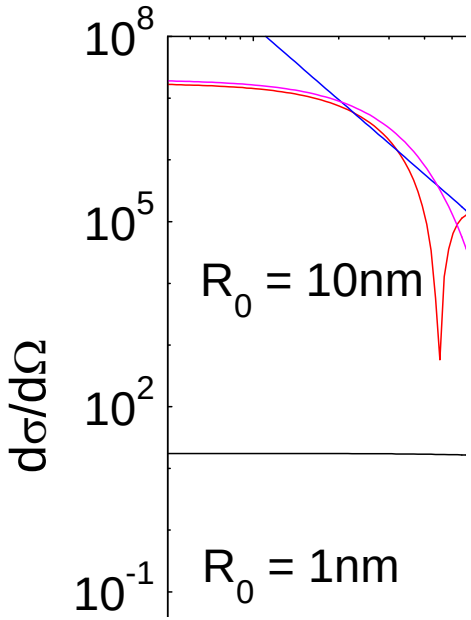

Guinier-approximation:
(for $QR_g < 1.5$)

$$I(Q) = \Delta\eta^2 V_p^2 \exp-(R_g^2 Q^2/3)$$

$$I_0 = \Delta\eta^2 V_p^2$$

$$R_g = (3/5)^{1/2} R_0$$

Porod approximation:
(for $QR_g > 2.5$)

$$I(Q) = 2\pi\Delta\eta^2 S^* Q^{-4} = P\, Q^{-4}$$

$$S = 4\pi R_0^2 \quad , V_p = 4\pi/3 R_0^3$$

$$R_0^4 = 9\, I_0 / 2\, P$$

$$I(Q) = 9\, \Delta\eta^2 V_p^2 [(\sin(QR)-(QR)\cos(QR))/(QR)^3]^2$$

Choice of Q-range

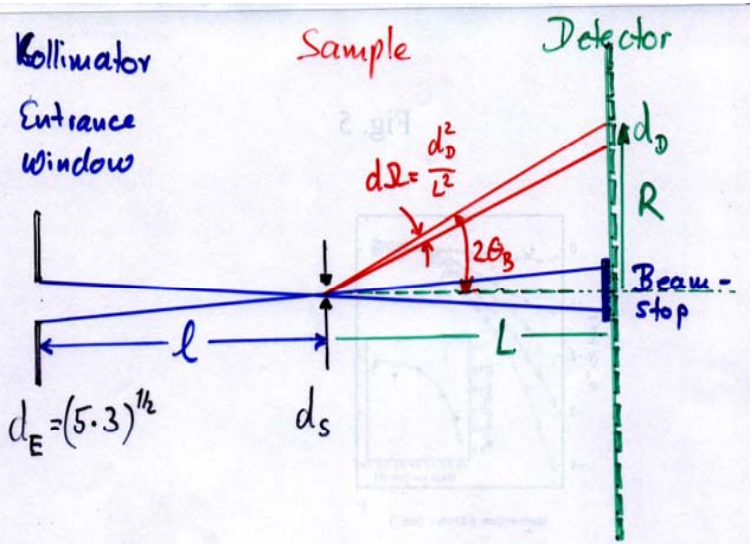

Q - range (KWS I)

$$Q = \frac{4\pi}{\lambda} \sin\theta_B = \frac{2\pi}{\lambda} \cdot \frac{R}{L}$$

$$Q_{max} = \frac{2\pi}{\lambda_{min}} \frac{R_{max}}{L_{min}} = 10\ nm^{-1}$$

$R_{max} = 62\ cm$
L_{min} 100 cm
$\lambda_{min} = 0.38$

$$Q_{min} = \frac{2\pi}{\lambda_{max}} \frac{R_{min}}{L_{max}} = 0.008\ nm^{-1}$$

$R_{min} = \frac{BS}{2} = 5$
$L_{max} = 1600\ cm$
$\lambda = 2\ nm$

1 Extended Q-range: Different sample-detector distances

Example: demixion in amorhous alloys

- ■ λ=0.6nm , l=2m, L_1=1.2m + Lift of detector by 0.2m λ·L= 72
- ● λ=0.6nm , l=2m, L_1=2m 120
- X λ=0.6nm , l=4m, L_1=4m 240
- ⌒ λ=0.6nm , l=8m, L_1=8m 480

Maximal factor: 16

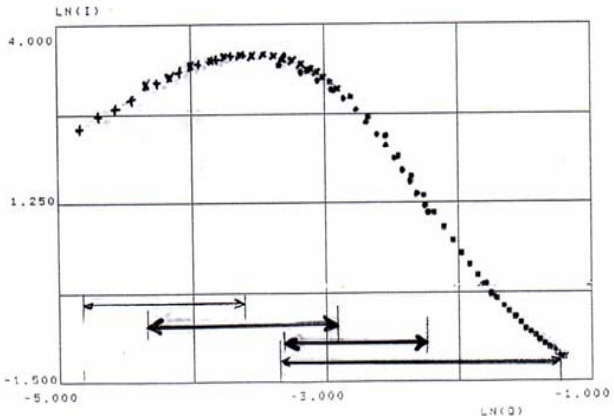

Intensity *versus* resolution

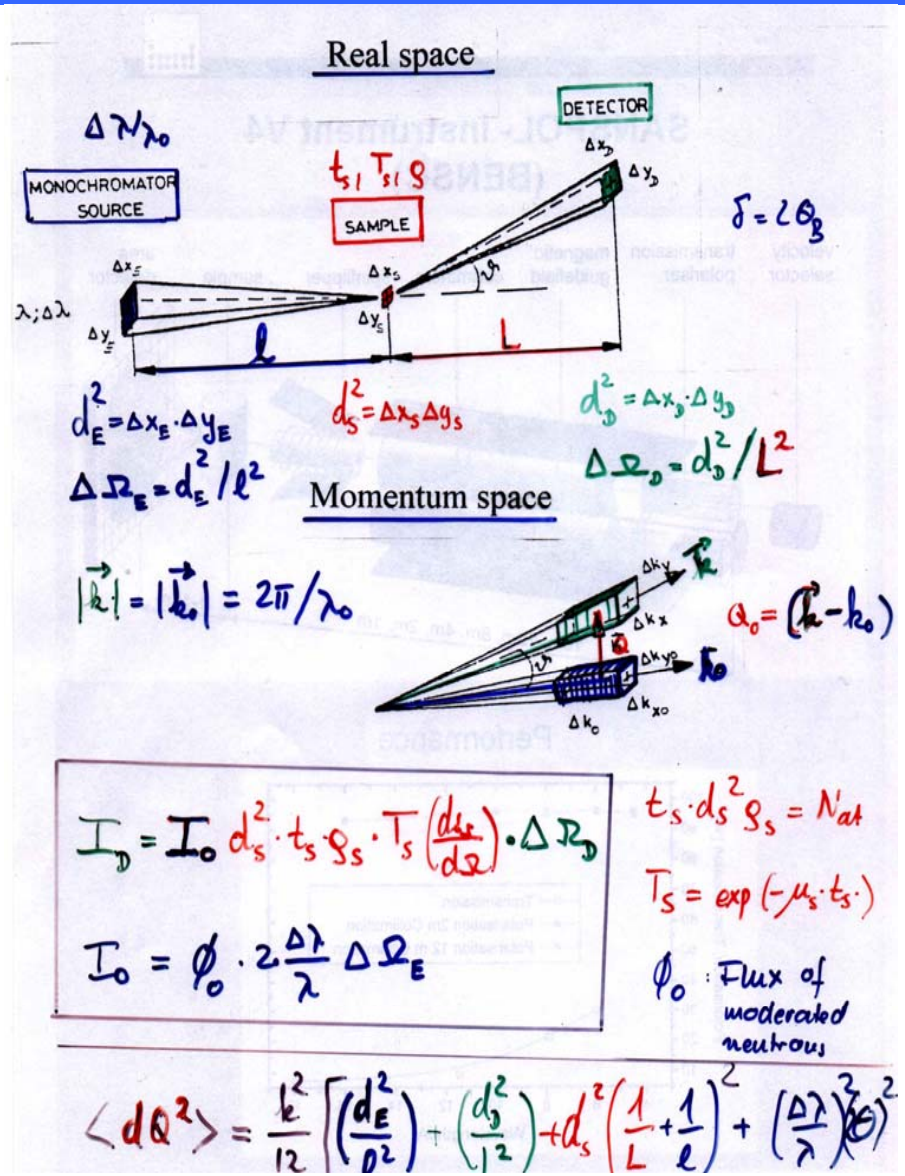

Optimized Conditions:

L = l

$d_E = 2d_s$

Practice: Intensity contributions

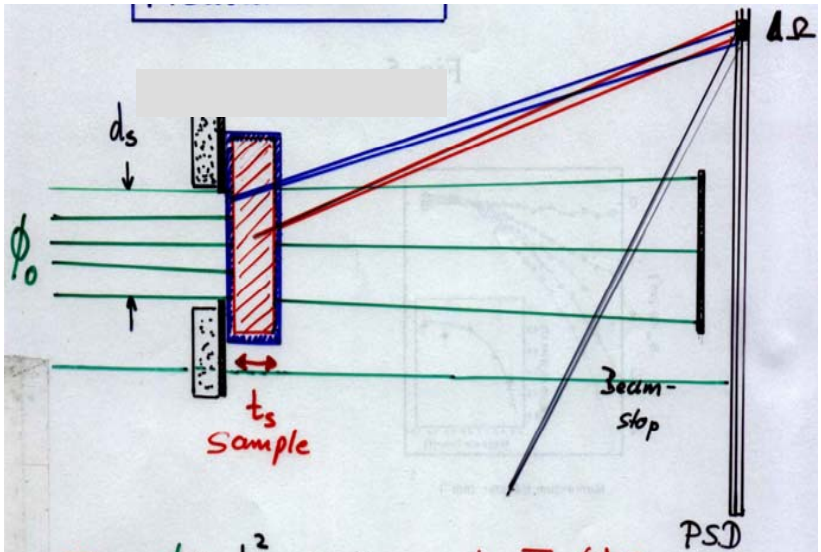

$$I_s = \underbrace{\phi_0(\lambda) \cdot d_s^2 \cdot \varepsilon(\lambda) \cdot \Delta\Omega}_{} \cdot t_s \cdot T_s \left(\frac{d\sigma}{d\Omega}\right)_s$$

$$I_s = C(\lambda) \cdot t_s \cdot T_s \left(\frac{d\sigma}{d\Omega}\right)_s$$

I_{BG} = Scattering from sample holder
↳ depends on sample transmission

I_0 = Sample independent noise
Scattering from air, electronic noise ...

Intensity at the detector:

$$I_D = I_0 + I_{BG} \frac{T_s}{T_{BG}} + I_s$$

Differential scattering cross section of sample

$$\boxed{\left(\frac{d\sigma}{d\Omega}\right)_s = \frac{I_D - I_0 - \frac{T_s}{T_{BG}} \cdot I_{BG}}{C(\lambda) \cdot t_s \cdot T_s}}$$

1. Scattering with sample + holder : I_D
2. Scattering of holder alone : I_{BG}
3. Residual noise : I_0
4. Transmission of sample + holder : T_s
5. Transmission of holder alone : T_{BG}
6. Absolute calibration : $C(\lambda)$

Must be measured for each spectrometer configuration $L, \ell, d_E, d_{SF}, \lambda, \ldots$

Transmissions and beam-center

Calculated

$$T = \exp-(\sigma_{tot}\, t_s / \rho_s)$$

t_s : Thickness of sample
ρ_s : Atomic density
σ_{tot} : Total cross section

$$\sigma_{tot} = \sigma_{abs}(\lambda) + \sigma_{coh} + \sigma_{inc}$$

$\sigma_{abs}(\lambda)$: absorption cross section (tabulated for λ=1.8A)

$$\sigma_{abs}(\lambda_1) / \sigma_{abs}(\lambda_2) = \lambda_1 / \lambda_2$$

Measured : Direct beam :

$$T = I_s(0) / I(0) = \frac{\sum \text{(counts) with sample}}{\sum \text{(counts) without s.}}$$

- Attenuation of primary beam f_a = 10..200
- Saturation corrrections
  I (true)= I (measured) *[1-t_1* I(measured)]
- Good collimation (small profile- low contributions of scattering contained in primary beam)

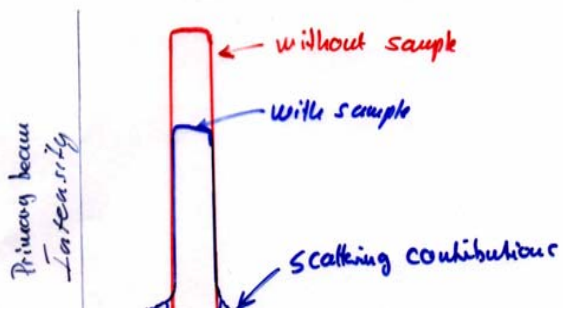

Measurement of empty can with attenuator f_a=270

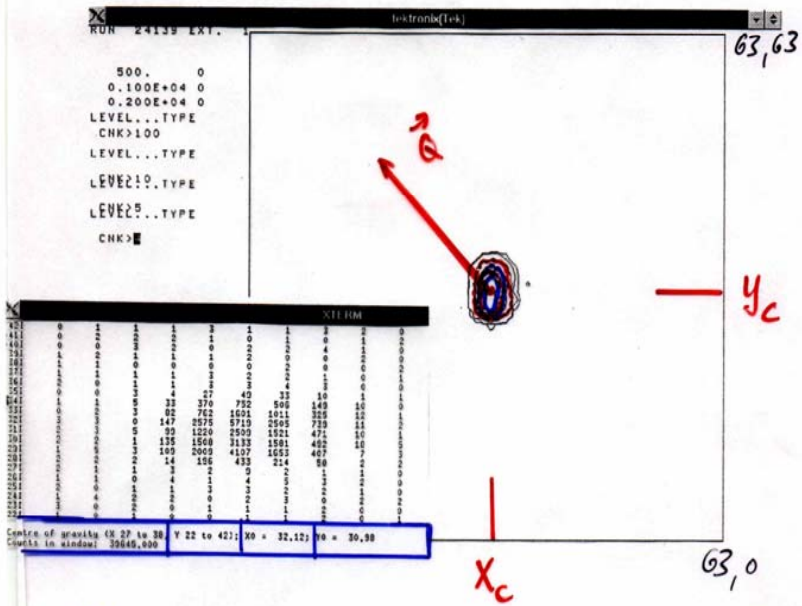

Determination of center of gravity:

$$x_c = \frac{\sum_i^n I(x_i, y_i) \cdot x_i}{\sum I(x_i, y_i)}$$

$$y_c = \frac{\sum_i^n I(x_i, y_i) \cdot y_i}{\sum I(x_i, y_i)}$$

Calibration of absolute intensity

$$C(\lambda) = \phi_0(\lambda)\,\varepsilon(\lambda)\cdot\Delta\Omega\cdot d_s^2$$

$\uparrow$ d_s^2/L^2

Must be known cell by cell.

[1] Using standards with known $(d\sigma/d\Omega)$

1a) • eg H_2O $\sigma_{inc.} = 160$ barn/at

• Vanadium $\sigma_{inc} = 5$ barn/at

Incoherent scattering independent of Q:

$$I(Q) = C(\lambda)\cdot(1-T_s)/4\pi \cdot g(\lambda)$$

all not transmitted neutrons are scattered in 4π!

•• H_2O: $g(\lambda)$ • ~0.8–1.3 inelastic contribu

• multiple scattering.

•• Vanadium: only for larger Q due

– to SANS from impurities

– H_2 = increases incoherent BG.

• Compressibility of a liquid

• Porous system with grain size > μm

$$\left(\frac{d\sigma}{d\Omega}\right) = 2\pi\,(\Delta b)^2\,\frac{S}{V}\,\frac{1}{Q^4} \quad \text{Porod}$$

• Glassy carbon: well-know pre calibrated Q-dependency

• Ceramics.

[2] Direct beam measurements

$$I_D = f_a(\lambda)\cdot\phi_0\,\varepsilon(\lambda)\cdot\Delta\Omega$$

with attenuator factor $f_a(\lambda)$ known:

$f_a(\lambda) = \Sigma'$(counts) of strong scatterer Att / Unattenuated.

$$\phi_0\,\varepsilon(\lambda)\cdot\Delta\Omega = I_D / f_a(\lambda)$$

No calibration of individual cells: $\varepsilon_i(\lambda)$!

Data reduction : cell by cell corrections

Anisotropic raw data:

"SC 16", λ = 1.2 nm, SD = 16 m / 4 m (water)

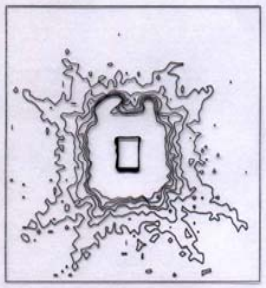

sample
150 min, 26 n/s

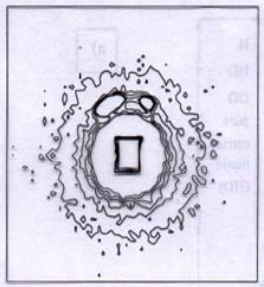

sample holder
180 min, 16 n/s

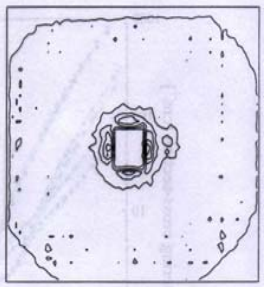

water cell
120 min, 93 n/s

empty cell
120 min, 64 n/s

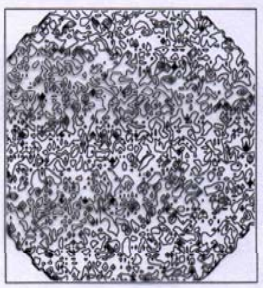

cadmium
180 min, 2.4 n/s

Anisotropic reduction procedure:

- corrected intensity

$$I = \frac{\left(\frac{S - Cd}{Transmission(S)}\right) - \left(\frac{SB - Cd}{Transmission(SB)}\right)}{\left(\frac{W - Cd}{Transmission(W)}\right) - \left(\frac{WB - Cd}{Transmission(WB)}\right)} * \frac{ScalingFactor(W)}{ScalingFactor(S)}$$

- error of corrected intensity

$$\Delta I = \sqrt{\left(\frac{\partial I}{\partial Cd} * \Delta Cd\right)^2 + \left(\frac{\partial I}{\partial W} * \Delta W\right)^2 + \left(\frac{\partial I}{\partial WB} * \Delta WB\right)^2 + \left(\frac{\partial I}{\partial SB} * \Delta SB\right)^2 + \left(\frac{\partial I}{\partial S} * \Delta S\right)^2}$$

- masking
- result: corrected anisotropic data file

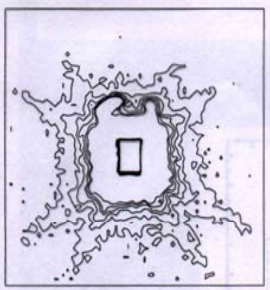

raw data

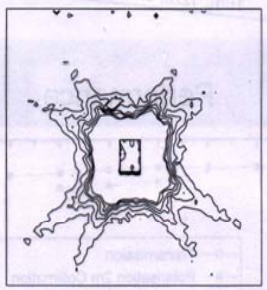

corrected data

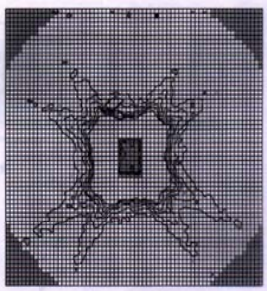

mask

Azimutal averages

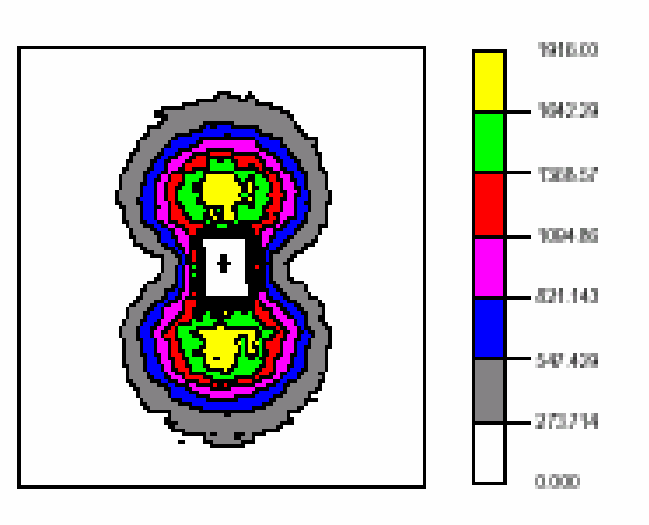

Radial averages in angle segments

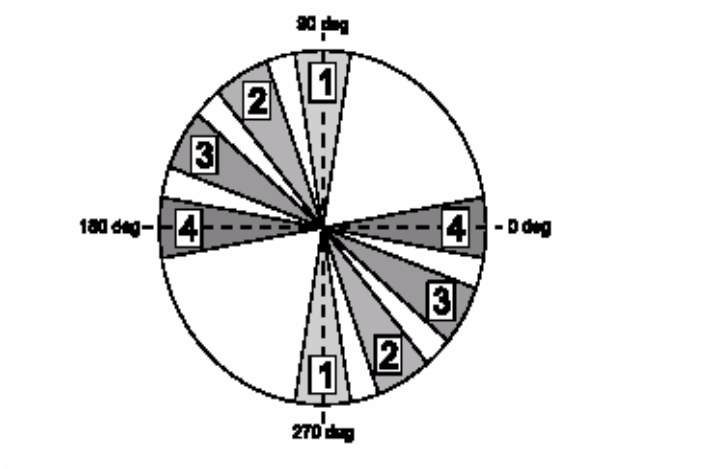

Cuts starting from beam-centre

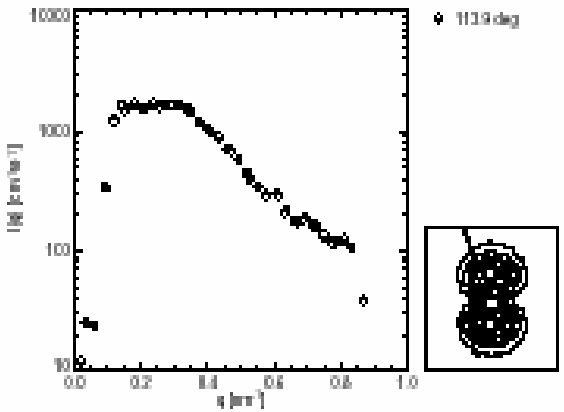

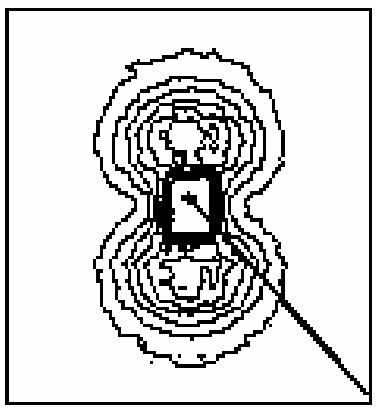

Data reduction software: BERSANS

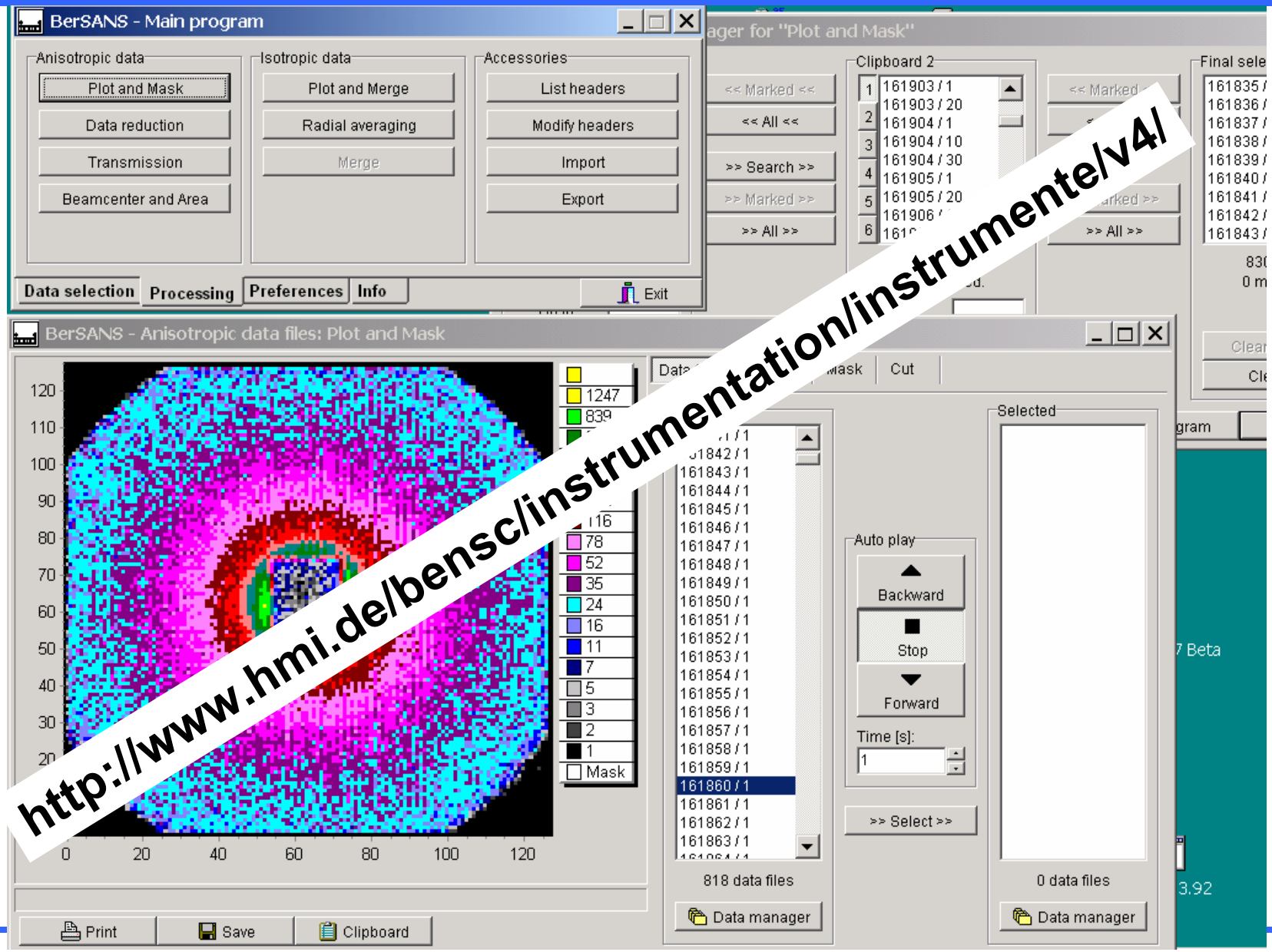

http://www.hmi.de/bensc/instrumentation/instrumente/v4/

Data analysis: Model fitting (SASFIT, FISH..)

$$I(Q)=N_p \int \{\Delta\eta\, V_p(R)\, f(QR)\}^2\, S(QR_{hc})\, N(R)\, dR \otimes RESU(Q)$$

Size distribution

Inter-particle Interference

Particle shape factor

Contrast: $\Delta\eta = \eta_{particle} - \eta_{Matrix}$

Instrument resolution

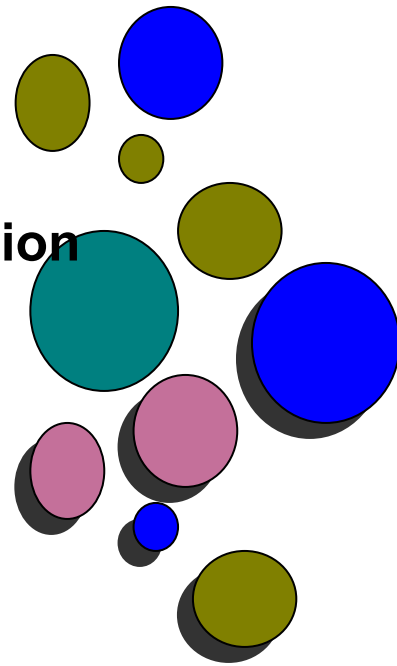

Analytical functions

N(R): e.g. lognormal distributions: <R>, σ

f(QR) sphere,ellipsoids,core-shell, cylinders..

S(QR): hard sphere potential..

Non-linear least-squares fit

$$\chi^2 = \sum \{(I(Q_i)_{exp} - I(Q_i)_{calc})/w_i\}^2 \quad \Rightarrow \quad \langle R_1\rangle, \sigma_1, f_1, \eta_1\ \langle R_2\rangle, \sigma_2, f_2\ \eta_2 \ldots$$

Data analysis: (Inverse Fourier transform)

$$I_A(Q) = \sum_{\nu=1}^{N} c_\nu \psi_\nu(Q) \qquad p(r) = \sum_{\nu=1}^{N} c_\nu \cdot \varphi_\nu(r)$$

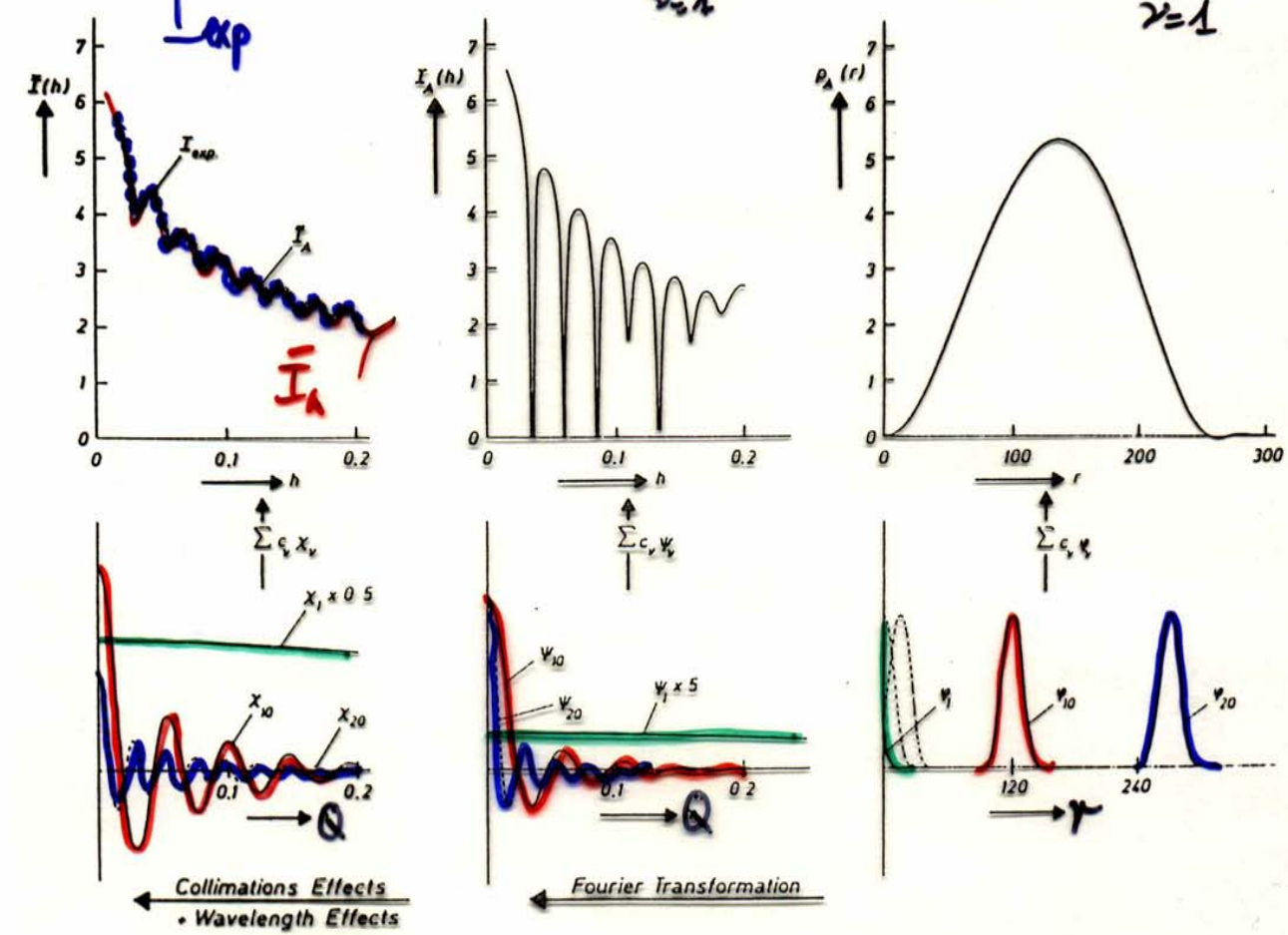

Glatter
ITP

Pair distance distribution function p (r)

$$p(r) = 4\pi r^2 \gamma(r)$$

e.g: spheres of Radius R

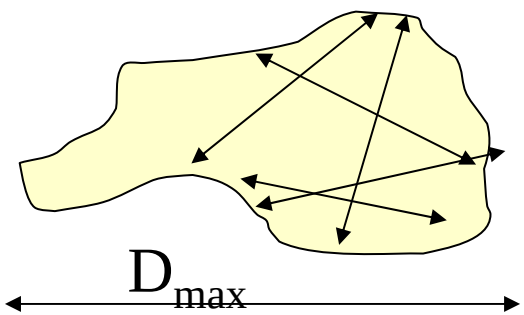

$r = 0$

$p(r)=0$

$r > D_{max}$

$p(r)=0$

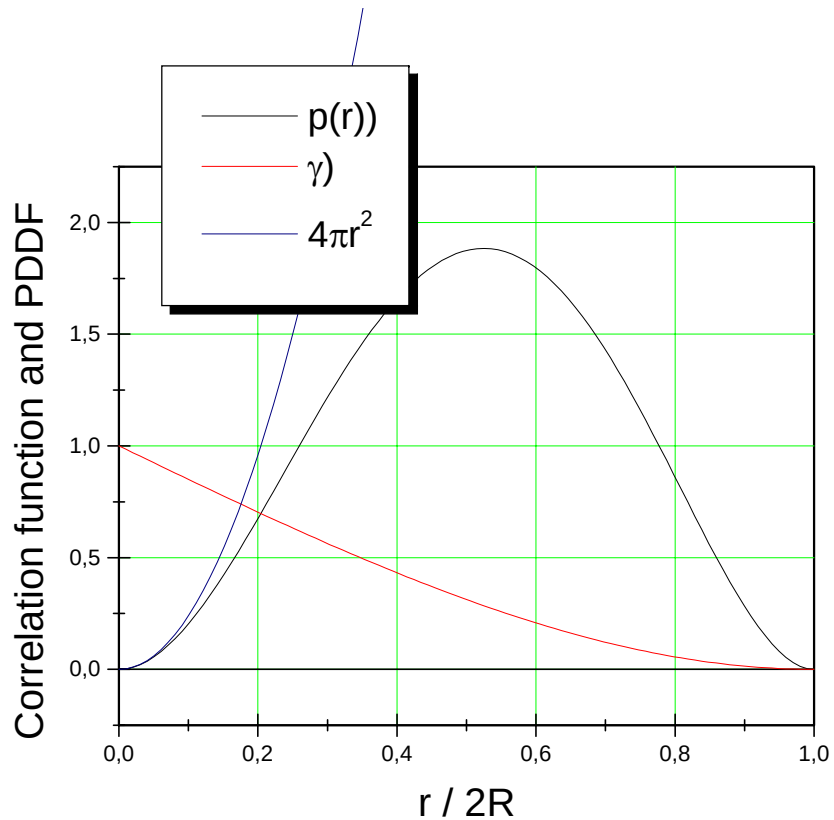

III. Practice of SANS

Instrument V4

SANS-Experiment, Data Reduction and analysis

Examples

Example 1: Contrast (η_1-η_2)

Suspension of latex (C_8H_8) in D_2O

	Latex	Heavy water
Molecular weight	104	20
Number of electrons	56	10
Mass-density/ gcm^{-3}	1.0	1.1
Scattering length density		
(X-ray)	$0.281e\text{-}12 * 56N_l/104$	$0.281e\text{-}12*1.1*10N_l/20$
Neutrons	$N_L/104\ (8b_c+8b_H)$	$1.1*N_L / 20(2b_D+b_O)$

Contrast

X-ray $(\eta_1-\eta_2) = -0.195\ e^{10}\ cm^{-2}$

neutrons $(\eta_1-\eta_2) = -4.970\ e^{10}\ cm^{-2}$

Example 2: Contrast-variation

Scattering lengths densities

η (H_2O)= -0.56 e^{10} cm^{-2}
η (D_2O)= 6.34 e^{10} cm^{-2}

D_2O / H_2O mixtures with volume fraction f D_2O

$$\eta_0(f) = (-0.56\,(1-f) + 6.34\,f)\ 10^{10}\ cm^{-2}$$

Intensity

$$\sqrt{I(Q)} \propto (\eta_1 - \eta_0(f))$$

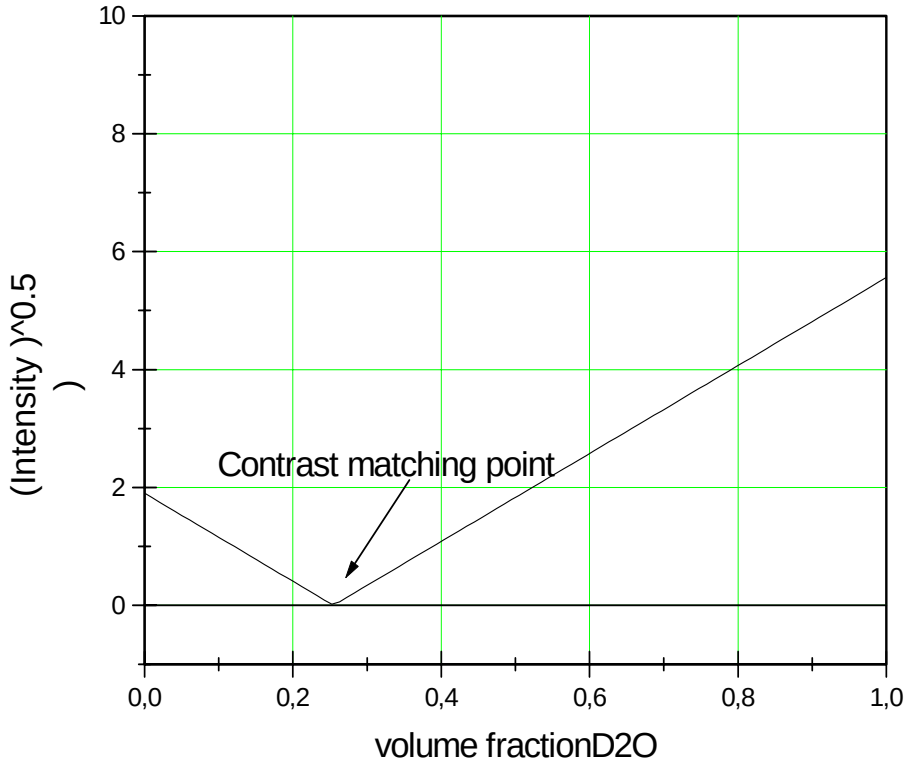

Example 3:Sintering of nano-ceramics

Sample n-Al_2O_3 CVS production:
45mol%Al_2O_3 55% Zr_2O_3 pressed 800MPa

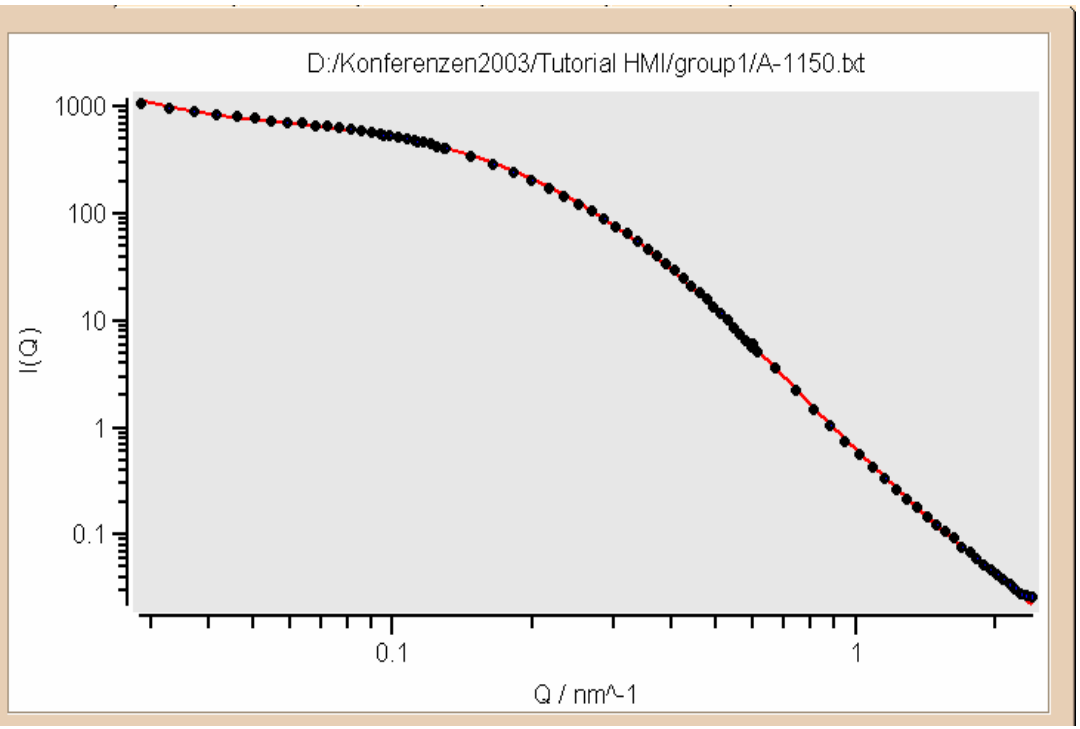

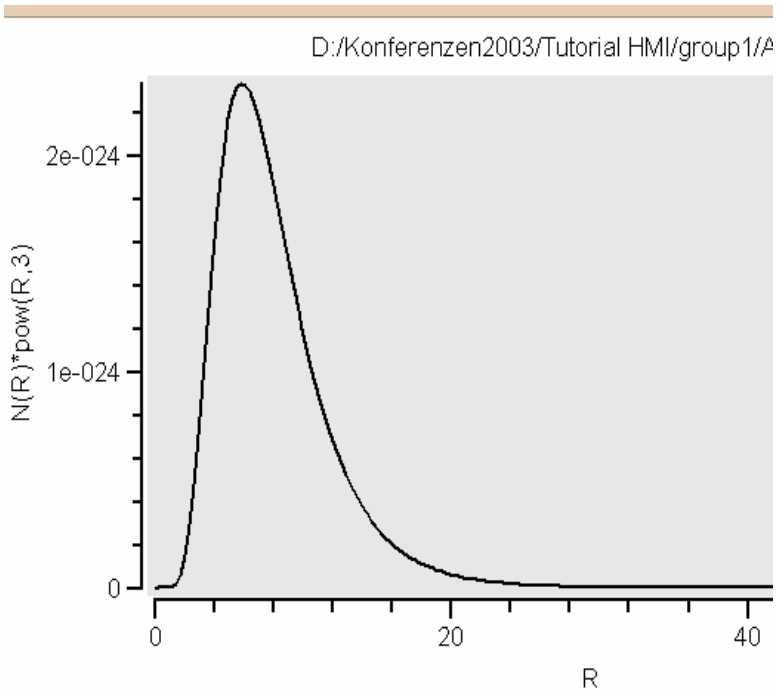

Example3:Sintering of nano-ceramics

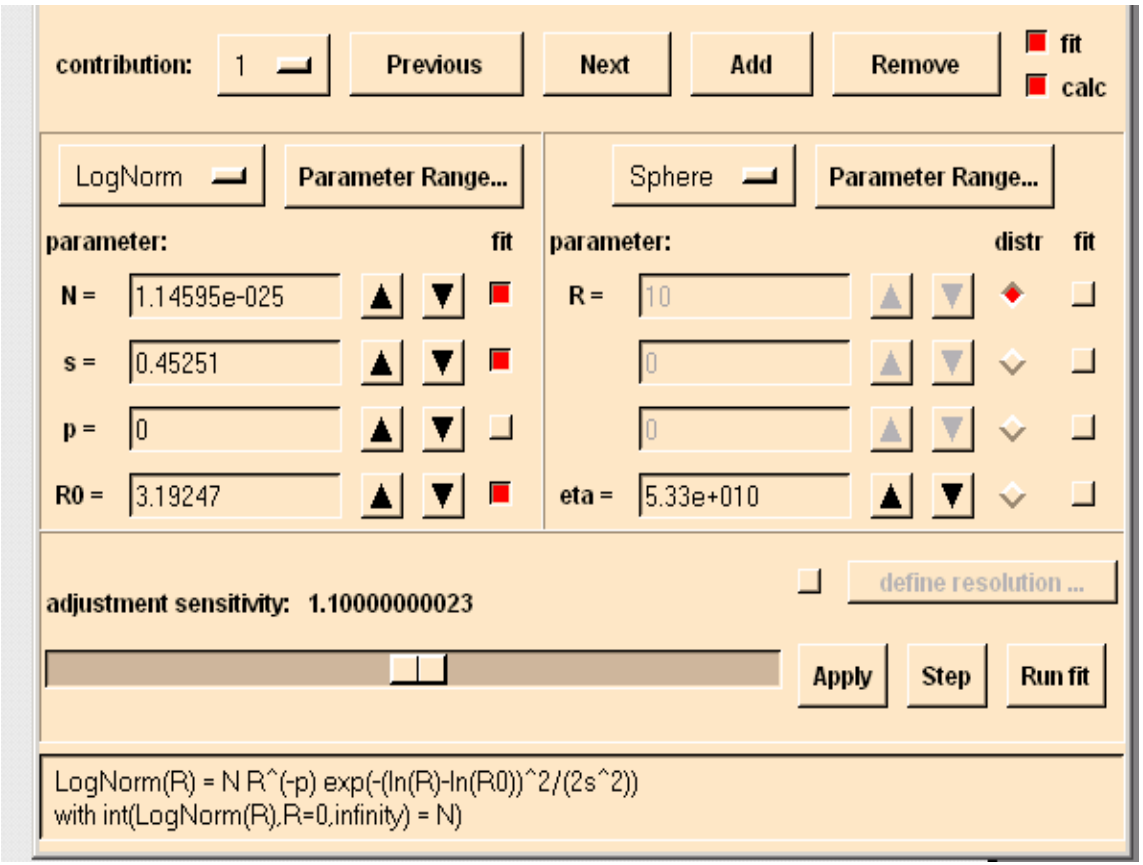

Moments of distribution

1. scatt. contrib.:	calc: yes
LogNorm	Sphere
<R^1> = 4.3403	<R^5> = 11935.4
<R^2> = 23.1189	<R^6> = 144147
<R^3> = 151.127	<R^7> = 2.13335e+006
<R^4> = 1212.39	<R^8> = 3.85619e+007
R_Ic = 8.0223	Ic = 5.3482
R_Ii = 6.53696	Ii = 4.90272
R_Ac = 8.88684	Ac = 31.4235221923
R_VP = 9.8436	VP = 227.705365117
R_RG = 16.356	RG = 12.6693031221

$R^2 = \langle R^8 \rangle / \langle R^6 \rangle = 16.3$

$RG = (5/3)^{0.5} R = 12.7$

Number density: $n_p (1-f) = N\ 10^{42} = 1.14\ 10^{21}$ T cm^{-3}

Volume fraction: $f(1-f) = n_p 4/3\pi \langle R^3 \rangle = 1.15\ 4/3\pi\ 151.12\ 10^{21} 10^{-21} = 0.07$

Example3 :Sintering of nano-ceramics

Guinier approx.: I(Q) = I0 exp(-Rg^2*Q^2/3)	integral structural parameters:
Guinier radius RG = 11.6391	correlation length lc = 12.1618
forward scattering I(0) = 842.265	correlation area Ac = 206.135
chisq(Guinier) = 13.7106	intersection length li = 8.69719
	Porod volume VP = 4114.79
Porod approx.: I(Q) = c0+c4*Q^(D-4)	Porod radius RP = 9.94076
background c_0 = 0.00671764	specific surface S/V = 0.459918
Porod constant c_4 = 0.59151	scattering invariant Inv = 4.04046
potential law D = 0	integrated intensity il = 15.6416
chisq(Porod) = 0.858593	Q_max = 0.02844
	Q_min = 2.398

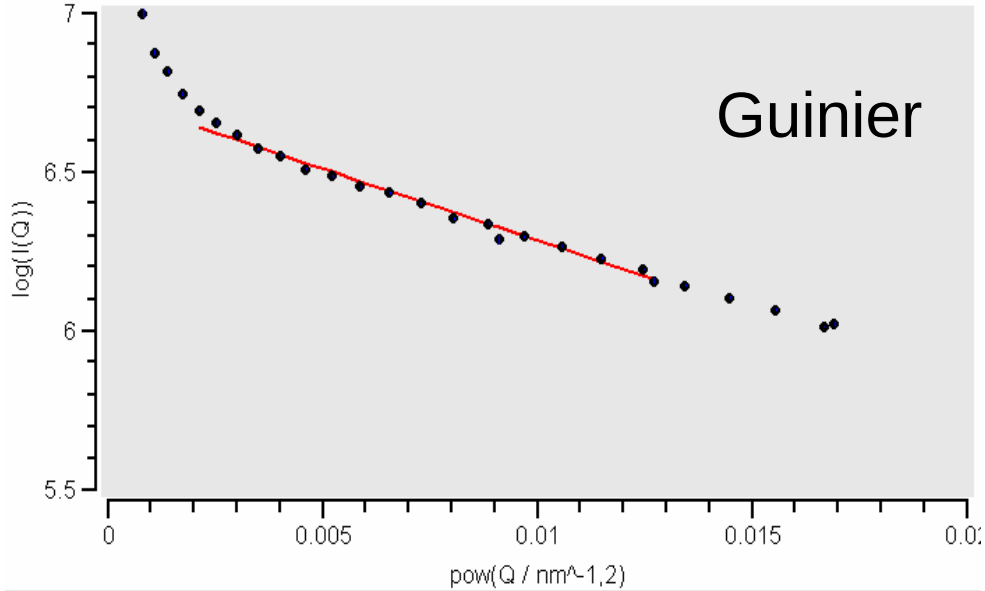

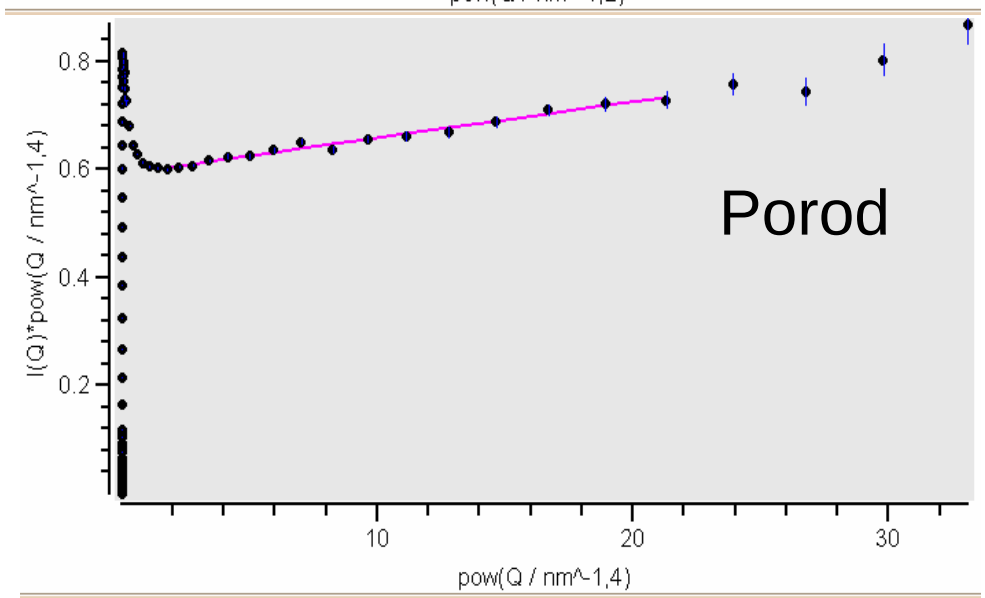

Guinier radius: 11.65 nm

Invariant $=f(1-f)/2\pi^2\Delta\eta^2$

$\Delta\eta=5.33\ 10^{10}\ cm^{-2}$

$f(1-f)=4.04\ 10^{21}/\ 2\pi^2\Delta\eta^2$

$=0.07$

Example 4: 2 D-scattering pattern

background

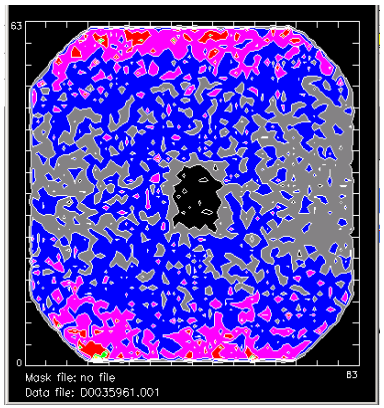

empty beam

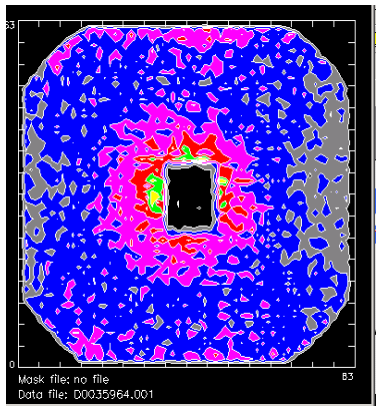

sample

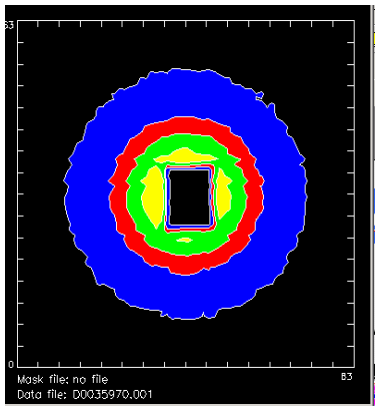

water

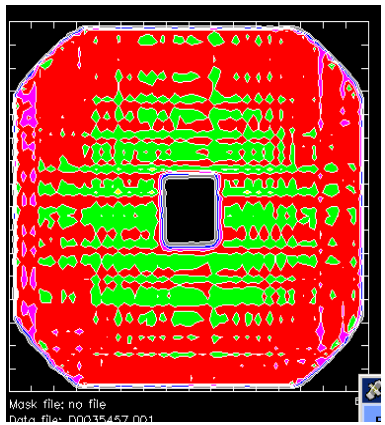

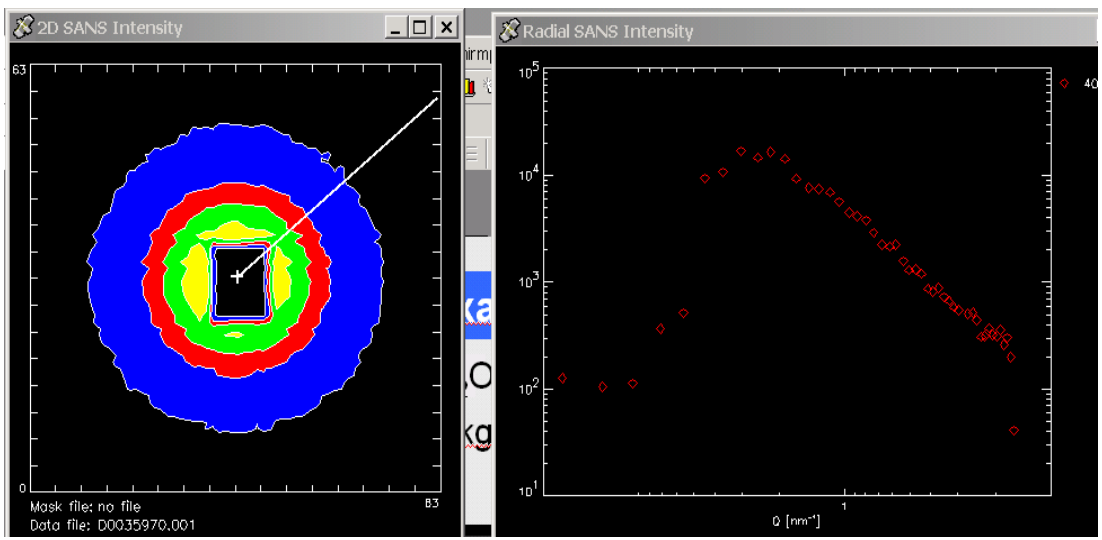

Correction for background, efficiency.
Beam center
Cuts and radial averages

Example 4 : Co-FF in Toluol (43%D)

H →

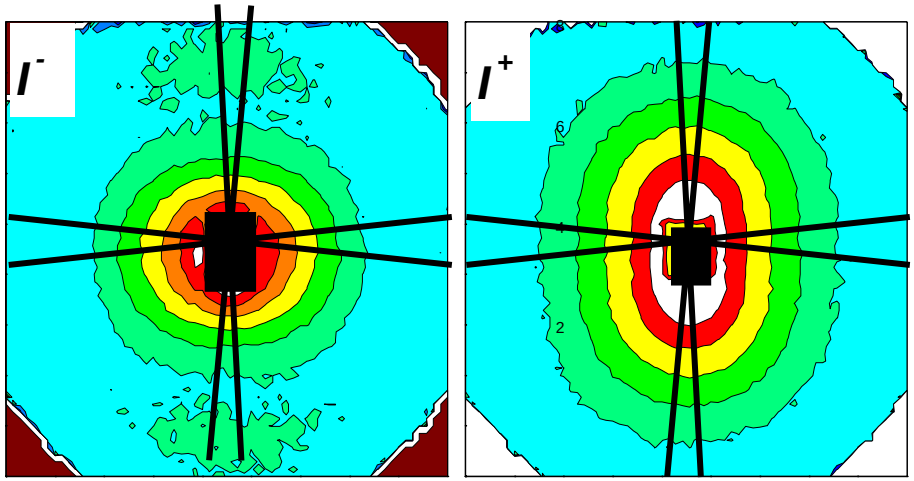

2 D-fit:
$I=A+B^{\pm}\sin^2\alpha$
or segments:

$I(Q//H)= I_{nuc}(Q)$
$I(Q\perp Q) \;=A+B^{\pm}$

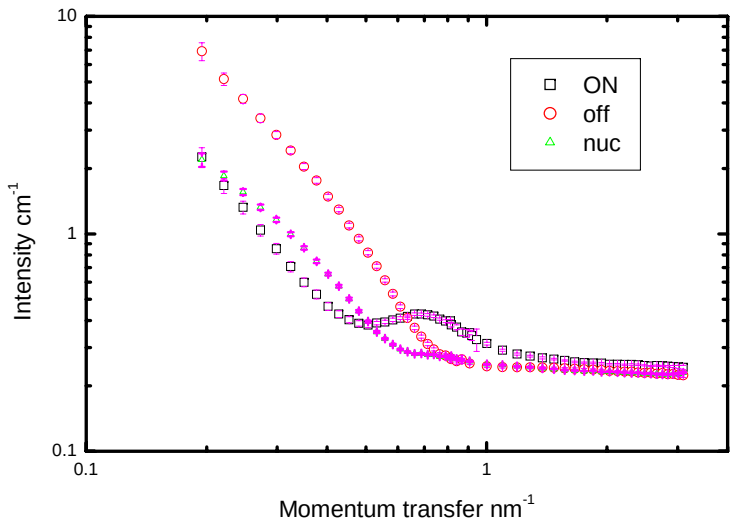

Scattering length density profile in Co-Ferrofluid

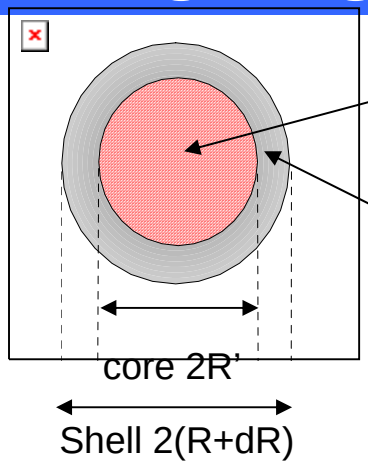

$$\Delta\eta_1^{(\pm)} = \eta_1^{nuc} \pm \eta_1^{mag} - \eta_{matrix}$$

$$\Delta\eta_2 = \eta_2^{nuc} - \eta_{matrix}$$

Core-shell model

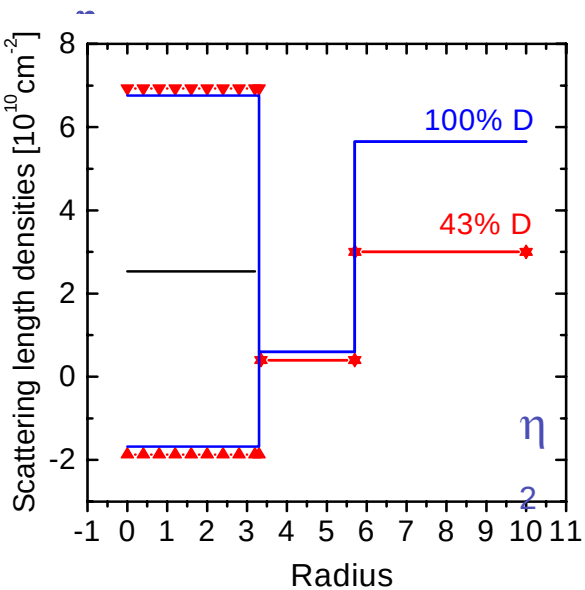

$$F_{shell}(Q) = [(\Delta\eta_1 - \Delta\eta_2)\, f_{sph}(QR') + \Delta\eta_2\, f_{sph}(QR)]\, V_p$$

$$f_{sph}(x) = 3\,[\sin(x) - x\cos(x)] / (x)^3$$

Example 4 :Co-FF in Toluol (43%D)

Scattering length densities

1. **Solvent: 43% D / H mixture of Toluene:**
   $\eta(x) = -0.7(1-x) + 6.8\,x$ — $\eta(solv) = 3.0\ 10^{10}\ cm^{-2}$
2. **Non-deuterated shell (C_{21}-H_{39}-N-O_3)** — $\eta(shell) = 0.3\ 10^{10}\ cm^{-2}$
3. **Nuclear sld (Co)**
   $\Omega(Co) = 0.\ 0.01099\ nm^3/at$,
   $b = 10^{-12} cm$ — $\eta(Co) = 2.56\ 10^{10}\ cm^{-2}$
4. **Magnetic sld Co**
   $m_0 = 1.715\ \mu_B$/ atom
   $\eta(mag) = 0.27\ 10^{-12}\ m_0/\Omega$ — $\eta(mag) = 4.3\ 10^{10}\ cm^{-2}$

Contrasts for SANSPOL

core - solvent : $\Delta\eta_1$ (on) = $\eta(Co) + \eta(mag) - \eta(solv) = 2.56+4.3-3.0 = 3.83\ 10^{10}$

$\Delta\eta_1$ (off) = $\eta(Co) - \eta(mag) - \eta(solv) = 2.56-4.3-3.0 = -4.70\ 10^{10}$

Shell-solvent $\Delta\eta_2 = \eta(shell) - \eta(solv) = 0.3-3.0 = -2.73\ 10^{10}$

Example 4: Co-FF in Toluol (43%D)

Fit of nuclear scattering (I(Q) // H)

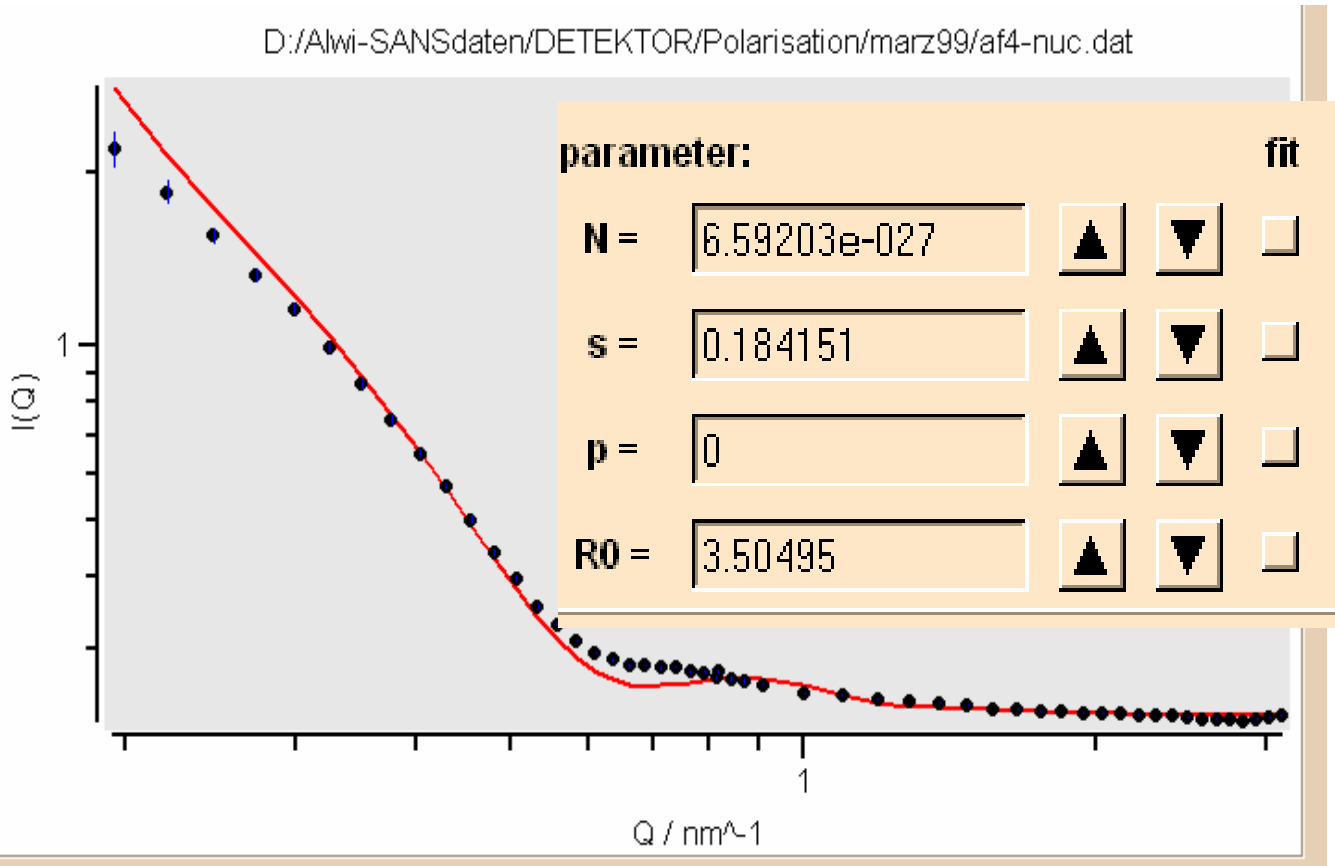

parameter:		fit
N =	6.59203e-027	
s =	0.184151	
p =	0	
R0 =	3.50495	

parameter:	
R =	5.8
dR =	1.90082
eta1 =	-4.30306e+009
eta2 =	-2.7e+010

Example 4: Co-FF in Toluol (43%D)

I(Q) – on (I perp. H)

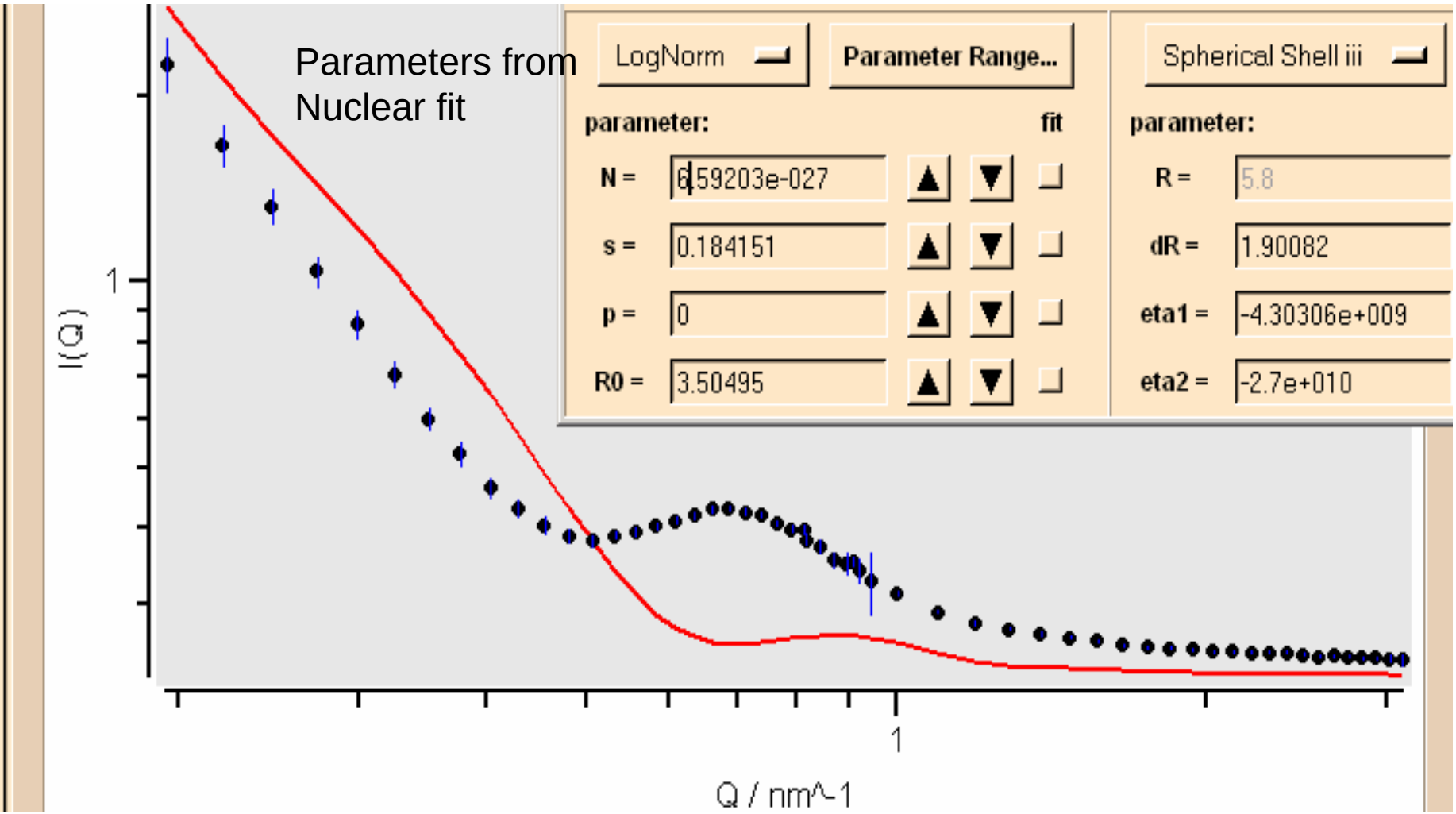

Example 4: Co-FF in Toluol (43%D)

I(on) same parameters –except η_1(on)

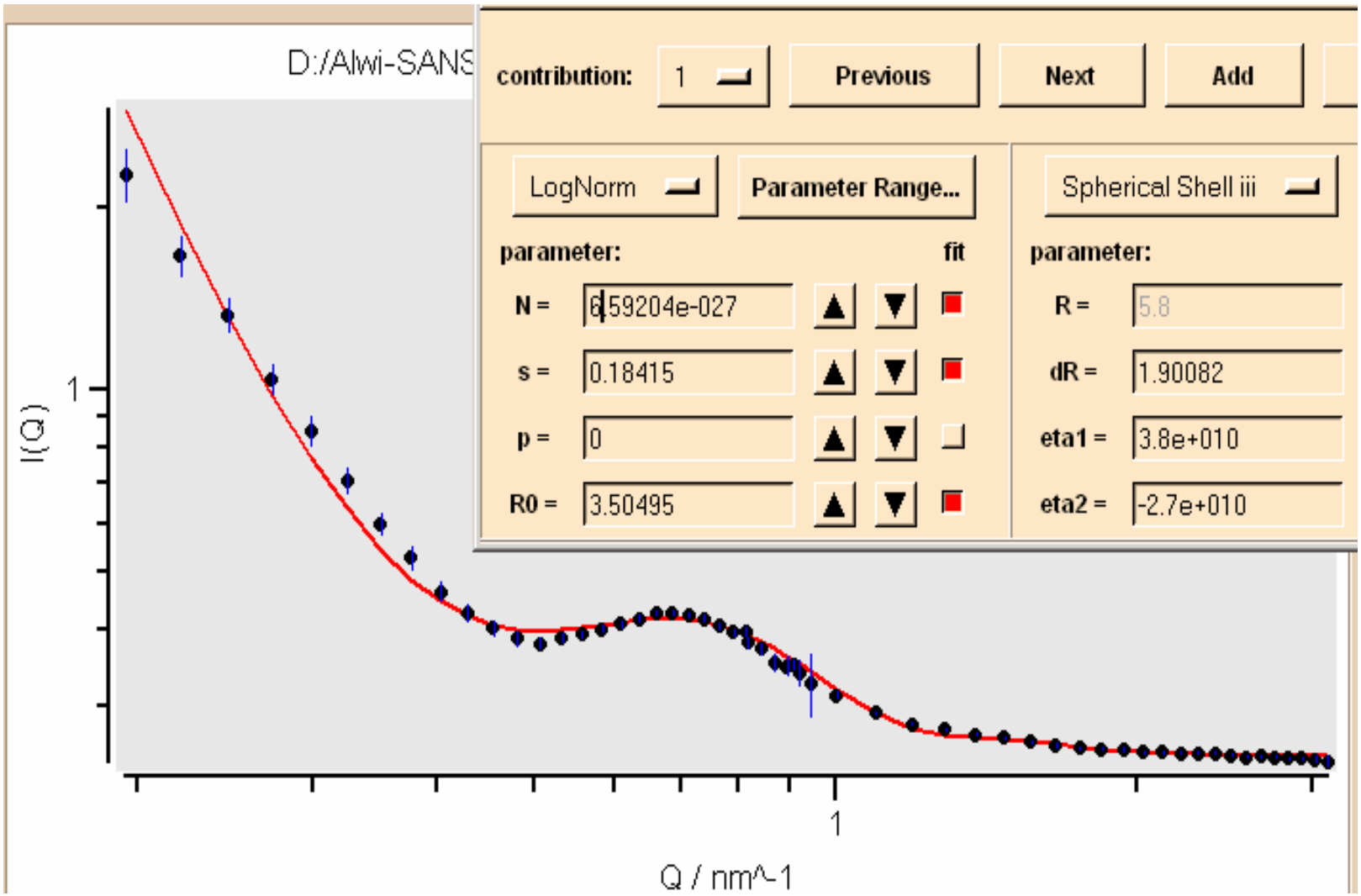

Example 4: Co-FF in Toluol (43%D)

I(off) same parameters –except η_1(off)

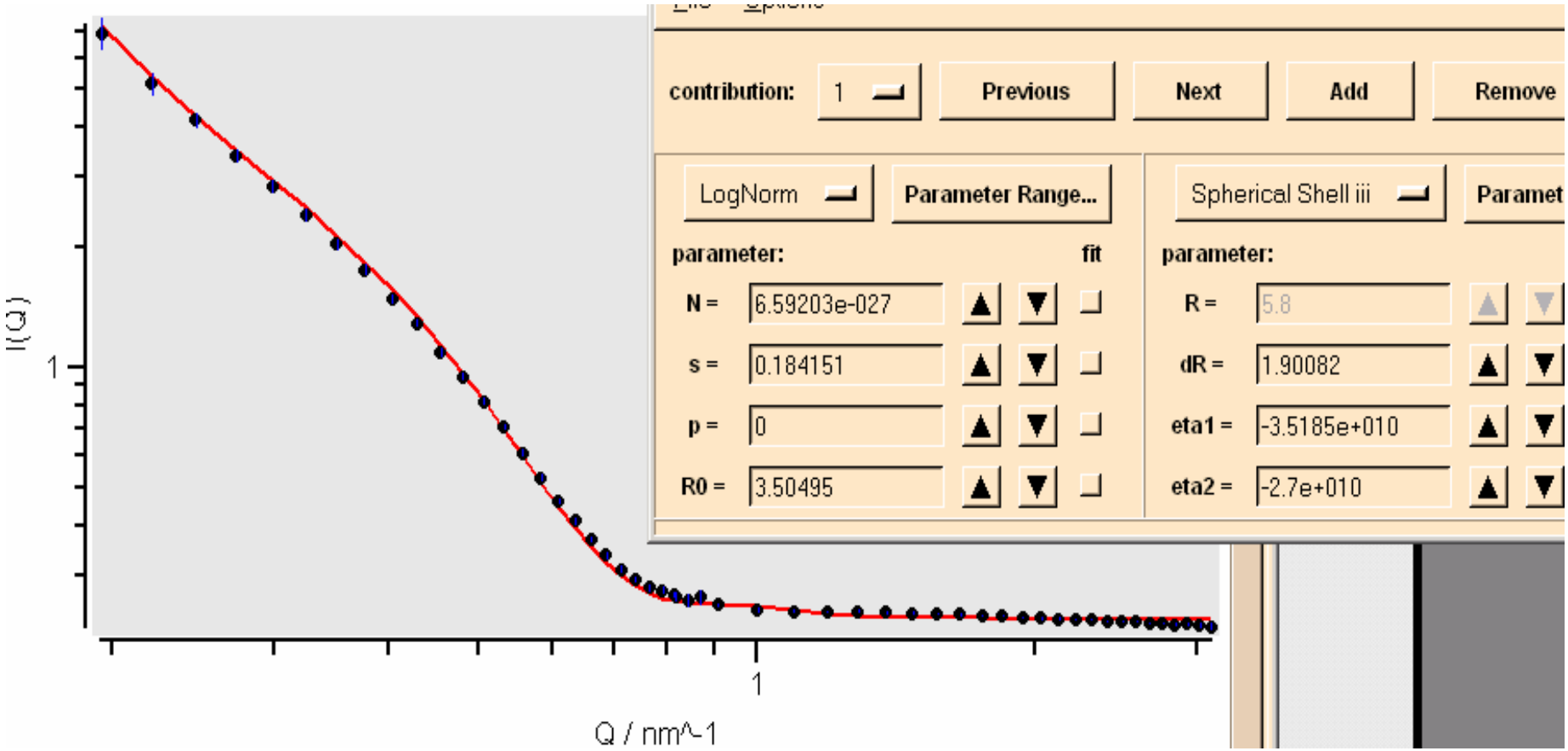

Example 4: Co-FF in Toluol (43%D)

Optimisation by simultaneous fits

I(on)
I(off)

and

I(nuc)
or I(mag)

using contraints on parameters e.g.:

$\Delta\eta_1$ **(on)=** $\Delta\eta_1$ **(nuc)+** η_1**(mag)**
$\Delta\eta_1$ **(off)=** $\Delta\eta_1$ **(nuc)-** η_1**(mag)**

Software: SASFIT (J. Kohlbrecher , PSI)
FISH (R. Heenan ISIS)
MATHematica (A.Heinemann, hmi)
Max Entropie: (Tatschev, hmi)

Example 4: Co-FF in Toluol (43%D)

Distribution of core size

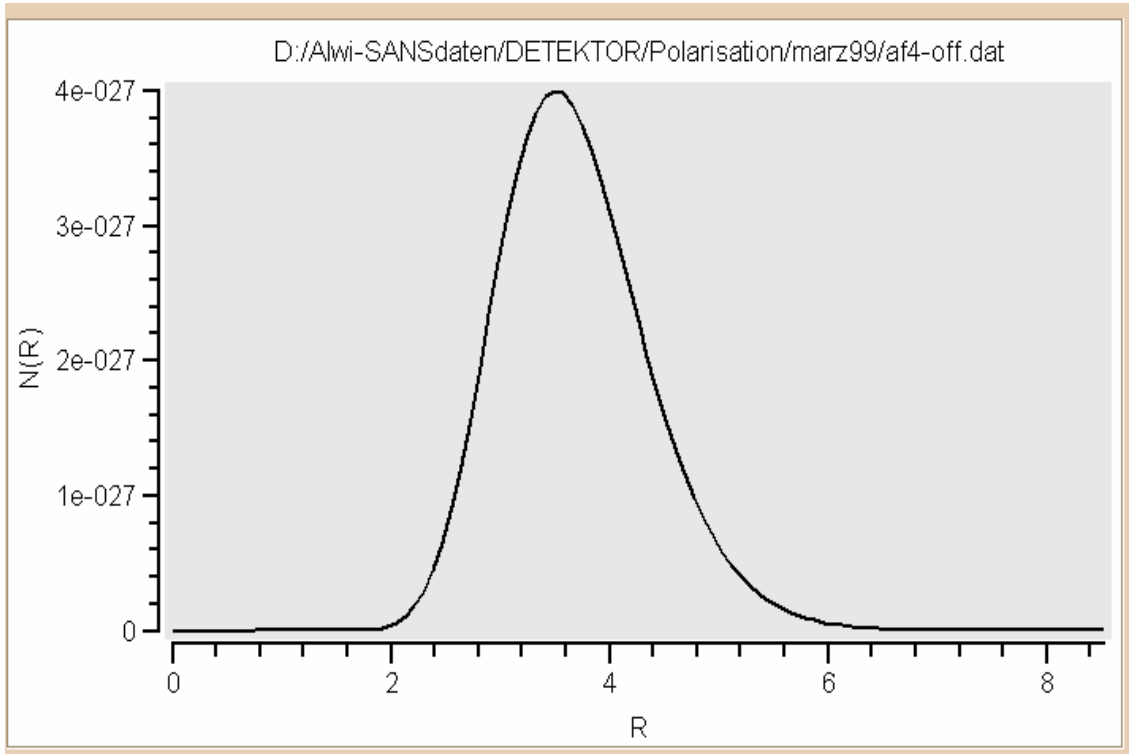

Moments of distribution

1. scatt. contrib.:	calc: yes
LogNorm	Spherical Shell iii
<R^1> = 3.68784	<R^5> = 957.413
<R^2> = 14.0692	<R^6> = 4182.78
<R^3> = 55.5257	<R^7> = 18902.4
<R^4> = 226.693	<R^8> = 88353.1
R_Ic = 4.08268	Ic = 2.72178666667
R_Ii = 3.9466	Ii = 2.95995
R_Ac = 4.15243	Ac = 6.86064235721
R_VP = 4.22335	VP = 17.983847565
R_RG = 4.59598	RG = 3.5600307999

$RG^2 = \langle R^8 \rangle / \langle R^6 \rangle = 21.1$

$R = (3/5)^{0.5} RG = 3.6$ nm

Number density: $n_p\,(1-f) = N\,10^{42} = 6.59\,10^{15}$ T cm^{-3}

Volume fraction: $f(1-f) = n_p 4/3\pi \langle R^3 \rangle = 6.59\ 4/3\pi\ 55.5\ 10^{15} 10^{-21} = 0.0015$

Problem class

1.) Calculate the nuclear and magnetic scattering contrast of ferromagnetic Co-particles wiith fully aligned magnetic moments in a solvent of a mixture of 40% D_2O and 60% H_2O.

H_2O: density 1 g/cm^3
D_2O: density 1.1 g/cm^3

H: Scattering lenght b= -0.374 10^{-12}cm
D: Scattering lenght b= 0.667 10^{-12}cm
O: Scattering lenght b= 0.581 10-12cm
Co: Atomic volume Ω(Co)=0. 0.01099 nm^3 /at , Scattering lenght b= 0.278 10^{-12}cm, Magnetic Moment m0 = 1.715 μB/ atom

V. New developments-Dynamical SANS

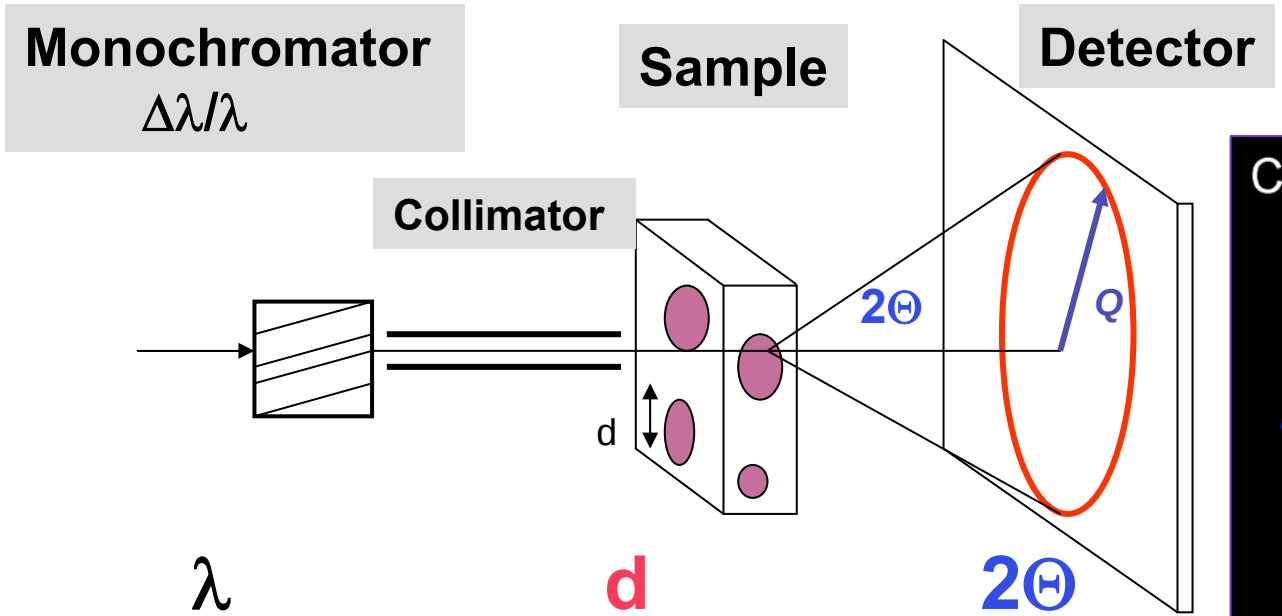

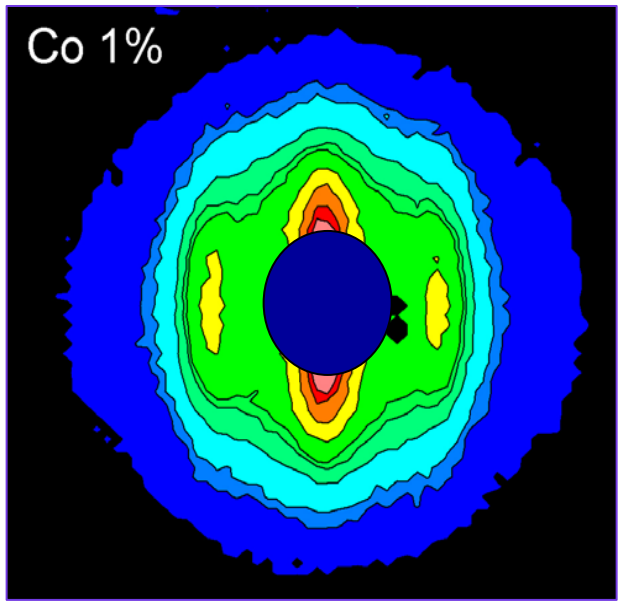

λ	d	2Θ
0.4-2 nm	0.5-300 nm	0.1-20°

Spacial fluctuations of density, composition, magnetization

Dynamical fluctuations- What time range ?

Dynamics of ordering and relaxation

Relaxation of field-induced order:
Time-resolved SANSPOL

Ordering and re-ordering in oscillating external field:

Continuous stroboscopic SANS
Pulsed stroboscopic „TISANE“

Time-resolved SANSPOL

B Intensity

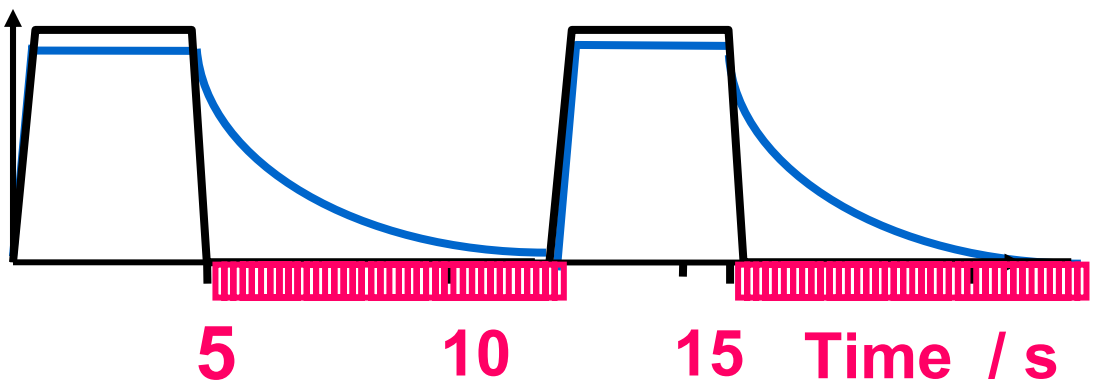

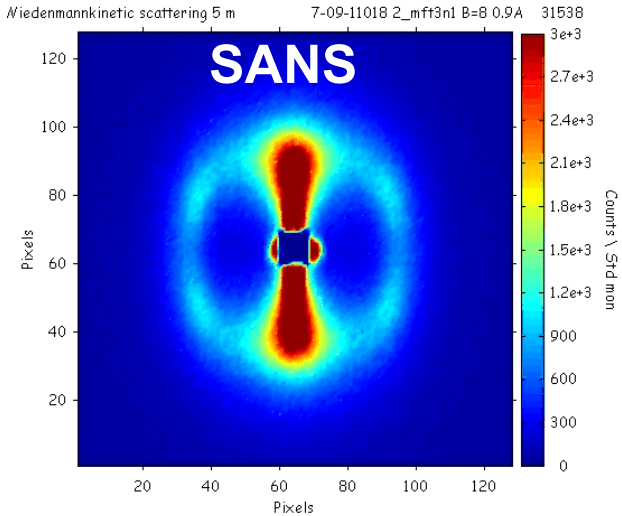

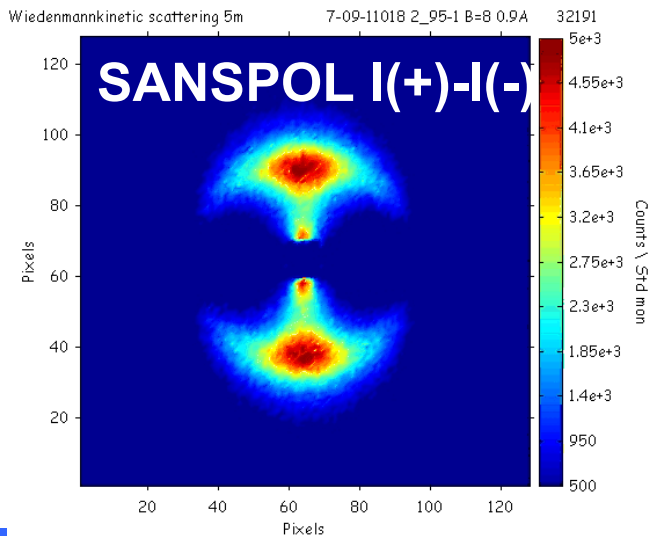

Decay of nuclear and magnetic correlations measured in time slices of 0.1 s

Duty cycle 15-30 s

MFT3N1: 6% Co in oil L9 H=0.5T

SANS cross-section

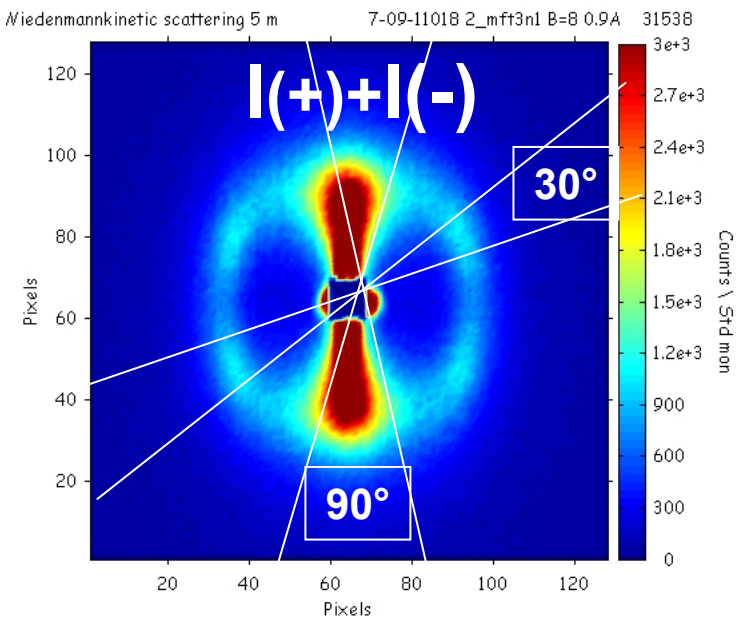

SANSPOL Difference cross-section

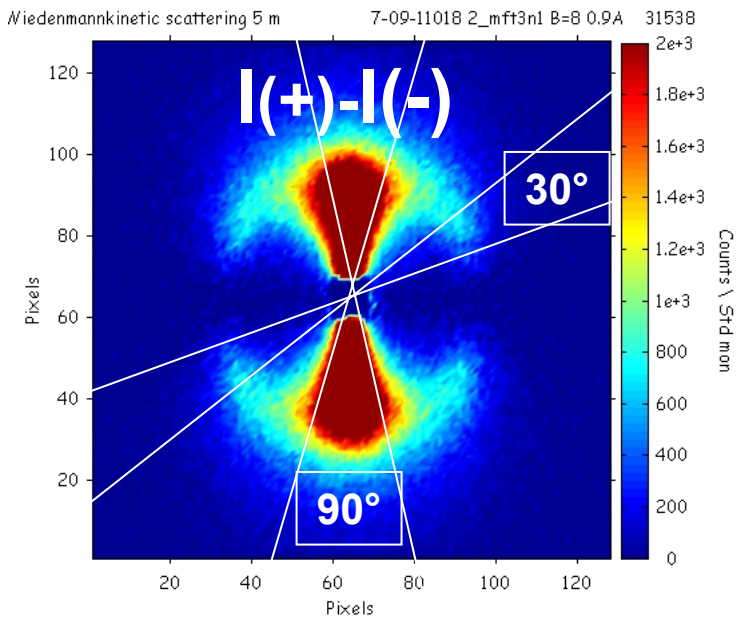

Magnetic and Nuclear correlations
+ Misalignment of magnetic moment
+ Nomagnetic contributions

Magnetic-Nuclear correlations

SANSPOL Differences

Loss of inter-plane correlations

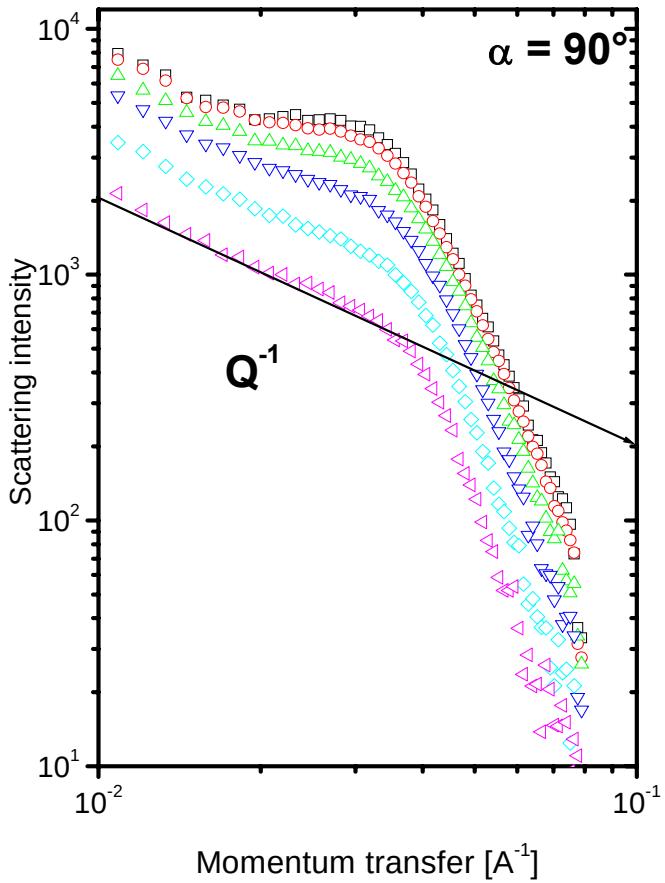

Loss of intra-plane correlations

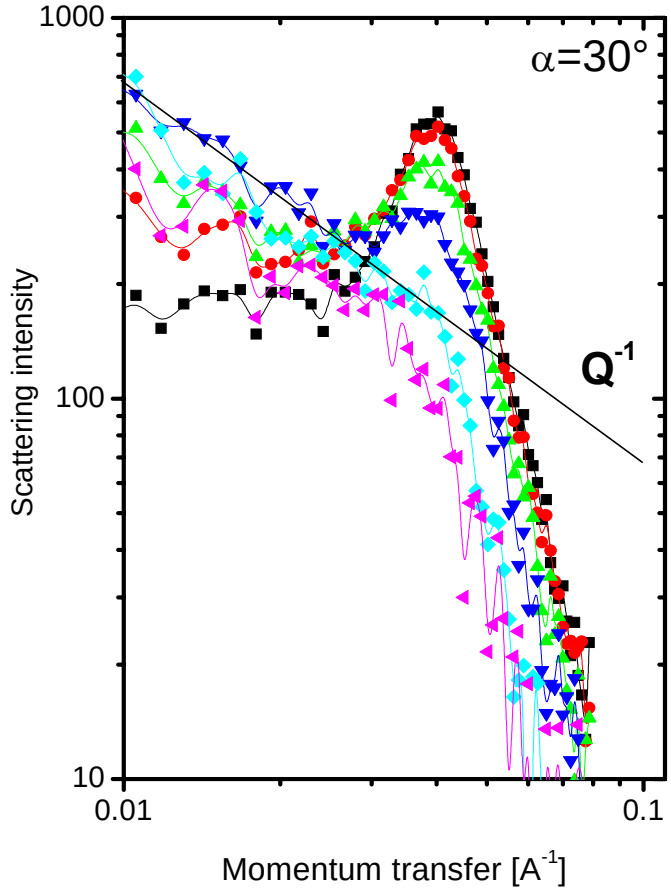

Chain segments remain partly aligned along remanent field

Time dependence of I(+)- I(-)

Sectors α = 90° (Q⊥ H)

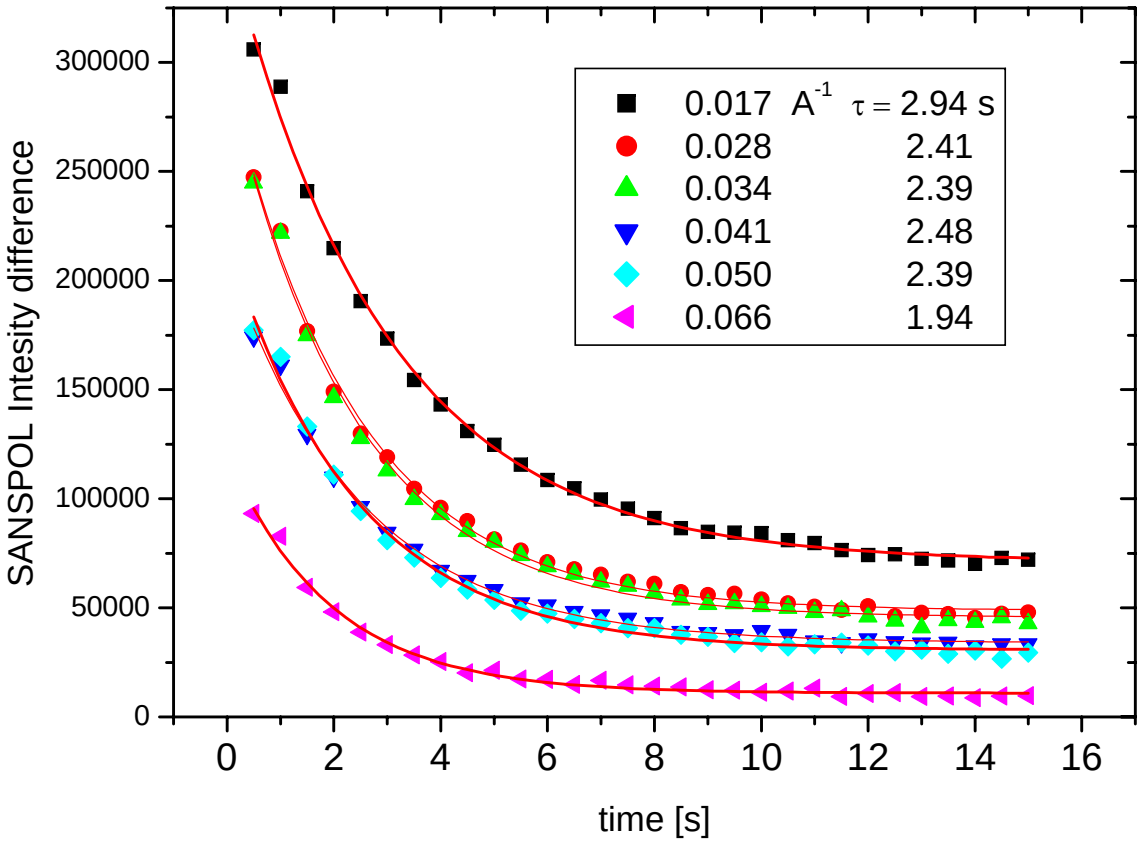

intra-chain correlations

τ > 3 s

Hexagonal Ínter-plane correlations:

$\tau \approx 2$ s

Exponential decay: $I(t)=I_0 + A \exp^{-t/\tau}$

Time dependence of I(+)- I(-)

Sectors α = 30°

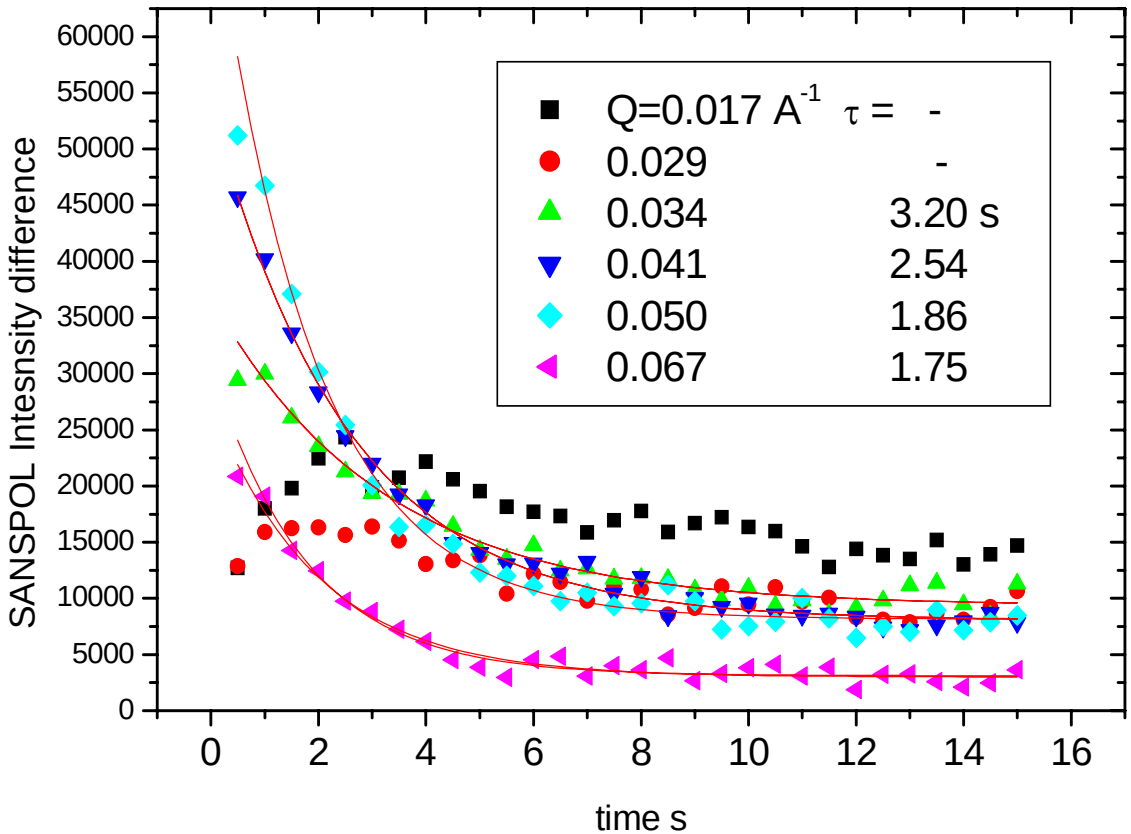

Hexagonal intra-plane correlations:

$\tau \approx 3.2$ s

Exponential decay: $I(t)=I_0 + A \exp^{-t/\tau}$

A. Wiedenmann, U. Keiderling, R. P. May, C. Dewhurst Physica B 2006

Time-resolved SANSPOL

Switch-off of B:

- Slow decay of field-induced ordering (few seconds).
- Fully reversible relaxation onto equilibrium
- Single exponential decay:
  Time constants depending on Q and B_{max}
  τ(intra-chain) > τ (in-plane) > τ (inter-plane)

Switch-on of B:

Reordering follows B-sweep rate: Process too fast!

Response from oscillating magnetic field

$$B(t)=B_0*\sin(2\pi\nu t+\phi)$$

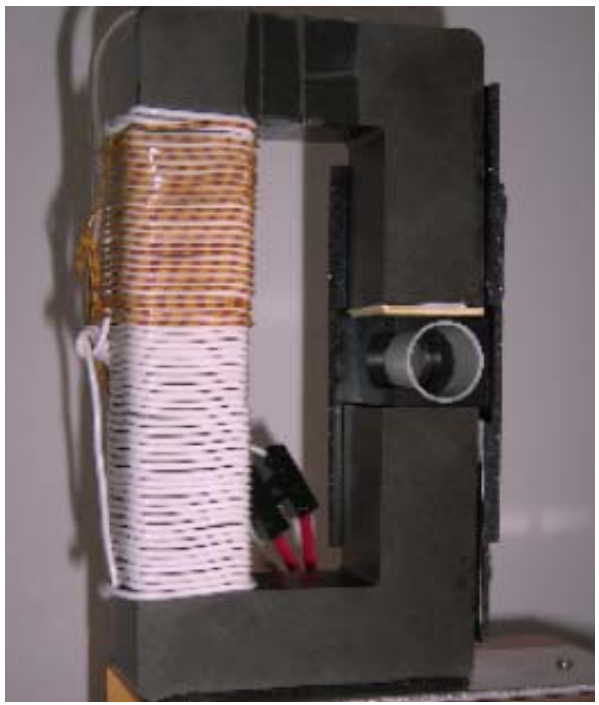

B_0 =20mT

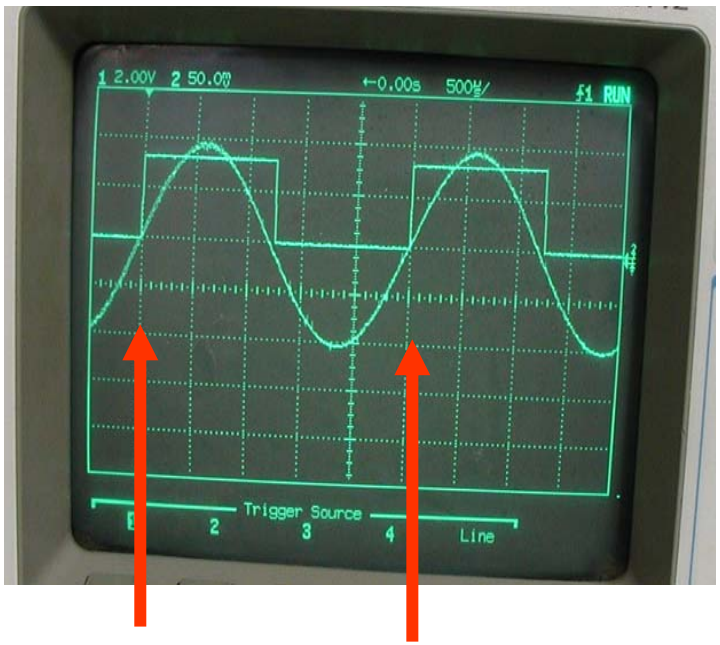

Frequency ν= 50 - 2200 Hz

Duty cycle: 3-5 orders of magnitude shorter

Trigger for list-mode data acquisition in 2 D detector

Continuous stroboscopic SANS

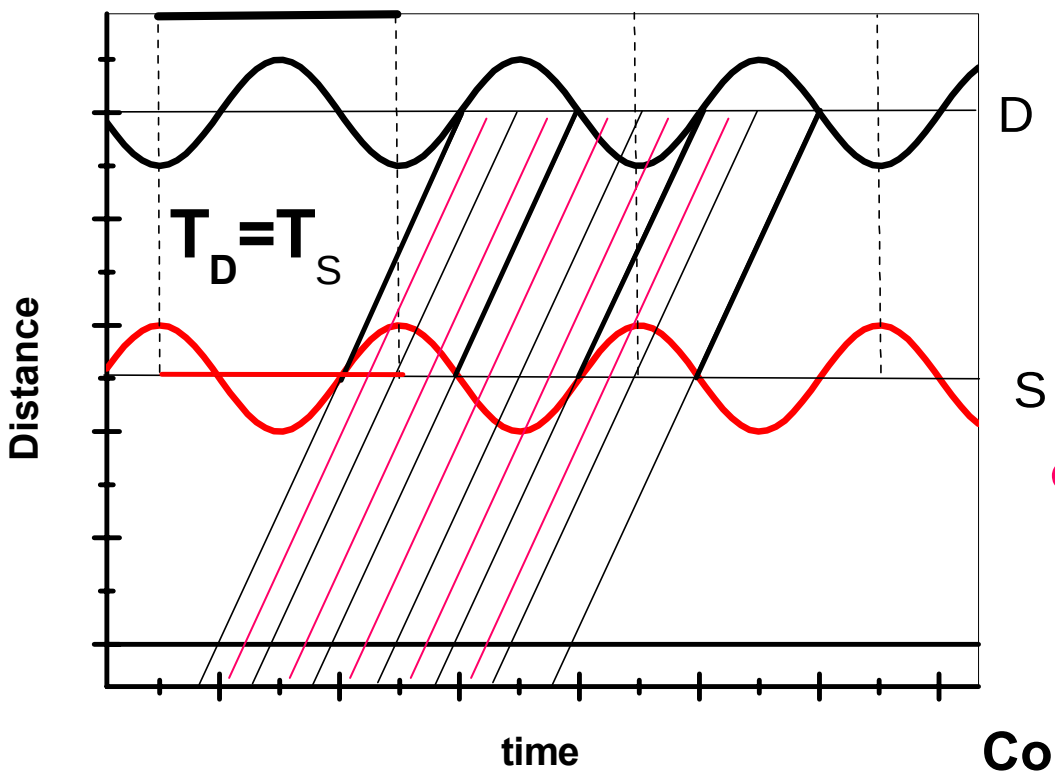

2D- Detector:
Time stamped recording of each scattered neutron

Sample
Oscillating magnetic field: oscillating magnetic contrast

Continuous monochromatic flux

$$t_{TOF}[ms] = \lambda[nm] * L_2[m] * 2.52778$$

Continuous stroboscopic SANS at V4

Wavelength distribution $\Delta\lambda / \lambda = 0.11$

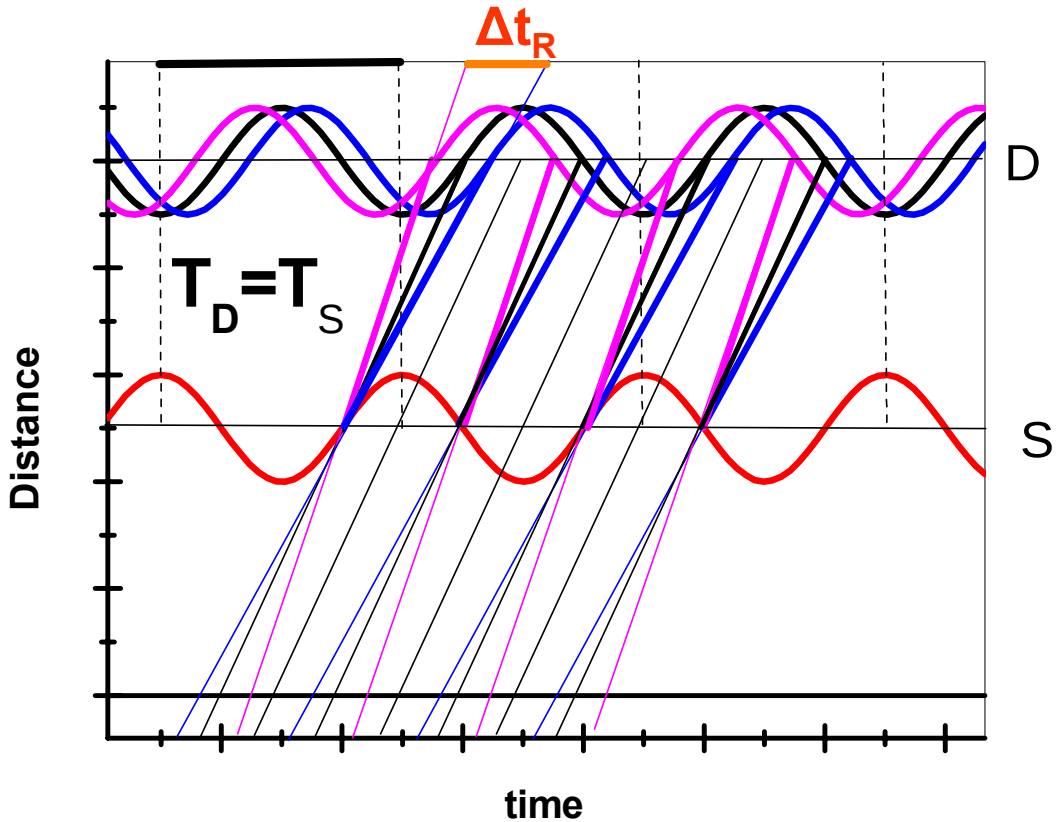

Damping

λ=0.6 nm, L_2=4m

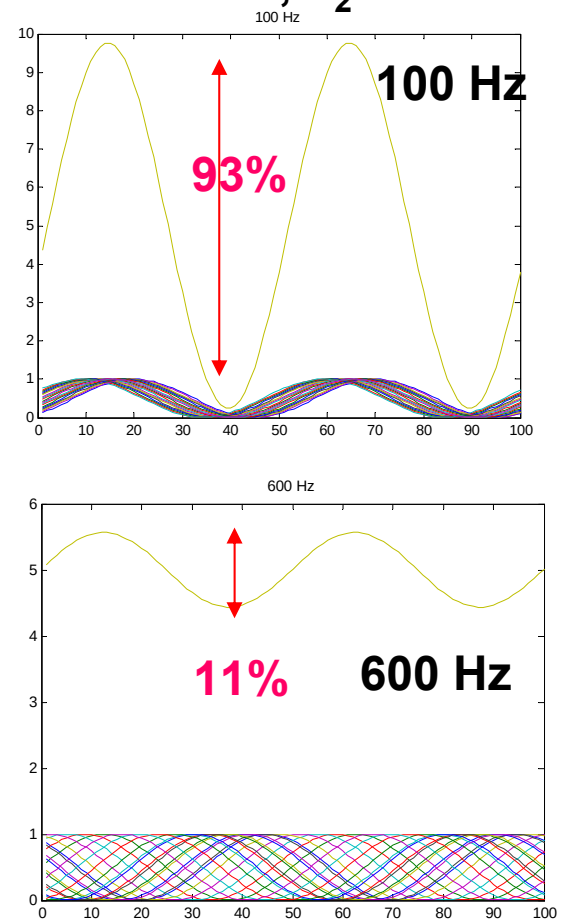

Relative time spread:

$$\Delta t_R / T_s = \Delta\lambda * t_{TOF} * \nu_s$$

Pulsed time-involved SANS (TISANE)

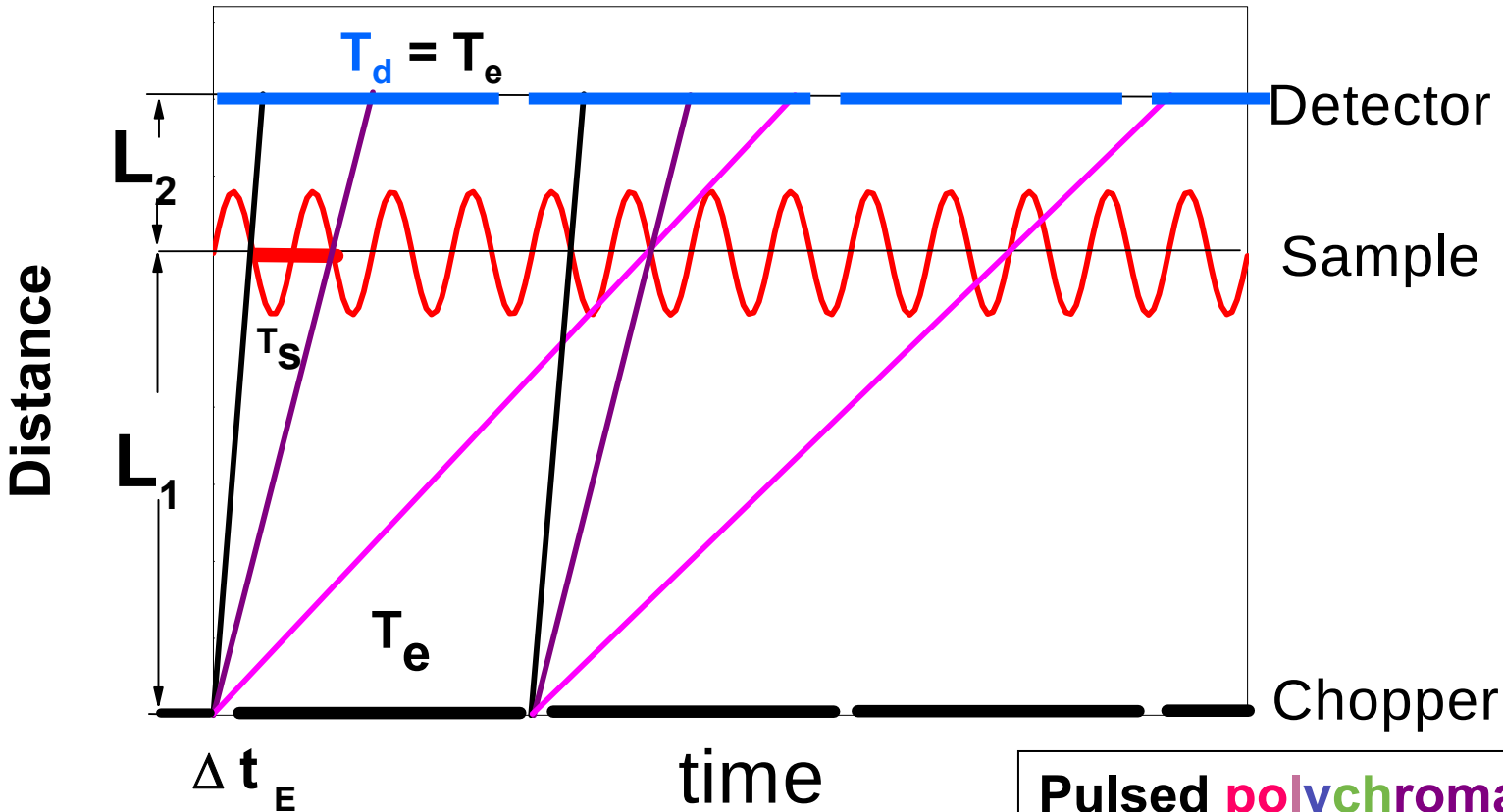

Pulsed polychromatic beam
λ: 0.2-1.6 nm

Pulsed time-involved SANS (TISANE)

R.Gähler et al 1984

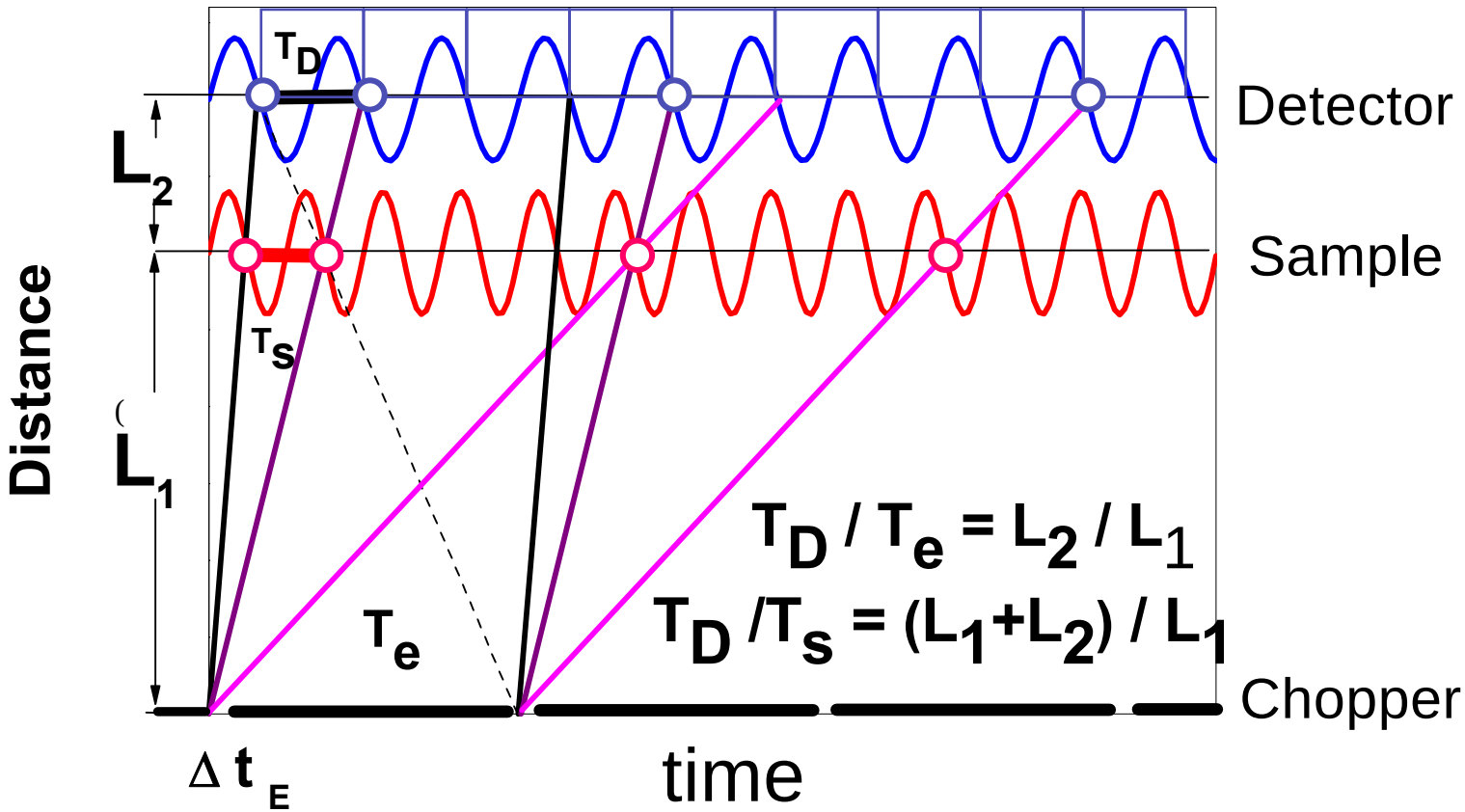

All neutrons scattered at the sample in the same oscillation state are recorded in the same time channel

Pulsed time-involved SANS (TISANE)

R.Gähler et al 1984

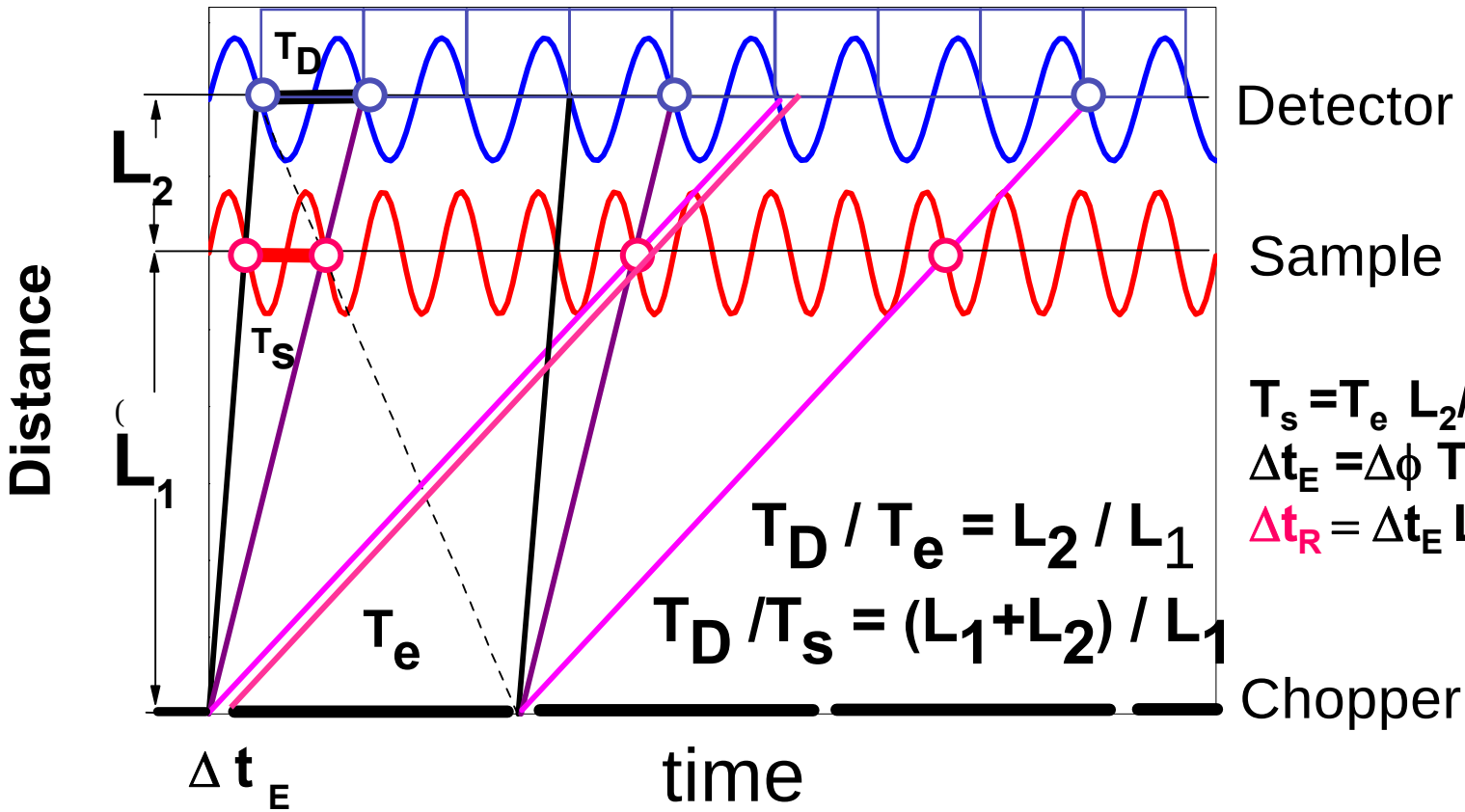

$T_D / T_e = L_2 / L_1$

$T_D / T_s = (L_1+L_2) / L_1$

$T_s = T_e \; L_2/(L_1+L_2) \sim T_e$

$\Delta t_E = \Delta\phi \; T_e$

$\Delta t_R = \Delta t_E \; L_2/L_1 \sim T_e$

Relative time spread:

$\Delta t_R / T_s = \Delta\phi \; (L_1+L_2) / L_1$

independent of frequency

TISANE@NEAT

L_1=13 m, L_2=4 m, ν_E (max)=666 Hz , ν_s(max)=2800 Hz

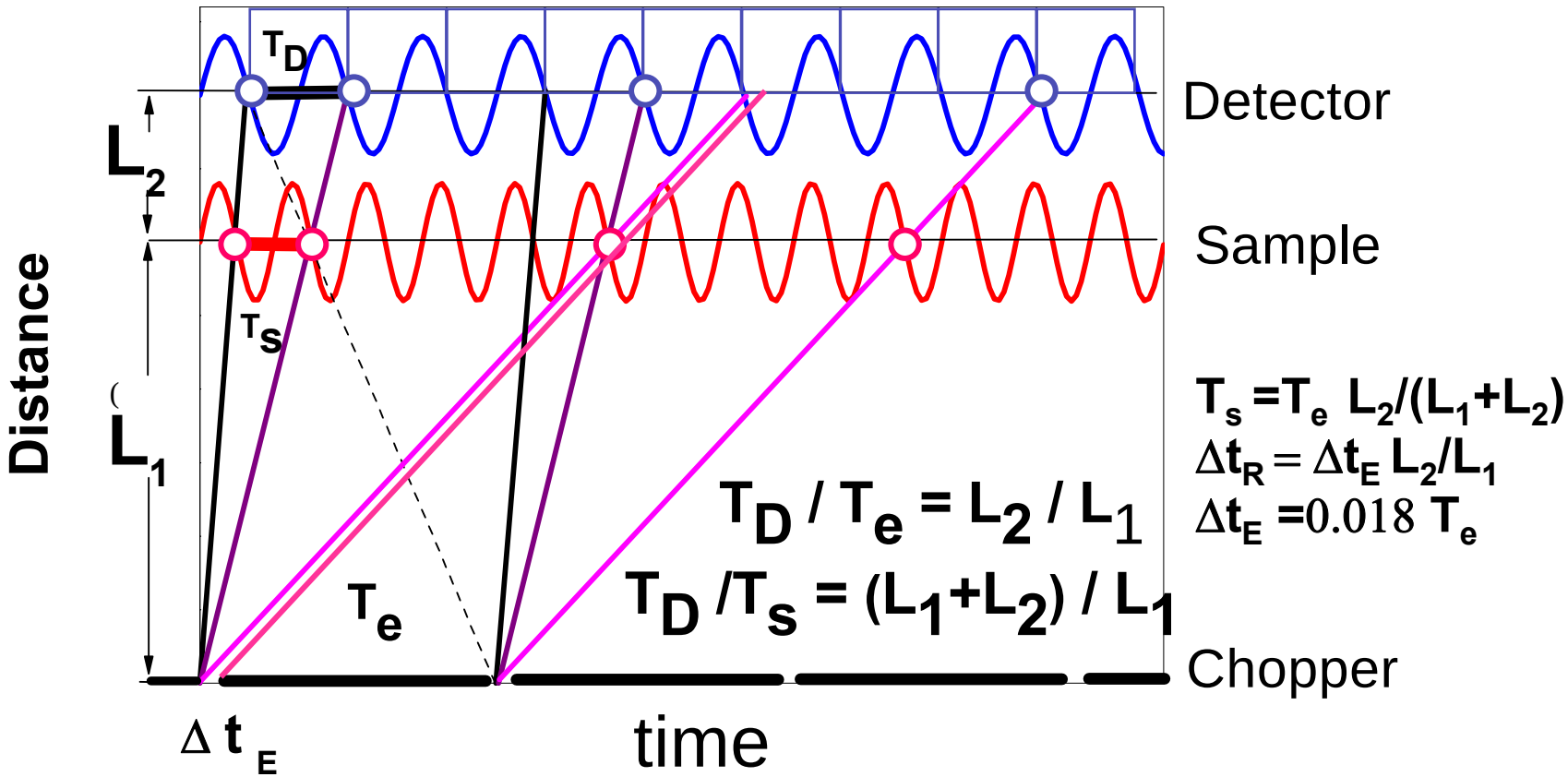

Relative time spread:

$\Delta t_R / T_s = 0.018\ (L_1+L_2) / L_1$

independent of ν_s !

2.3%

TISANE@NEAT

L_1=13 m, L_2=4 m, ν_E (max)=666 Hz , ν_s(max)=2800 Hz

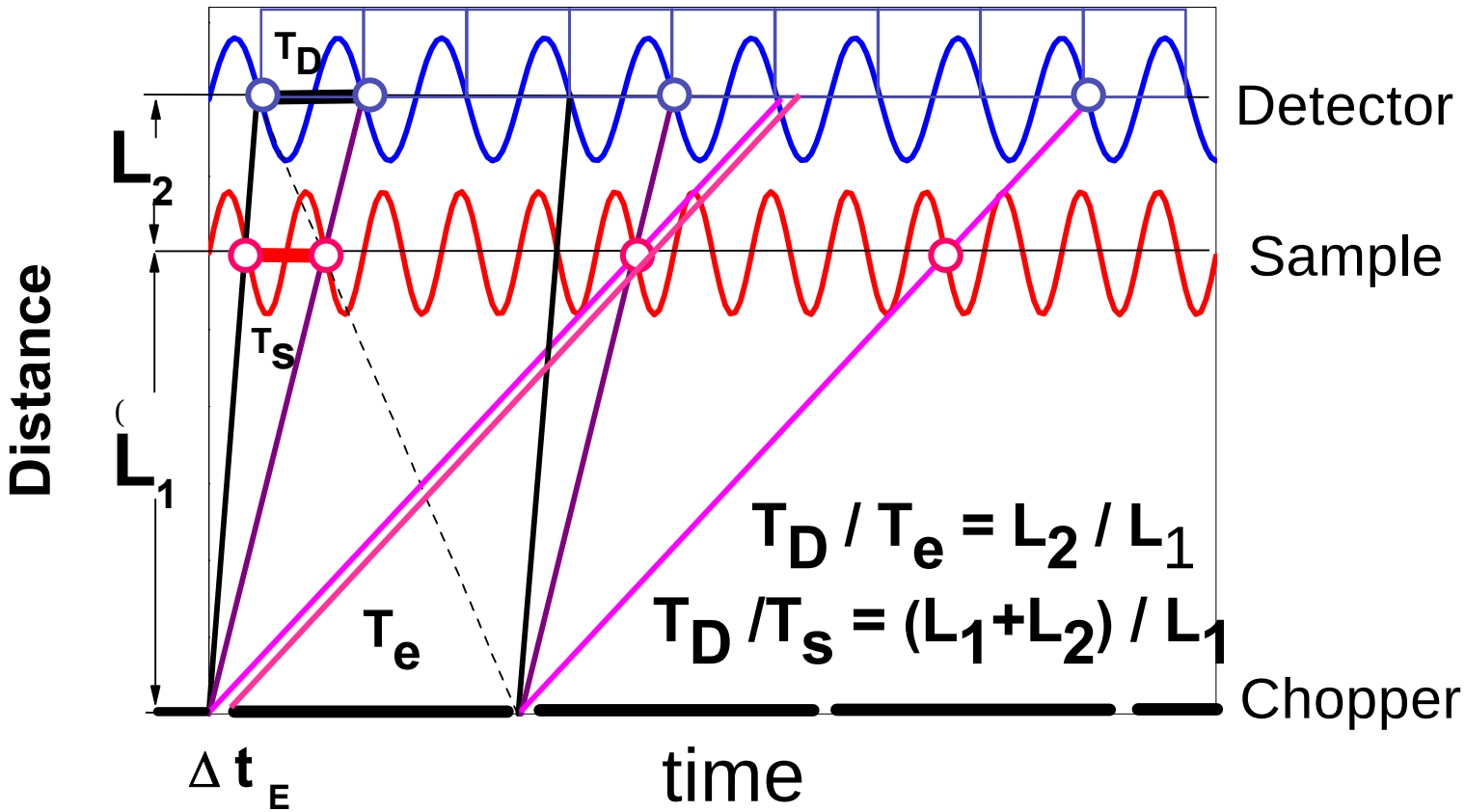

Precision:

nominal	$t_{mes} = T\ N_c$, **Deviation** $T_2\ (N_c\text{-}1)$
for t_{mes}=1h	$\Delta\nu/\nu < 10^{-7}$ **e.g.** 1531.393(5) Hz

Results: Continuous stroboscopic SANS

ν_s = 100 Hz B_0= 20 mT

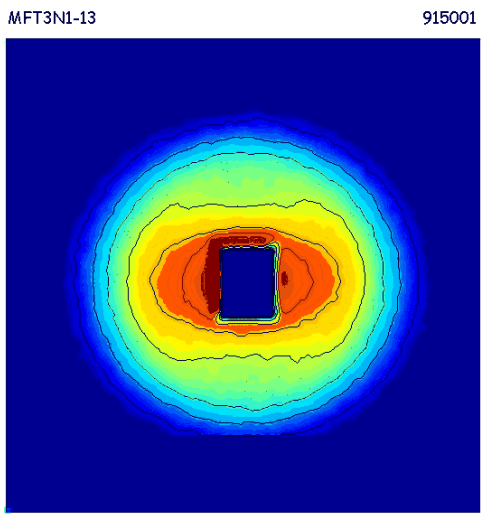

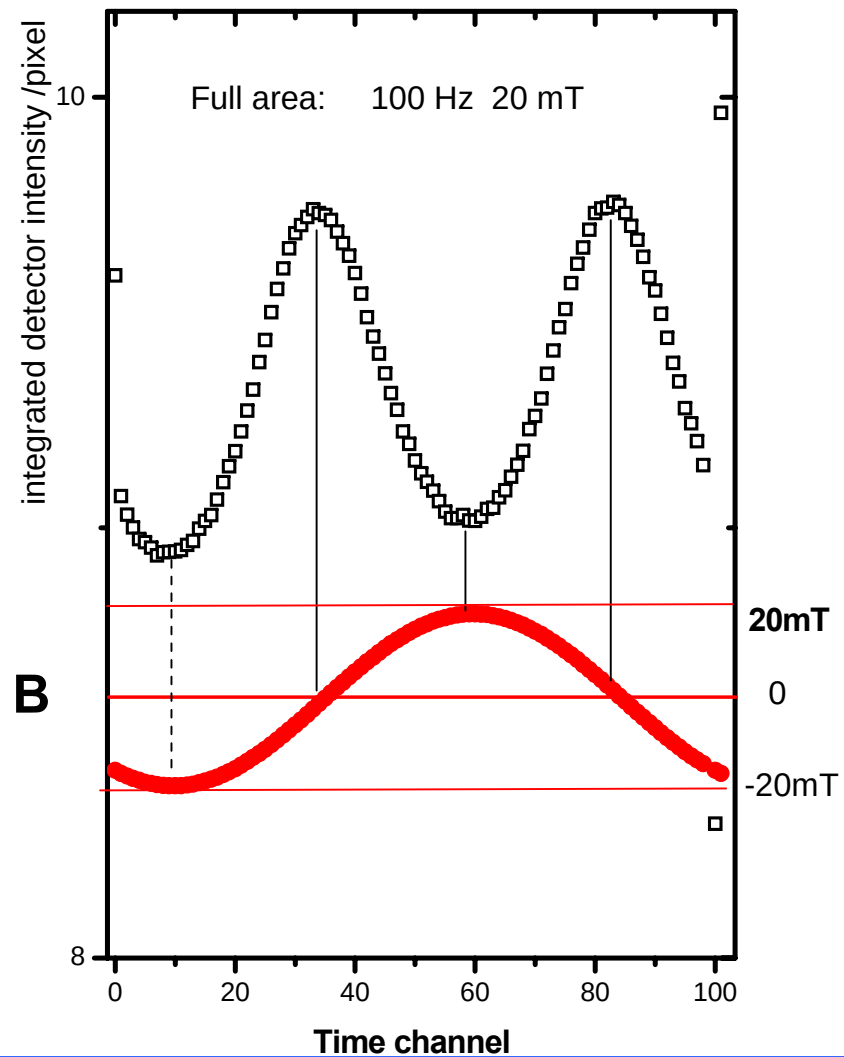

Frequency of response twice of B-field

Results: Static SANS

B_0= 20 mT

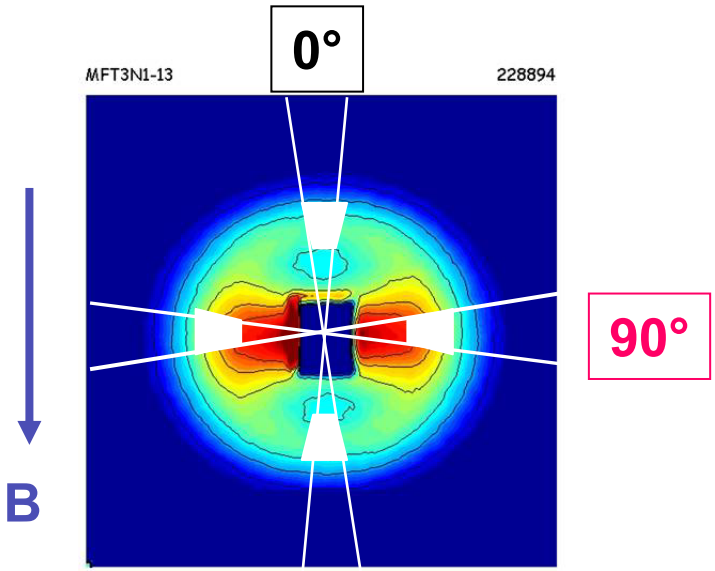

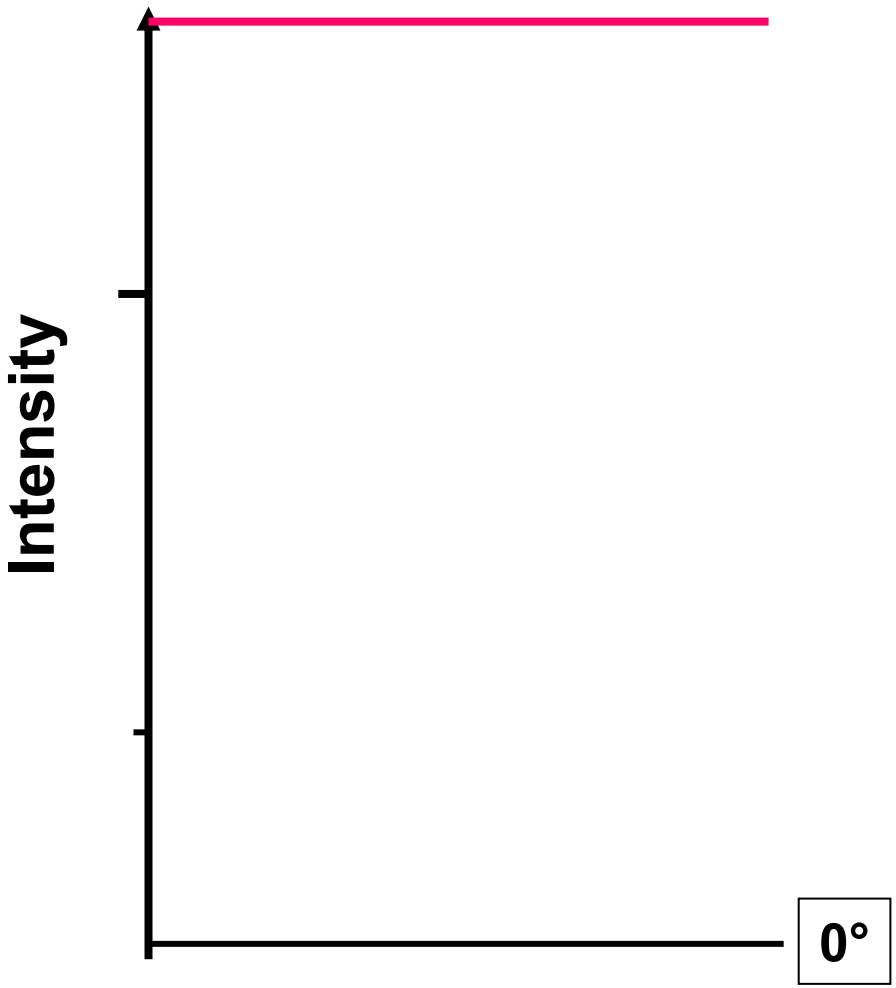

Results: Static SANS

B_0= 0 mT

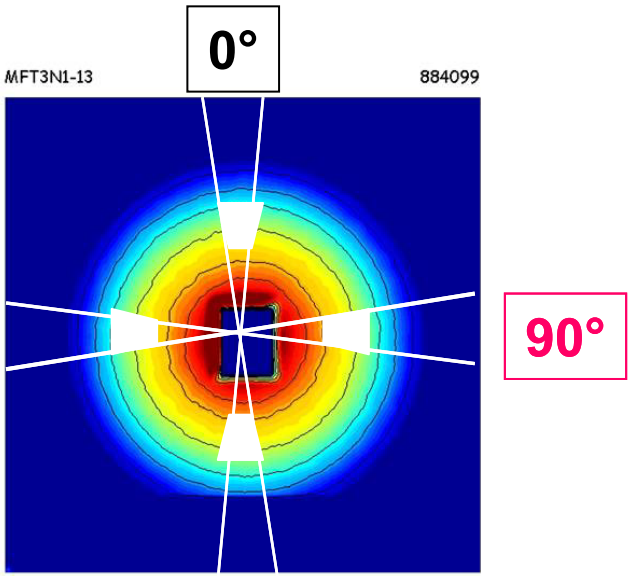

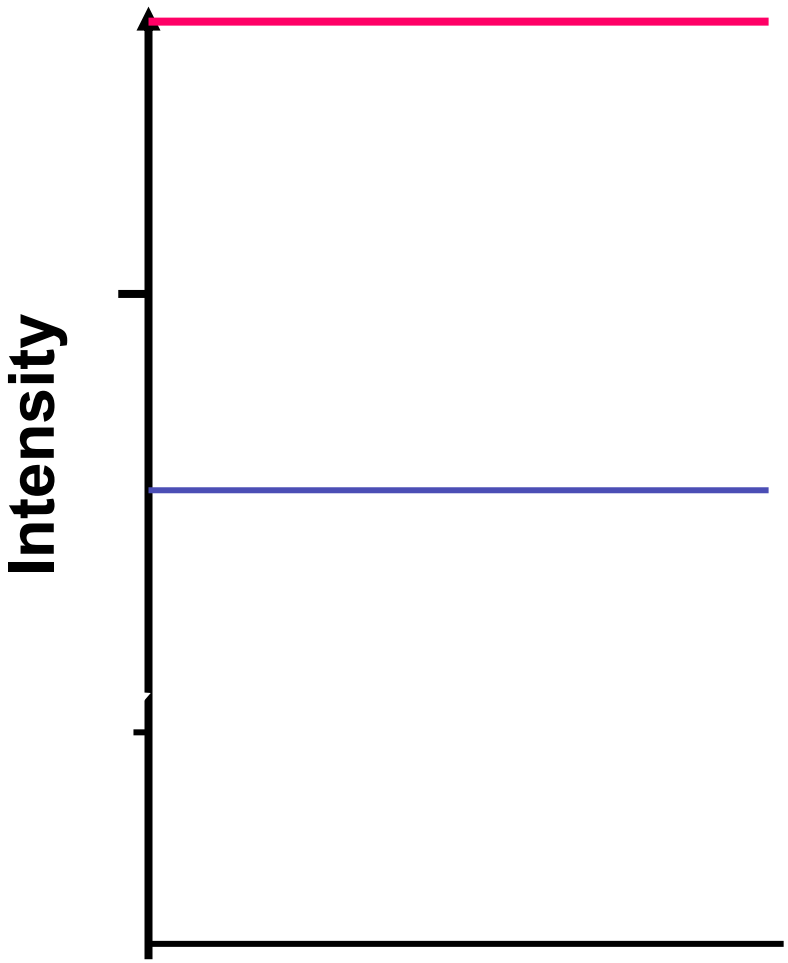

Results: Continuous stroboscopic SANS

ν_s = 100 Hz B_0= 20 mT

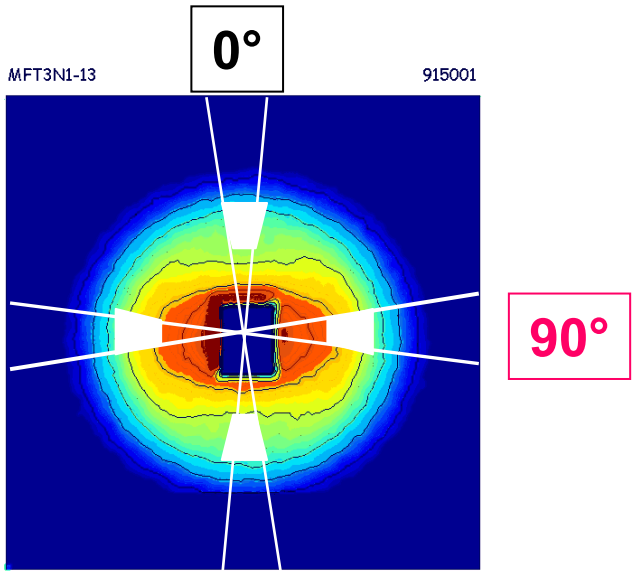

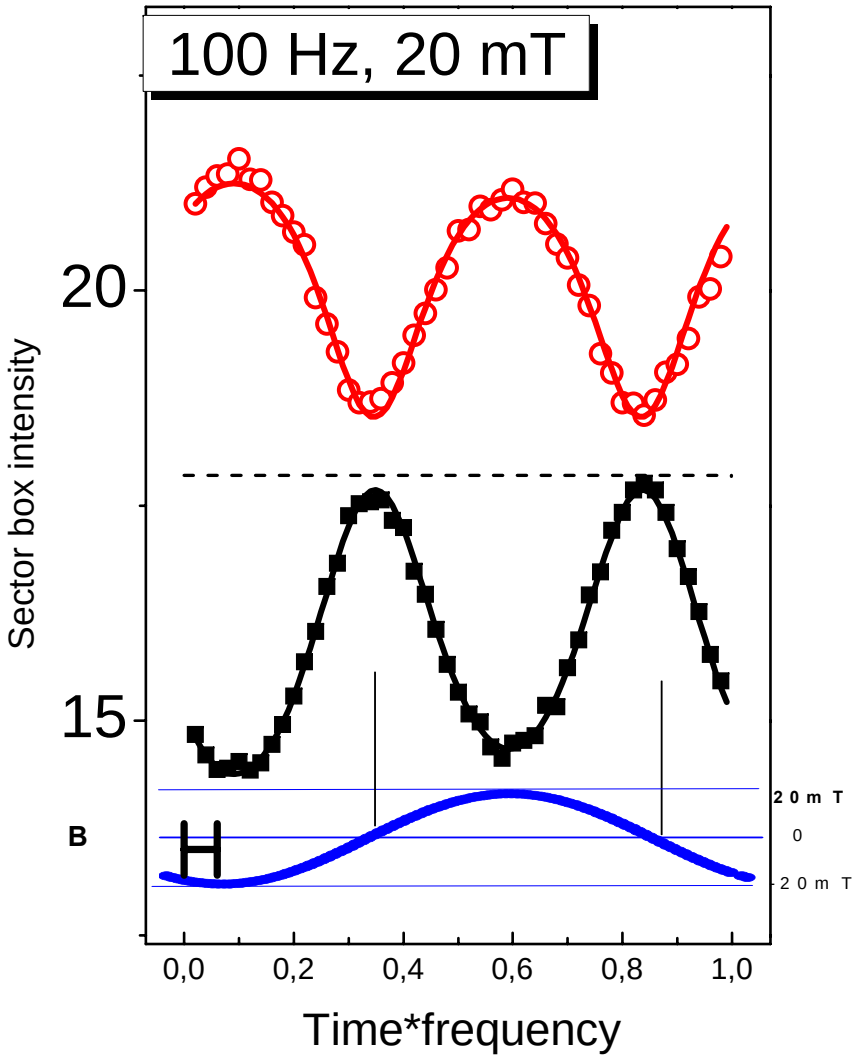

Frequency of response twice of B-field

Results: Continuous stroboscopic SANS

ν_s = 300 Hz B_0= 20 mT

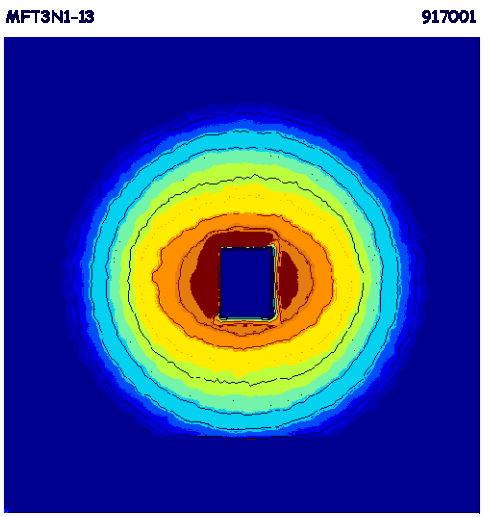

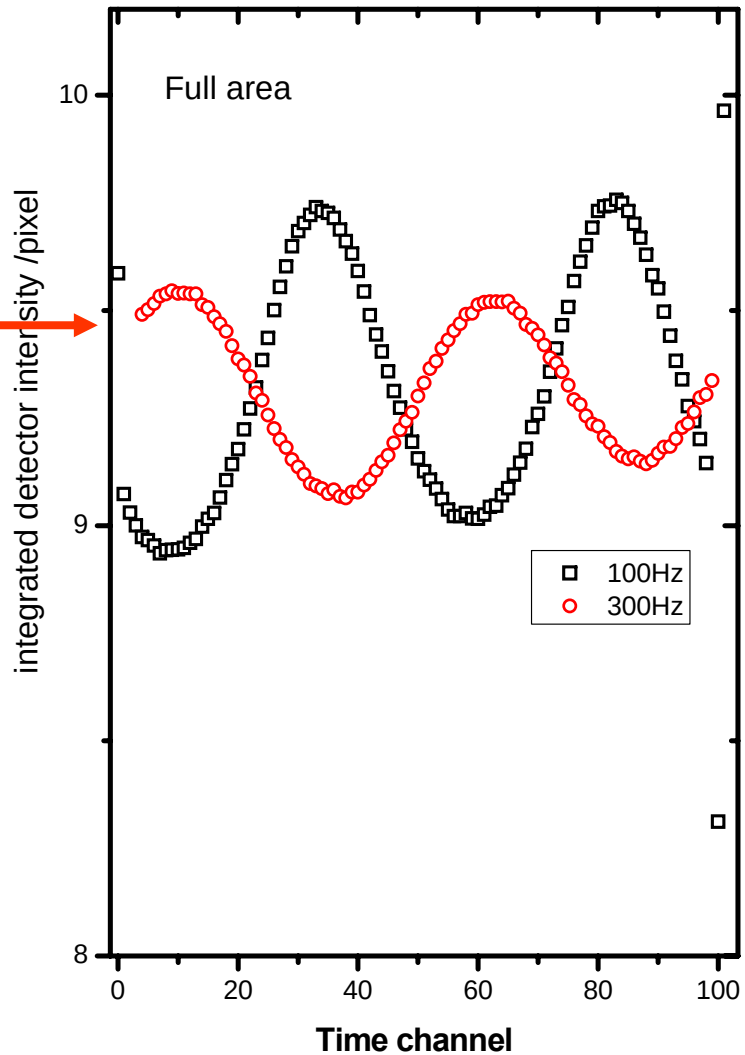

Results: Continuous stroboscopic SANS

ν_s = 300 Hz B_0= 20 mT

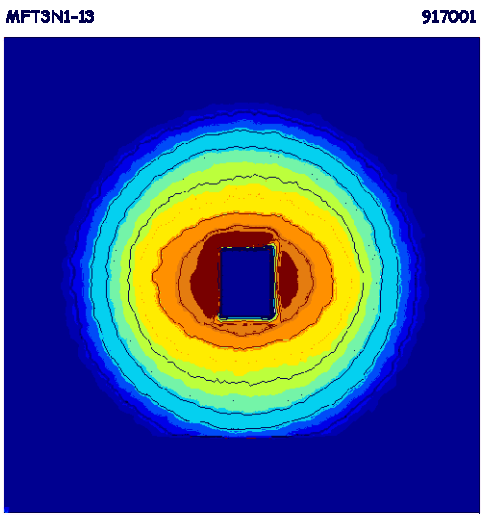

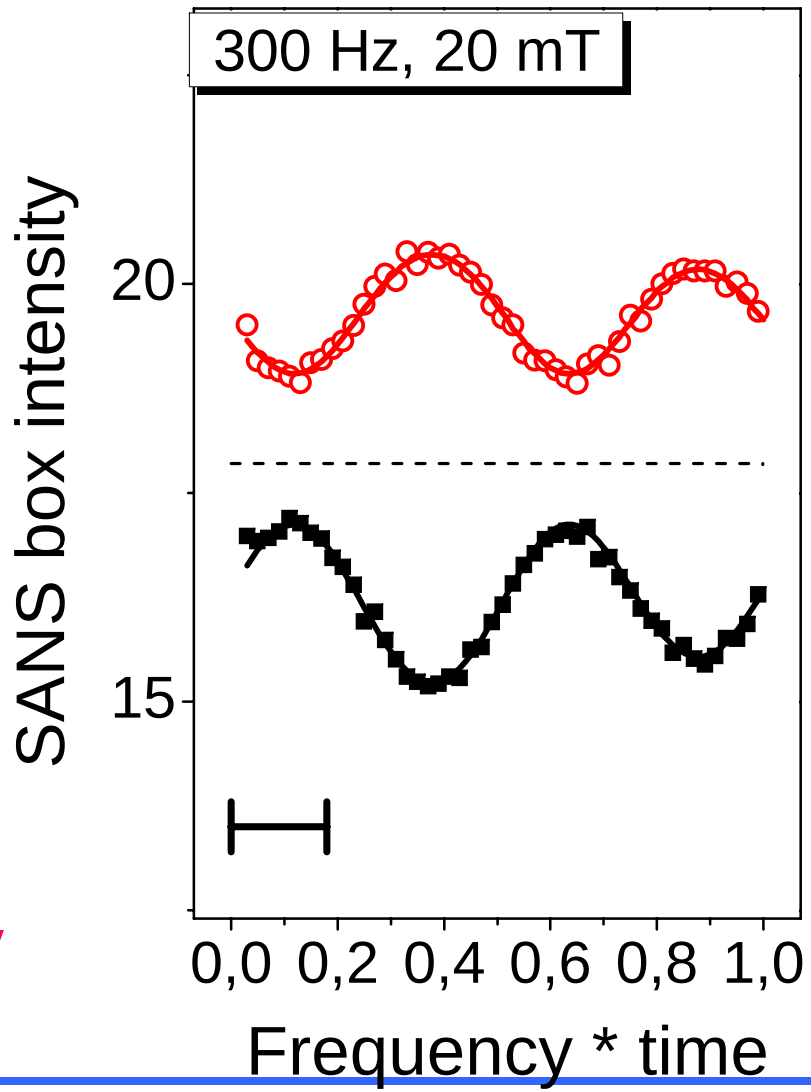

Damping of oscillations with increasing frequency

Results: Continuous stroboscopic SANS

ν_s = 600 Hz B_0= 20 mT

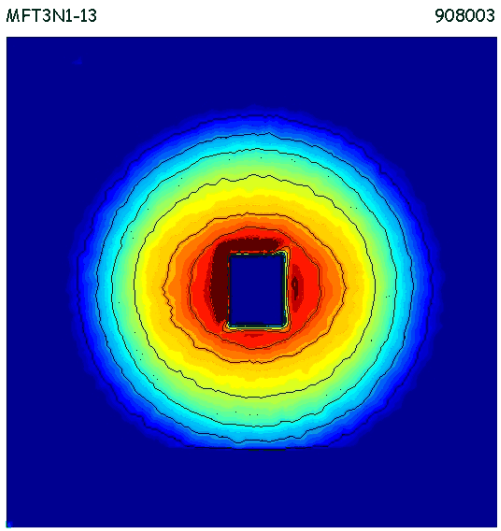

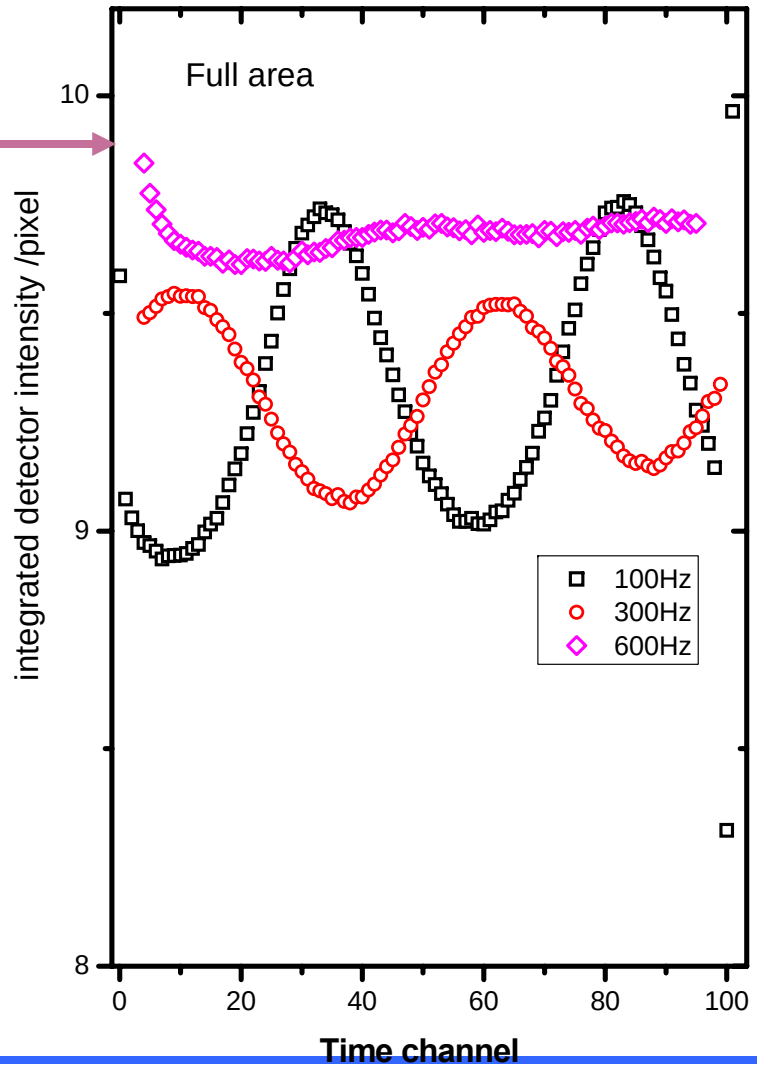

Damping of oscillations with increasing frequency

Results: Continuous stroboscopic SANS

ν_s = 600 Hz B_0= 20 mT

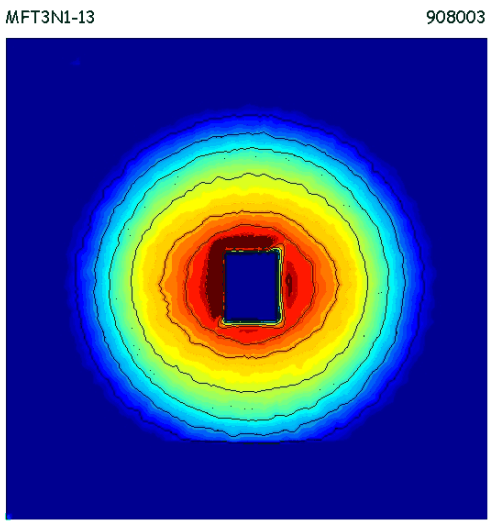

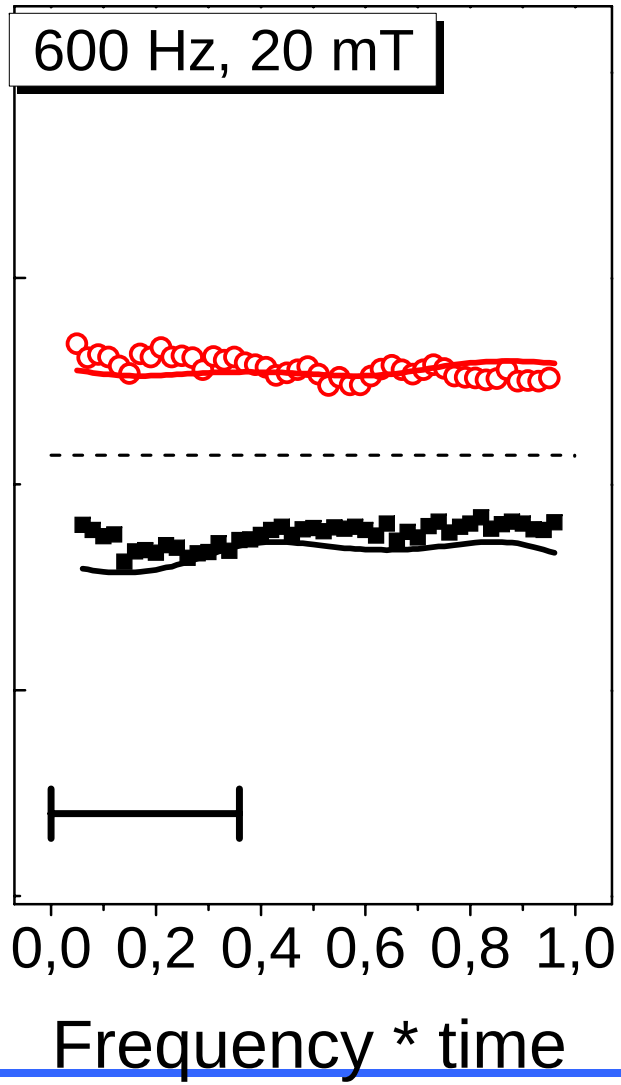

Damping of oscillations with increasing frequency

Continuous SANS

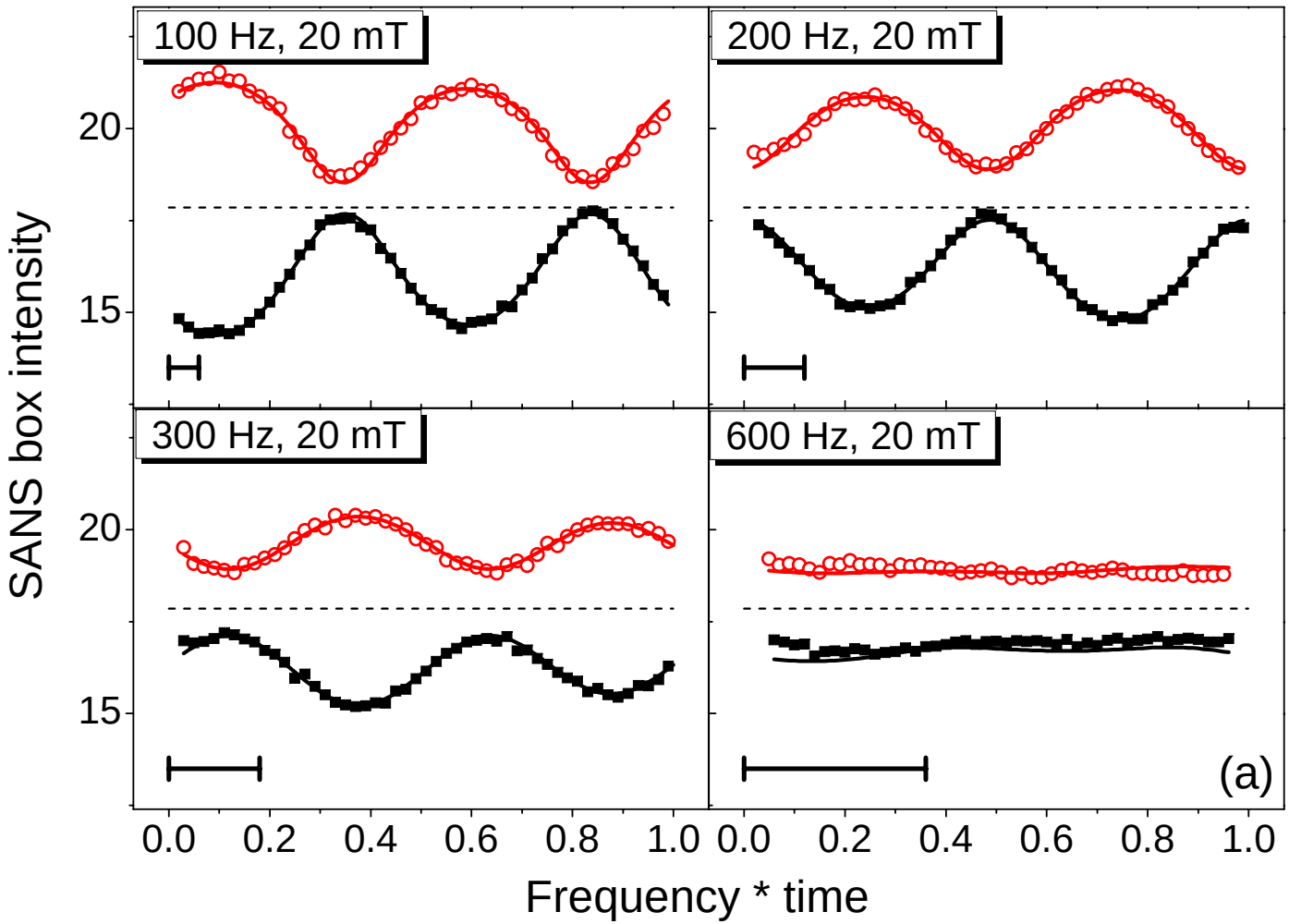

$\alpha = 90°$

$\alpha = 0°$

$\Delta t/T_s$

Pulsed TISANE:

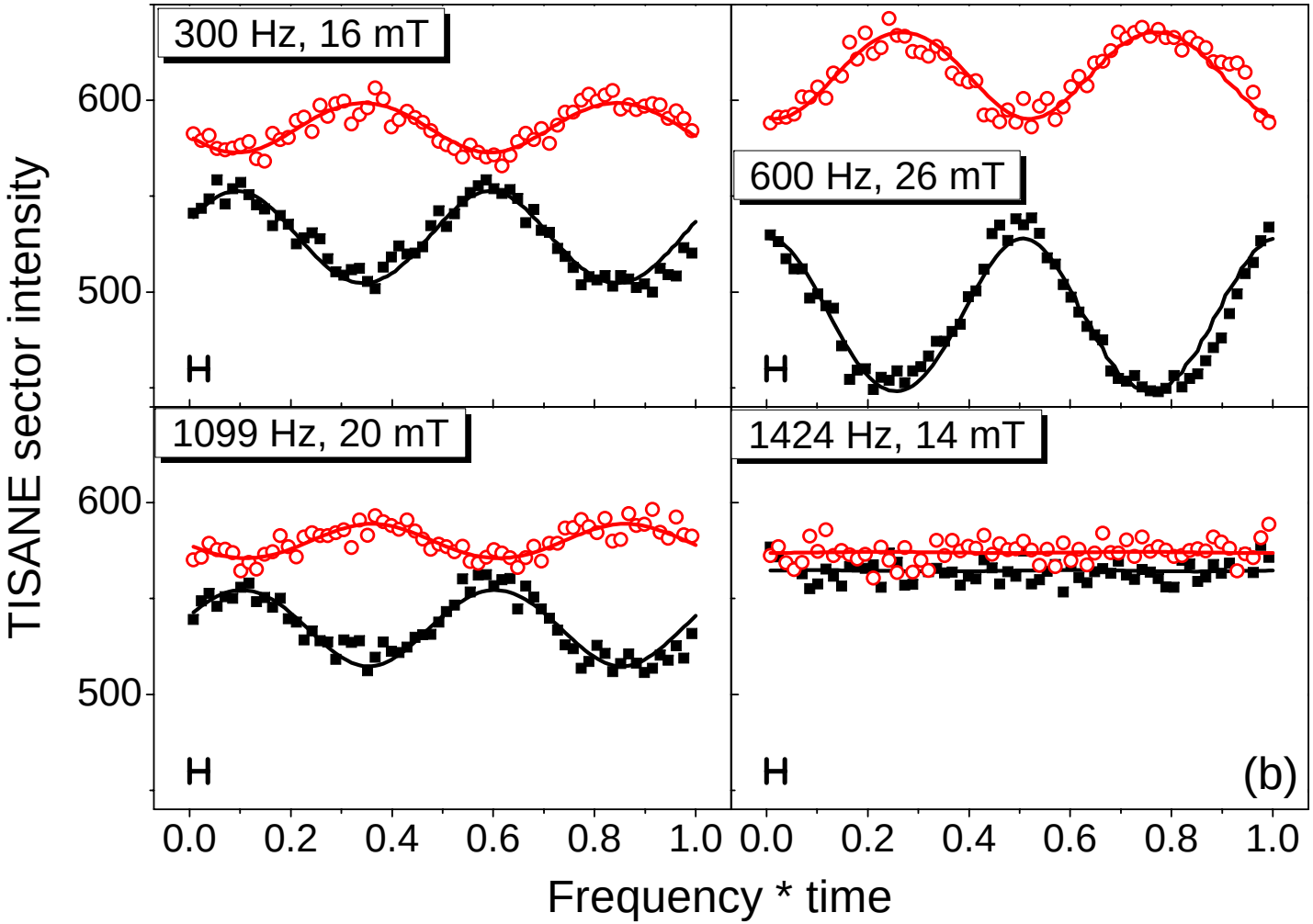

$\alpha = 90°$

$\alpha = 0°$

Magnetic single-domain particles

Superparamagnetic behaviour

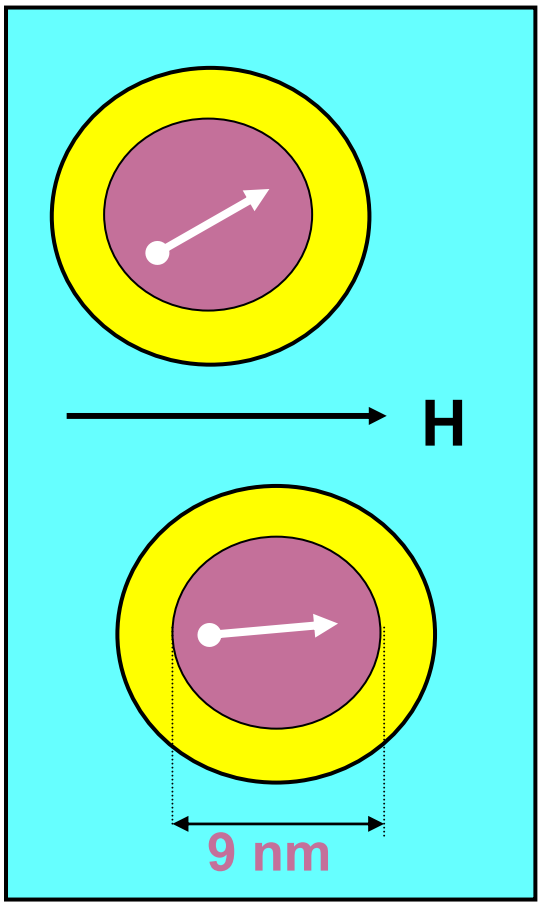

$$\sigma/\sigma_\infty = L(M_{cr}V_p\mu_0H_{eff} / kT)$$

Langevin function:

$$L(x)=\coth(x)-1/x$$

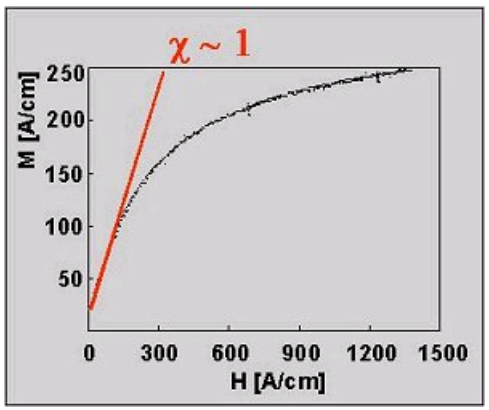

Known from SANS:

V_p Particle volume

M_{cr} Magnetic particle moment

Magnetic single-domain particles

Static SANS cross-section

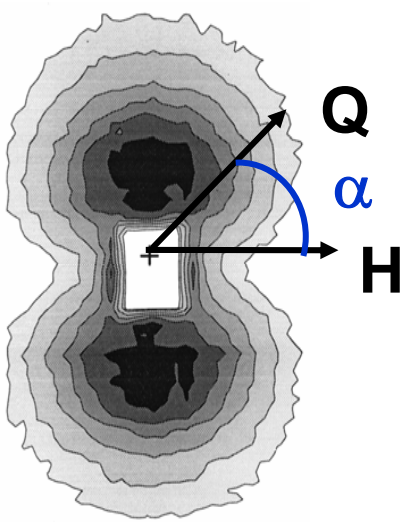

$$[\, F_M^2\, L^2(x)\, \sin^2\alpha + F_N^2]\;\; S(Q,\alpha)$$

$$+\, F_M^2\, [2L(x)/x - (L^2(x)-1+3\, L(x)/x\,)\sin^2\alpha]$$

R. Pynn et al (1983), J. Kohlbrecher , AW 1997

Magnetic single-domain particles

Static SANS cross-section

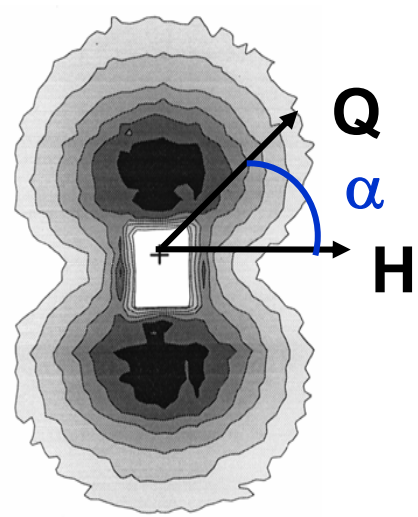

Magnetic and Nuclear correlations

+ Misalignment of magnetic moments

Magnetic single-domain particles

SANS cross-section in oscillating field

$$B(t)=B_0 \sin(2\pi\nu\, t) + B_{st}$$

$$x(t) = M_p V_p\, B(t) / kT)$$

$$\int \{ [\, F_M^2\, L^2(x) \sin^2\alpha + F_N^2]\; S(Q,\alpha)$$

$$+ F_M^2\, [2L(x)/x - (L^2(x)-1+3\, L(x)/x\,)\sin^2\alpha] \}$$

$$D(\Delta\lambda,\nu_s)\, d\Delta\lambda$$

Stroboscopic *versus* static SANS

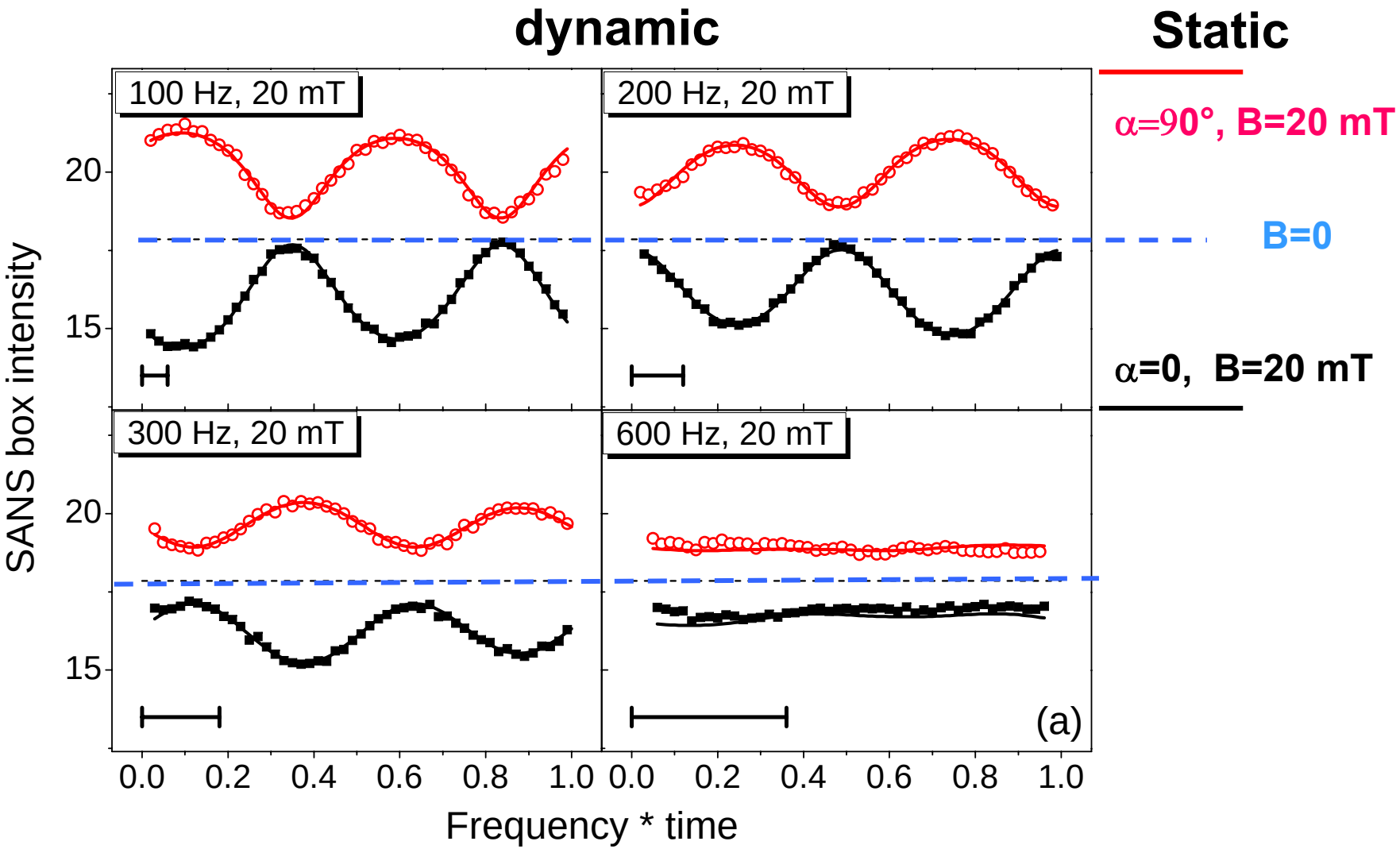

Magnetic single-domain particles

SANS cross-section in oscillating field

$$B(t)=B_0 \sin(2\pi\nu t) + B_{st}$$

$$f^* \int \{ [F_M^2 L^2(x) + 2 F_M F_N L(x)] \sin^2\alpha + F_N^2 \} S(Q,\alpha)$$

$$+ F_M^2 \{L(x)/x - (L^2(x)-1+3 L(x)/x)\sin^2\alpha \} D(\Delta\lambda,\nu_s) d\Delta\lambda$$

Oscillating part

$$+ \quad (1- f) U_{static}$$

Fraction of freely rotating moments

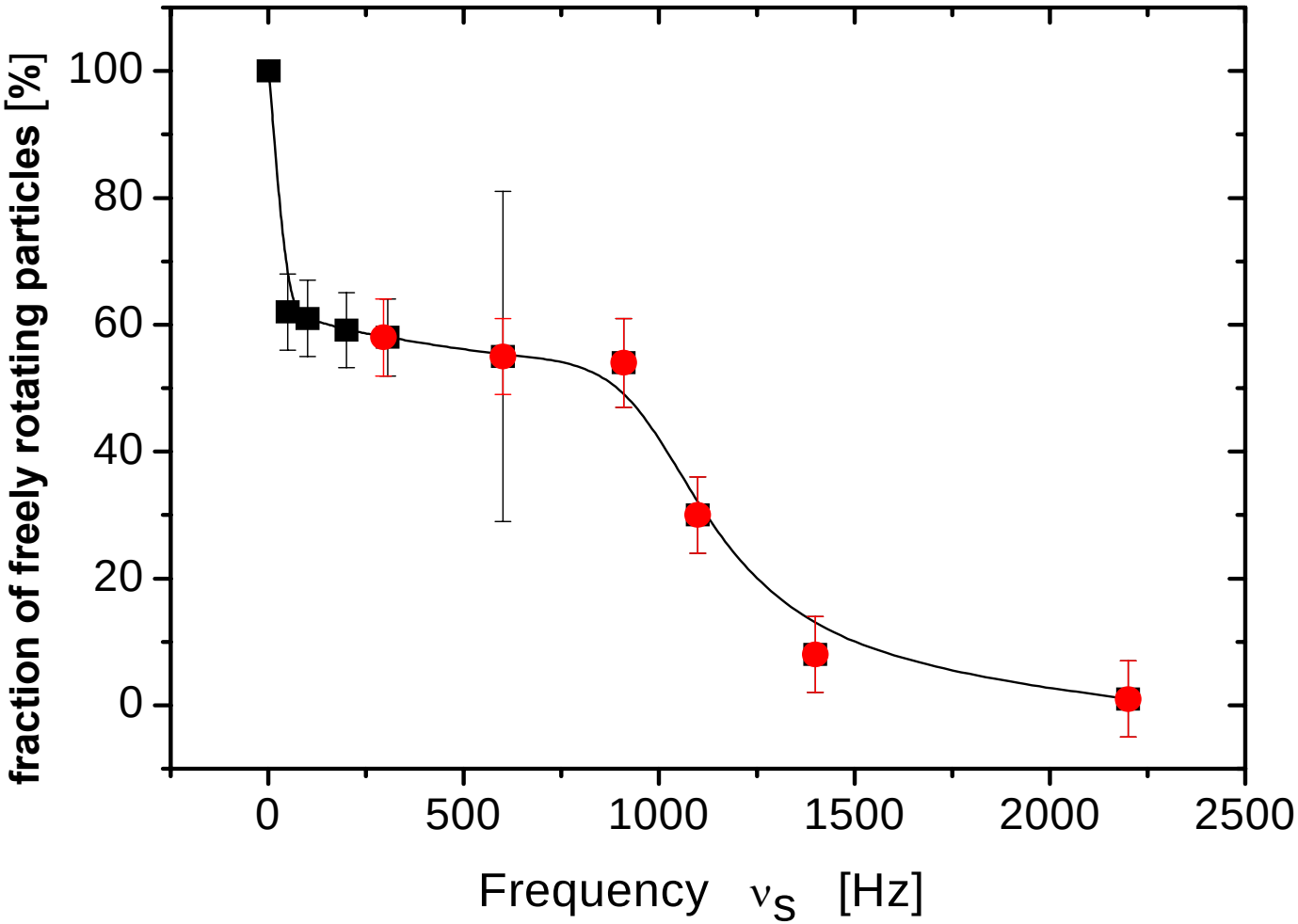

Fraction of freely rotating moments

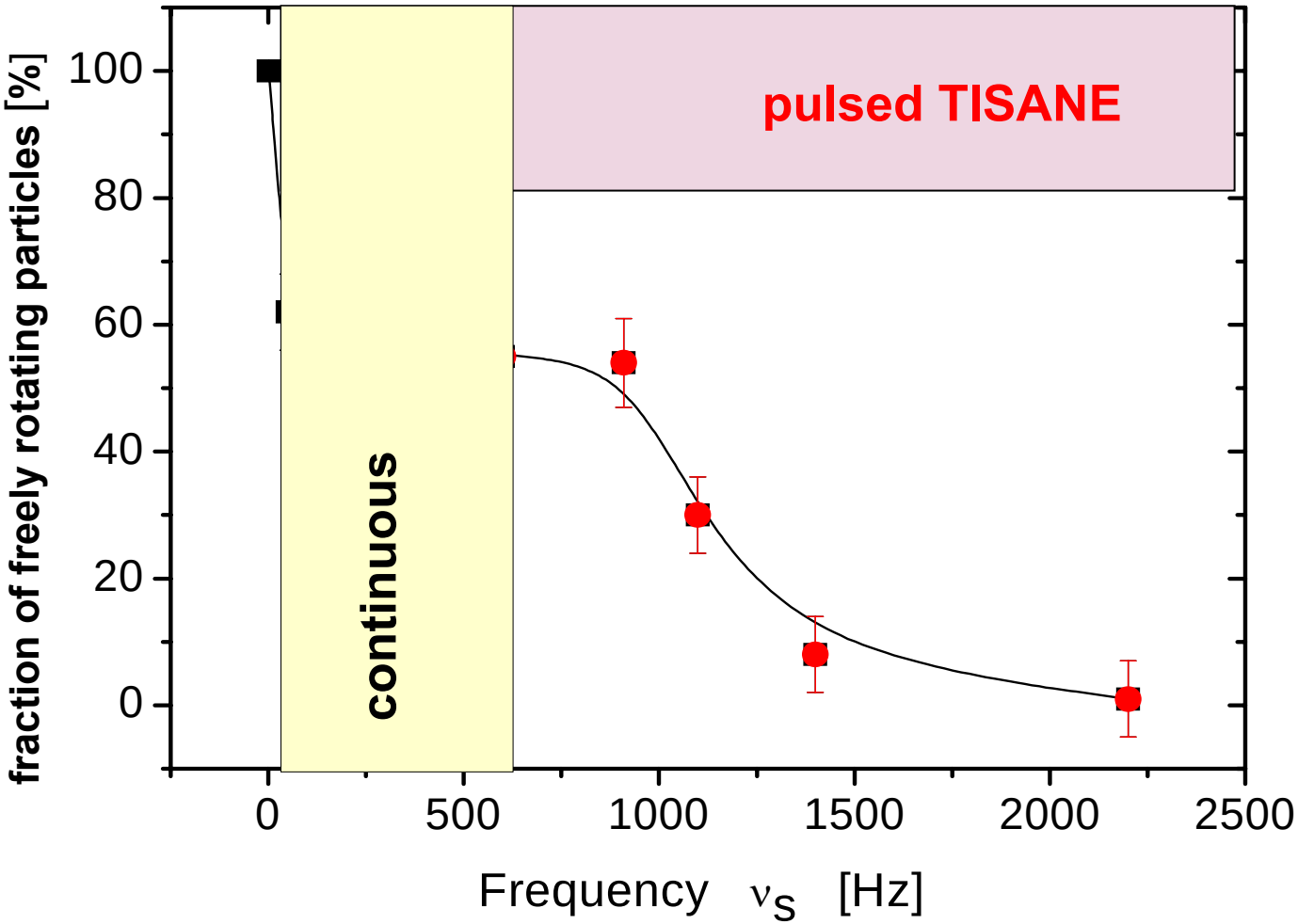

Relaxation mechanisms

Neel-relaxation of single particle moment

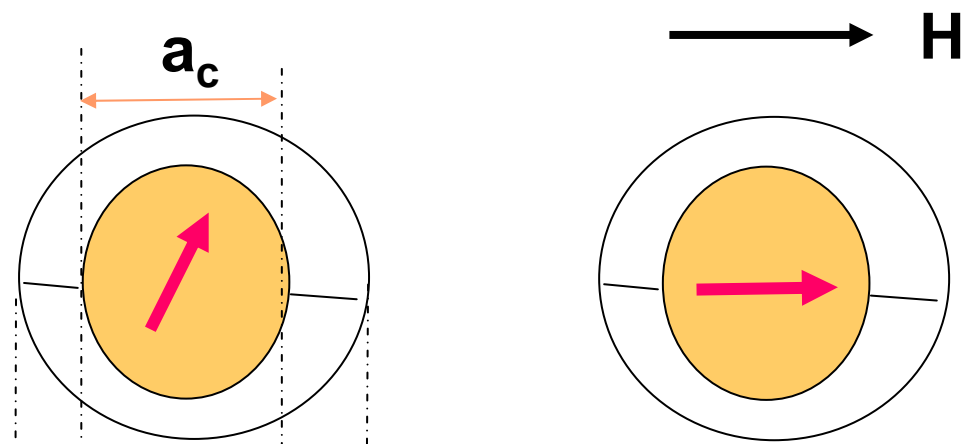

$$\tau_N = \tau_0 \exp (K V_c / k_B T)$$

Brown-rotation of single particle

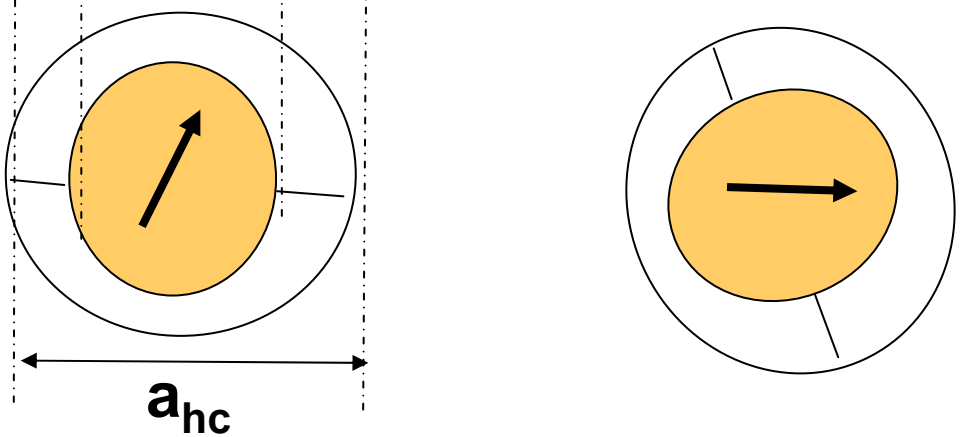

$$\tau_B = 4\pi\eta\, a_{hc}^3 / k_B T)$$

Relaxation mechanisms

Néel-relaxation of particle moment

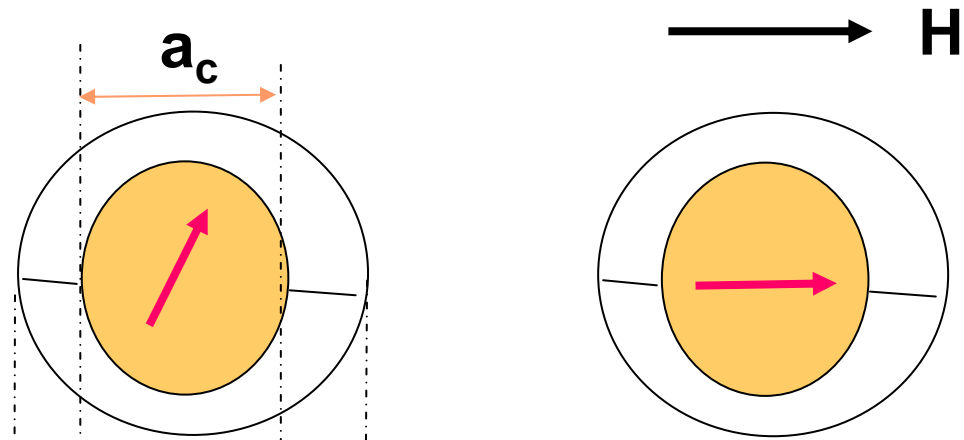

τ_0 = 10^{-9} s

K (fcc-Co) = 2.6 10^5 J/m^3

R_c = (4.2 4.4 4.6) nm

τ_N = (0.2 3.5 80) s

Brown-rotation of single particle

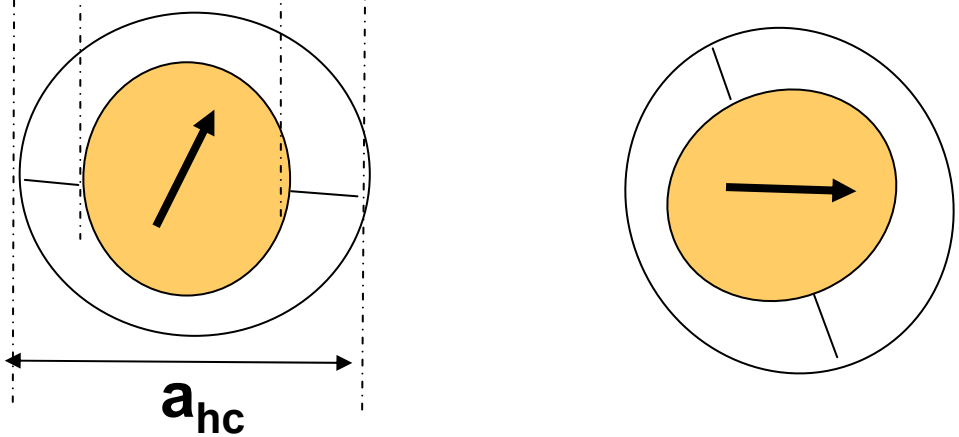

η = 0.1 - 0.2 Pas

a_{hc}= 6.0 - 7.0 nm

τ_B = 160 - 100 μs

ν_B =1000-1600 Hz

Relaxation mechanisms

Néel-relaxation of particle moment

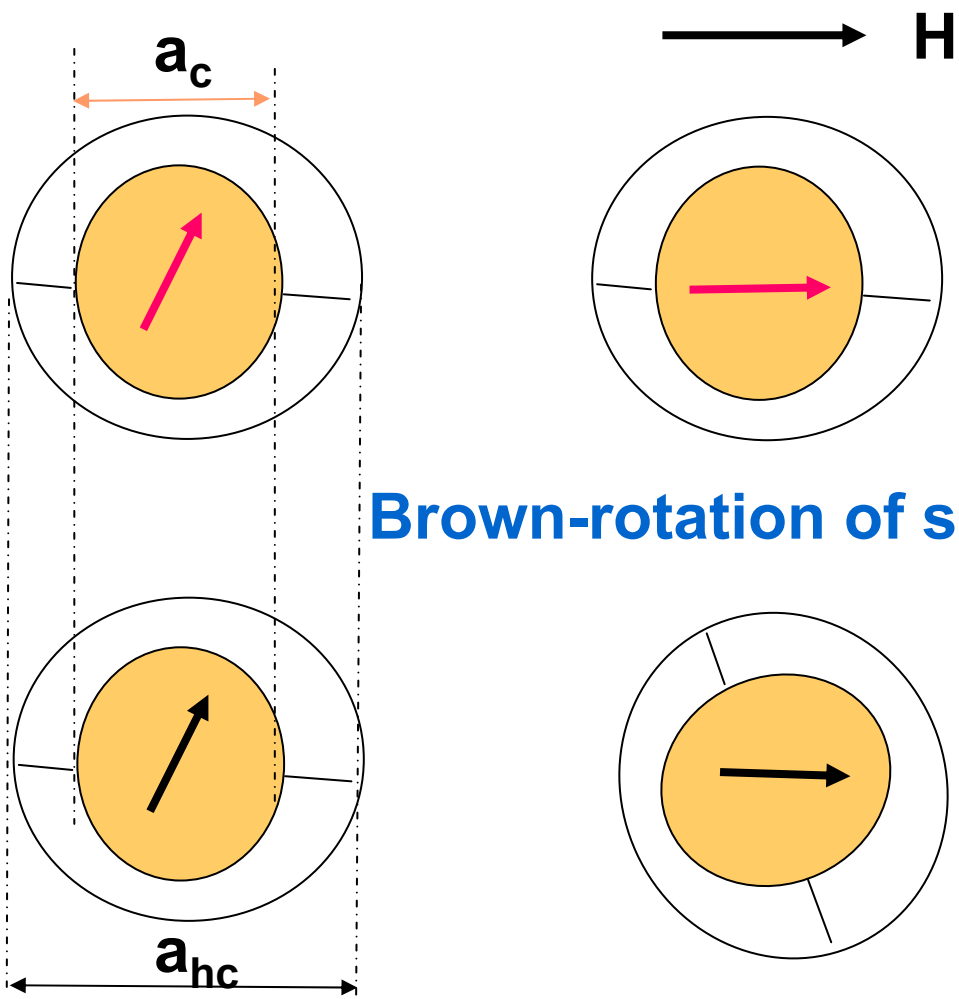

Magnetic moments almost blocked inside particle

Brown-rotation of single particle

Observed threshold for free rotation ν_{obs} =1000-1600 Hz

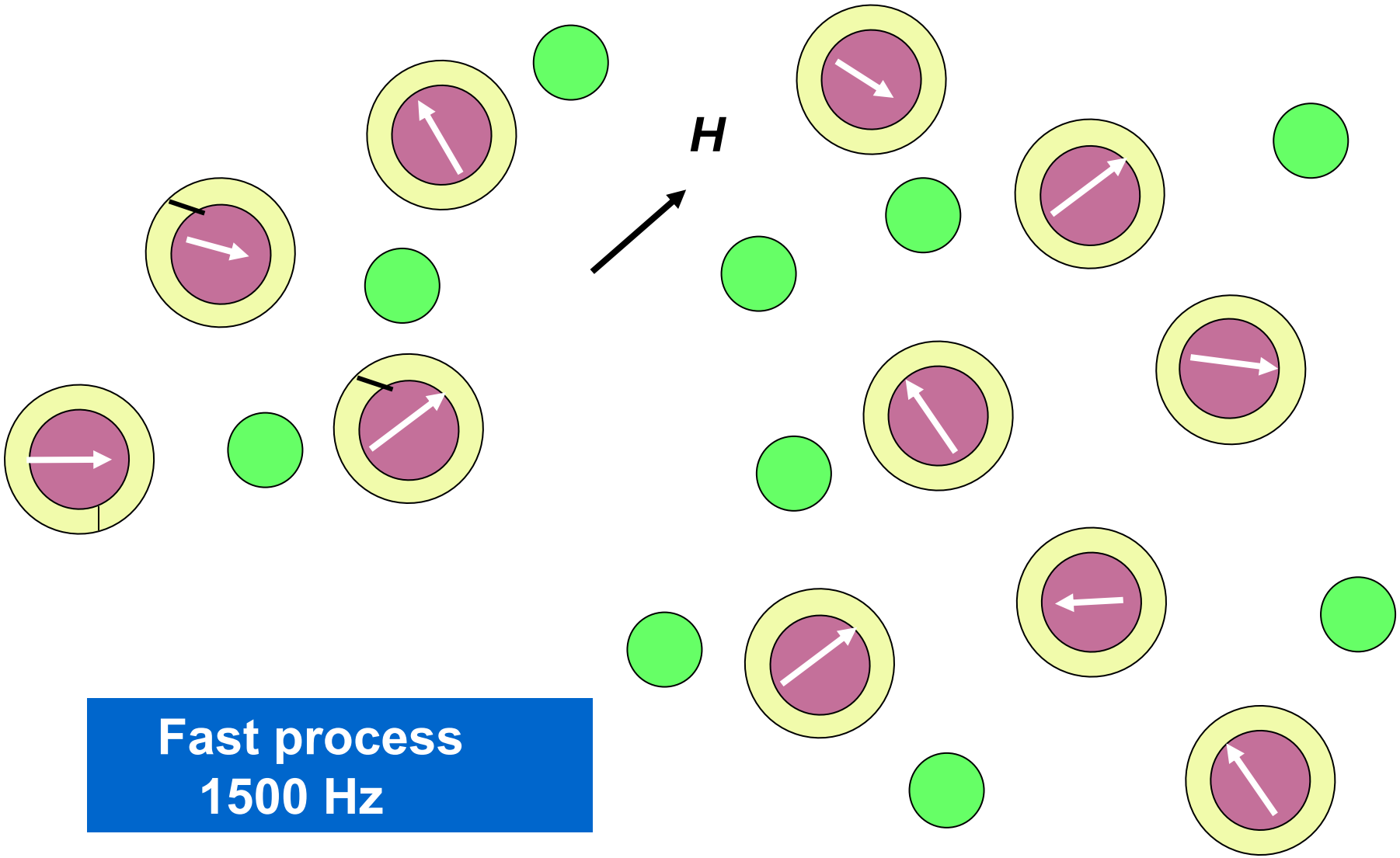

Fast process
1500 Hz

Attractive interactions

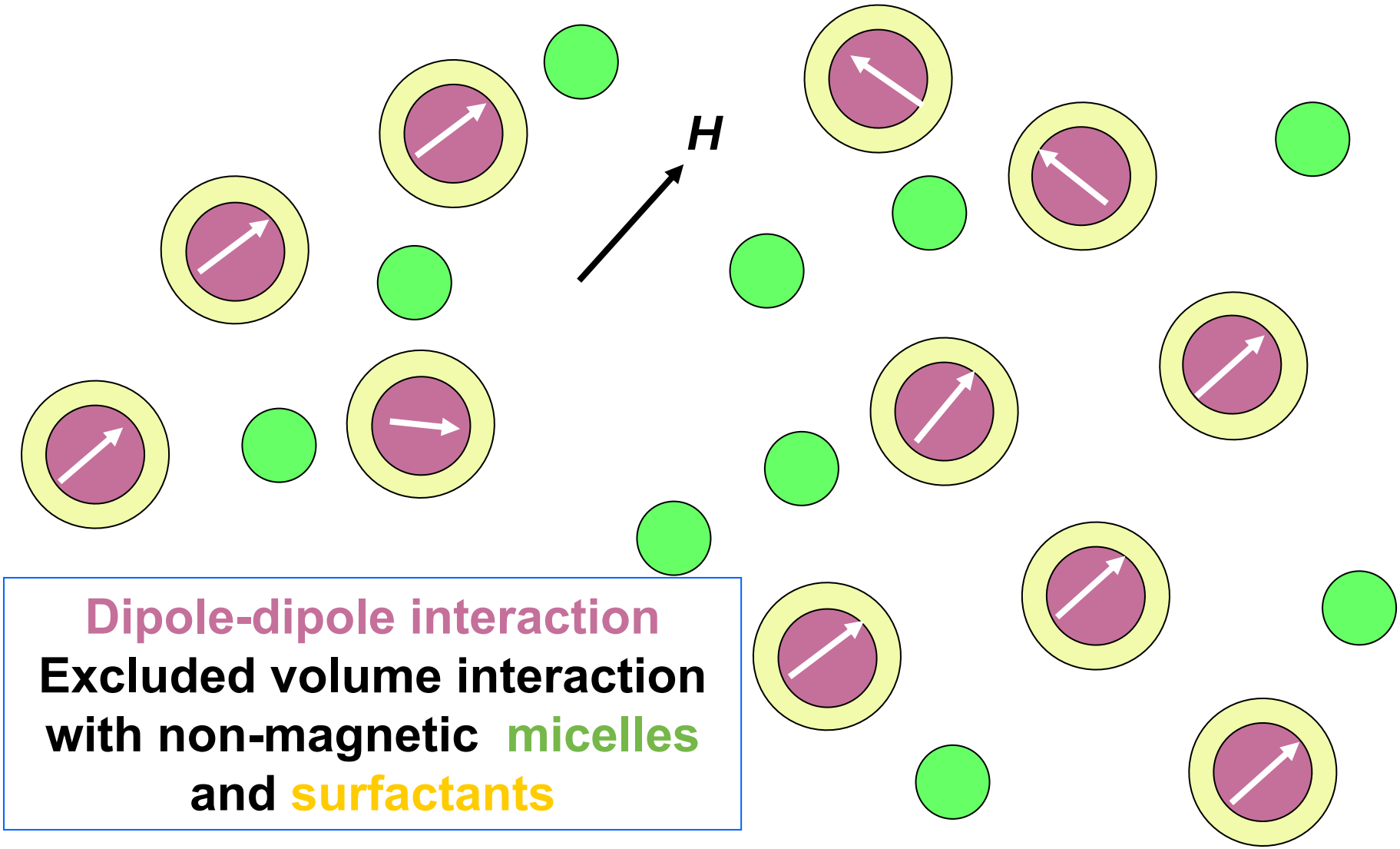

Dipole-dipole interaction

Excluded volume interaction with non-magnetic micelles and surfactants

Formation of ordered domains

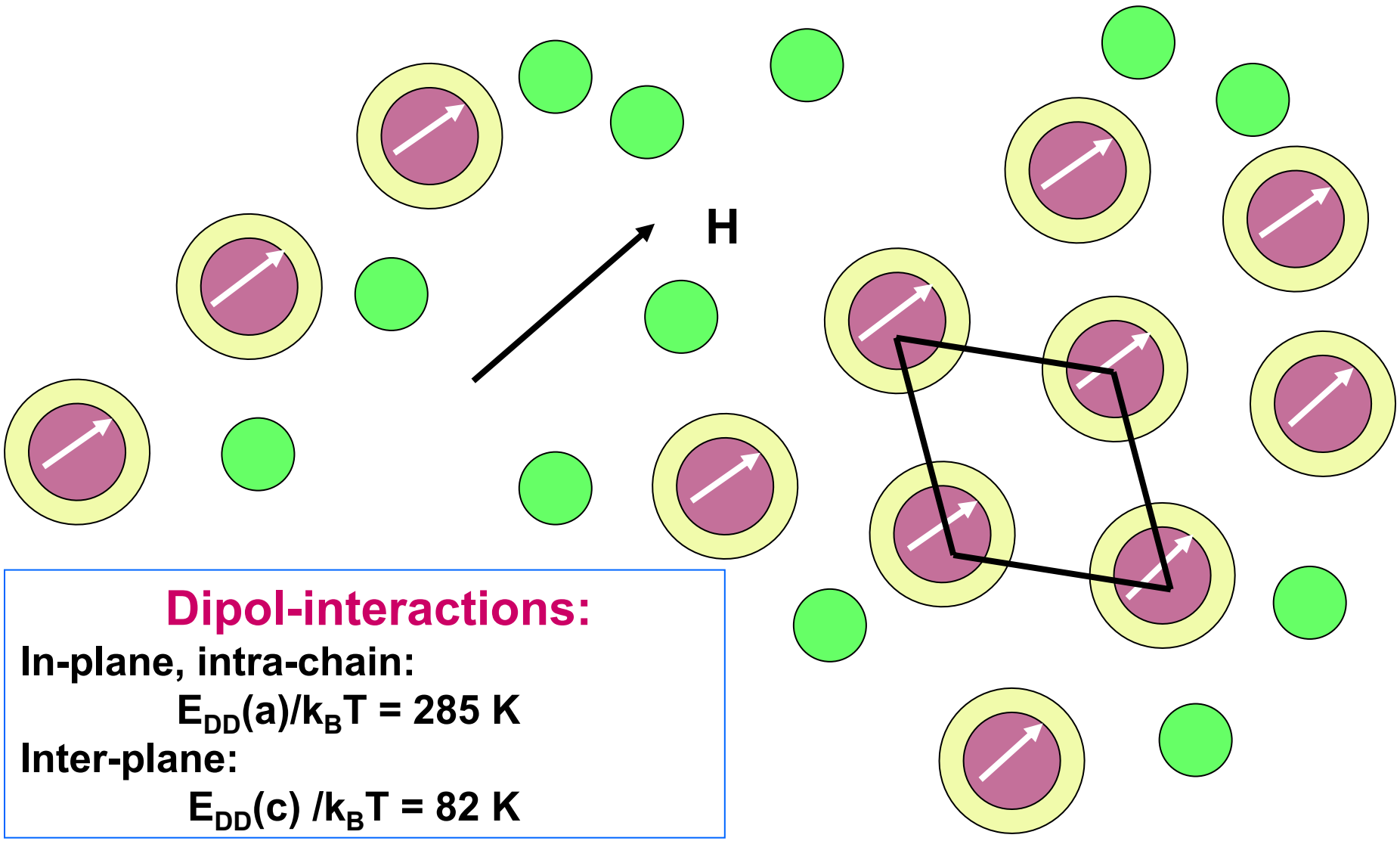

Dipol-interactions:

In-plane, intra-chain:

$$E_{DD}(a)/k_BT = 285\ K$$

Inter-plane:

$$E_{DD}(c)/k_BT = 82\ K$$

Relaxation: Rotation of ordered domains

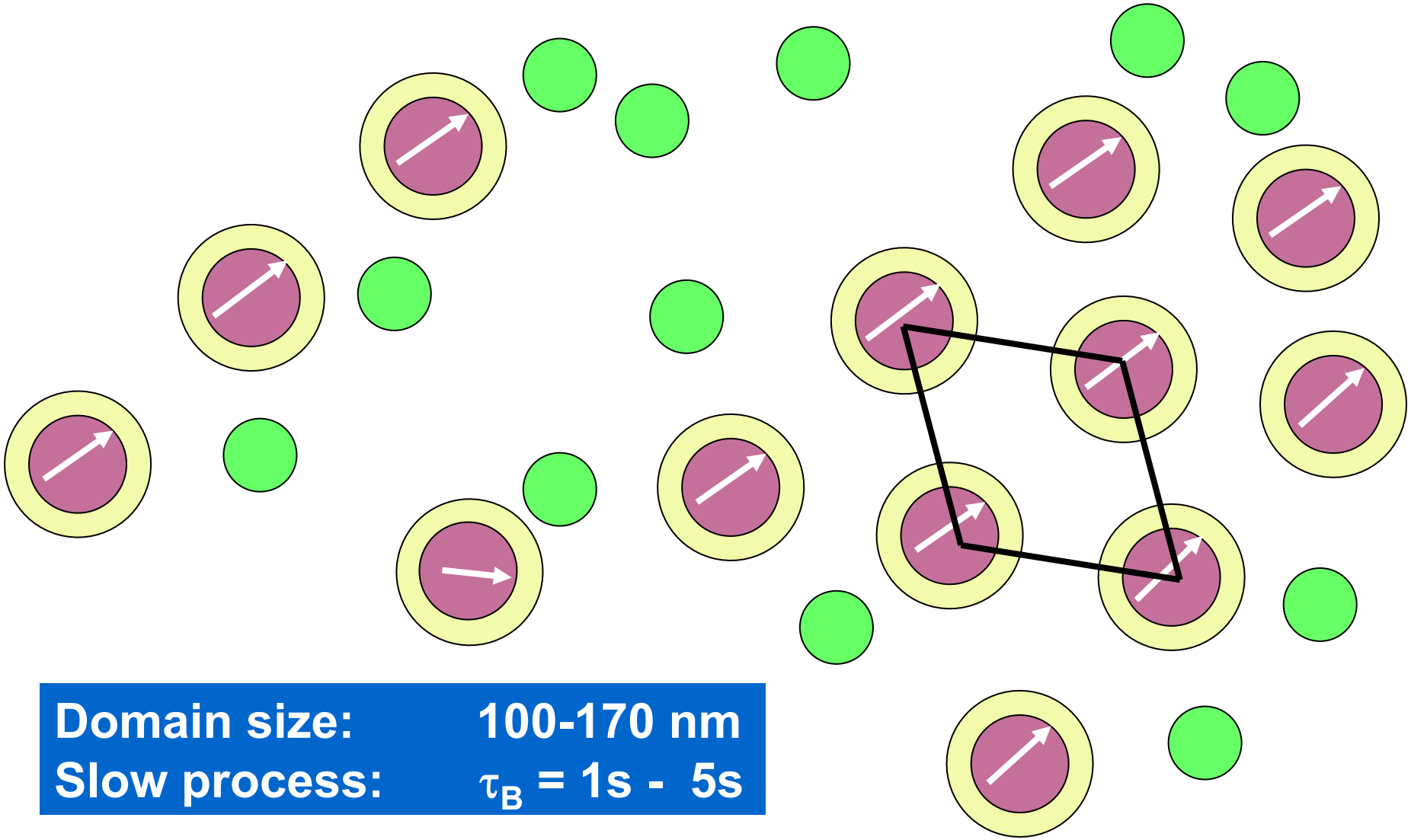

Domain size: 100-170 nm

Slow process: τ_B = 1s - 5s

Relaxation: Rotation of ordered domains

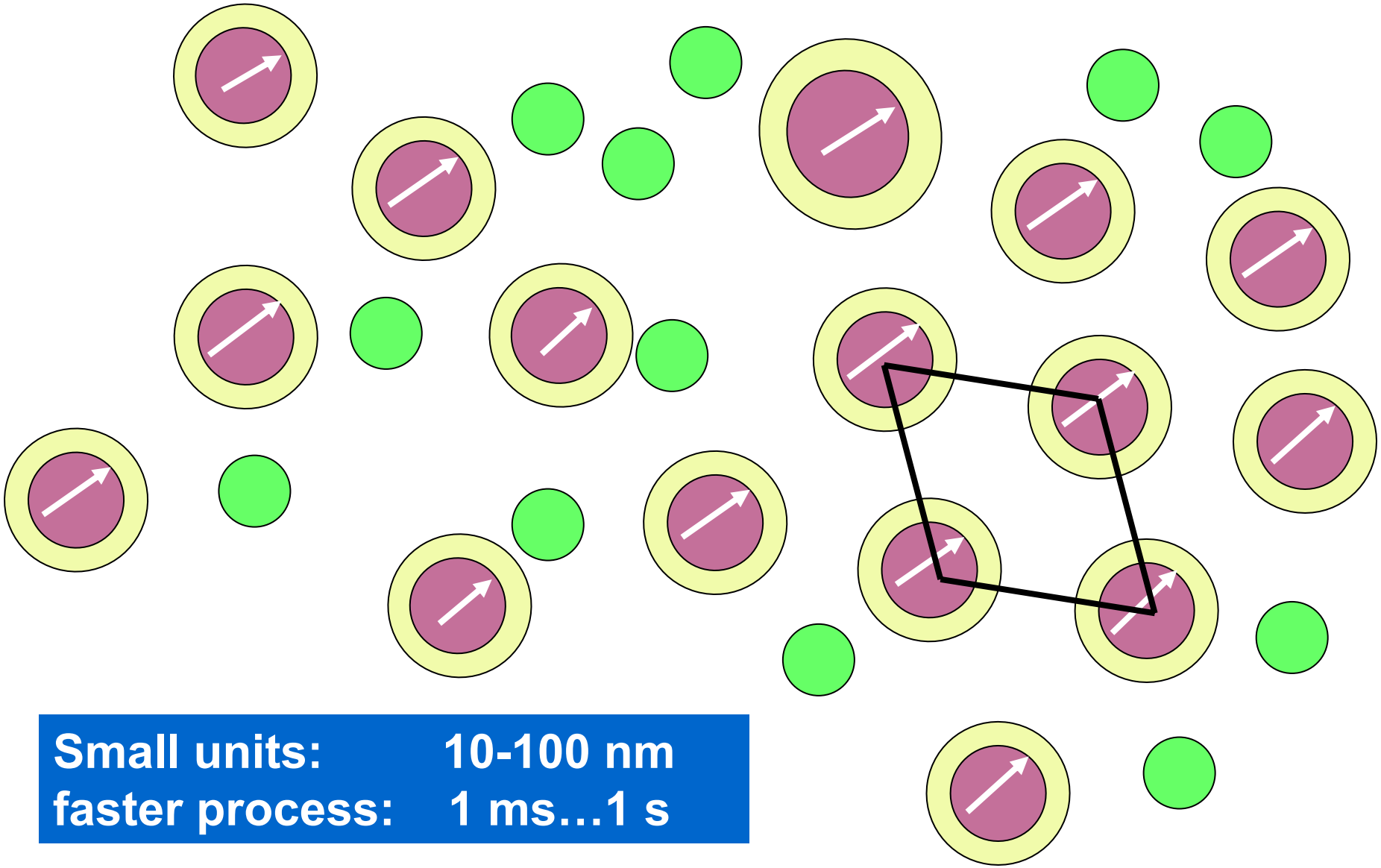

Small units: 10-100 nm
faster process: 1 ms…1 s

Summary

Mechanisms and dynamics of field-induced ordering in Co-Ferrfluids determined by Brownian relaxation

Dynamical processes in nanoscaled inhomogeneities are observable by time-resolved SANS

Limitation of continuous techniques: $\Delta\lambda/\lambda$
Pulsed TISANE technique: Sub-millisecond range

Complementary to Photon correlation spectroscopy (PCS,XPCS), Forced Raleigh scattering, ac-χ

Closes the gap between inelastic neutron scattering/ Mössbauer (10^{-12}- 10^{-6} s) and static measuremets

A. Wiedenmann, U. Keiderling, K. Habicht, M. Russina, R. Gähler PRL 97 057202 (2006)

Conclusion

Combining *"SANS, SANSPOL, POLARIS "*
Contrast variation technique for magnetic materials

Weak magnetic *versus* strong nuclear contributions and *vice-versa*:

Density profiles, interfaces
Sign and magnitude of contrast

Separation of magnetic and nuclear contributions

Dynamics in nanoscaled materials in sub-ms range

TISANE @ NEAT October 2005

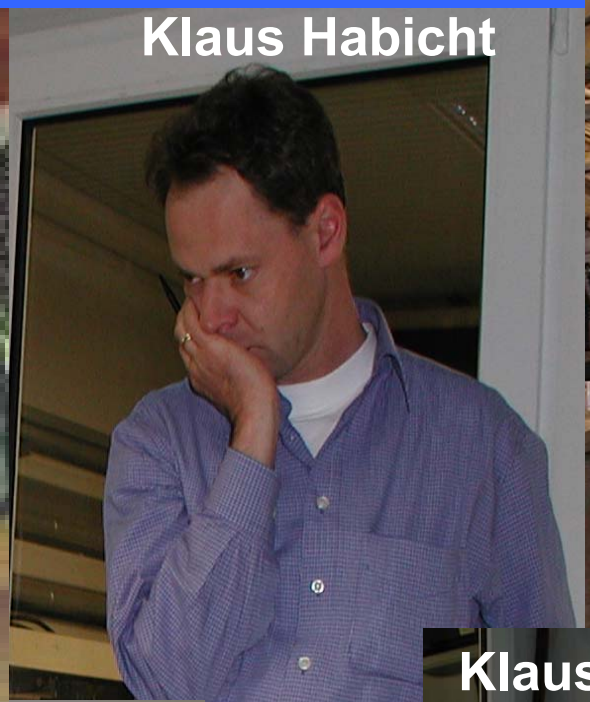

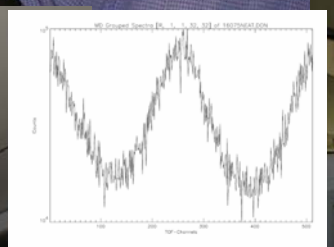

References

A. Guinier , G. Fournet: Small angle scattering of x rays, John Wiley New Yorck 1955

O. Glatter O. Kratky edt. Small angle scattering of x ray, Academic Press, London,1982

L.A. Feigin D.I. Svergun Structure Analysis by Small Angle X-ray and Neutron Scattering Plenum Press New Yorck, 1987

G. Kostorz in Neutron Scattering ed. Kostorz Academic New Yorck 12979 p 227

T. Keller, T. Krist, A. Danzig, U. Keiderling, F. Mezei, A. Wiedenmann, J. Nuclear Instruments A451(2000),474-479

A. Wiedenmann, A. Hoell, M. Kammel, P. Boesecke, Phys Rev. E 68 (2003) 031203, 1-10

A. Wiedenmann, J. Appl. Cryst. 33 (2000)428-432

A. Wiedenmann, Physica B297(2001)226-233

A. Wiedenmann, A. Hoell and M. Kammel ,J. Magn. Magn. Mater. 252 (2002)83-85

A. Wiedenmann ,Lecture Notes in Physics, Springer, editor S. Odenbach (2002), S. 33-61

A. Heinemann, A. Wiedenmann ,J. Appl. Cryst. 36 (2003),845-849

J. Teixeira, J. Appl. Chryst., 21 (1988) 781-785

J. Kohlbrecher et al J, Zeitschrift für Physic B, 104 (1997) 1

U. Keiderling et al, physica B, 213 214 (1995) 895-897

D.I. Svergun, H.B. Stuhrmann, Acta Cryst., A47 (1991) 736-744

R. Pynn, Los Alamos Neutr. Sc. Center, ()

J.S. Pedersen, J. Appl. Chryst., 27 (1994) 595-608

A. Wiedenmann, Materials Science Forum, 312-314 (1999) 315-324

A. Heinemann, A. Wiedenmann, Acta Crystallographica Section A, A57 (2001) 1-4

A. Wiedenmann, Journal of Applied Crystallography, 33 (2000) 428-432

P. Fratzl, F. Langmayr and O. Raris, J. Appl. Cryst, 26 (1993) 820-826

U. Keiderling and A. Wiedenmann, Physica B, 213\&214 (1995) 895-897

A. Wiedenmann SANS investigations of magnetic nanostructures in “Neutron scattering from magnetic materials” ed. T. Chatterji Elsevier 2006, 473-520